# Functional analysis of MICA polymorphism with an emphasis on Behcet's Disease

Shafi, Seema

*Awarding institution:*
King's College London

# Functional Analysis of MICA Polymorphism With An Emphasis On Behcet's Disease

**Seema Shafi**

Thesis submitted for the degree of Doctor of Philosophy
at King's College London, as part of the University of London
January 2013

King's College London,
Guy's, King's and St Thomas' School of Medicine,
Peter Gorer Department of Immunobiology,
Guy's Hospital, Borough Wing, 2nd Floor,
London, SE1 9RT.

# Abstract

Behcet's disease (BD) is a multi-organ inflammatory pathology. A main factor of genetic predisposition locates to HLA-B*51, but MICA*009 is also reported to be strongly associated with BD. The aim of the thesis is to undertake a functional analysis of MICA polymorphism, and determine the functional effects of the HLA-B*51-MICA*009 combination.

Isogenic stable cell lines expressing MICA*009,*008,*009v and ULBP2 were separately created. These were used in killing assays to compare the cell biology of the different MICA isoforms and to assess whether that encoded by MICA*009 varies from other isoforms in its capacity to promote killing by NKG2D positive cells from healthy controls and BD patients. Similarly, double transfectants: HLA-B*51-MICA*009 and HLA-B52*MICA*009 (control) were created and used in similar assays to determine the inhibitory effect, if any, of HLA-B*51 on the targeting of $MICA^+$ cells by patients' lymphocytes.

Data from killing assays show a most unanticipated, donor-to-donor variation in the hierarchy with which different transfectants are targeted by lymphocytes from healthy controls and from patients. These hierarchies seem stable longitudinally and are validated by the CD107a assay. Differential killing cannot easily be explained by an affinity hierarchy because people's cells kill different targets with different hierarchies. Variation among patients is even greater: Approximately 25% of patients preferentially target cells expressing MICA*009 *versus* cells expressing other MICA isoforms. HLA-B*51 and HLA-B*52 comparably inhibit the targeting of $MICA*009^+$ cells by lymphocytes from healthy controls but for 45% of patients, HLA-B*51 shows distinctively stronger inhibition of the targeting of $MICA*009^+$ cells. The variation is killing is not explained by either the number of $NKG2D^+$ or $KIR3DL1^+$ cytotoxic cells nor the expression level of these molecules.

In conclusion, this thesis advances the current understanding of human MICA biology by presenting novel data detailing the expression and function of MICA proteins. The data in this study provide insight into the "tuning" of the lymphocyte stress surveillance response and the impact upon this of HLA-B*51, with implications for the pathogenesis of Behcet's disease.

# Acknowledgements

I would like to begin by acknowledging my supervisors, Professor Adrian Hayday, Professor Miles Stanford, Dr Graham Wallace and Dr Robert Vaughn for their support, advice and guidance and for giving me the opportunity to carry out this research. I have been very fortunate with my supervisors as they all complemented each other wonderfully well. Professor Adrian Hayday (as my daily supervisor) who provided me with a great insight into the world of research and whose wisdom and knowledge inspired and motivated me. Dr Graham Wallace brought a thorough eye and great enthusiasm with him, which I greatly benefited from. Professor Miles Stanford not only provided me with samples for this study, he also always supported me with his positive attitude and good humour, and would kindly treat me to extravagant weekly Sushi lunches. Thank you! I would also like to thank the other members of my thesis committee, Dr Deborah-Dunn-Walters, Professor Salim Khakoo and Professor Dorian Haskard for their advice and guidance.

For this research, a lot of data were essential. Many people helped with this, for which I would like to thank them whole heartedly: the blood donors in the department who provided blood to me on numerous occasions. Thank you so much. I highly appreciate the work carried out by; Pierre Vantourout, who not only carried out experiments to complement my project, but also took the liberty of taking over the project when I left the lab (I am sure he is very thrilled about this!) and Harry Petrushkin, who despite being an opthamologist, was dangerously addicted to lab work. Furthermore everyone in the department has been very helpful and extremely friendly. Most credit goes to my lab colleagues in Prof Hayday's group at Guy's and Cancer Research UK, who have been a source of friendships as well as good advice and collaboration. I would like to thank them all, past and present for always providing support and a great environment to work in, specifically; Monica Correia, Yasmin Haque and Andrew Roberts who inspired me despite the enormous work pressures we were facing together.

Finally I would like to thank my parents who provided me with a loving home, one where an academic mind was celebrated. My parents and my sister always supported, encouraged and believed in me. My nieces (despite living in Dubai) provided

numerous moments of joy and happiness to me, even when I felt the pressures of lab work and thesis writing. I would like to thank my partner, who tirelessly provided me with every possible support through my PhD and reinforced the theory that patience and perserverance are key to success.

This thesis is dedicated to my parents for their love, endless support and encouragement.

# TABLE OF CONTENTS

# List of Figures

# List of Tables

# Abbreviations

| | |
|---|---|
| Ab | Antibody |
| ADAM | A Disintegrin And Metalloproteinase |
| ADCC | Antibody-dependent cell-mediated cytotoxicity |
| AECA | Anti-endothelial cell Antibody |
| Ag | Antigen |
| ANA | Anti-nuclear antibody |
| APC | Antigen presenting cell |
| BCA | Bicinchoninic acid |
| BD | Behcet's Disease |
| BSA | Bovine serum albumin |
| cDNA | Complementary deoxyribonucleic acid |
| CFSE | Carboxyfluorescein succinimidyl ester |
| CHO | Chinese hamster ovary cells |
| CTL | Cytotoxic T lymphocytes |
| DC | Dendritic cell |
| DDAO-SE | Dodecyldimethylamine oxide succinimidyl ester |
| DNA | Deoxyribonucleic acid |
| dNTP | Deoxyribonucleotide triphosphate |
| DTT | Dithiothreitol |
| E:T | Effector:Target ratio |
| EDTA | Ethylenediaminetetraacetic acid |
| Erp5 | Endoplasmic reticulum protein 5 |
| EtBr | Ethidium bromide |
| EtOH | Ethanol |
| FACS | Fluorescent activated cell sorting |
| Fc | Fragment, crystallizable |
| FcRn | Neonatal Fc receptor |
| FCS | Foetal calf serum |
| FITC | Fluorescein isothiocyanate |
| FRT | Flp recombinase target |
| GM-CSF | Granulocyte macrophage colony stimulating factor |

| | |
|---|---|
| GOI | Gene-of-interest |
| HCl | Hydrochloric acid |
| HCMV | Human cytomegalovirus |
| HEPES | 4-(2-hydroxyethyl)-1-piperazineethanesulfonic acid |
| HLA | Human leukocyte antigen |
| HRP | Horseradish peroxidise |
| HSP | Heat shock proteins |
| HSV | Herpes simplex virus |
| ICBD | International Criteria for Behcet's Disease |
| IEL | Intraepithelial lymphocyte |
| IFN | Interferon |
| Ig | Immunoglobulin |
| IL- | Interleukin |
| KIRs | Killer inhibitory receptors |
| LAMP-1 | Lysosomal-associated membrane protein 1 (CD107a) |
| LPS | Lipopolysaccharide |
| mAb | Monoclonal antibody |
| MCP-1 | Monocyte chemoattractant protein 1 |
| MCS | Multiple cloning site |
| MHC | Major histocompatibilty complex |
| MICA | MHC class I polypeptide-related sequence A |
| MICB | MHC class I polypeptide-related sequence B |
| mIgG1 | Mouse immunoglobulin G1 |
| MOPS | 3-(N-morpholino)propanesulfonic acid |
| mRNA | Messenger RNA |
| NCRs | Natural cytotoxicity receptors |
| NKG2D | Natural killer activating receptor 2 |
| NKG2DL | Natural killer activating receptor 2 ligands |
| NK | Natural killer |
| NSAIDs | Non-steroidal anti-inflammatory drugs |
| ORF | Open reading frame |
| pAb | Polyclonal antibody |
| PBMC | Peripheral blood mononuclear cells |

| | |
|---|---|
| PBS | Phosphate-buffered saline |
| PCR | Polymerase chain reaction |
| PI-3 kinase | Phosphatidylinositol 3-kinase |
| pMHC | Peptide-MHC |
| PTPN22 | Protein tyrosine phosphatase, non-receptor type 22 |
| RNA | Ribonucleic acid |
| SD | Standard deviation |
| SEM | Standard error of the mean |
| sMICA | Soluble MICA |
| SSC | **S**aline-sodium citrate |
| ss/ds | Single-stranded/double-stranded |
| TAE | Tris-acetate-EDTA |
| TEMED | Tetramethylethylenediamine |
| TCR | T cell receptor |
| TGF-β | Transforming growth factor β |
| TLR | Toll-like receptor |
| TMB | Tetramethylbenzidine |
| TNF | Tumour necrosis factor |
| TRAIL | Tumour necrosis factor-related apoptosis inducing ligand |
| Treg | T Regulatory cells |
| UV | Ultra Violet light |
| ZAP70 | Zeta-chain-associated protein kinase 70 |
| Zeo | Zeocin |

# CHAPTER ONE: INTRODUCTION

## 1.1 Behcet's Disease

Behcet's disease (BD) is a chronic, systemic inflammatory disease affecting a spectrum of tissues. It can present with mucosal ulceration, inflammation of the eyes, intestine, skin and joints, with additional neurological and vascular manifestations (Yaz et al., 1998). BD progresses by repeated cycles of attack, healing process, and remission. Muco-cutaneous manifestations generally have a short course of attack and healing, whereas ocular lesions generally have a longer course with new attacks occurring before the healing process is complete. Such repeated attacks severely impair vision and may lead to blindness (Le Thi Huong et al., 1991). BD is most prevalent in and around the ancient silk trading routes from the Mediterranean *via* the Middle East to Eastern Asian countries (Nussenblatt et al., 2004). It is of high prevalence and consequently of intense interest in Turkey, whereas it is significantly less common in Northern Europe, Northern Asia, most of continental Africa, Australia and North America (Verity et al., 1999; Zouboulis 2004). Diagnosis of BD is essentially clinical, most often based on the International Criteria for Behcet's Disease (ICBD), 1990 (Table 1).

| | |
|---|---|
| Recurrent oral<br>aphthous ulcers | Small or large aphthous or herpetiform ulcerations, recurring at least 3 times in a 12-month period |
| Plus two of the following | |
| Recurrent genital ulcerations | Aphthous ulcerations or scarring |
| Eye lesions | Anterior uveitis, posterior uveitis or cells in the vitreous on slit lamp examination or retinal vasculitis observed by an ophthalmologist |
| Skin lesions | Erythema nodosum, pseudofolliculitis, orpapulopustulous lesions or acneiform papules in postadolescent patients without steroid treatment |
| Positive pathergy testing | Intracutaneous needle stick with 21G on forearm read by a physician after 24–48 h |

**Table 1.1**: Criteria of International Study Group 1990 (Christoph et al., 2008), illustrating diagnosis by a "triad" of symptoms.

---

The core criteria for diagnosis are: oral and genital aphthosis, skin manifestations, and eye lesions (International Team for the Revision of International Criteria for Behcet's Disease 2008). However, because these criteria were mostly developed as a classification of the disease in its earlier stages, the diagnosis of BD can be difficult and uncertain (Lee 1997), and other sets of diagnostic criteria were previously described by Mason and Barnes (1969), O'Duffy (1974), and Dilsen et al (1986), and in Asia by Mizushima (1988). BD manifestations also show regional differences. Thus, a positive pathergy test is common among patients from Turkey, other Mediterranean countries and Japan, but is less frequent in Northern Europe and the USA (Yazıcı et al., 1984). Gastrointestinal manifestations are common in patients from the Far East (Shimizu et al., 1979), but less common in Turkey (Yurdakul et al., 1996).

BD affects every age group, although mostly post-puberty and prior to the sixth decade, with a peak in the third decade (Ando et al., 1999; Yazici et al., 1984; Zouboulis, 2003, Altenburg et al., 2006). However, childhood cases have been reported (Kone-Paut et al., 1998). Disease prevalence was at one time higher in females, although there has been roughly comparable incidence in males and females for the past twenty years (Nakae et al., 1993; Ando et al., 1999; Zafirakis and Foster, 2002; Zouboulis, 2003; Altenburg et al., 2006).

The cause of BD remains a mystery. Naturally an infectious aetiology has been considered, and agents such as *Streptococcal spp*. that are common in oral fauna and *Herpes simplex virus* (HSV) have been implicated, as has exposure to toxins. Peripheral blood monocytes and skin monocytes from patients have been reported to produce a hypersensitivity reaction to *Streptococcus sanguis* antigens that was less evident in healthy controls (Kaneko et al., 1997). Some such antigens share amino acid sequences common with heat shock proteins (HSP) and it was reported that *S sanguis* and human HSP60/65 activate γδ T cells from patients but not from healthy controls (Lehner et al., 1997; Direskeneli et al., 2000). Although no mechanistic insight for these observations was provided, recently described antigen-driven expansions of peripheral human γδ T cells (Willcox et al., 2012) suggest a scenario whereby long-term activation of auto-specific γδ cells (that may have been initiated by microbial antigens) might be sustained by self-antigens. Indeed it was reported that following initial bacterial challenge, antigenic HSP were expressed on oral mucosal cells. Given that human γδ T cells commonly express inhibitory NK receptors, it is also conceivable that such T cell dysregulation could be influenced by certain HLA types (Verity et al., 2003; Lafarge et al., 2005).

The involvement of HSV as a triggering factor in BD was suggested by Heluci Behcet himself. Serum antibodies to HSV-1 and circulating immune complexes with HSV-1 are elevated in BD patients (Lehner, 1997). Fifteen years' ago, an animal model for BD was developed, wherein 30% of mice inoculated with HSV exhibited BD-like symptoms: the involvement of skin, genital, tongue and gastrointestinal ulcers, ocular inflammation and arthritis (Sohn et al., 1998). Although HSV-1 infection and immunity is common, there is again a possibility that in individuals of certain genetic haplotypes, infection triggers a hyper-active and sustained mucosal immune response

(Denman et al., 1979). Nonetheless, there is as yet no concrete evidence to support a causative role of HSV-1 or any other virus or microbe in the pathogenesis of BD.

## 1.2 Behcet's disease: An autoimmune or autoinflammatory disorder?

BD is commonly regarded as a T lymphocyte driven disease (Turan et al., 1997; Gul 2001), with immunological features including oligoclonal expansions of αβ T cells and increased numbers of γδ T cells, both in the peripheral blood and in mucosal lesions (Freysdottir et al., 1999; Nagafuchi 2005). However, cellular pathology alone is insufficient to identify the driving features of disease progression, since there is also conspicuous neutrophil infiltration, endothelial swelling, and fibroid necrosis, all in the context of enhanced inflammatory cytokines. Nonetheless, patients with active disease have a Th1-skewed cytokine profile (elevated levels of TNF, IFN-γ and IL-12), whereas patients in remission display a Th2-skewed cytokine profile (IL-4, IL-6 and IL-10) (Hamzaoui et al., 2002). Interestingly, a genetic variant that produces low mRNA and protein for the inhibitory cytokine, IL-10, was recently associated with BD, consistent with the perspective that patients suffer from uncontrolled T cell expansions (Remmers et al., 2010). IL-10 polymorphism has likewise been causally associated with lymphocyte dysregulation in early-Inflammatory Bowel Disease (Glocker et al., 2011).

Given the uncertainty of any causal role for T and B lymphocytes in BD, there has been much debate on whether it should be classified as an autoimmune or an autoinflammatory disease. The former type of disease would be exemplified by Type I diabetes, with patients displaying overt titres of autoantibodies and cytolytic T cells reactive to auto-antigens such as Glutamic Acid Decarboxylase (GAD65) and insulin (Bulek et al., 2012). Autoimmune diseases are more common in one gender, and may co-present with other autoimmune diseases. Autoinflammatory diseases are typified by Familial Mediterranean Fever (FMF) and Muckle-Wells syndrome, with severely dysregulated inflammatory responses to stress but no overt causative autoreactivities (Centrola et al., 1998; McGonagle and McDermott 2006).

In support of the notion that specific antigens might drive lymphocyte dysregulation in BD, oligoclonal TCRVβ subset expansions were documented in the peripheral $CD4^+$ and $CD8^+$ T cell compartments of patients (Direskeneli et al., 1999), and there are additional reports of autoantibodies against cell surface antigens, e.g. anti-endothelial cell antibody (AECA); against tropomyosin, enolase, and kinectin; as well as anti-lymphocyte antibodies and a generalised state of B cell activation (Eksioglu-Demiralp et al., 1999; Direskeneli et al., 1995; Mor et al., 2002; Lee et al., 2003; Lu et al., 2005; Feng, 2007). However these antibodies are not present in many patients, are of low affinity, and are suspected to result from BD rather than being causative. As alluded to above, the most extensively investigated autoantigen in BD is HSP60, which contains four immunodominant T and B cells epitopes (Direskeneli and Saruhan-Direskeneli 2003). From among these, the HSP60-peptide, 336-51, provokes a Th1-type proinflammatory response in PBMC of BD patients that over-express the Th1-skewing transcription factor, Txk (Nagafuchi et al., 2005). However, 336-51 responsive T cell lines could also be obtained by continuous and repetitive stimulation *in vitro* of PBMC from healthy controls (Saruhan-Direskeneli et al., 2001). Indeed when viewed overall, BD patients do not show high titres of autoantibodies such as anti-nuclear antibody (ANA); show no consistent autoantigen-specific T cells; and show neither female dominance nor association with other autoimmune diseases (Yazıcı 1997; Direskeneli 2006). Thus, while lymphocytes are strongly implicated in the pathology of BD, the cause(s) of their dysregulation are unelucidated and hence may or may not be primary initiating events.

Like BD, autoinflammatory diseases are characterised by periods of seemingly unprovoked, repeated inflammatory attacks by cells of the innate immune system, primarily neutrophils (Stojanov et al., 2005). Hence, BD has been considered to be in this category (Gul, 2005), added to which, many FMF patients also present defining symptoms of BD (Livneh, 2001). Taken together, available data suggest that BD has autoinflammatory causes inducing unrestrained inflammation that, in combination with specific microbial challenges, gradually provoke the dysregulated activation of lymphocytes that then assert a pre-eminent role in pathology (Fig 1). This perspective accommodates the common emergence of BD in adults rather than children, and the

genetic linkage of the disease to loci, such as HLA, that regulate lymphocyte responses, as considered below.

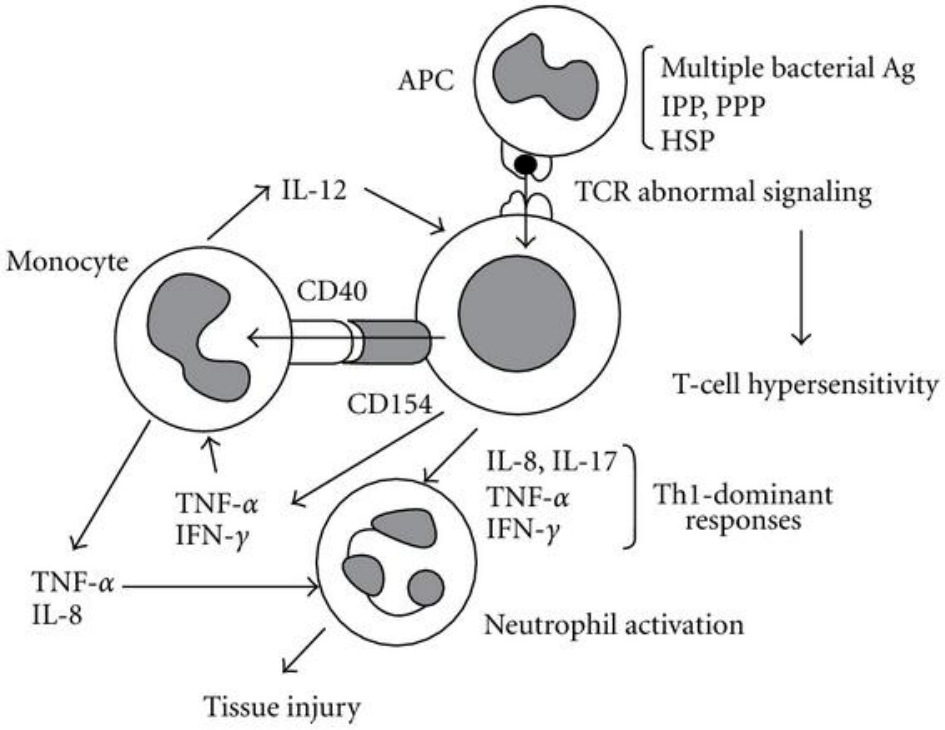


**Figure 1.1:** Proposed pathogenesis model of Behcet's disease. Ag: antigen; APC: antigen-presenting cells; HSP: heat shock protein; IFN: interferon; IL: interleukin; IPP: isoprenyl pyrophosphate; PPP: prenyl pyrophosphate; TCR: T-cell receptor; Th1: T-helper cells type 1; TNF-$\alpha$: tumor necrosis factor $\alpha$. (Tursen, 2012).

---

## 1.3 The involvement of immune cells in Behcet's disease: a more detailed consideration

Figure 1 illustrates the potential for positive reinforcing interactions between cells of the innate immune system (neutrophils, monocytes, APC) and T cells, particularly if defects in IL-10 and/or other regulators fail to constrain it (Remmers et al., 2010). Neutrophils may be activated by cytokines such as IL-18, IFN-γ and TNF-α that can all be produced by activated T cells in BD (Tursen, 2009; Hirohata and Kikuchi 2003). Of note, Shimizu et al (2012) reported in BD an excessive representation of T cells

producing both IL-17 and IFN-γ which in combination have been commonly linked with other inflammatory immumnopathologies (Kullberg et al., 2006). Additionally, BD patients reportedly show decreased numbers of naïve $CD4^+CD45RA^+$ T cells *versus* increased numbers of $CD4^+CD29^+$ T cells (Kahan et al., 1991). The relevance to BD of Th2 skewing is uncertain, with reports that Th2 lymphocytes and cytokines are generally low in BD (Frassanito et al., 1999; Mantaş et al., 1999), in seeming contrast to reports that cells from BD patients make high levels of IL-4, IL-10 and IL-13 *in vitro* (Raziuddin et al., 1998).

A particularly recurrent implication of T cells in BD relates to cytotoxicity. Thus, multiple studies have shown elevated numbers of circulating $CD8^+$ T cells and reduced numbers of $CD4^+$ T cells in the peripheral blood of patients (Valesini et al., 1985; Savage et al., 1988; Fortune et al., 1990). There are increased numbers of $CD3^+CD56^+$ cytotoxic T cells, including a minor subset of $CD4^+$ T cells that may be enriched in tissues (Hamazaoui et al., 1988; Hamazaoui et al., 1994; Levitz et al., 1995; Dummer et al., 1996). CD56 expression has also been reported to be high on Natural Killer (NK) cells of patients with active disease (Kaneko et al., 1985), and as considered above, expanded $\gamma\delta^+$ T cell compartments seem common in BD. The peripheral expansion and intraocular infiltration of $TCR\alpha\beta^+$ $CD8^{bright}$ $CD56^+$ T cells was shown to be a signatory feature of BD patients with uveitis compared to those with uveitis of other aetiologies (Yu et al., 2004). The function of these cells in Behcet's uveitis has not been determined, but they are downregulated upon treatment with cyclosporine and prednisone (Ahn et al., 2005). Pathological studies have implicated T cells and polymorphonuclear leukocytes within vasculitic lesions in BD patients with arterial and central nervous system involvement (Hirohata, 2008; Hasan et al., 1996).

T regulatory (T-reg) cells suppress and dampen effector T cell responses. The lack of T-reg cells in humans and mice results in excessive T cell activation and early death (Gavin et al 2006). Human T-reg cells are $CD4^+CD25^+$, although it is important to note that these markers are also expressed by highly activated T-effector cells. T-reg cells are also $CCR4^+$ and $CCR8^+$, responding to chemokines such as CCL1, CCL17 and CCL22, which seemingly steer the cells to secondary lymphoid tissue and inflamed sites (Iellem et al., 2001). Two groups have described elevated numbers of $CD4^+$ $CD25^+$ T-reg cells in the peripheral blood of patients with active BD (Hamzaoui et al.,

2006b; Suzuki et al., 2006). However, using foxp3 as a marker for Tregs, some groups have reported a decreased frequency of $CD4^+$ $foxp3^+$ cells in active BD (Geri et al., 2011) by comparison to a significant increase in Tregs in BD patients with recurrent apthous ulcerations (Pekiner et al., 2012).

Neutrophils are the most abundant leucocytes and form the first line of defence against infectious agents. They respond to chemotactic stimuli, phagocytose and destroy foreign bodies using oxidative and non-oxidative mechanisms. In BD, neutrophils reportedly show increased adhesion, chemotaxis, and superoxide dismutase levels, but have reduced phagocytic activity (Efthimiou et al., 1989; Pronai et al., 1991; Mege et al., 1993; Dogan et al., 1994; Carletto et al., 1997). The causes for such an altered phenotype are unknown, but contributing to this may be the persistent pro-inflammatory cytokine milieu, including IL-1β, IL-6, IL-8, GM-CSF and TNF (Akoglu et al., 1990; Niwa et al., 1990; Mege et al., 1993, Iper et al., 1998; Mantas et al., 2000; Akdeniz et al., 2004; Kotter et al., 2005; Oztas et al., 2005; Pay et al., 2006).

IL-8 serum levels correlate with disease activity (Aki et al., 2006; Gur-Toy et al., 2005), consistent with which anterior uveitis and joint lesions in BD patients mostly contain a neutrophilic infiltrate that is driven by IL-8. Elevated levels of IL-8 together with IL-12, MCP 1, IFN-γ and IL-12 are found in mucocutaneous biopsies of BD patients (Ben Ahmed et al., 2004), and IL-8 and TNF have jointly been implicated in vasculitis. IL-8 is most commonly attributed to activated monocytes (Fig 1), and may therefore be a product of a reinforcing loop of T cells and APC, as considered above.

Soluble levels of CD28 have been reported to be elevated in the serum of BD patients with active disease. At minimum, therefore, CD28 concentration may be a disease-activity biomarker in BD (Hamzaoui et al., 2005). Since CD28 is a key co-stimulator of T cells, this biomarker may also indicate that there is T cell dysregulation. Likewise, antibodies against the negative regulator of T cells, CTLA-4, have been reported in some BD patients, which may be produced as a consequence of recurrent T cell activation and which may impair natural mechanisms of T cell downregulation.

In sum, it is clearly the case that BD patients display activation and dysregulation of immune cells in both the innate and adaptive compartments. The relative importance of any one cytokine in BD is hard to assess given the complexity of the cytokine

milieu. Indeed, it was reported that there was no pattern of cytokine expression clearly relating to disease activity or treatment (Curnow et al., 2008). Nonetheless, the seemingly increased representation and activities of CD8 T cells, γδ T cells, NK cells, and neutrophils provide a strong potential for autoreactive tissue damage consistent with BD symptoms.

## 1.4 Treatment for Behcet's disease

Systemic corticosteroids and other immunosuppressive drugs have been the most commonly selected drugs for the initial treatment of BD, although they seldom result in stable, long-term remission, particularly in ocular disease. However, the treatment of patients is likely to be transformed by the application of recently developed biologics, although there have as yet been only few, large-scale randomised trials of biologics in BD. Overall, BD patient treatment can currently be considered in three categories: symptomatic drugs; disease-modifying drugs; and biological agents.

### Symptomatic drugs

Local antiseptics and antibiotics are used to treat infected giant aphthous lesions. For skin and joint manifestations, non-steroidal anti-inflammatory drugs (NSAIDs) have some effect in mild to moderate erythema nodosum and in mono or oligoarthritis. NSAIDs, along with heparin and anti-coagulants, are also used for phlebitis. Prednisolone may be used to ameliorate more severe skin manifestions, while local corticosteroids are prescribed for mild anterior uveitis.

### Disease-modifying drugs

Colchicine, levamisole, thalidomide, dapsone, corticosteroids, cytotoxic drugs and cyclosporine A comprise the major forms of disease-modifying drugs applied to BD. Colchicine has been used to treat every manifestation of BD (Mizushima et al., 1977), and is particularly effective for mucocutaneous and joint lesions (Davatchi et al., 2009). Levamisole is used for mucocutaneous lesions, joint manifestations and mild uveitis (Davatchi et al., 1984). Thalidomide is predominantly used in recurrent and resistant mucous membrane manifestations (Hamza, 1986; Hamuryudan et al., 1998).

Dapsone is used in mucocutaneous lesions as an anti-leprotic agent (Hamza et al., 1989). The use of corticosteroids is most commonly associated with the use of other immunosuppressive drugs, such as cyclosporine. Methylprednisolone is often given intravenously, but usually only provides short periods of disease improvement.

The main cytotoxic drugs prescribed are chlorambucil (Davatchi et al., 2009), azathioprine (Yasici et al., 1990), cyclophosphamide (Hamza et al., 1989), pulse cyclophosphamide (Davatchi et al., 2004) and methotrexate (Davatchi et al 2003). These drugs are used specifically for eye lesions, neuro-Behcet's syndrome, pulmonary vasculitis, severe gastrointestinal manifestations and arterial and large vein thrombosis, and usually only in patients with severe forms of BD. Cytotoxic drugs and cyclosporin A show comparable efficacy in ameliorating ophthalmologic manifestations (Al-Rawi et al., 1986).

**Biological agents**

Anti-TNF drugs – notably infliximab (a chimeric monoclonal antibody directed against TNF) or adalimumab have shown good efficacy in several case-controlled studies, predominantly for patients with severe ocular manifestations. (Mushtaq et al., 2007 and Van Laar et al., 2007) Adalimumab has a lower risk of allergic reactions compared to infliximab. It has been suggested that TNF blockade reduces the number of tissue-associated T cells expressing TNF, by retaining Th1 cells in circulation as a result of inhibition of TNF-induced endothelial activation (Misumi et al., 2003). Both entanercept (TNF-blocker) and rituximab (anti-CD20) are used for mucocutaneous and ophthalmologic manifestations when cytotoxic drugs are inefficient. In a recent comparative study between infliximab and conventional therapy, BD patients had significant decreases in inflammation, reduced ocular complications and a reduced number of relapses following treatment with infliximab (Tabbara and Al-Hemidan, 2008). Similarly, a study carried out on 369 patients showed that TNF blockade represents an important therapeutic advancement for patients with severe and resistant, or intolerant, to standard immunosuppressive regimens BD (Arida et al., 2011).

IFN-α is a member of the type-I-IFN family and can be produced by all somatic cells post viral infection. IFN-α exerts antiviral, antiproliferative, immunomodulatory and antiangiogentic effects (Kotter et al., 2003a). The efficacy of IFN-α for severe ocular

BD has been demonstrated in a number of case reports and open studies, with several showing that treatment leads to partial or complete improvement of visual activity in most patients (Kotter et al., 2003b; Krause et al., 2003; Kotter et al., 2004; and Tugal-Tutkun et al., 2006a). The mechanism of disease reduction by IFN-α is unknown, but it might help eradicate viral or microbial components of BD pathogenesis (Kotter et al., 2004).

Despite progress in treatment, there is no cure for BD, with the age of onset being sufficiently young that many patients die from the disease itself. One approach to developing a cure is to gain a better understanding of pathogenesis that can be greatly informed by genetics.

## 1.5 HLA-B*51 and HLA-B*52

BD does not show a Mendelian inheritance pattern, occurring sporadically in most families (Gul et al., 2000; Remmers et al., 2010). However, a familial aggregation of BD is evident, along with an increased disease risk among first-degree relatives. Sibling recurrence rate was assessed at 4.2% in Turkish patients. In 1982, an association with HLA-B*5 in the human MHC locus was identified as a heritable risk for BD ($p<0.0001$). HLA-B molecules bind antigenic peptide fragments that they present to the TCRs of $CD8^+$ T cells. This seems particularly significant given the prevalence in BD pathology of $CD8^+$ T cells, and may be interpreted as asserting T cell dysregulation as a primary cause of disease initiation and/or progression. However, HLA-B molecules also regulate NK cells *via* engagement of Killer-Inhibitory Receptors (KIRs).

HLA-B*51 is present in 40-80% of all BD patients (Mizuki et al., 1997), compared to 24% among healthy populations in Turkey and the Middle East and 8% in Northern Europe (Verity et al., 1999). Microsatellite analysis of eight polymorphic microsatellite markers within 1100kb showed a direct association of HLA-B*51 with BD (Gul et al., 2001b; Muftuoglu et al., 1981). Using genome-wide association studies, the HLA-B*51 gene was reported to have the strongest genetic association with Behcet's disease (de Menthon et al., 2009; Remmers et al., 2010 ; Mizuki et al

2010). However, it may still be the case that HLA-B*51 is associated with a more severe outcome or specific manifestations of disease (Gul et al., 2001b; Muftuoglu et al., 1981).

Among the 21 different isoforms that exist at the HLA-B*51 locus, B*5101 and B*5108 are associated with BD disease and its severity. The HLA-B*5 locus also includes the HLA-B*52 isoforms, which are not associated with BD risk. In seeking to explain the differential association of these isoforms with BD, different components of their protein products have been considered. For example, B*51 and B*52 both display the BW4 motif that is associated with NK cell regulation (see Section 1.9, below). The Bw4 epitope is highly conserved and is determined by five polymorphic positions [residues 77,80,81,82 and 83] in the helical part of the α1 domain of MHC Class I (Wan et al., 1986). Nevertheless there is some variability within this epitope with eight Bw4 variants defined by polymorphisms at positions 77, 80 and 81 (Vilches et al., 1994; Adams et al., 2001), whereas positions 82 and 83 are invariant among $Bw4^{+}$ HLA-A and HLA-B allotypes. Some of the polymorphic residues that define the Bw4 epitope are speculated to interact with bound peptides, which may influence peptide specificity (Barber et al., 1993), MHC stability and T cell recognition (Clayberger et al., 1990). Morevoer, the Bw4 residues are in close proximity to asparagine 86, which is the highly conserved site of N-glycosylation on MHC Class I molecules (Grossberger et al., 1992).

Provocatively, HLA-B*52 (B*5201 isoform) differs from HLA-B*51 by two amino acids in the α helix of the heavy chain: HLA-B*51 carries asparagine and phenylalanine residues at positions 63 and 67, respectively, in the B pocket of the antigen-binding groove, which are replaced by glutamic acid and serine in the corresponding site in HLA-B*52 (Falk et al., 1995). Of 116 subtypes of HLA-B*51 (IMG/HLA Database Release 3.5.0, 14 July 2011), only B*5107 and B*5122 differ in the B pocket sequence. The most frequent HLA-B*51 subtype is HLA-B*5101 which was the isoform first associated with BD (Mizuki et al., 1993).

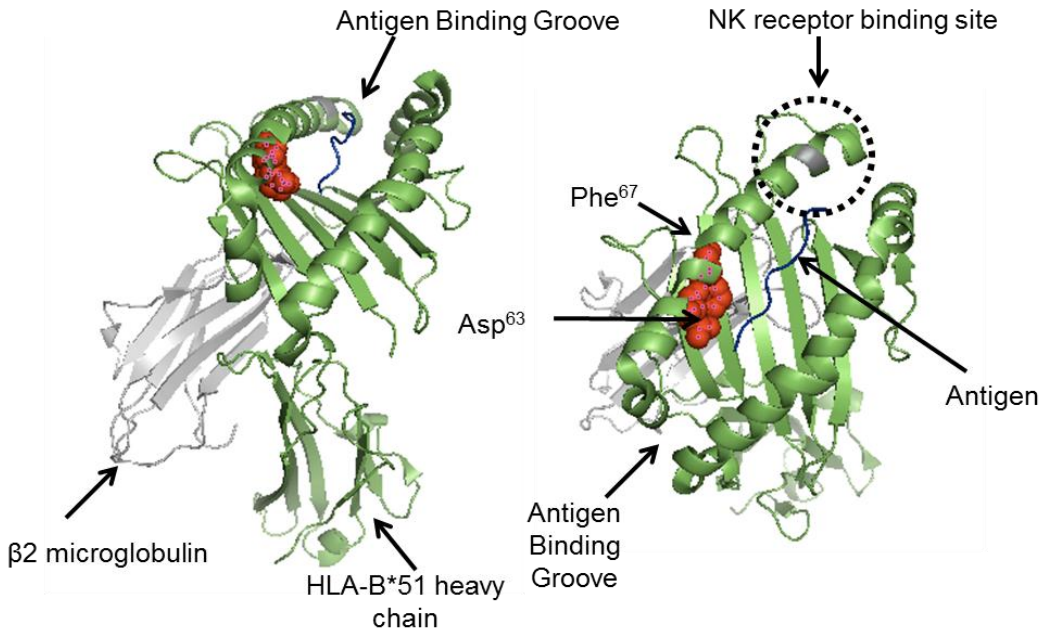


**Figure 1.2**: A crystallography model of the HLA-B*51 molecule. Illustration of the crucial asparagines and phenylalanine at positions 63 and 67 in its antigen-binding groove. The KIR3DL1 binding site is shown as a dotted circle. This diagram is a gift from Dr Ahmet Gul, Istanbul University.

---

The peptides bound by HLA-B*51 and HLA-B*52 differ considerably (Falk et al., 1995). Because auto-specific T cells are ordinarily deleted or anergised in the thymus by high affinity interactions with thymic antigen presenting cells (Gascoigne and Palmer, 2011), the combination of broad and low-affinity peptide binding by HLA-B*5101 may pose particular problems for tolerance, permitting the periphery to populated by large numbers of potentially self-reactive $CD8^+$ T cells, and thereby predisposing for the development of the disease (Kikuchi et al., 1996; Sakaguchi et al., 1997; Gebreselassie et al., 2006). Since peptides are required to stabilise MHC Class I, low affinity peptide binding leads to HLA-B*51 being slow to assemble (Sakaguchi et al., 1997). In sum, the two residue differences between HLA-B*51 and B*52 may appear subtle, but may cause the biochemistry and biology of the two Class I molecules to be profoundly different, thereby differentially contributing to the pathogenesis of BD (Falk et al., 1995).

Among populations, HLA-B*51 is more common where BD is common and is absent where disease is absent (Deuter et al., 2008). Nonetheless, approximately one third of patients in countries with prevalent disease do not carry the HLA-B*51 gene, therefore suggesting that other structurally-related HLA types e.g. B*27, B*15 and B*57 (see below) may also be causally associated with BD.

An HLA-B*51-restricted peptide from MICA was shown to stimulate $CD8^{+}$T cells from BD patients to produce IFN-γ (Yasuoka et al., 2004). Similarly, an HLA-B*51 related peptide (also present in HLA-B*27) initiated proliferation of PBMC's only from HLA-B*51-positive BD patients with posterior uveitis (Kurhan-Yavuz et al., 2000). Notwithstanding these data, there has been little functional insight into how HLA-B*51 may promote Behcet's disease. One approach to addressing this challenge was to determine whether other genes are causally associated with BD, thereby suggesting other functional components of pathogenesis.

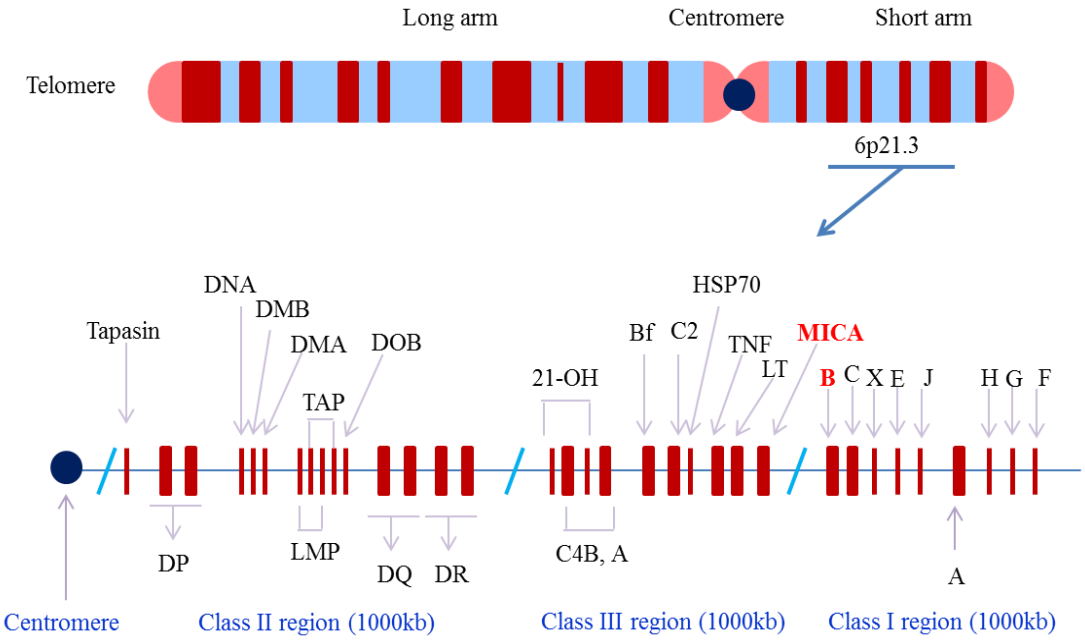


**Figure 1.3**: A map of the Major Histocompatibility complex (MHC) on chromosome 6. The map outlines the genes in close proximity to HLA-B. MICA and HLA-B are denoted in red. Other genes within the locus are transporter of antigenic peptides (TAP), steroid 21-hydroxylase enzyme (21-OH), the complement loci (C4A and B), properdin factor B of the alternate complement pathway (Bf), complement factor 2 (C2), tumour necrosis factor (TNF) and lymphotoxin (LT).

## 1.6 Other genes associated with Behcet's disease

Over the past two decades other genes associated with BD have included those encoding TNF; proteins from the complement system; HSPs; IL-10 ; IL-23; and/or IL-12, and MHC class I related genes, such as MICA.

The human MHC region consists of 3.6Mb on the short arm of chromosome 6 and contains 224 gene loci (The MHC sequencing consortium 1999; Horton et al 2004) (Fig 1.2). Not surprisingly therefore, some of the genes that are genetically associated with BD (Fig 1.3) sit within the MHC locus, and are in linkage disequilibrium with MHC Class I. As an example, one can consider the case of TNF. Association of BD with allelic variation in the TNF promoter region was initially reported in Japanese patients (Mizuki et al., 1992) and then validated among Middle Eastern patients (Verity et al., 1999). There are two variants, TNFB*1 and TNFB*2, of the promoter, with the TNFB*2 variant in linkage disequilibrium with HLA-B*51, implying that they compose a co-inherited haplotype. In such cases, the challenge is to assert whether the increased prevalence of TNFB*2 in BD patients reflects its passive linkage to HLA-B*51 and/or its own functional contributions. Interestingly, TNFB*2 has been associated with higher TNF production by stimulated monocytes, with the potential to contribute to dysregulated inflammation.

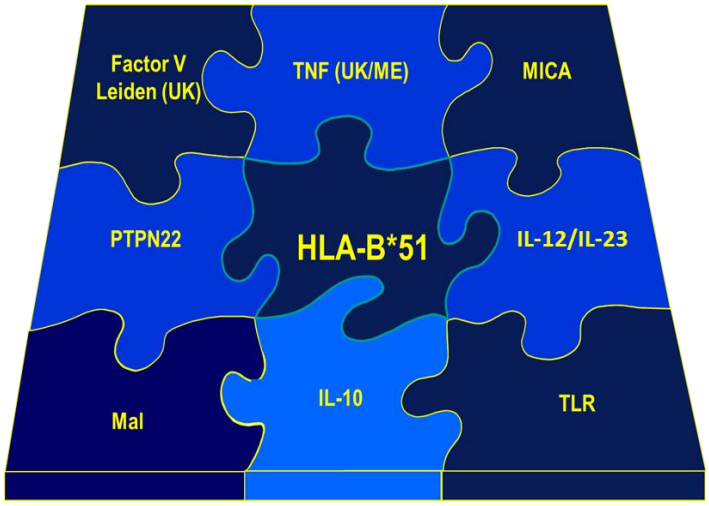


**Figure 1.4**: "The Behcet's Jigsaw": Outline of the genes associated with disease. Central and most important is HLA-B*51, with evidence existing for the association of the additional genes shown. The second most important gene is MHC Class I chain related gene (MICA). Other genes associated are outlined above: Tumour necrosis factor (TNF) Interleukin-10 (IL-10), Factor V Leiden, Toll like receptor (TLR), myelin and lymphocyte gene (Mal) and IL-12/IL-23 are all positively associated with BD, and Protein tyrosine phosphatase non-receptor type 22 (PTPN22) is inversely associated with BD. This diagram is a gift from Dr Graham Wallace, Birmingham University.

---

## 1.7 MHC Class I chain related (MIC) gene

One locus in linkage disequilibrium with HLA-B*51 encodes the MICA and MICB gene products. The MIC locus is located approximately 46kb from HLA-B (Shina et al., 1999) between HLA-B and TNF-α (Bahram et al 1994). The MICA transcript of 1482bp encodes a 383 amino acid polypeptide of 43kDa (Bahram et al., 1994) that is structurally very similar to classical MHC class I molecules: it is composed of 3 extracellular domains referred to as α1 (encoded by exon 2), α2 (encoded by exon 3) and α3 (encoded by exon 4), a transmembrane region (encoded by exon 5) and a carboxy-terminal cytoplasmic tail (encoded by exon 6) (Bahram et al., 1994; 2000). However, it does not carry peptide cargo; is not complexed to β2-microgloubulin; and does not associate with TAP (transporter associated with antigen processing) (Groh et al., 1996; Groh et al., 1998). It is closely related to a sister protein, MICB, encoded

from the same locus. Both proteins are ligands for a C-type Lectin receptor, NKG2D, expressed primarily by subsets of cytolytic $CD8^+$ T cells, γδ T cells, and NK cells (Bauer et al., 1999; Wu et al., 1999).

Studies have shown that MICA proteins are expressed on primary tumours of epithelial origin (Paschen et al., 2009; Unni et al., 2008); on leukaemias (Kato et al., 2007); and on virus-infected cells (Chalupny et al., 2006; Tosh et al 2006). MICA is also upregulated by physico-chemical or infectious stress on gut epithelial cell lines (Groh et al., 1996), epithelium-derived tumour cell lines, monocytes, keratinocytes, dendritic cells, fibroblasts (Zwirner et al., 1998), on activated $CD4^+$ and $CD8^+$ T cells (Molinero et al., 2006) and on several freshly isolated human tumours (Groh et al., 1999).

The MICA and MICB genes have functional heat shock response elements in their promoter region (Groh et al., 1996). Heat shock of epithelial cell lines (Hela cells: a human cervical epithelial carcinoma cell line) at 42˚C for 2 hours initiated cell surface MICA upregulation (Groh V et al., 1996). Other stressors such as virus infection (e.g. by human cytomegalovirus (HCMV), inflammation and DNA damage also cause MICA upregulation albeit with different kinetics (Groh et al., 1996; Groh et al., 1998; Groh, et al 2001; Schreiner et al. 2006; and Tang et al. 2008). Signalling *via* Toll like receptors (TLRs) was also reported to increase the surface expression of MICA (Schreiner et al., 2006).

MICA is recognised as the most polymorphic human non-classical class I gene with at least 65 alleles (http://www.ebi.ac.uk/imgt/hla/). Also there are ≥13 known MICB alleles (http://www.ncbi.nlm.nih.gov). The term allele will be used in this thesis to describe genetic variants of MICA and the term isoform to describe forms of the protein, with slightly different amino acid sequences, but with the similar activity. The 65 known human MICA alleles have been branched into two different lineages (LI and LII) based on phylogenetic tree construction, using a common 821-nucleotide MICA sequence spanning exons 2-4 (Figure 1.4) (Choy et al., 2003). The main differences between LI and LII are at 4 positions: 684, 685, 697 and 713 in exon 4, encoding the α3 domain. The mutation at position 684 is a synonymous substitution. Positions 685 and 697 are substitutions of G-A and T-C, respectively,

which result in the non-conservative substitutions of Gly-Ser and Trp-Arg at residues 206 and 210 of the peptide sequence. Position 713 encodes a conservative substitution at position 215 on the polypeptide. These polymorphic sites lie close to one of the MICA glycosylation sites (Bahram et al., 1994). The MICB alleles are very similar to the LII lineage MICA alleles because they encode polypeptides with Ser, Arg and Thr at positions homologous to 206, 210 and 215 in MICA. 49 of 65 MICA isoforms exhibit changes in the extracellular and transmembrane domains (exons 2-4). The transmembrane region of MICA includes a triplet repeat-length microsatellite polymorphism ([GCT]*n*) of a variable number of repeats designated as A4, A5, A6, A8, A9, A10 and A5.1. Note that A5.1 defines a guanine insertion (GCT → GGCT) that leads to a frameshift mutation and a premature stop codon within the transmembrane domain (Mizuki et al., 1997) thus preventing synthesis of the 42 amino acid cytoplasmic tail. Such a truncated protein is encoded by the MICA*008 isoform and it was reported that this protein product could not be expressed stably at the cell surface (Bahram, 2000). MICA*A5.1 and A6 forms are found in both the LI and LII lineages, whereas A4, A7, A8, A9 and A10 are found only in the LI lineage and A5 is found only in the LII lineage (Choy et al., 2003). Several studies have shown MICA*008/A5.1 to be the most frequent allele in populations of distinct ethnicities: for example, most Caucasian populations carry this allele (Fodil et al., 1999; Petersdorf et al., 1999; Fischer et al., 2000; Bahram, 2000). Conversely, MICA*008 and MICA*00201 are frequent among African Americans, whereas MICA*027, *00201 and *010 are most frequent among South American Indians (Zhang et al., 2002).

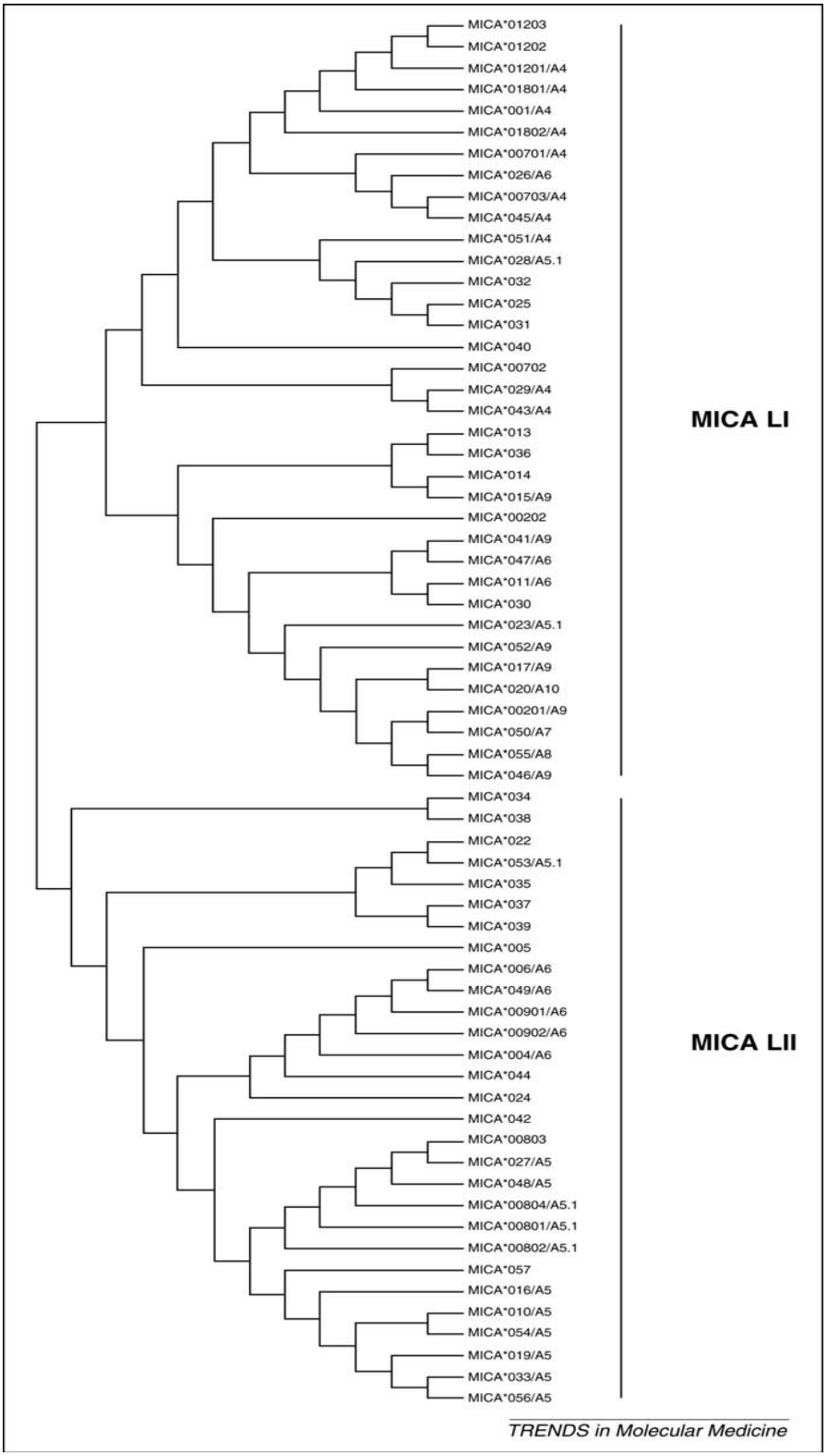


**Figure 1.5**: Phylogenetic tree of MICA: The 65 human MICA alleles branch into 2 lineages based on the common 821 nucleotide covering exons 2-4 of the MICA sequence. 36 alleles are listed in lineage 1 (LI) and 29 in lineage 2 (LII) (Choy et al., 2003).

MICA*009, is strongly associated with HLA-B*51 and HLA-B*52. However, in BD patients, it was striking that it co-segregated only with HLA- B*51 which is disease-associated (Wallace et al., 1999). MICA*009 is an A6 gene and a triplet repeat region polymorphism in the transmembrane region of A6 MICA genes has shown significant association with BD in both Japanese and Middle Eastern patients (Mizuki et al., 1997). This very strong association of MICA*009 with BD and its strong linkage to HLA-B*51 may indicate that these molecules functionally interact and may both contribute to the pathogenesis of BD.

The functional effects of MICA polymorphisms have not been fully investigated. However, one hypothesis would be that they engage NKG2D with different affinities. From crystallographic analysis of unliganded MICA, the structure seems quite distinct from MHC Class I. For example, the α2 helix, which is defined as the groove helix, appears to be flexible and thus not visible in the crystal structure (Li et al., 1999). The region equivalent to the MHC Class I antigen presenting platform formed by the α1 and α2 domains flips over by an angle of 113.5° and points down to the cell membrane, rather than facing upward into the intercellular space. There are amino acids in MICA that disrupt any potential binding of $\beta_2$m (Li et al., 1999).

However when MICA binds to NKG2D, the flexible α2 reforms with 2 additional α-helical turns to allow the ligand-receptor complex to form. This leads to a 96° flip of the α1 and α2 structure thereby bringing the α1 and α2 region into direct contact with NKG2D. This reflects critical flexibility in the region between the MICA α3 stalk and the overlying platform. These structural analyses depict some polymorphic residues as being in direct contact with NKG2D (Li et al., 1999, 2001; Strong, 2000).

However, binding affinity may also be affected indirectly by polymorphism in MICA. For example, using soluble recombinant NKG2D, it was determined that the main differentiating factor between affinities of different MICA isoforms for NKG2D, was a methionine/valine bi-morphism at position 129 (Steinle et al., 2001). Structural analysis of MICA isoforms *01,*04*07,*08 and *16 reported that a valine at position 129 was associated with reduced affinity for NKG2D that was increased when substituted by methionine. The crystal structure of MICA*01 shows amino acid 129 to be located in the β-pleated sheet in the α2 domain, and since the side chain of

methionine 129 is buried, the substitution with valine may result in conformational change which indirectly affects the binding and affinity of MICA for NKG2D. However the protein encoded by MICB*01 with a valine at position 129 also showed strong binding to soluble NKG2D, suggesting that further polymorphisms within and perhaps outside the NKG2D binding site may play a role in differential affinity of MICA isoforms for the receptor. (Steinle et al., 2001).

Within their cytoplasmic tails, some proteins that carry organelle-specific retention sequences or subcellular sorting motifs (Pelham, 1999; Mostov et al., 2000). This may be the case for MICA proteins, given their localisation predominantly on the basolateral surface of intestinal epithelial cells. The intestinal epithelium is the site of most extensive exposure to the environment (Shao et al., 2001) and is composed of sheets of polarised cells, whose plasma membranes are separated by tight junctions into apical (luminal) and basolateral domains with distinct functional characteristics. The basolateral surface mediates contact with large numbers of intraepithelial lymphocytes (IELs), including T cells and NK cells, many of which express NKG2D and act to protect the gut from microbial or tumoral challenge (Lefrancois et al., 1997; Hayday et al., 2001; Lopez-Larrea 2008). Highlighting the potential of epithelial cells expressing MICA to regulate such cells, a dihydrophobic basolateral sorting motif was identified in the cytoplasmic tail of MICA. Interestingly, this is missing from MICA A5.1 isoforms, which are common in Caucasian populations, and in tissue culture experiments, those protein products localise atypically to the apical surface of epithelial cells, where they may be impaired in their capacity to regulate IEL (Suemizu, 2002)

## 1.8 MICA, MICB and Stress

MICA and MICB are regarded as stress antigens due to their low mRNA and protein expression in primary cells and in many cell lines, however this is increased following various types of "stress". Hence, the regulation of MICA and MICB facilitates NKG2D-mediated immune recognition of stressed cells by NK cells and $NKG2D^{+}$ subsets of T cells. The same appears to be true other for MHC Class I-related ligands for NKG2D encoded by the murine or human Rae-1 genes and this form of immune

recognition has by now been intensively studied in both human and murine contexts (Hayday, 2009; Strid et al., 2008; 2011). Of note, it was shown in mice that the acute upregulation of a transgene-encoded NKG2D ligand, Rae-1, on keratinocytes was sufficient to activate adjacent $NKG2D^+$ dendritic epidermal T cells (DETC) *in vivo*. Moreover, this led not only to local T cell responsiveness but to the rapid induction of high levels of IgE, attesting to the potential impact of NKG2D ligands such as MICA as acute regulators of immune responses (Strid et al., 2008; 2011).

Conversely, the chronic upregulation of transgenic MICA/Rae-1 provoked the downregulation of surface expression NKG2D receptors and the impairment of NK cell responsiveness, which was manifest in an impaired ability to reject tumours and to respond to infection (Weimann et al., 2005; Oppenheim et al., 2005). Related to this, NKG2D can also be internalised and degraded by chronic exposure to soluble MICA which appears frequently to be shed from the surface of human tumour cells by directed proteolysis (Salih et al., 2002; Groh et al., 2002, 2006; Doubrovina et al., 2003). The α3 domain of MICA on the surface of the tumour cells forms a complex with a disulphide isomerase/chaperone, endoplasmic reticulum protein 5 (ERp5) thereby provoking a conformational change that facilitates proteolytic cleavage by ADAM (a disintegrin and metalloproteinase) proteases (Kaiser et al., 2007; Waldhauer et al., 2008). Consistent with this, sera from many patients with various malignancies have tested positive for sMICA (Duan et al., 2011; Arreygue-Garcia et al., 2008; Salih et al., 2003; Salih et al., 2002; Groh et al., 2002). These findings underline a potentially important role of sMICA in tumour immune escape, with some studies reporting that serum sMICA levels may be an important negative prognostic factor for hepatocellular carcinoma (Li et al., 2012). In sum, MICA is a highly regulated protein, with powerful functional potential. Its profound biological significance is not limited to tumour immune-surveillance. Rather, viruses of many classes show diverse capacities to evade activation of immune cells *via* the NKG2D receptor, such as ubiquitination of MICA; targeting MICA or MICB via microRNA; or encoding of MICA-like decoys that compete for NKG2D binding (Stern-Ginossar et al., 2007, 2008; Campbell, 2007; Thomas et al., 2008; Vivier et al., 2008).

Given this, genetic polymorphisms in MICA might affect the function of the NKG2D pathway at any of several levels, including the direct interaction of MICA with

NKG2D; the induction and stability of MICA mRNA; and/or the synthesis, stability, and/or shedding of MICA protein. This thesis will provide a system for assessing the impact of MICA polymorphism on key aspects of its biological function, namely its capacity to provoke NK cells and T cell responses. This approach can cast light on the potential significance of MICA polymorphism to BD and other inflammatory pathologies.

## 1.9 Natural killer (NK) cell recognition

The association of MICA and MHC Class I haplotypes with BD, coupled to the cellular data described above, suggests a major role in the disease for cells regulated by these molecules including NK cells and subsets of T cells.

NK cells are bone marrow-derived cells, traditionally considered as part of the innate immune response because for the most part they lack pathogen-specific antigen receptors. They commonly comprise 10-15% of circulating lymphocytes in humans, falling mostly into two distinct populations. About 90% are $CD56^{dim}CD16^{+}$ cells that are capable of natural killing and antibody dependent cell cytotoxicity, but do not produce much IFN-γ. Conversely, about 10% are $CD56^{bright}CD16^{-}$, are weakly cytotoxic, do not proliferate vigorously in response to IL-2, but produce substantial amounts of IFN-γ. It has been suggested that $CD56^{bright}CD16^{-}$ cells utilise their cytokine production to play a regulatory role in immune responses while $CD56^{dim}CD16^{+}$ cells are terminally differentiated cytotoxic effector cells (Cooper et al., 2001; Inngjerdingen et al., 2011).

Developmental studies have suggested that the $CD56^{dim}$ NK-cell subset is derived directly from the $CD56^{bright}$ NK subset (Lanier et al., 1986; Moretta et al., 2006; Chan et al., 2007; Ouyang et al., 2007; Takahashi et al., 2007). $CD56^{bright}$ cells from lymph nodes and tonsil could be induced by IL-2 to adopt the function and phenotypic appearance of $CD56^{dim}$ cells (Freud et al., 2005). However, other data confound this picture. For example, it was reported that $CD56^{dim}$ cells can acquire a $CD56^{bright}$ cell phenotype upon stimulation with IL-12, and that tissue $CD56^{bright}$ cells are $CD56^{dim}$ cells that had been activated *in situ* by tissue cytokines (Walzer et al., 2005).

Upon activation, NK cells can kill transformed, infected and allogeneic cells by the granule exocytosis pathway. In this process, cytotoxic granules containing perforin, members of the granzyme family of proteases, and granulysin (in humans only) translocate to the surface of NK cells, where their contents are secreted into the immunological synapse formed between the NK cell and the target cell. Inside the target cell, granzymes cleave caspases that activate the target cell's intrinsic cell death machinery. Direct activation of cysteine-aspartate directed proteases caspase 3 and 7, by granzyme B leads to caspase-dependent degradation of specific protein substrates that cause apoptosis (Martin et al., 1996; Adrain et al., 2005; Cullen et al., 2007).

To control the action of NK cells there is a complex balance between the activating and inhibitory receptors on their surface that use opposing signalling motifs (Figure 1.6). NK cells *in vivo* are constitutively suppressed by the interaction of inhibitory receptors with self MHC Class I ligands.

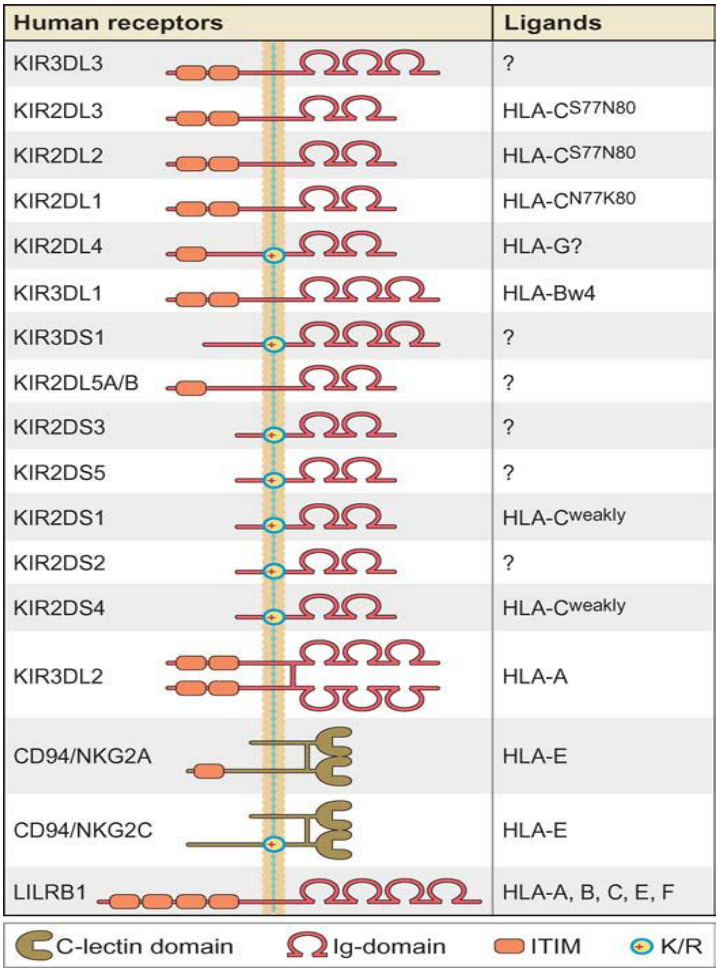


Figure 1.6: Graphic depiction of human NK cell receptors for MHC class I. Inhibitory KIR (i.e., KIR2DL and KIR3DL), LILRB1, and CD94/NKG2A contain ITIMs in their cytoplasmic domains. CD94/NKG2C and the KIR molecules lacking ITIMs and having a charged residue in their transmembrane domains (i.e., KIR2DS and KIR3DS) likely pair with the DAP12 signaling adapter. KIR2DL4 is an exception; it possesses an ITIM in its cytoplasmic domain and is associated with the Fc$\varepsilon$RI$\gamma$ signaling adapter. MHC class I ligands for the receptors, if known, are shown. Figure reproduced from Lanier, 2005.

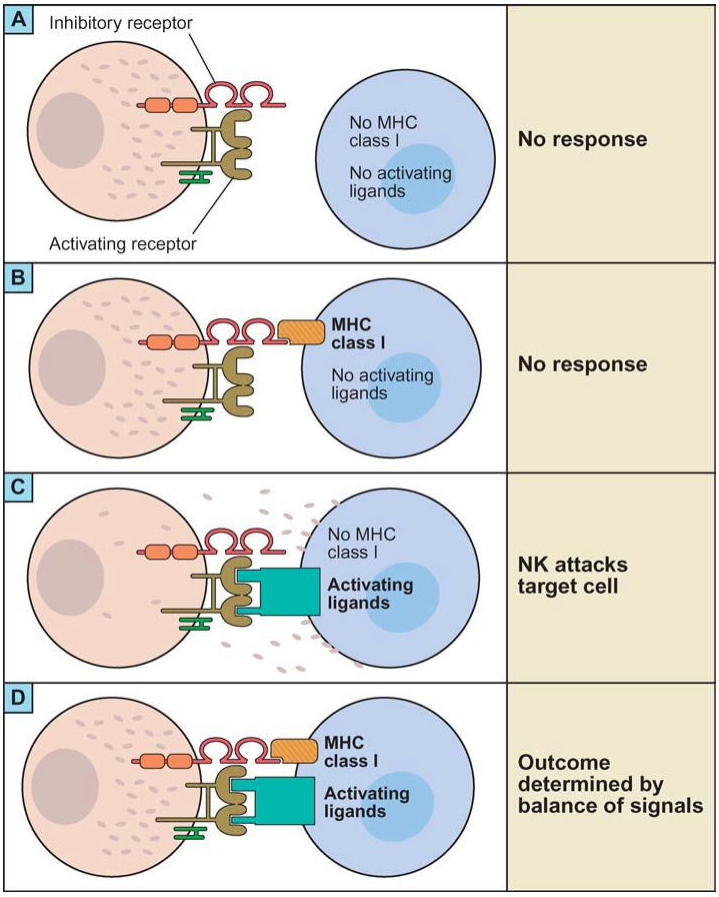


**Figure 1.7** "Missing-self" revisited. Graphic depiction of encounters between NK cells and potential targets and possible outcomes. In some circumstances, inhibitory receptors recognizing ligands other than MHC class I proteins may suppress NK cell responses. When interacting with target cells expressing ligands for both inhibitory and activating receptors, the outcome is determined by the summation of the strength of signals. The amount of activating and inhibitory receptors on the NK cells and the amount of ligands on the target cell, as well as the qualitative differences in the signals transduced, determine the extent of the NK cell response. Figure reproduced from Lanier, 2005.

---

In humans inhibitory receptors belong to either the Immunoglobulin-like superfamily (IgSF) or the C-type lectin-like receptor (CTLR) superfamily. The IgSF inhibitory receptors include the killer immunoglobulin-like receptors (KIR) that are specific for determinants shared by groups of HLA-A, B or C allotypes (Lanier, 1998). KIRs (see section 1.10) like other members of the immunoglobulin (Ig) superfamily have either

2 or 3 extracellular Ig-like domains. The KIR locus encodes several proteins known generically as KIR2DL or KIR3DL, which are inhibitory and have immunoreceptor tyrosine-based inhibitory motifs (ITIM -Ile/Val- Leu/Ser-x-Tyr-x-x-Leu/Val) in the intracellular region that are phosphorylated upon engagement by ligand (Trowsdale, 2001) [considered further below].

By comparison KIR2DS and KIR3DS which have shorter intracellular regions lacking the ITIM domain and that function as activating receptors via charged transmembrane residues. KIR2DL4 is unusual as it consists of a long intracellular region but only one ITIM and a positively charged amino acid in the transmembrane region. Unlike other clonally distributed KIRs, KIR2DL4 is transcribed by all NK cells (Valiante et al., 1997; Cantoni et al., 1998; Rajagopalan et al., 2001) and acts as an activating receptor on recognition of sHLA-G. KIR2DL4 is not normally expressed on the NK cell surface but in endosomes using a novel endosomal signalling pathway that involves the serine/threonine kinases PKCs and Akt and has been implicated in regulating cytokine and chemokine production at the materno-foetal interface to promote foetal health (Rajagopalan and Long, 2012).

KIR expression on NK cells is reported to be random and is regulated by the methylation of KIR gene loci (Chan et al., 2003). The overall KIR repertoire is determined by KIR genotype, however there is evidence of some modulation of KIR expression on human cells by HLA Class I molecules (Yawata et al., 2006). The repertoire of KIR genes expressed on different NK cells within one individual can vary with respect to allelic variants and expression levels whereby each individual has different populations of NK cells expressing a combination of KIRs (Gardiner et al., 2008). The repertoire of KIR genes forms a KIR haplotype, and expression of each KIR gene varies between haplotypes, but three KIR genes are common to all haplotypes (KIR3DL3, KIR2DL4 and KIR3DL2).

Members of the CTLR family in humans include the CD94–NKG2A/C/E heterodimers. The inhibitory, ITIM-containing CD94-NKG2A receptor and activating DAP12-associating CD94–NKG2C receptor both recognise MHC class I-

leader peptides presented by HLA-E (Lee et al., 1998; Carretero et al., 1998; Braud et al 1998), whereas the corresponding mouse heterodimers recognize $Qa1^b$ (Vance et al., 1998).

In mice Ly49 receptors are type II transmembrane receptors and are members of the CTLR superfamily that regulate the balance of NK cell activation and tolerance. Most of the Ly49 receptors are inhibitory and signal through an ITIM, while activating receptors contain a charged residue in their transmembrane domain and signal via DAP12. (Smith et al., 1998). Ly49 receptors mainly bind to MHC class I molecules and related proteins; Ly49A binds $H\text{-}2D^d$, $H\text{-}2D^k$ (Tormo et al., 1999) and Ly49C binds $H\text{-}2K^b$ and $H2D^b$ (Dam et al., 2003). Activating receptors include Ly49P and Ly49W are reported to recognise and interact with $H\text{-}2D^d$ (Silver et al., 2001; Silver et al., 2000) and Ly49D, has been shown to bind $H\text{-}2D^d$ although this remains debatable (Mason et al., 2000; Ortaldo et al., 2001). Ly49 is an unusual receptor as it contains both an ITIM-like motif and a charged transmembrane residue. Recognition of MHC class I molecules by Ly49 receptors require the presence of a peptide bound in the groove of the MHC class I molecule. The specificity of this peptide-binding differs between Ly49 receptors (Orihuela et al., 1996 ; Correa et al., 1995; Hanke et al., 1999; Michaelsson et al., 2000). The Ly49 repertoire on NK cells is found to be highly polymorphic (Mehta et al., 2001) and the level of expression of Ly49 genes on NK cells is influenced by the level of MHC class I expression in the particular mouse (Mehta et al., 2001; Veinotte et al., 2003 ; Raulet et al., 1997).
Another family of receptors in the mouse is the NKRP1 receptor family. NKRP1C is an activating receptor and contains a positively charged amino acid in its transmembrane domain and associates with the Fcγ chain and on cross linking with appropriate mAbs triggers cytokine secretion and cytotoxic activity (Karlhofer et al., 1991; Arase et al., 1997). Similarly, NKRP1A and NKRP1F also contain charged residues in their transmembranes which indicate that these may be activatory receptors. NKRP1D and NKRP1B are ITIM-containing receptors, that lack charged transmembrane residues, and on cross linking with mAbs or ligands associate with SHP-1 and deliver inhibitory signals (Carlyle et al., 1999; Kung et al., 1999; Plougastel et al., 2001; Iizuka et al., 2003). NKRP1B and NKRP1D are reported to recognise mouse C-type lectin related (Clr) protein b (Clr-b) (Plougastel et al., 2001;

Iizuka et al., 2003) and NKRP1F specifically recognises C1r-g (Iizuka et al., 2003) and can recognise CLR-x (Aust et al., 2009).

Signalling by the inhibitory and activating NK cell receptors is mediated by conserved sequences within the cytoplasmic domains of these receptors or their associated adapter proteins (figure 1.6). As stated before, signalling of inhibitory receptors is mediated by ITIM. Upon inhibitory receptor-ligand engagement, ITIM are phosphorylated and associate with Src-homology domain bearing tyrosine phosphatases SHP (SH2-containing protein-tyrosine phosphatase)-1 and SHP-2, or the phospholipid-specific phosphatise SHIP (SH2-containing inositol polyphosphate 5-phosphatase), depending on the particular receptor analysed, which results in the inhibition of the activation signalling cascade (Long et al., 2001) and decreased phosphorylation of several intracellular signalling proteins including FcεRIγ , ZAP70, Syk, PLCγ 1, PLCγ 2, SLP76, and Vav-1. SHIP functions to degrade phosphatidylinositol-3,4,5-trisphosphate to phosphatidylinositol-3, 4-bisphosphate, thus preventing sustained Ca2+-dependent signaling (Valiante et al., 1996; Binstadt et al., 1996; Binstadt et al., 1998; Palmieri et al., 1999; Stebbins et al., 2003).

The activating NK cell receptors transduce signals through association with adapter molecules such as CD3ζ (Anderson et al., 1989) and DAP12 (Lanier et al., 1998) that contain an immunoreceptor tyrosine-based activation motifs (ITAM). The ITAM are defined by the prototype sequence, Asp/Glu-x-x-Tyr-x-x-Leu/Ile x6−8 Tyr xx Leu/Ile, where x denotes any amino acid with 6 to 8 amino acids between the two Tyr xx Leu/Ile elements (Reth, 1989). Upon tyrosine phosphorylation of the ITAM, the tyrosine kinases $p72^{syk}$ and ZAP70 are recruited via their SH2 domains and causing a Ca2+ influx, degranulation, and transcription of cytokine and chemokine genes (Biassoni et al., 2001; Biassoni et al., 2002; Moretta et al., 2000).

Another signalling pathway in NK cells results from stimulation of the 2B4 (CD244) receptor present on all human and mouse NK cells, which binds to CD48, which is expressed on all hematopoietic cells (Brown et al., 1998; Latchman et l., 1998; Garni-Wagner et al., 1993; Valiante et al., 1993). There are conflicting reports

regarding the outcome of stimulation through this receptor in both humans and mice. Activation or inhibition results from the signaling induced by the recruited adapter proteins (Lee et al., 2004; McNerney et al., 2005; Garni-Wagner et al., 1993). Human 2B4 is expressed as one of two isoforms, of which only one has been shown to activate NK cell cytotoxicity (Mathew et al., 2009). The cytoplasmic tail of the 2B4 receptor contains an immunoreceptor tyrosine-based switch motif, which recruit Src homology 2 domain containing adapter proteins; SLAM associated proteins (SAP) which results in activation of NK cell function, or ERT which results in inhibition of NK cell function (Veillette 2006).

An additional set of receptors on NK cells is made up of the natural cytotoxicity receptors (NCRs). These receptors belong to the Ig-superfamily (McQueen et al., 2002) and include NKp46 (Sivori et al., 1997; Pessino et al., 1998), NKp44 (Vitale et al., 1998; Cantoni et al., 1999) and NKp30 (Pende et al., 1999). NCR expression is largely restricted to NK cells. All NK cells express NKp46 and NKp30 whereas only activated NK cells express NKp44. These receptors may recognise pathogen-specific moieties: thus, NKp44 and NKp46 have been reported to recognise virus-specific haemagglutinins and mediate NK cell lysis of virally infected cells (Mandelboim et al., 2001; Arnon et al., 2001). NKp46 and NKp30 have also been shown to bind heparin sulfate proteoglycans and NKp80 binds activation-induced C-type lectin (Bloushtain et al., 2004; Welte et al., 2006). More recently, NKp30 has also been shown to bind B7-H6, a tumour cell ligand and triggers antitumor NK cell cytotoxicity and cytokine secretion (Brandt et al., 2009). In a multiple myeloma model, the NKp30 receptor reportedly recognises and binds to the nuclear factor HLA-B associated transcript 3 (BAT3), which can be released from tumour cells and trigger NKp30-mediated cytotoxicity which was necessary for tumour rejection (Pogge von Strandmann etal., 2007). NKp30 and NKp46 utilise $\zeta\gamma$ chains as signalling polypeptides, while NKp44 utilises DAP12.

Impairment in the engagement of KIRDL receptors by self-MHC would be predicted to provoke an inappropriately activated state of NK cells, whereas impairment in engaging KIRDS receptors might limit NK cell activation. Indeed, certain combinations of KIR and HLA molecules can affect the outcome of different diseases.

Thus, KIR3DS1 (activating) and HLA-Bw4 co-expression is linked to delayed progression to fully developed AIDS in HIV positive individuals. In the absence of KIR3DS1, HLA-Bw4 has no effect; in the absence of Bw4, KIR3DS1 still is protective (Martin et al., 2002). The ligand for KIR3DS1 is not known but presumed to be Bw4. (Alter et al., 2007) Similarly, patients homozygous for KIR2DL3 are more likely to clear hepatitis C virus if they are also homozygous for HLA-C isoforms that recognise KIR2DL3 (Khakoo et al., 2004). Likewise resistance to papilloma virus and to developing neoplasia was associated with specific inhibitory KIR and HLA genotypes (Arnheim et al., 2005). Such data emphasise the point that disease-associations of polymorphisms in MHC Class I may not simply reflect the impact upon the αβ TCR repertoire. To overcome constitutive suppression, NK cells require [1] "missing self" (Karre, 2008), as would occur for example, when CMV promotes self-MHC downregulation on infected cells so as to limit their targeting by $CD8^+$ T cells and/or [2] upregulation of activating "stress ligands" such as MICA. Failure of NK cells to respond to a target can be due to strong inhibitory signals mediated by the inhibitory receptor-ligand interaction or by the lack of activation signals (Figure 1.7).

NK cells are not the only cell type to be regulated in this fashion, most γδ T cells and a subset of antigen-experienced $CD8^+$ T cells express NKG2D and KIRs (Vilches et al., 2002; Ugolini et al., 2001; Hayday, 2009), particularly γδ cells that may also express NCRs (Correia et al., 2011).

Effector $CD8^+$ cytotoxic T lymphocytes (CTL) in tissues do not express CD28, and NKG2D can serve as a potent co-stimulatory molecule (Rajasekaran et al., 2010; Groh et al., 2001; Jamison et al., 2002). Whereas NKG2D is constitutively expressed by NK cells, its expression by T cells is selectively upregulated by IL-15, released by epithelial cells from inflamed or otherwise stressed epithelium (Sutherland et al., 2006). This might promote CTL responses in the context of low concentrations of antigen (Roberts et al., 2001). NKG2D is also upregulated, albeit to lesser degrees, by IL-10, IL-12 and IFN-α (Sutherland et al., 2002).

Human γδ T cells can also be co-stimulated by NKG2D engagement coincident with TCR engagement (Nedellec et al., 2010). However, as was stated above, acute

upregulation of Rae-1 on keratinocytes *in vivo* was sufficient to activate intraepidermal γδ T cells (Strid et al., 2008; 2011). Whether NKG2D activation is likewise sufficient to activate other T cells *in vivo* is unresolved, although studies of human peripheral blood γδ T cells *in vitro* have indicated that this may occur (Das et al., 2001). We shall now consider two receptor-ligand sets in more detail: KIRs and MHC Class I, and NKG2D and its ligands.

## 1.10 Genetic basis of KIR polymorphism

KIRs are encoded by 15 genes with two additional pseudogenes (KIR2DP1 and KIR3DP1) on chromosome 19q13.4. Two groups of haplotypes have been defined (Uhrberg et al., 1997): Group A haplotypes comprise seven genes which are mostly inhibitory and two pseudogenes, whereas group B haplotypes include many activating KIR genes. Overall, the KIR locus is characterised by extensive genetic polymorphism (Uhrberg et al., 1997), in which respect non-allelic homologous recombination within the locus may be facilitated by the very high sequence homology that the different KIR genes exhibit (Carrington et al., 2004).

KIR proteins with 2 extracellular Ig-like domains are designated KIR2D, and those with 3 extracellular Ig-like domains are designated KIR3D (Figure 1.8). While KIRDL are inhibitory, and KIRDS activating (see above), KIR2DL4 encodes a protein that seemingly shares structural features with both the activating and inhibitory KIRs (Rajagopalan et al., 2001).

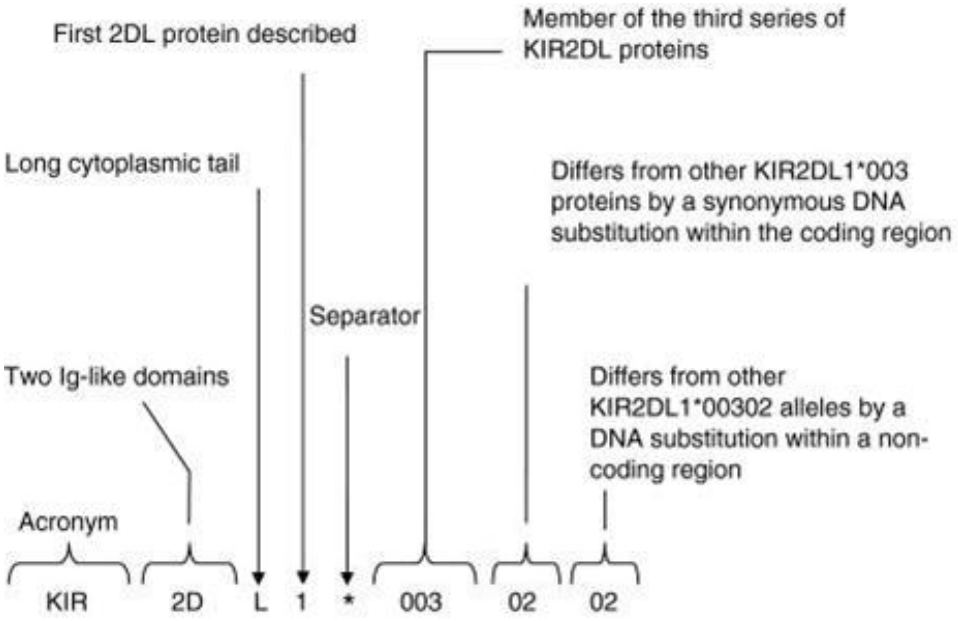


**Figure 1.8**: Diagrammatic description of the nomenclature of KIRs. The KIRs are separated into 2 groups according to whether the proteins have either 2 or 3 extracellular domains (2D or 3D). They either have a long or short (L or S) cytoplasmic tail which corresponds to the inhibitory or activating (respectively) potential of the KIRs. The first 3 digits of the KIR nomenclature refers to the alleles that differ in the exon sequence that lead to the non-synonymous changes whereas the next 2 digits refer to alleles that differ in exon sequence but leads to synonymous changes. The last 2 digits indicate alleles that differ in either an intron, promoter or another non-coding region. The last digit of the KIR nomenclature refers to the difference between 2 or more genes that are very similar in structure and sequence, example KIR2DL5A and KIR2DL5B. Figure reproduced from Middleton et al., 2010.

---

Activating KIR proteins bind HLA class I molecules with a reduced affinity relative to the paired inhibitory KIR (Trowsdale et al., 2001), fuelling the view that inhibition is dominant. The ligands for KIR3DL1 are HLA-B51 and B52, which are recognised *via* the so-called Bw4 eptiope (residues 77-83 in the α1 domain; see above) that is common to both isoforms and to some other HLA-A isoforms whose gene products are also recognised by KIRs (Cella et al., 1994; Thananchai et al., 2007). KIR3DL1 can be grouped in both A and B haplotypes, while the activating gene, KIR3DS1, is found

only in haplotype B. As judged by population and disease association studies, KIR3DS1 may bind HLA-Bw4 molecules with isoleucine at position 80 (Bw4-80I) (Martin et al., 2002; Single et al., 2007). KIR3D proteins do not recognise other HLA molecules, with, for example, Bw6 motifs in place of Bw4. Thus, KIR3DL1$^{+}$ cells could only be inhibited by cells expressing HLA-Bw4$^{+}$ molecules (see also below).

Antibody blocking studies (using anti-KIR3DL1 specific monoclonal antibody, DX9) have shown that the quantity of KIR3DL1 on the surface of NK cells can influence the inhibition of cells (Carr et al., 2005; Yawata et al., 2006). Moreover, KIR polymorphism directly affects the recognition and binding of Bw4 molecules with specific peptides sitting in their binding groove (Thananchai et al., 2007). Thus, the regulation of KIR3DL1-expressing (NK and T cells) can be substantively affected by polymorphisms in KIR3DL1, in KIR3DS1, and in HLA-B*51/52.

KIR3DL1 is highly polymorphic (Gardiner et al 2001). KIR3DL1 isoforms have been divided into three groups according to cell surface expression: high expressers (*001, *002, *008,*015 and *020), low expressers (*005, *006 and *007) or null expression (*004) which could potentially be due to polymorphisms in promoter regions (Pando et al., 2003; Gardiner et al., 2001; Yawata et al., 2006; Li H et al., 2008). The proximal promoter of the KIR genes has bi-directional transcriptional activity (Stewart et al., 2003; Davies et al., 2007) thus implying that the strength of the competing promoters may affect the number of NK cells expressing a given KIR within a given individual. Indeed, the KIR3DL1 proximal promoter is polymorphic at the transcription factor binding sites which are known to affect promoter activity (Davies et al., 2007).

## 1.11 KIRs and Licensing

The combined impact on NK cell biology of polymorphism and variable expression of isoforms in both the KIR and HLA Class I loci has been articulated in a concept termed “licensing”. More specifically, this concept takes into account the following points: first, KIRs are not uniformly expressed on NK cells, either qualitatively or quantitatively; second, the KIR locus segregates independently of the MHC locus. Thus, in any one individual, some NK cells would not have a corresponding inhibitory

HLA ligand present in a given individual, for example, KIR3DL1$^+$ cells in a Bw6 homozygote. As such it was unclear how these cells would be prevented from killing self cells. Yokoyama and colleagues proposed that KIR on NK cells must recognise their cognate HLA molecule in order to acquire functional competence through "licensing" (Kim et al., 2005). Hence, paradoxically, an inhibitory receptor interaction appears to be required in an active way for an NK cell to acquire function, before that cell is then inhibited by interaction with the same self-MHC. Unlicensed cells that do not engage self MHC do not acquire functional competence, but might become active in response to cytokines and other activating molecules during infections. This might permit a broader repertoire of NK cells to contribute to the response to pathogens without the risk of autoimmunity (Kim et al., 2005; Kim et al., 2008). This concept has been supported by studies showing that NK cells from MHC class I deficient mice are defective in target cell killing. Moreover, the licensing concept embraces gene dosage, consistent with which KIR3DL1$^+$ cells in donors with two Bw4 genes displayed increased responsiveness to tumour stimulation compared with KIR3DL1$^+$ cells from individuals with either one or no Bw4 genes. By contrast NK cells lacking KIR3DL1 showed no difference in activity (Kim S et al., 2008). It should be noted that no clear molecular mechanism for licensing has been defined, and that there has been considerable disagreement over how MHC Class I might determine the functional activity of NK cells (Raulet and Vance, 2006). In this regard, the "Rheostat model" of Hoglund and colleagues argues that peripheral NK cells exist with a continuum of functional potentials that reflect their quantitative exposure to self MHC Class I during development (Brodin et al., 2009). Thus, each individual would harbour cells with different potentials to respond to specific targets as a result of "developmental tuning". As already stressed, above, the cells' responses will also be dictated by the status of their activating receptors.

## 1.12 NKG2D

The receptor for MICA, NKG2D, is a type II transmembrane C-type lectin that assembles as a homodimer and that is encoded by the killer cell lectin-like receptor subfamily member-1 (KLRK1) gene on human chromosome 12. NKG2D has low homology (only 21% amino acid sequence identity) to other members of the NKG2 family, and thus is regarded as an atypical member of that family. NKG2D has no signalling motif itself, but upon binding to target cells expressing its ligands, it initiates intracellular signalling through phosphatidylinositol 3-kinase (PI-3K) and Grb2 *via* its association with the adaptor protein, DAP10 (Bauer et al., 1999; Wu et al 1999). DAP10 has a cytoplasmic domain with an YXXM motif, which binds to the p85 subunit of PI3K (Vivier et al., 2004). An NKG2D homodimer can bind 4 DAP10 chains *via* transmembrane arginine residues. Binding a single ligand can thus result in phosphorylation of 4 DAP10 molecules, suggesting a high sensitivity of NKG2D receptor signalling (Garrity D et al., 2005). In some cells in the mouse, NKG2D can also associate with the activating adaptor, DAP12 (Gilfillan et al., 2002).

Although NKG2D is an activating receptor in its response to acutely upregulated ligands, its engagement of ligands results in its surface modulation and reduced function upon subsequent ligand encounter (see above). Persistent encounter with tumour cell-bound ligand could completely uncouple the NKG2D receptor from intracellular mobilization of calcium and cytotoxic activity due to reduced expression of DAP-10 and DAP12, but was reversible when the NK cells were removed from the inhibiting environment (Coudert et al., 2005). Curiously, IFN-γ production was sustained under these circumstances. As introduced above, in transgenic animals constitutively and ubiquitously expressing MICA under the control of the H-2K$^{b}$ promoter, NKG2D-mediated cytotoxicity was severely impaired–reflecting significant downregulation of surface expression of NKG2D. Associated with this, these mice failed to reject MICA-expressing tumours and to mount a normal response upon *Listeria* infection (Wiemann et al., 2005). Interestingly, sustained NKG2D engagement had collateral yet non-reciprocal effects on other receptors not utilizing DAP10 and DAP12, including the IL-2/IL-15 pathway. Thus, sustained NKG2D stimulation was associated with reduced cellular size and expansion of NK cells (Coudert et al., 2008). Oppenheim and colleagues likewise reported that murine NK

cells chronically exposed *in vivo* to transgenic Rae-1 showed reduced responses both to NKG2D-ligand-expressing target cells, and to cells from β2-microglobulin-deficient mice that expressed reduced levels of MHC Class I (Oppenheim et al., 2005).

The contributions of NKG2D to pathophysiology have been clarified to some extent by the development and investigation of NKG2D-deficient mice (Guerra, 2008; Zafirova, 2009). Predictably, there was reduced targeting of NKG2D-ligand-expressing tumour cells, but unexpectedly the mice were more resistant to CMV-infection, seemingly reflecting an hitherto unappreciated role of NKG2D in regulating NK cell subset development and status (Zafirova, 2009). Thus genetic polymorphisms that influence NKG2D engagement of its ligands might dysregulate cellular immune responses through developmental effects as well as their direct impact on effector-target cell interactions.

NKG2D also has a role in regulating the adaptive immune response, in that NK cells can kill recently activated $CD8^+$ cells in an NKG2D- and perforin-dependent fashion, thereby biasing the differentiation of $CD8^+$ cells away from a central memory phenotype and toward an effector memory (Tem) phenotype. Hence, under conditions where NKG2D interactions are impaired, tumour control may ironically be enhanced *via* increased $CD8^+$ T cell activity (Soderquest et al., 2011).

Likewise, whereas NK cells have negligible direct effects on cells infected with lymphocytic choriomeningitis virus (LCMV), they can have a major indirect impact on infection *via* their NKG2D-mediated targeting of activated $CD4^+$ T cells that provide help to anti-viral $CD8^+$ T cells (Waggoner et al., 2011). Because CD8 T cells mediate both virus clearance and immunopathology, the impact of NKG2D-mediated interactions on helper-$CD4^+$ T cells had very distinct effects at different doses of virus infection. At high doses, NK cell-mediated limitation of T cell numbers prevented virus clearance, but also prevented death due to pathology, whereas at moderate doses of virus, NK cell regulation of the T cell response was incomplete and there was increased mortality due to immunopathology. These data emphasise the complexity of phenotype that can result from altered NKG2D-mediated responses in different contexts, and points to the potentially complex impact of polymorphisms in MICA set against different genetic backdrops.

In pregnancy, tolerance has been attributed to down-regulation of NKG2D on PBMC by soluble MICA (sMICA) [see above]. MICA expression in the placenta was restricted to the syncytiotrophoblast, but sMICA was elevated in maternal blood throughout pregnancy, and was released by placental explants *in vitro*. Cell surface NKG2D expression on maternal PBMC was down-regulated compared to non-pregnant controls. Moreover, sMICA in the sera of pregnant women could downregulate NKG2D on PBMC from healthy donors with consequent inhibition of NKG2D-dependent cytotoxic responsiveness (Mincheva-Nilsson et al., 2006). Although NKG2D$^{-/-}$ mice were outwardly healthy with no obvious breeding problems (Guerra, 2008; Zafirova, 2009), it should be noted that there are differences between mice and humans in the immunological regulation of pregnancy: thus, adaptive T cell responses seem more important in mice (Munn et al., 1998), while NK responses are possibly more important in humans (Trowsdale and Moffett, 2008).

## 1.13 NKG2D ligands

In mice and in humans, there are several, diverse NKG2D ligands (NKG2DL) inevitably provoking the question of whether there are distinct features and/or distinct outcomes of NKG2D engagement of different ligands. Crystallographic studies have revealed a unique induced-fit mode of recognition which allows NKG2D a high degree of variability in its ligands (Radaev et al., 2001; and see above).

The human NKG2D ligands and can be subdivided into two families: the MHC class I related chain (MIC) proteins and the ULBP molecules (Table 1.2). The MICA family consists of seven genes, MICA, B, C, D, E, F and G, but only MICA and MICB appear to encode functional transcripts (Shiina et al., 1999).

| NKG2D ligands | Chromosomal location | Structures |
|---|---|---|
| MICA | Encoded within MHC locus on chromosome 6, 6p21.3 | α 1, α2 and α3 extracellular domains, transmembrane region and a cytoplasmic tail |
| MICB | | |
| ULBP1 | Encoded within the long arm of chromosome 6, 6q24.2 | α 1 and α2 extracellular domains are GPI linked to membrane |
| ULBP2 | | |
| ULBP3 | | |
| ULBP4 | | α 1 and α2 extracellular domains, a transmembrane region and a cytoplasmic tail |
| RAETIG | | |

**Table 1.2**: The human NKG2D ligands: The human ligands can be subdivided into two families, the MHC class I related chain (MIC) proteins and ULBP molecules.

---

The ULBPs were identified as cellular targets of the human cytomegalovirus (HCMV) glycoprotein, UL16 (Cosman et al., 2001), that the virus uses as a method of immune-evasion. The ULBP molecules: ULBP1-3, ULBP4/RAET1E and RAET1G are encoded on the long arm of chromosome 6, position 6q24.2. All NKG2DL have MHC class I like α1 and α2 domains, which mediate binding to NKG2D, but only MICA and MICB have the additional α3 domain. ULBP1-3 are associated with the cell membrane as glycosylphosphatidylinositol (GPI)-linked proteins, as are murine Rae-1 proteins, whereas MICA, MICB, ULBP4/RAET1E and RAET1G have transmembrane and cytoplasmic tail sequences (Eagle et al., 2006). Despite their overall similarity to MHC Class I, none of the NKG2D-ligands presents peptides to T cells. ULBPS are 55-60% identical in amino acid sequences and are distantly related to the MICs (23-26% homology) and to other MHC class I family members. ULBP1, ULBP2 and MICB bind to UL16 whereas ULBP3 and MICA do not bind to UL16 (Cosman et al., 2001). Thus, perhaps the repertoire of NKG2D ligands offers the host the means to

circumvent immune-evasion (Eagle et al., 2006), in which regard, polymorphism in the ULBP genes and in UL16 genes from diverse viral strains is still being studied. HCMV immunoevasion is also contributed to by virus-encoded micro-RNA, hcmv-miR-UL112, that specifically targets and downregulates MICB expression during infection (Ambros, 2004). Hence, differences in ligand RNA sequences may likewise confer host benefit.

ULBP transcripts are expressed in a wide range of tissues, including heart, testis, bone marrow, thymus and lung, and in several cell lines (Cosman et al., 2001), although ULBP protein expression has remained undetected on normal peripheral blood mononuclear cells (Sutherland et al., 2001). Nonetheless, different expression profiles of different ULBPs may underpin different biologies. At the same time, different ULBPs have different functions even when expressed from the same cells: thus, ULBP1, but not other ULBP molecules, conferred on lymphomas the capacity to be killed in an NKG2D-dependent fashion by human γδ T cells (Lanca et al., 2010). Interestingly in this regard, ULBP1 has an intermediate affinity for NKG2D between ULBP2 (highest) and ULBP3 (lowest) (Kubin et al., 2001). Thus, the biological effects of NKG2D ligands do not simply reflect a hierarchy of NKG2D binding affinity, which is a key point returned to in this thesis. MICA binds to NKG2D with an affinity of 1μM (Li et al., 2001). The realisation that all NKG2D ligands are not equivalent in their effects on NKG2D attaches potentially considerable importance to polymorphism among NKG2D ligands, as is the case for MICA and MICB.

## 1.14 Summary

BD is a serious unmet clinical need with no cure. In pursuing its pathogenesis, investigations of BD genetics and pathology have focussed attention on a limited set of cells and the genes that regulate them. Among these, the regulation of NK cells and T cells by the NKG2D receptor and its ligand MICA, and by the KIR3DL1 receptor and its ligands, HLA-B*51 and HLA-B*52 is conspicuous. Genetic associations of BD with HLA-B and with MICA could conceivably reflect NK and/or T cell dysregulation caused by a coincident combination of inappropriate cell activation (MICA-NKG2D) and inhibition (KIR-HLA-B). However, there has to date been little elucidation of how human NK and T cell responses are affected by polymorphisms in MICA and how

those responses are in turn affected by polymorphisms in HLA-B. This thesis investigates these issues. While such interactions alone will not elucidate the pathogenesis of BD, it is hoped that they will clarify key aspects of human NK and T cell regulation that will be of benefit to understanding many aspects of human cell-mediated immune responses in health as well as in disease. Indeed, the results identify an unanticipated level of inter-individual variation in NK cell and γδ T cell responsiveness that may reflect a form of tuning reminiscent of the rheostat model (above).

## 1.15 Hypothesis

I hypothesise that different MICA isoforms, including MICA*009, expressed under equivalent conditions, will show differential capacity to provoke human T cell and NK cell activation. I further hypothesise that the MICA-dependent killing responses by lymphocytes of Behcet's disease (BD) patients may be differentially regulated by HLA-B*051 *versus* HLA-B*052. Experimental support for this hypothesis would add weight to the prospect that disease-associated isoforms of MICA and HLA-B may contribute to lymphocyte dysregulation in BD. Conversely, refuting the hypothesis might reduce support for this perspective.

## 1.16 Aims of the thesis

(a) To generate isogenic cell lines expressing different isoforms of MICA, and to compare the expression levels of the gene products encoded by those different MICA isoforms.

(b) To use the isogenic cell lines to determine whether MICA*009 differs from other isoforms in its capacity to provoke killing by NKG2D-expressing lymphocytes from healthy individuals and from Behcet's Disease patients.

(c) To determine whether HLA-B*51 and HLA-B*52 differentially affect the cytolytic response to MICA*009-positive cells.

(d) To determine whether specific populations of cytolytic leukocytes differ in patients with BD and healthy controls and how this might relate to the results of Aims (b) and (c)

# CHAPTER TWO– DEVELOPMENT OF A FUNCTIONAL ASSAY FOR MICA POLYMORHISM

The functional analysis of MICA polymorphism is not clearly understood and no direct assessment of the impact of this on lymphoid stress-surveillance has been studied. Consequently, the functional role for the different isoforms in terms of evoking the responses of $NKG2D^+$ lymphocytes from healthy donors and patients with BD has not been studied. The following study aims to advance the current understanding of these issues.

In order to better understand the role of MICA*009 in Behcet's disease, I embarked on a series of investigations to compare the various properties of the MICA*009 protein to other MICA isoforms, such as surface protein expression, intracellular expression, DNA and RNA expression and the capacity of MICA to regulate the responses of $NKG2D^+$ lymphocytes by healthy donors. Studies of this nature have not been tackled before and thus to study these properties of the highly polymorphic MICA, a functional genomics model was designed whereby different MICA isoforms and ULBP2 (non-polymorphic NKG2D ligand) were transfected into a system (Flp-In system) to generate isogenic cell lines with single copies into the same genomic site of Chinese Hamster Ovary (CHO) epithelial cells via an FRT recombinase. The CHO cells were ideal for the model designed to study the functional effects of MICA polymorphism, as they do not express any endogenous MICA or HLA-ligands for the killer inhibitory receptors and thus the biology of the different MICA isoforms could be compared.

These transfectants would then be used to study the differences, if any, between different MICA isoforms. Several questions arise which require investigation. Some studies report that MICA*008 is the most abundant MICA gene in Caucasians and is non-functional due to a premature termination in the transmembrane domain (Suemizu et al., 2002; Eleme et al., 2004), therefore does this imply that MICA*008 is invisible to lymphoid surveillance? Are all individual responses to the non-polymorphic NKG2D ligand, ULBP2 similar, while being more or less responsive to their own versus allotypic MICA isoforms?

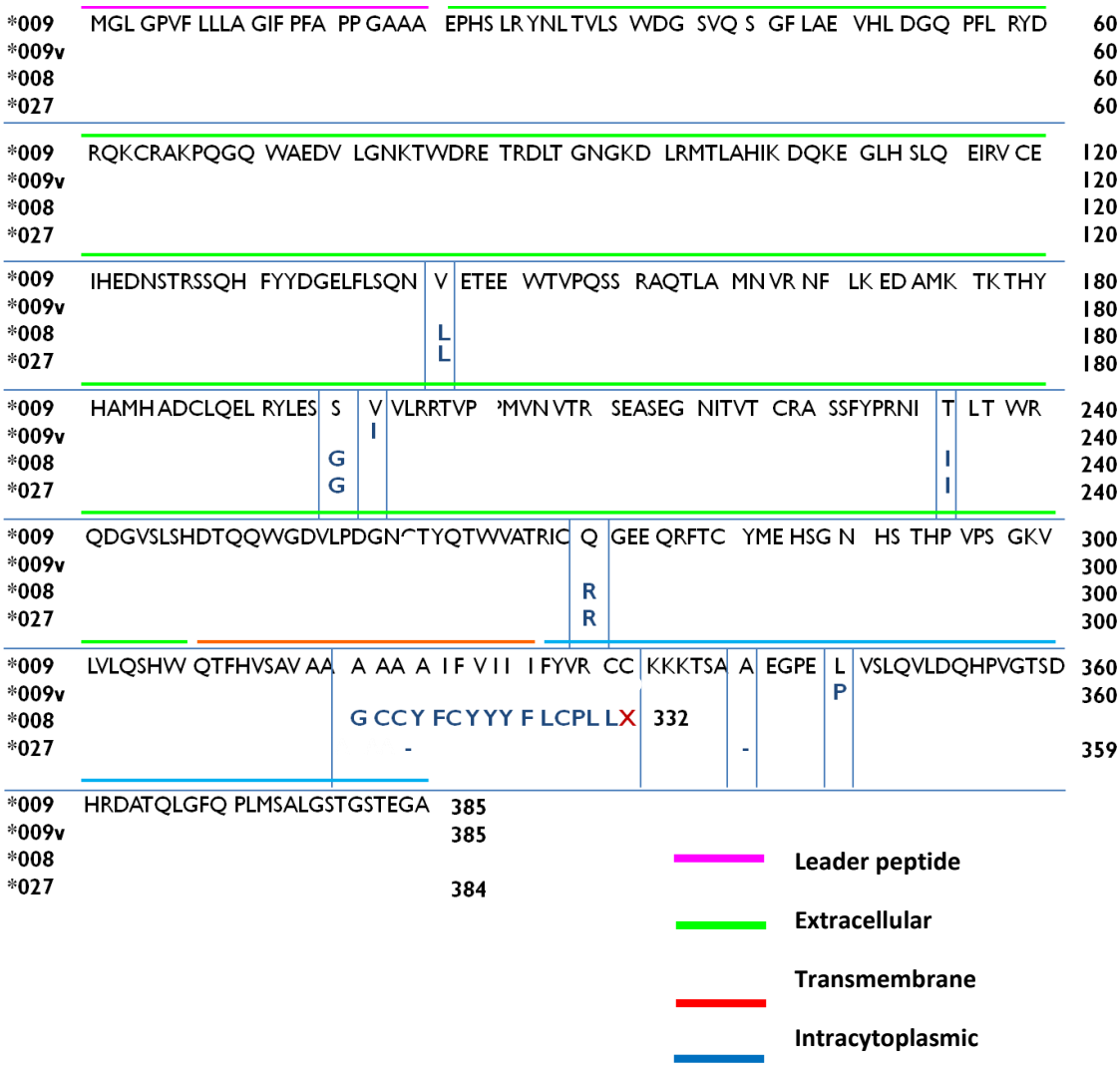


**Figure 2.1**: Illustration of the protein sequence of the different MICA isoforms used in this study. Sequences were obtained using the online translation tool from expasy.org and aligned with Clustal series of programs (Chenna et al., 2003). The amino acids highlighted in blue represent the differences in sequence. The red X in the MICA*008 sequence indicates the position of the premature stop codon.

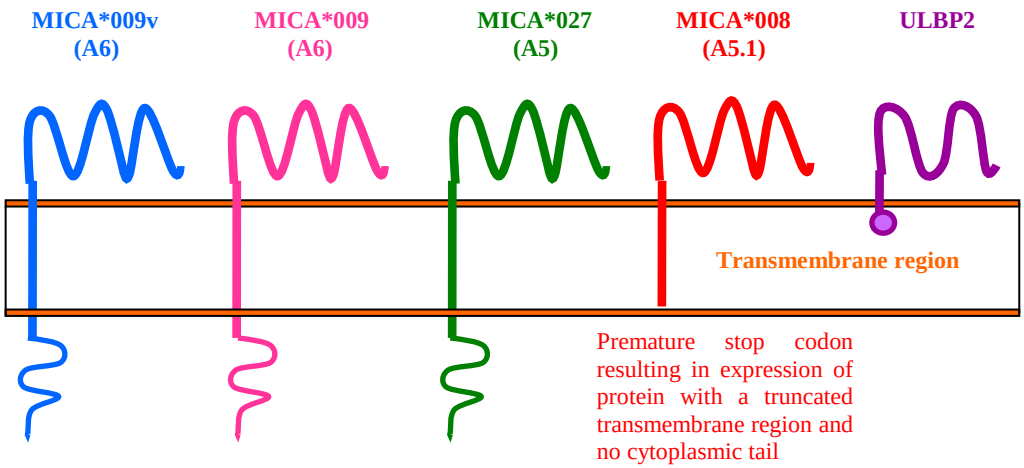


**Figure 2.2**: Diagrammatic illustration of the different MICA isoforms and ULBP2 protein structures based on the sequence data. The MICA protein has 3 extracellular domains (α1, α2 and α3), one transmembrane region and a cytoplasmic domain. Within the transmembrane region consists a series of alanine (GCT) repeats (the number of repeats depends on the MICA isoform) denoted as (A*). MICA*009v and *009 are structural similar. The extracellular domain of MICA*008 is structurally identical to MICA*027, however MICA*027 retains the transmembrane region and the cytoplasmic domain. The ULBP2 protein structurally has 2 extracellular domains (α1 and α2) is anchored in the transmembrane region with the help of a GPI-linker.

---

## 2.1 Comparative analysis of MICA allele sequence and structure

In order to analyse the biological impact of MICA polymorphism on the recognition by NKG2D$^{+}$ cells, a functional genomics system was developed and used (FRT system, Figure 2.9). The isoforms chosen for comparative analysis were the following: MICA*009v, MICA*009, MICA*027 and MICA*008. Another NKG2D ligand, ULBP2, was also chosen as a control for the MICA isoforms, to determine differences, if any, were exclusive to the polymorphisms in MICA and not extended to other NKG2D ligands.

The MICA protein consists of 3 extracellular domains referred to as α1 (encoded by exon 2), α2 (encoded by exon 3) and α3 (encoded by exon 4), a transmembrane region (encoded by exon 5) and a carboxy-terminal cytoplasmic tail (encoded by

exon 6) (Bahram 2000). The polymorphisms exist in the extracellular and transmembrane domains (exons 2-4). A variable number of GCT repeats in exon 5 have been identified which encode four, five, six, nine or 10 alanine (A) residues called A4, A5, A6, A9 and A10, respectively. MICA*009. MICA*027 (A5) has an identical ectodomain to MICA*008 but carries a full transmembrane domain with a cytoplasmic tail. MICA*009, the allele genetically associated with Behcet's disease, encodes a protein with a full length transmembrane domain and cytoplasmic tail with an ectodomain that differs from MICA*027 by 4 residues. MICA*009v (A6) is our term for an unreported isoform which was derived from a B lymphoblastoid tumour cell line, MOU, and it differs from MICA*009 by 2 amino acids and MICA*006 by 1 amino acid in the ectodomain.

MICA*008 (A5.1), the most common isoform in Caucasian populations and has a distinct structure: there is an insertion of a guanine (Mizuki et al., 1997) after the second GCT (alanine) repeat which leads to a frameshift mutation, resulting in a premature stop codon (Fodil et al., 1996) which chops off the 42 amino acid cytoplasmic tail. Due to this, MICA*008 is expressed as a truncated protein. The ULBP2 protein is structurally similar to MICA; however it consists of only 2 extracellular domains (α1 and α2) and is anchored in the transmembrane region with the help of a GPI-linker, thus lacking a transmembrane region and cytoplasmic domain.

The alleles are strikingly similar and thus it is intriguing to comparatively analyse if the coding sequence polymorphisms substantially affect MICA RNA, protein and cell surface expression of these molecules.

## 2.2 Cloning and transfection of MICA and ULBP2 genes

MICA*009v, MICA*008, MICA*009, MICA*027 and ULBP2 were PCR amplified from the cell lines: MOU, Int407, C1R, SWEIG007 and Hacat cell lines respectively, using MICA and ULBP2 specific primers and using a proof reading DNA polymerase enzyme. The PCR products were run on a 1% agarose gel. The bands corresponding to MICA (1158bp) and ULBP2 (740bp) were cut out of the gel and purified, then cloned into a TOPO cloning vector (Figure 2.3 and 2.6). The chemically competent *Escherichia coli* (E.coli) bacteria ((TOP10 bacteria) were transformed with the recombinant plasmids plated onto ampicillin for 24 hours growth. Positive colonies were screened for the correct integration of the cDNA using restriction enzyme digestion and subsequently sequenced to confirm the successful inheritance of the correct ORF (Figure 2.5, 2.6 and 2.8). The genes were then sub-cloned in to a pcDNA5-FRT vector that contains a hygromycin resistance gene which lacks a start codon, immediately downstream of a homologous FRT site and upstream of the multiple cloning site (MCS), in to which the gene of interest (GOI) is inserted. The pcDNA5-FRT vector containing the GOI's were transfected into CHO-FRT cells which results in a homologous recombination event between the FRT sites. This results in GOI integration into the CHO cell genome downstream of the CMV promoter, disruption of the Zeocin resistance gene and gain of a start codon for the hygromycin resistance. Positive cells expressing the GOI are then selected for hygromycin resistance (Figure 2.4 and 2.7).

The chemically competent *E. coli* bacteria (TOP10) were transformed with the pcDNA5-FRT-GOI vectors onto ampicillin for 24 hours. The positive colonies were analysed for orientation of the GOI by restriction enzyme digestion. The vectors were then transfected into the CHO-FRT cells by electroporation. The transfected cells were then grown in hygromycin selective medium. A small aliquot of positive cells were then tested for zeocin sensitivity. To ensure that the GOI had been integrated at only the FRT site and no other sites in the CHO genome, a control transfection was carried out whereby the pcDNA5-FRT-GOI was transfected without the pOG44 vector (vector carrying the Flp recombinase enzyme) and this did not produce any hygromycin resistant cells with the GOI integrated at random

integration sites. As a negative control, CHO-FRT cells were transfected with the parental pcDNA5-FRT vector with the pOG44 vector for the generation of CHO-FRT hygromycin resistant cells. After growth of the positive cells in hygromycin resistant medium, the cells were then stained with anti-MICA and anti-ULBP2 antibodies and analysed for surface expression of the appropriate genes.

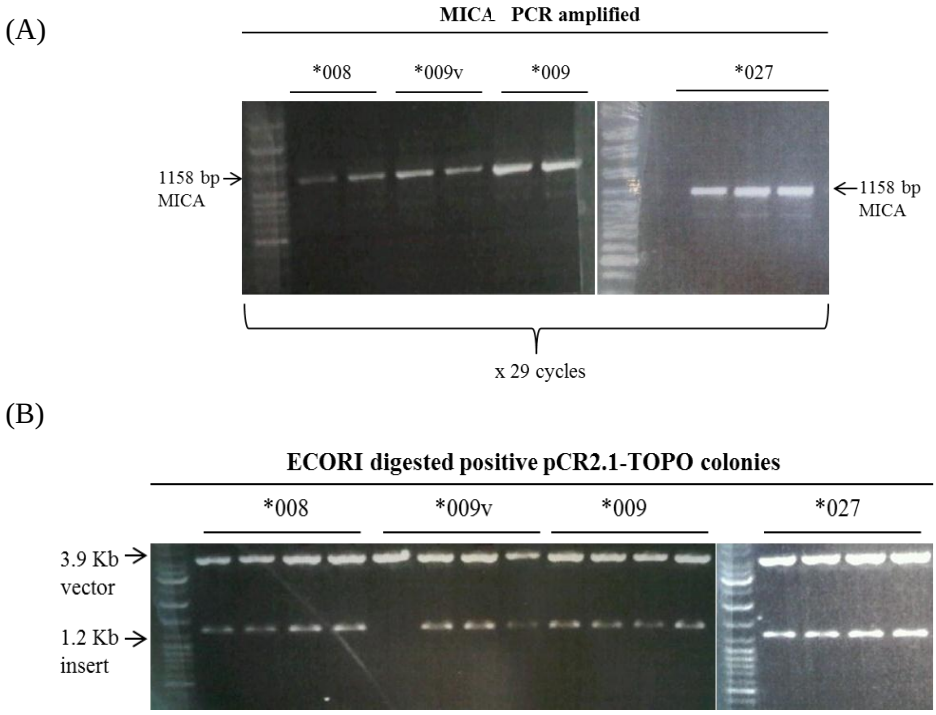


**Figure 2.3**: PCR amplification and cloning of MICA alleles (A) PCR amplification of MICA alleles from the various cell lines: Int407 (MICA*008), MOU (MICA*009v), C1R (MICA*009) and MICA*07 (SWEIG007). The PCR products were cloned into the pcr2.1 TOPO vector and (B) the positive colonies were digested with the ECORI restriction enzyme to determine which colonies incorporated the inserts (MICA*009,*008,*009v and *027).The positive colonies were then sequenced to obtain the colonies with sequence in agreement with that in the data base (http://www.ebi.ac.uk/imgt/hla/).

(A)

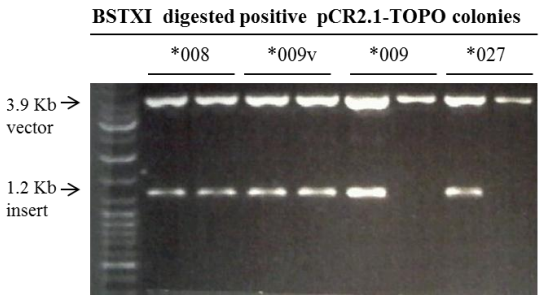


(B)

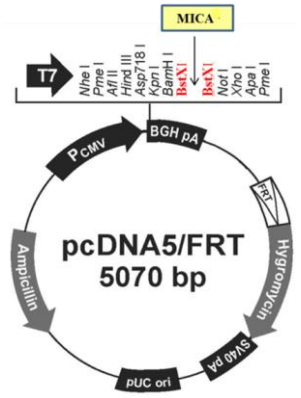


(C)

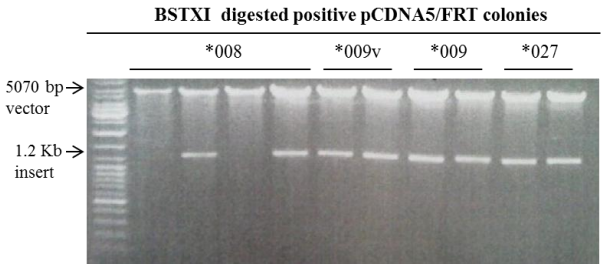


**Figure 2.4**: Subcloning of the MICA alleles into the pcdna5/FRT vector. MICA*009v,*008,*009 and *027 were subcloned into the pcdna5/FRT vector (expression vector) in the multiple cloning site (MCS), between the 2 BSTXI sites: (A) the MICA allelic products were cut out of the pcr2.1 TOPO vector, run on an agarose gel, gel purified and subcloned into the pcdna5/FRT vector. (B) Map of the pCDNA5/FRT- MICA vector with the multiple cloning site, showing where MICA was inserted during cloning. (C)The positive colonies were digested with the BSTXI restriction enzyme to determine if any of the inserts had incorporated into the vector.

(A)

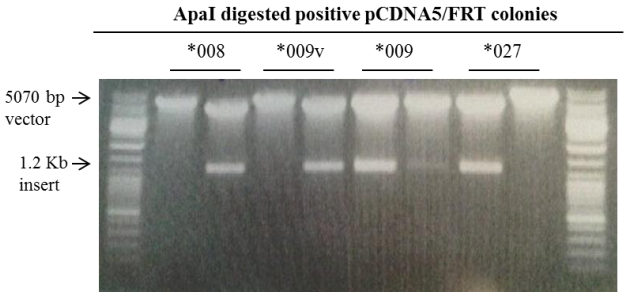


(B)

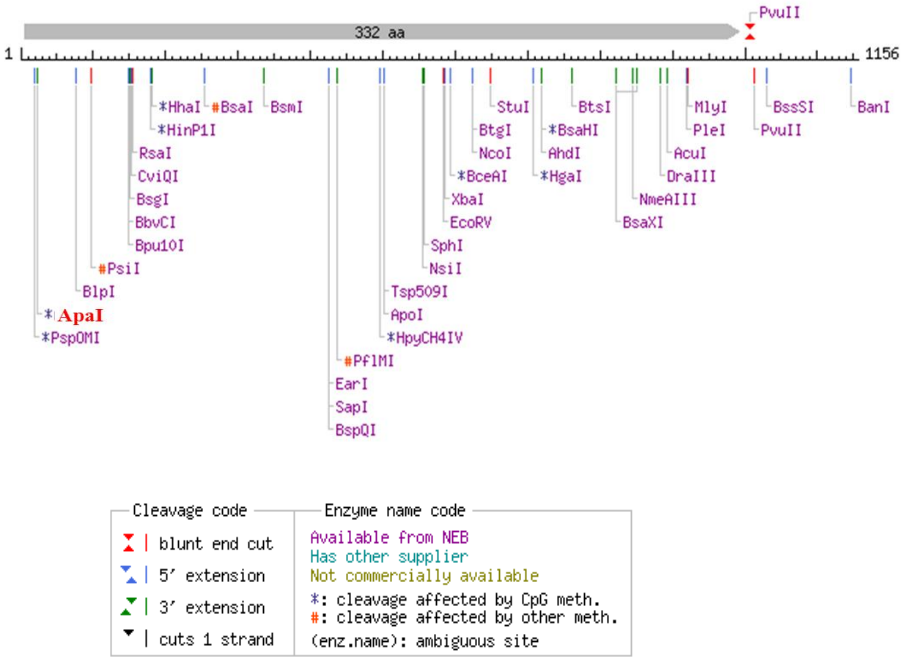


**Figure 2.5**. Determining positive vectors for correct orientation of the MICA alleles in the expression vector, pcdna5/FRT. (A) to investigate which positive vectors (with the insert (MICA) had incorporated the insert in the correct orientation, the vectors were digested with the restriction enzyme ApaI, which cuts into the different MICA genes at base pair 13 and is also in the MCS of the pcdna5/FRT vector. Vectors with the correct orientation when digested would yield the 1.2 kb band of MICA. (B) Restriction enzyme map of the MICA gene highlighting ApaI (in red).

(A)

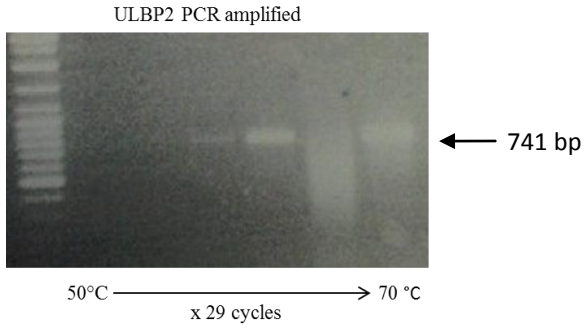


(B)

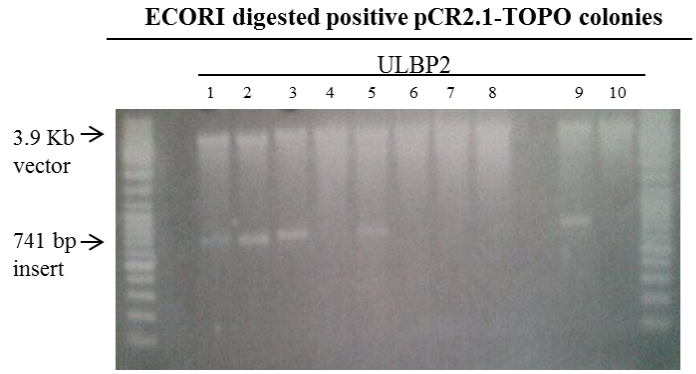


**Figure 2.6**: PCR amplification and cloning of ULBP2 (A) PCR amplification of ULBP2 from Hacat cells UV treated for 24 hours (Human keratinocyte cell line). The PCR product was cloned into the pcr2.1 TOPO vector and (B) the positive colonies were digested with the ECORI restriction enzyme to determine which colonies incorporated the ULBP2 gene.

(A)

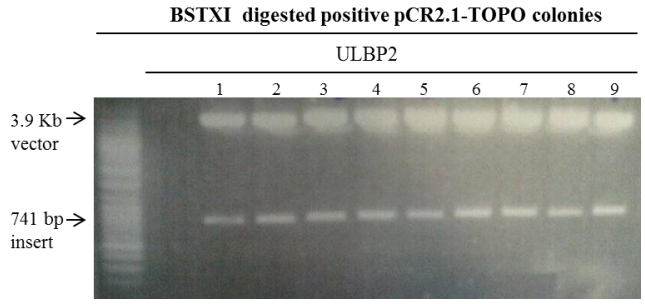


(B)

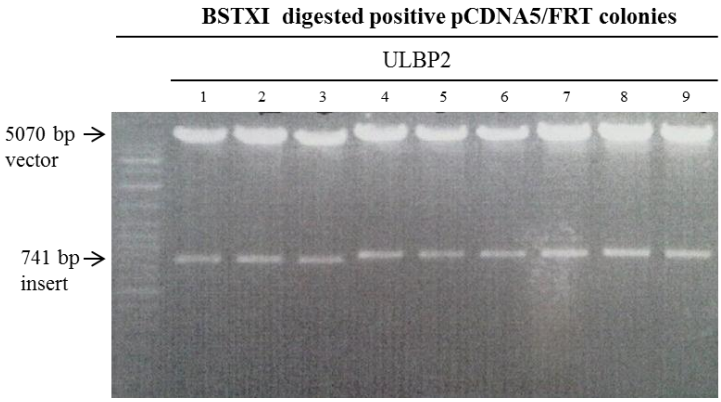


**Figure 2.7**: Subcloning of ULBP2 into the pcdna5/FRT vector. (A) The positive colonies were then sequenced to obtain the colonies with perfect sequence data. (B) These colonies were subcloned into the pcdna5/FRT vector (expression vector) in the multiple cloning site, between the 2 BSTXI sites: the ULBP2 gene were cut out of the pcr2.1 TOPO vector, run on an agarose gel, gel purified and subcloned into the pcdna5/FRT vector. The positive colonies were digested with the BSTXI restriction enzyme to determine if any of the inserts had incorporated into the vector.

(A)

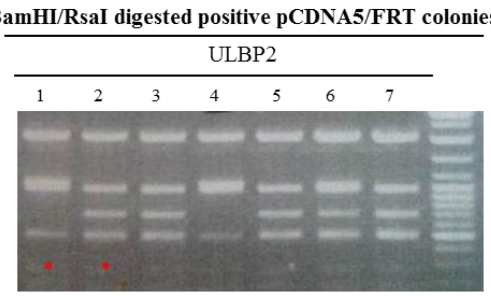


(B)

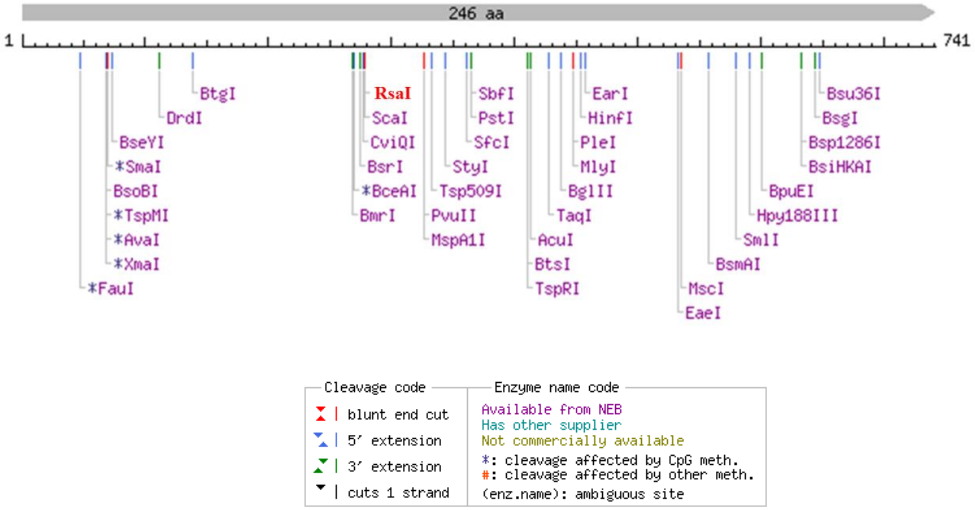


**Figure 2.8:** Determining positive vectors for correct orientation of ULBP2. (A) To investigate which positive vectors had incorporated the ULBP2 gene in the correct orientation, the vectors were digested with various combinations of restriction enzymes: BamHI which is in the MCS of the pcdna5/FRT vector before the first BSTXI enzyme site and RsaI cuts into the ULBP2 gene at base pair 278. Star activity of BamHI was observed in all the digests, however it was clear to see the 2 types of vectors (annotated by the *), and thus both were sent for sequencing, to determine the vector with the ULBP2 gene in the correct orientation. (B) Restriction enzyme map of the MICA gene highlighting RsaI (in red).

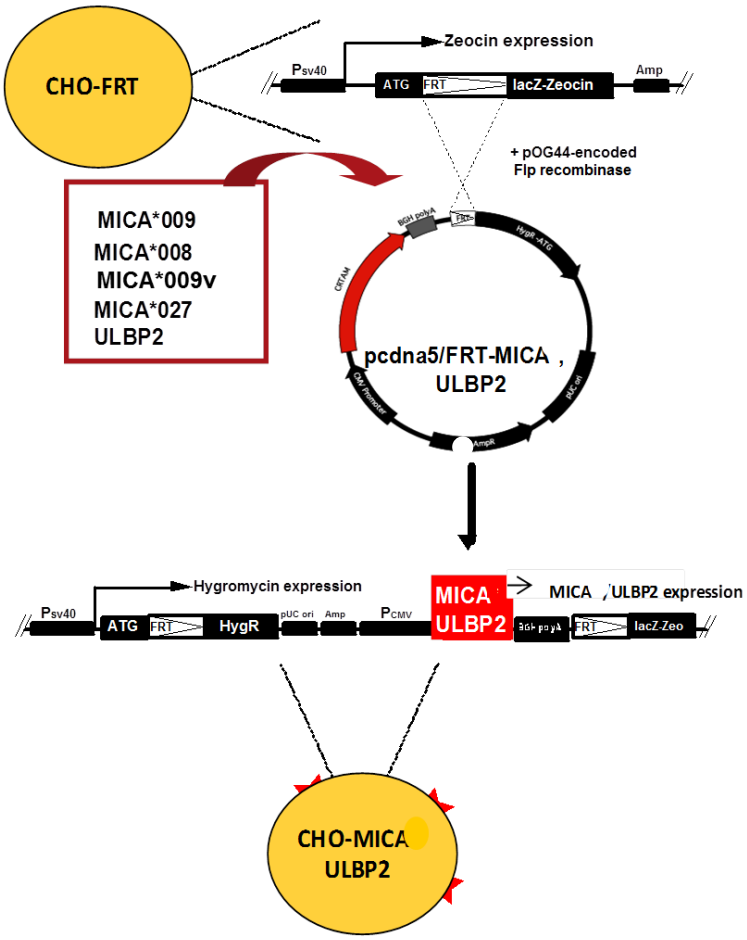


**Figure 2.9**: Diagrammatic illustration of the Flp-In system method used in CHO cells to generate the CHO cell lines. The FRT modified CHO cells (CHO-FRT) contains: a Flp recombinase target (FRT) site (immediately downstream of the start codon) in the same location in the genome of every CHO-FRT cell and also contains a zeocin resistance gene. The GOI's (MICA*009v,*009,*008,*027 and ULBP2) were PCR amplified from various cell line cDNA's using MICA specific primers and separately cloned into the pcdna5/frt expression vector, which contains a homologous FRT sequence and a hygromycin resistance gene that lacks a start codon. Following transfection of the CHO-FRT cells with the pcDNA5-FRT-GOI in combination with the pOG44 vector (encoding the Flp recombinase enzyme) the GOI is integrated into the CHO genome simultaneously disrupting the zeocin resistance gene and full functionality of the hygromycin resistance gene. This allows for transcription of the genes under the control of the human CMV promoter and confers hygromycin resistance and zeocin sensitivity.

## 2.3 Analysis of MICA and ULBP2 structure and cell surface expression

The different MICA alleles and ULBP2 were stably integrated separately into CHO-FRT cells as single copies into the same genomic site via a Flp recombinase enzyme. This allowed for the generation of isogenic stable cell lines which expressed either MICA*009v, MICA*009, MICA*027, MICA*008 and ULBP2 thus eliminating variation among transfectants caused by random integration of genes into the genome.

The expression of each MICA allele and ULBP2 gene is driven by the exact same transcriptional promoter in all the transfectant cell lines under the influence of the FRT system, therefore differences, if any in cell surface expression is due to allelic varaiation. MICA protein expression was examined by surface staining using Flow cytometry analysis (Figure 2.10) using three different anti-MICA antibodies. The analysis showed each cell line expressed the desired protein alone, with no detectable staining of homologous endogenous proteins. Interestingly, MICA*009, MICA*009v and MICA*027 expression patterns were similar, whereas. MICA*008 was expressed weakly on most CHO-Flp-In cells, with only approximately 11% expressing the protein at much higher levels, higher than those observed with MICA*009v, MICA*009 and MICA*027 transfectants. This weak expression of the MICA*008 isoform at the surface of most cells was not due to poor translocation of the protein to the plasma membrane, as most MICA*008 was expressed at the cell surface rather than intracellularly (Figure 2.10 B and figure 2.11 A and B). ULBP2 cell surface expression was similar to MICA*009 and MICA*009v (Figure 2.10 A).

The differences in cell surface protein expression of the MICA isoforms may be attributable to the structures of these alleles (Figure 2.1 and 2.2). MICA*027 surface expression is lower than MICA*009v and MICA*009, but higher than MICA*008. (Fodil et al.,1999). These patterns of MICA expression remained consistent using the three different antibodies (Figure 2.10 A) thus ruling out the possibility of different anti-MICA antibodies displaying selective reactivity against particular allelic forms. Surface expression of ULBP2 was similar to MICA*009

and *009v where 99% of cells were positive for cell surface expression. In order to further examine these possible differences in MICA isoform expression, the CHO transfectants were analysed by immunofluorescent microscopy. The results show very few cells expressing MICA*008 protein at the cell surface (Figure 2.11 C). By comparison, MICA*027 and MICA*009 are expressed at the cell surface by almost all of the CHO transfectants (Fig 2.11 A and B). These data confirm the flow cytometry analysis (Figure 2.10) of surface MICA*008 compared to the other MICA isoforms.

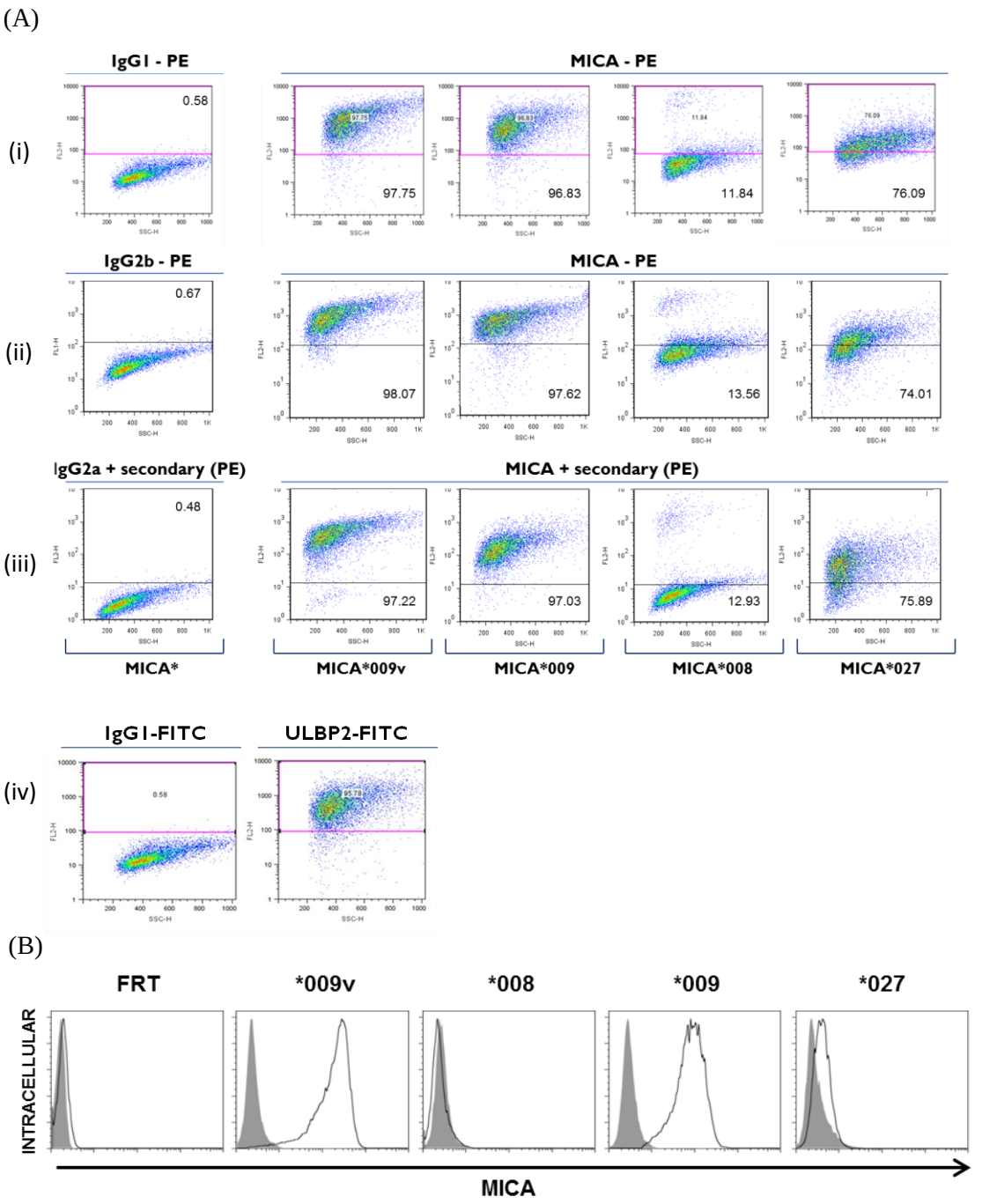


**Figure 2.10**: Cell Surface and Intracellular expression profiles of the MICA and ULBP2 transfectants. A) Surface expression profiles of MICA*009v,*009,*008,*027 and ULBP2 compared to the control CHO-FRT-hygro cells analysed by flow cytometry. Data shown are representative dot plots of multiple stainings with isotype control (not shown), with three different MICA antibodies (i) anti-human MICA-PE antibody, (ii) mouse anti-human MICA-PE antibody and iii) purified anti-human MICA/B antibody + secondary Goat Anti-Mouse IgM Phycoerythrin (iv) ULBP2-PE conjugated antibody.(n >3) B)

Intracellular staining of the transfectants using the same antibodies as in (A i). (Representative of n=2).

---

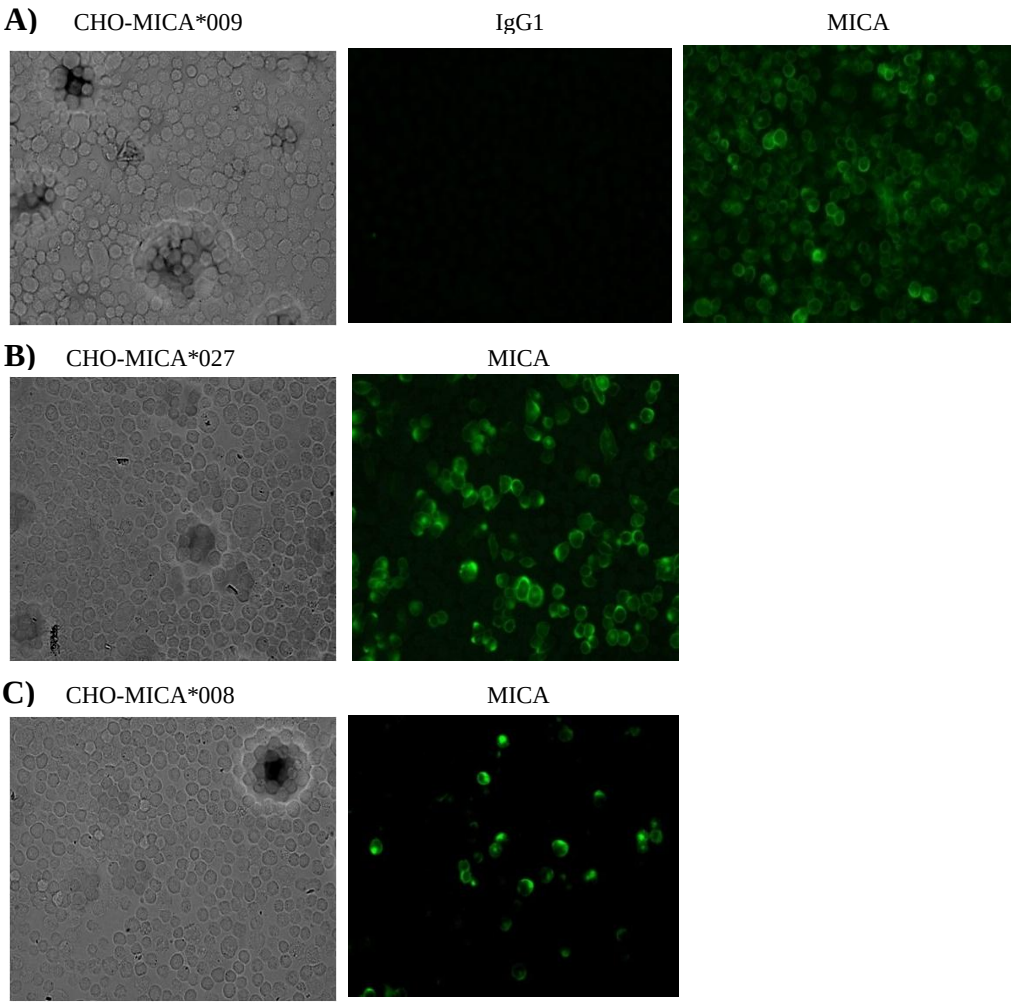


**Figure 2.11**: Immunofluorescence microscopy showing intracellular staining of CHO-MICA*008, *009 and 027 transfectants, original magnification, x 63. a) shows the number of CHO-MICA009 cells on the coverslip(left), the cells stained with isotype control mouse IgG1 + secondary FITC Rat Anti-Mouse IgG1 (center) and mouse anti-human MICA + secondary FITC Rat Anti-Mouse IgG1 (right) b) CHO-MICA*027 (total cells, left, and MICA-stained, right) and c) CHO-MICA*008 (representative of n=2).

## 2.4 Analysis of MICA DNA, RNA and protein expression

Upon integration of the MICA alleles into the CHO-FRT cells, the resulting transfectant cell lines were analysed to determine single integration of the alleles in the CHO-FRT genome. This was assessed by a southern blot. A 4975bp BlpI cut fragment was indicative of the introduction of the different MICA cDNAs into the LacZeo cassette present in the CHO-FRT cells (Fig 2.12 C). The very faint band of approximately 5000bp is a flanking fragment confirming that the integration site of each MICA allele is the same in each fragment. The absence of further bands indicates and confirms that all MICA alleles were integrated only once (single copy) into the CHO-FRT genome without random integration.

The FRT system controls the expression of each allele from the same transcriptional promoter and termination elements, therefore any differences in expression are directly attributed to intragenic allelic variation. Consequently, similar to the differences observed in cell surface expression of the MICA isoforms (Figure 2.10 A) there was a clear hierarchy of RNA expression where MICA*009v>MICA*009>MICA*027>MICA*008 where MICA*009v RNA was 1.3x the level of MICA*009 RNA, 1.8x the level of MICA*027 RNA and 7.1x the level of MICA*008 RNA. This indicates that polymorphisms in MICA affect RNA expression levels potentially through stability and transcript elongation (see discussion, chapter five).

This quantitative variation in mRNA expression (Figure 2.13) was mirrored by the steady state protein expression determined by western blot analysis (Figure 2.14). MICA*009v, MICA*009 and MICA*027 were all detected on the blot at 76Kda, whereas MICA*008 protein on the gel migrated faster due to its truncated sequence and was detected at 71Kda. This hierarchy was paralleled by the cell surface expression of the different MICA proteins (Figure 2.10), for example; the poor cell surface expression of MICA*008 was not due to inadequate translocation to the cell surface membrane, indicated by the inconspicuous levels of intracellular protein expression, rather most MICA*008 was expressed at the cell surface. This implies

that the poor level of cell surface expression reflected overall poor RNA and protein expression.

(A)

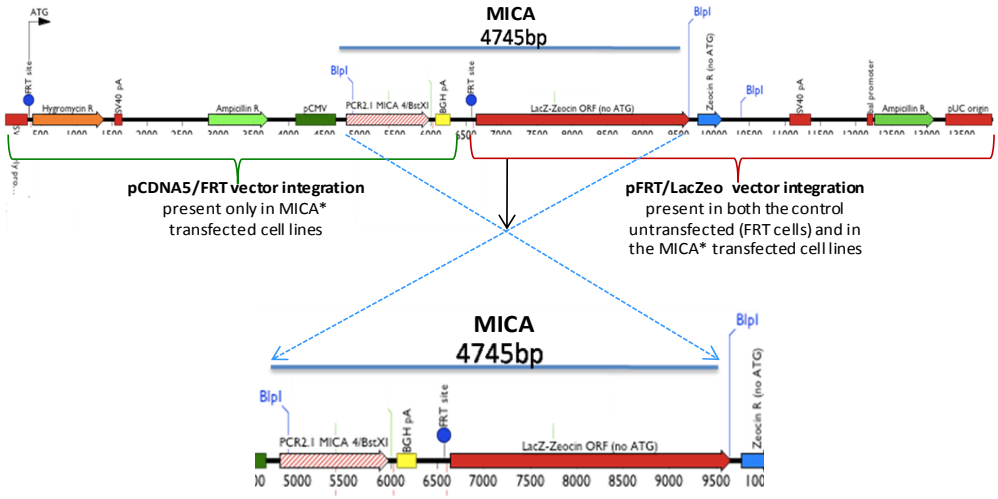


(B)


(C)

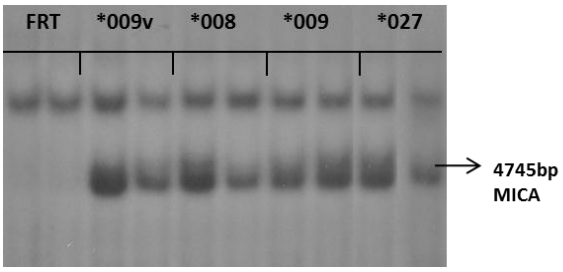


**Figure 2.12**: Southern Blot analysis of MICA*009, *009v, *008 and *027 transfectants. Cloning of MICA*009, *009v, *008 and *027 transfectants in to CHO cells via the flp-frt system is a practical means for generating isogenic cell lines to test the impact of polymorphisms on gene function in the following way: Southern blot. The restriction enzyme chosen and used to cut the DNA from the

MICA transfected cell lines was BlpI, which also cuts into the MICA gene at position 71bp after the ATG (start codon). This way it was possible to identify single integrants from multiple ones using: Single integrants produce one band of size 4745bp (with MICA in the FRT site). Multiple integrants would produce the band of 4745bp (with MICA in the FRT site) plus bands of different sizes. (A) Schematic representation of the size of the region in the CHO genome cut by BlpI (which incorporates the MICA gene). (B) Restriction enzyme digested DNA (15µg) from CHO-FRT (control) and MICA transfectant cell lines. Duplicates of each DNA were digested and run on a gel (C) indentification of single integrants, 4745bp MICA band (representative of n=2).

---

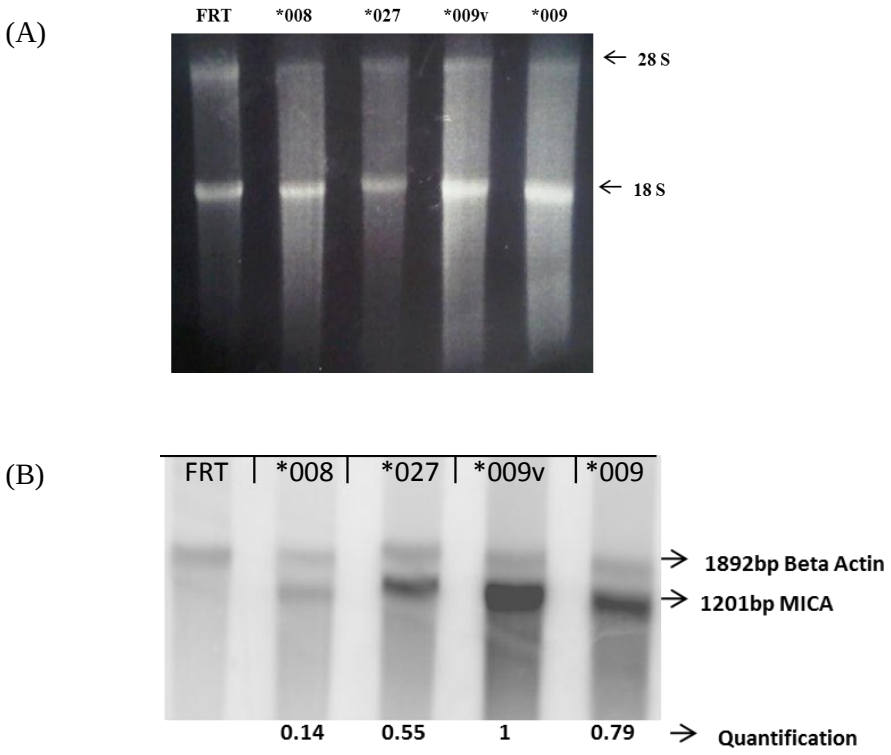


**Figure 2.13**: Northern blot analysis of MICA*009, *009v, *008 and *027 RNA: (A) RNA (15µg) from MICA*008, *027, *009v and *009 transfectants was run on a formaldehyde gel. (B) Detection of beta actin (1892 bp) and MICA (1201 bp) on the membrane by full length probes for both (detected and quantified by the Image Quantifier machine (representative of n=2).

(A)

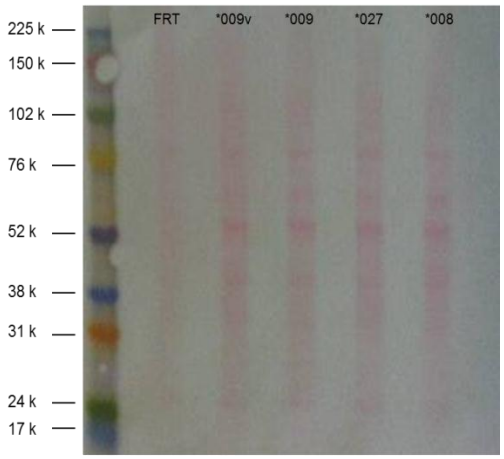


(B)

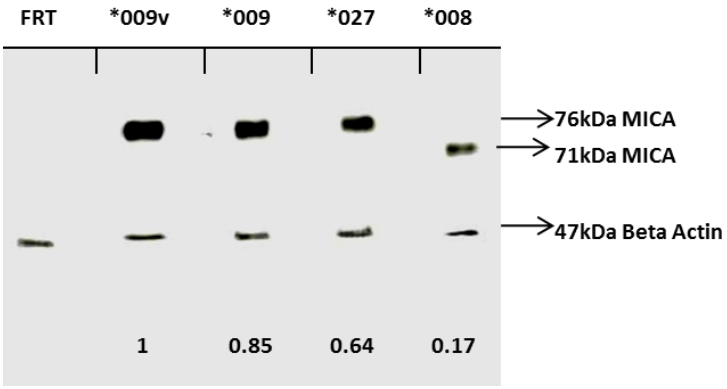


**Figure 2.14**: Western blot analysis of expression levels of MICA in the transfectants. (A) Ponceau stained western blot membrane detecting protein concentration of transfectants loaded (10µg). (B) Detection of MICA (76 kDa MICA*009v,*009 and *027 and 71 kDa MICA*008) and beta actin (47 kDa) on the membrane (representative of n>3).

---

## 2.5 Soluble MICA is detected in all the supernatants of the MICA transfectants.

Western blot analysis revealed the presence of soluble MICA in all the MICA supernatants after 6 hours in serum free medium. ELISA was used to quantify the concentration of soluble MICA at 2 hour intervals for 12 hours to determine if MICA was being shed from the cell surface (Fig 2.15). However, the highest concentration detected at every time point was from supernatants of MICA*009v

cells, being around 3 fold higher than MICA*008 and reached a maximum of 4700 pg/ml. The levels of soluble MICA*009 detected in the supernatant were approximately 1 fold lower than soluble MICA*009v levels. No soluble MICA was detected in the supernatants of the untransfected CHO-FRT cells. Thus it would be intriguing to investigate whether these levels of soluble MICA obtained from the transfectants would have any effect on rendering them as targets for killing by NKG2D$^{+}$ lymphocytes by donors, as previous reports have demonstrated that a high level of sMICA down-regulates the NKG2D receptor on NK cells, and thus impairs the cytotoxic response of the NKG2D$^{+}$ cells and their capacity to secrete IFN-γ (Groh et al., 2002). This issue is addressed in chapter three.

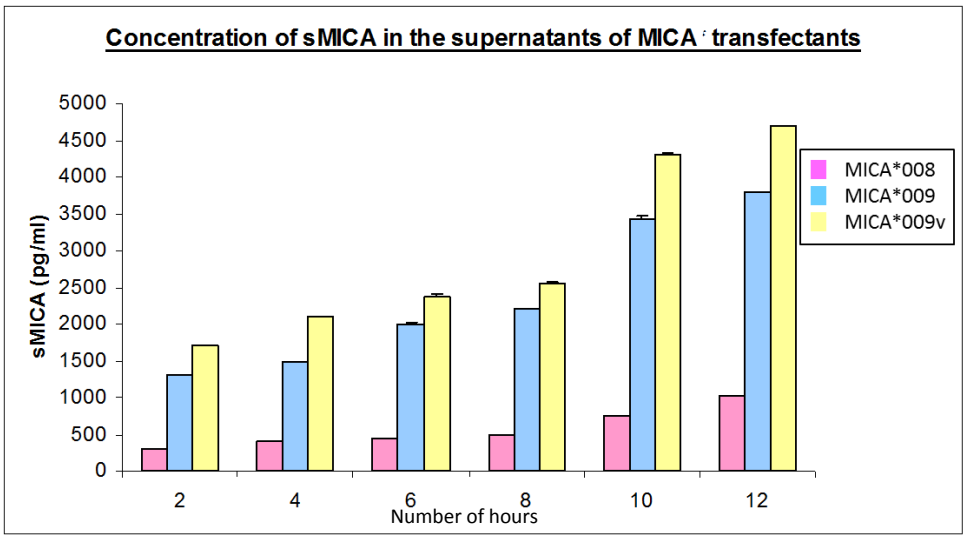


**Figure 2.15**: Analysis of soluble MICA protein in CHO transfectant supernatants at 2 hour intervals for 12 hours using a soluble MICA ELISA. Samples were normalised whereby lysates of 1 million cells were prepared and added to each well, and equal amounts of supernatant were added per well b) sMICA ELISA: equal amounts of supernatant were added to each well, and samples were analysed in duplicate (representative of n=2).

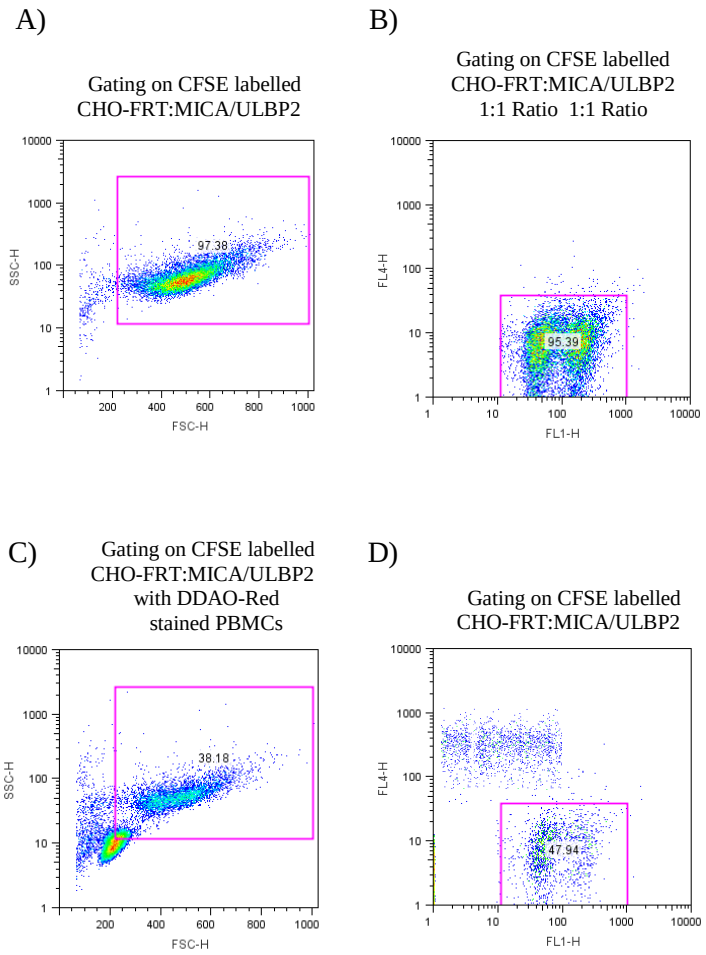


**Figure 2.16**. Representative flow cytometry data illustrating the CFSE *in vitro* killing assay strategy: A) Gating of CFSE labelled CHO-FRT:CHO-transfectant without PBMC's (control) on forward and light scatter, B) Gating on CFSE labelled CHO-FRT:CHO-transfectant to determine the 1:1 ratio, C) and D) gating to exclude the DDAO-Red labelled PBMC's and determine the ratio of CHO-FRT:CHO-transfectant after the duration of the assay (representative of n>3).

---

## 2.6 MICA provokes specific killing by NKG2D$^+$ cells

The capacity of the MICA transfectants to act as targets for killing by NKG2D$^+$ cells was assessed and analysed using an in vitro killing assay where the transfectants were labelled with a high concentration of the membrane intercalating dye, CFSE, and mixed in a 1:1 ratio with the control CHO-FRT cells labelled with a

low concentration of CFSE. After incubation with effector cells for 12 hours, the ratio of $CFSE^{hi}$ to $CFSE^{lo}$ cells was taken as a measure of specific target killing.

Initially the CFSE assay was subjected to optimisation to determine the optimal effector:target (E:T) ratio and duration of assay required. In accordance with this the CFSE killing assay was carried out at 3 time points: 4, 8 and 12 hours at 3:1, 10:1 and 20:1 E:T ratio using 3 healthy controls (representative data from 1 healthy control, Figure 2.17). The percentage specific lysis of transfected target cells was calculated, and maximum killing achieved was observed at the 10:1 and 20:1 E:T ratio.

A striking feature observed from these initial killing assays was the variability in killing of the different transfectants. Similar patterns were observed between the killing of MICA*009 and MICA*009v transfected cells at 4, 8 and 12 hours of the assay. However, most surprisingly, MICA*008 transfected cells were killed to approximately the same extent as MICA*009V and *009 transfectants, despite the weak protein cell surface expression where only approximately 11% of cells displaying high levels of surface MICA. According to the results obtained from these experiments killing of the MICA targets was optimal at the 1:10 and 1:20 E:T ratio after 12 hours.

(A)

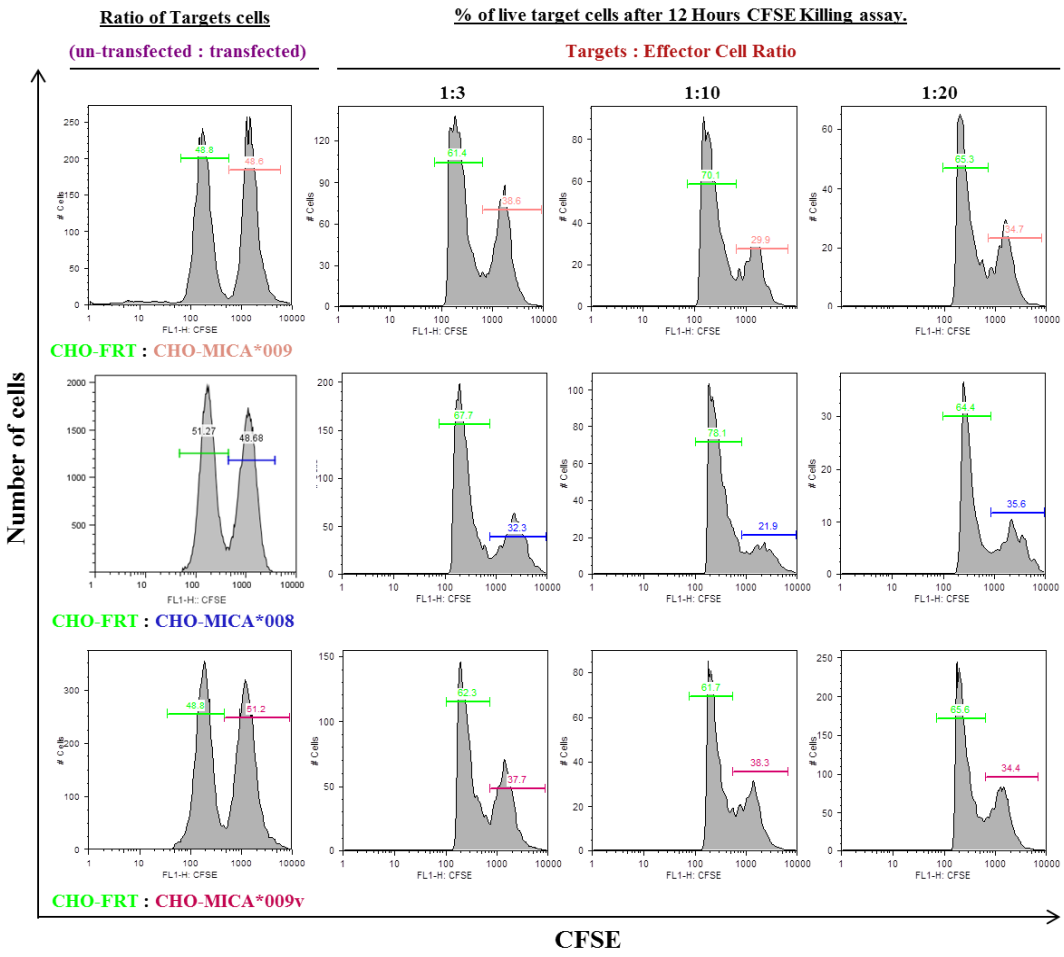
Ratio of Targets cells
(un-transfected : transfected)
% of live target cells after 12 Hours CFSE Killing assay.
Targets : Effector Cell Ratio
1:3
1:10
1:20
Number of cells
CFSE
CHO-FRT : CHO-MICA*009
CHO-FRT : CHO-MICA*008
CHO-FRT : CHO-MICA*009v

(B)

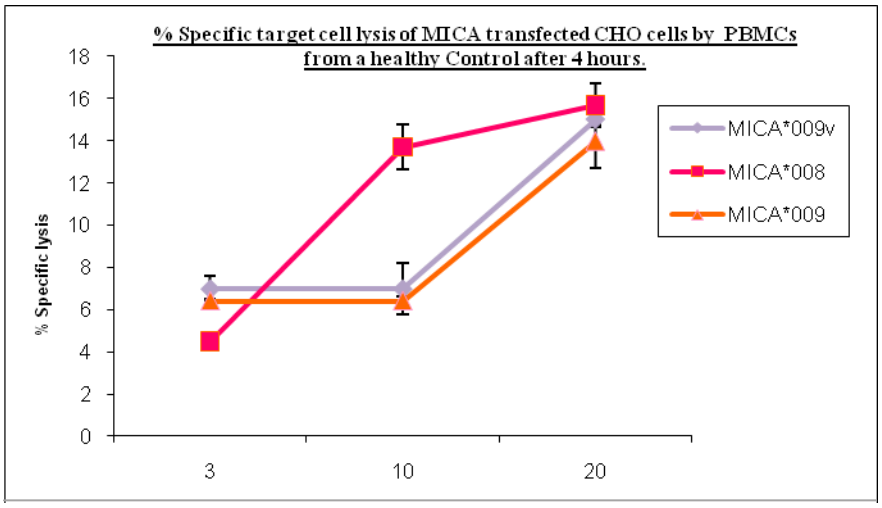
% Specific target cell lysis of MICA transfected CHO cells by PBMC's from a healthy Control after 4 hours.
% Specific lysis
MICA*009v
MICA*008
MICA*009

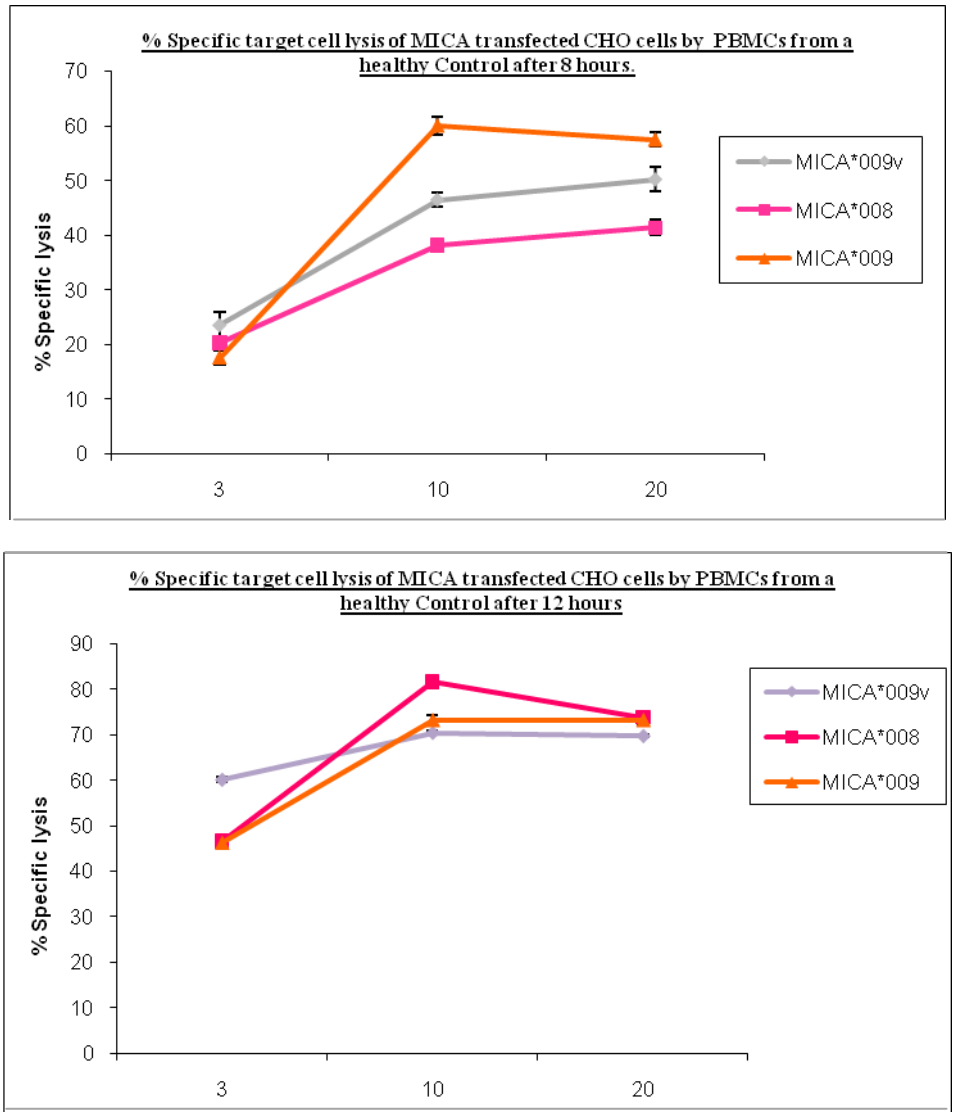


**Figure 2.17**: Optimisation of the *in vitro* CFSE killing assay: Cytolytic lysis of MICA*008,*009 and *004 CHO targets by PBMC's from one healthy control. The assay was carried out such that the control:target (CHO-FRT:MICA) was at a 1:1 ratio. Three different E:T (effector:target) ratios were used: 3:1, 10:1 and 20:1, and the duration of the assay was carried out at 3 different time points: 4, 8 and 12 hours. The assay was carried out in triplicate, where a mean of the results was obtained. (A) Histograms showing the percentage of killing of the MICA targets in relation to the control (CHO-FRT) at the 3 different E:T ratios. (B) Graphical representation of the calculated percentage of specific lysis of the MICA targets and the different E:T ratios and 3 different time points. (n=2).

## 2.7 MICA transfectants are killed in an NKG2D-dependent fashion

To determine if the MICA transfectants are killed in an NKG2D-dependent fashion, in vitro CFSE killing assays were carried out on 5 healthy controls (representative data from 1 healthy control, Figure 2.18) using the mouse anti-human NKG2D antibody and a mouse IgG1 isotype control antibody to block the NKG2D receptor. The results of this blocking assay were determined by calculating the percentage specific lysis of the transfectants, which revealed that the percentage killing of the transfectants obtained was similar when targets were incubated with PBMCs alone and those incubated with the isotype control (determined by the specific lysis of only the MICA transfectants compared to the CHO-FRT control targets). However targets incubated with the blocking NKG2D antibody (PBMC + α-NKG2D) showed no killing of the transfectants determined by the initial 1:1 ratio of CHO-FRT control: CHO-MICA transfectants. These results indicate that blocking the NKG2D receptor on the surface of $NKG2D^{+}$ lymphocytes completely inhibits killing of the MICA transfectants. This suggests that the cytolytic pathway and thus killing of transfectants is solely mediated by the NKG2D-MICA interaction.

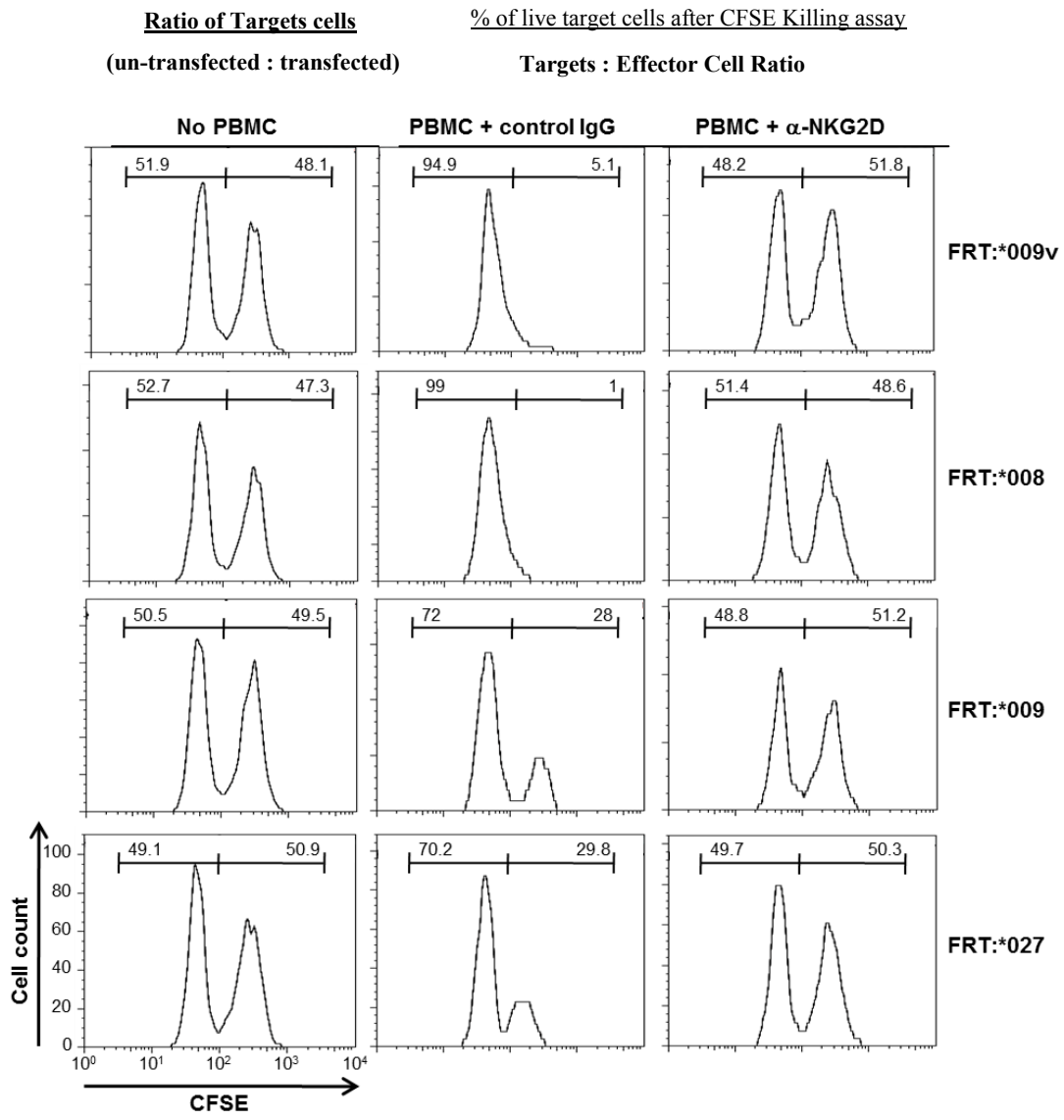


**Figure 2.18**. The NKG2D blocking assay. PBMCs (from one healthy control donor) were pre-incubated for one hour with a blocking mouse anti-human NKG2D antibody (10µg/ml azide free) prior to adding them to the target cells (MICA transfectants). The *in vitro* CFSE killing assay was carried out at a 20:1 E:T ratio and the duration of the assay was 12 hours. The assay was carried out in triplicate, where a mean of the results was obtained. The antibody was left in for the duration of the assay (representative of n=2).

## 2.8 Normalising the CFSE *in vitro* killing assay

To determine whether the variability in killing of the MICA transfectants was a property unique to individuals, a cell line, NKL (established from the peripheral blood of a patient with $CD3^{-}CD16^{+}CD56^{+}$ large granular lymphocyte (LGL) leukemia) was used in the killing assays. The NKL cell line exhibits cytolytic killing and antibody-dependent cellular cytotoxicity (ADCC) similar to normal $CD16^{+}CD56^{dim}$ NK cells and thus was an ideal choice to use as a control for donor NK cells in the cytolytic assays.

Initial optimisation of the killing assay using NKL was carried out using different E:T ratios: 3,5,7,20,30 and 40:1 with a duration of 12 hours. Variability in killing of the MICA and ULBP2 transfectants was evident but slight. The percentage specific killing of the ULBP2 transfectants was the highest at every E:T point showing that the ULBP2 transfectants are recognised as a target for killing. The optimal E:T ratio obtained was 5:1 as the variability in killing of the transfectants was easily visible (Figure 2.19 B). This killing of the MICA transfectants (including MICA*027) was carried out at the 5:1 E:T ratio over 3 time points (week 1, 4 and 6) to determine whether the killing observed at one time point would remain stable longitudinally (Figure 2.19 C). Killing of the MICA*027 transfectants showed MICA*027 as a functional target for killing. The slight variability in killing of the MICA transfectants by the NKL cell line can clearly be seen where MICA*027>MICA*009v>MICA*009>MICA*008. It is surprising that NKL recognises and lyses MICA*027 most efficiently than the other isoforms, since the difference between MICA*027 and MICA*009 is only 4 residues (Figure 2.1). It will be interesting to identify if this hierarchy of MICA*027 killing is reflected in killing assays using PBMCs from donors.

(A)

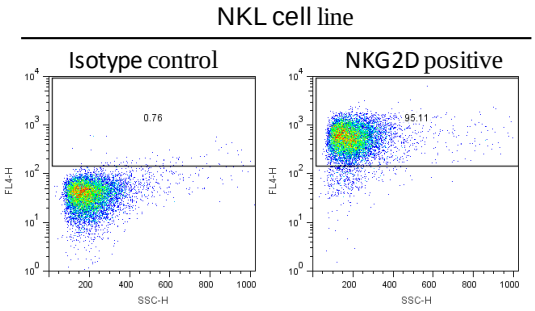


(B)

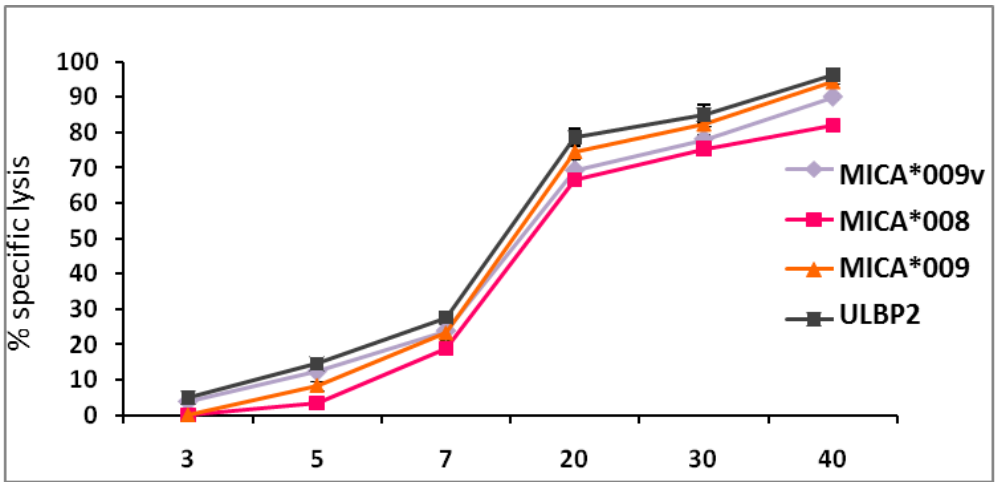


(C)

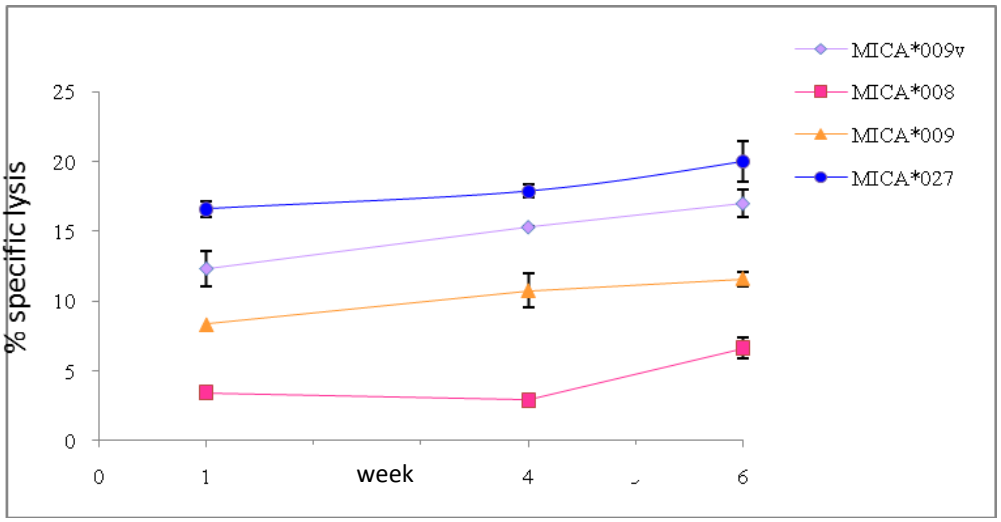


**Figure 2.19**: NKL cell line killing of MICA and ULBP2 transfectants: (A) NKL cell line expression of NKG2D when compared to isotype control (representative of n>3). (B) Optimisation of NKL killing assay of targets using different E:T ratios (3, 5, 7, 20, 30 and 40:1) to determine the most suitable ratio required for subsequent assays (n=2). (C) Killing of MICA*009V,*008,*009 and *027 transfectants by the

NKL cell line using a 5:1 E:T ratio (n=2). The assay was carried out in triplicate, where a mean of the results was obtained. Duration of the assays was 12 hours.

---

## 2.9 DISCUSSION

Previous data have reported MICA as a highly polymorphic gene, with about 65 known MICA alleles. The complete full length sequences of all alleles have been recorded, (Fodil et al., 1999), but how this affects MICA biology has not been investigated thoroughly. In order to study the effects of MICA polymorphism, new in vitro killing assays were designed. These techniques allowed monitoring of the stress surveillance in vitro.

The Flp-In sytem modified in CHO cells permits the study of the polymorphic aspects of MICA gene products, such as variation in RNA and protein expression. The small number of differences between the MICA alleles has important effects on RNA expression levels, even though the promoter and other regulatory sequences are normalized. These differences in RNA expression translate to the total and cell surface protein expression. The concept of the variation of RNA sequences regulating differential stability of RNA is currently under investigation.

The differences in cell surface expression show MICA*008 transfectants to poorly express the protein at their cell surface. A study by Suemizu et al (2002) using confoccal microscopy visualised the subcellular localization of the molecule in polarized Madin–Darby canine kidney (MDCK) epithelial cells, and identified that MICA*008 lacks a basolateral targeting motif. Thus the protein does not target to the basolateral membrane of human enterocytes, but instead it targets to the apical membrane. The expression studies and immunofluorescence microscopy (Figure 2.10 A and Figure 2.11) show that MICA*008 is in fact expressed mostly at the cell surface. Despite the differences in RNA and cell surface protein expression, all MICA isoforms can be recognised and targeted by $NKG2D^{+}$ cells. Surprisingly, MICA*008, which is poorly expressed at the surface of cells is targeted just as well as the other more strongly expressed MICA isoforms by donor PBMCs. Our

preliminary conclusions are either that lymphoid killing is extremely sensitive, detecting MICA on the surface of cells at lower levels than are detectable by cytometry, or that MICA*008 surface expression is very rapidly turned over, such that in the duration of the assay, approximately 100% of the cells do display surface MICA at some point, and hence become targets. To distinguish between these two possibilities, shorter incubation times with the killer cells will be utilised.

The initial studies with healthy donor PBMCs using the NKL cell line as a control, showed the responses to the different MICA proteins and ULBP2 protein being highly variable. Furthermore, it has not yet been elucidated whether different MICA proteins expressed at the surface of cells are targeted and killed differently by NKG2D positive NK cells, γδ T and $CD8^+$ αβ T cells from different individuals.

The unexpected inter-individual variation observed, needs further exploration by using a larger cohort of healthy donors. This further investigation was undertaken and is described at length (chapter three).

# CHAPTER THREE—ANALYSIS OF THE HIERARCHY OF INTER-INDIVIDUAL VARIATION

The capacity of MICA or ULBP to render CHO cells as targets for killing was assessed (see chapter two) using an assay in which MICA or ULBP FRT-CHO transfectants and the control CH0-FRT cells were used as targets with the $NKG2D^+$ human cell line, NKL cell line (control for PBMCs) and PBMCs from a healthy donor for optimisation of the *in vitro* CFSE killing assay. The assays with NKL, revealed a dose-dependent specific cytolysis of all MICA and ULBP2 transfectants (chapter two). Although MICA*009 targets were killed better than MICA*008 targets, the difference was minor relative to the substantial differences in surface expression, with MICA*008 conferring effective targeting, despite its very low surface expression. CHO-FRT-MICA transfectants were also targets for primary peripheral blood mononuclear cells (PBMC) from one healthy donor, with all specific killing completely inhibited by a blocking anti-NKG2D antibody.

Results from killing assays showed a hint of inter-individual variation in killing of the MICA transfectants. This phenomenon has not been seen before, and thus had to be explored in depth to identify whether this is a consistent finding. This issue is addressed in this chapter using a larger cohort of healthy control PBMCs in killing assays. Furthermore, the effect of a chronic disease state such as BD, in which MICA*009 has been implicated as one of the susceptibility genes was investigated, to determine how efficiently $NKG2D^+$ lymphocytes from a cohort of BD patients, would kill the MICA and ULBP2 transfectants. These studies would provide an insight into how $NKG2D^+$ lymphocytes from patients respond in immune surveillance of autologous transformed or otherwise dysregulated cells, and conversely differential propensity for NKG2D-dependent inflammation.

## 3.1 Inter-individual variation in killing of transfectants is a consistent finding

In order to determine if the hierarchy of specific cytolysis displayed inter-individual variation seen between individuals (Figure 3.1A), longitudinal assays were performed using PBMC's from four healthy donors used in killing assays to target the MICA and ULBP2 transfectants at 2 and 3 different time points, over a period of at least 4 months (Figure 3.1 B). The data from these studies showed that inter-individual variation in killing of the transfectants for any one donor was essentially stable longitudinally. This meant that individual AD who targeted MICA*008 better than MICA*009 remained consistent over time, likewsie donor M, who targeted MICA*009 consistently better than MICA*008.

(A)

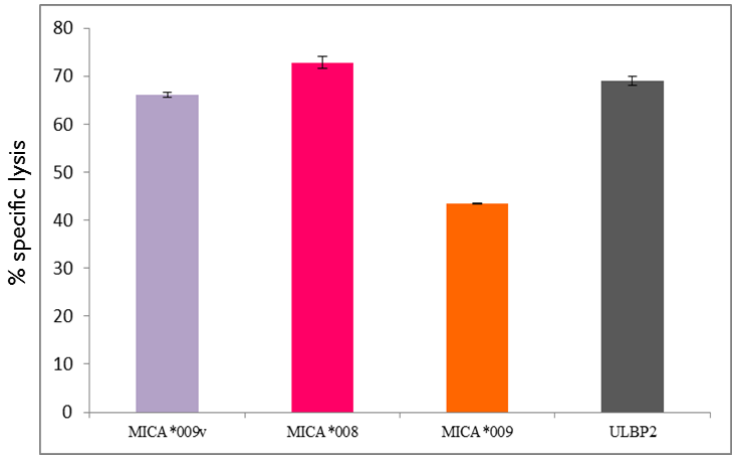


(B) i)

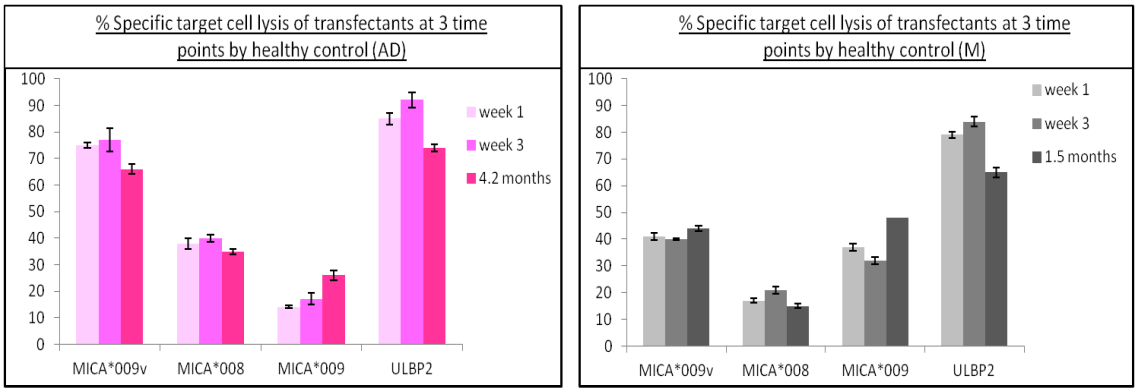


ii)

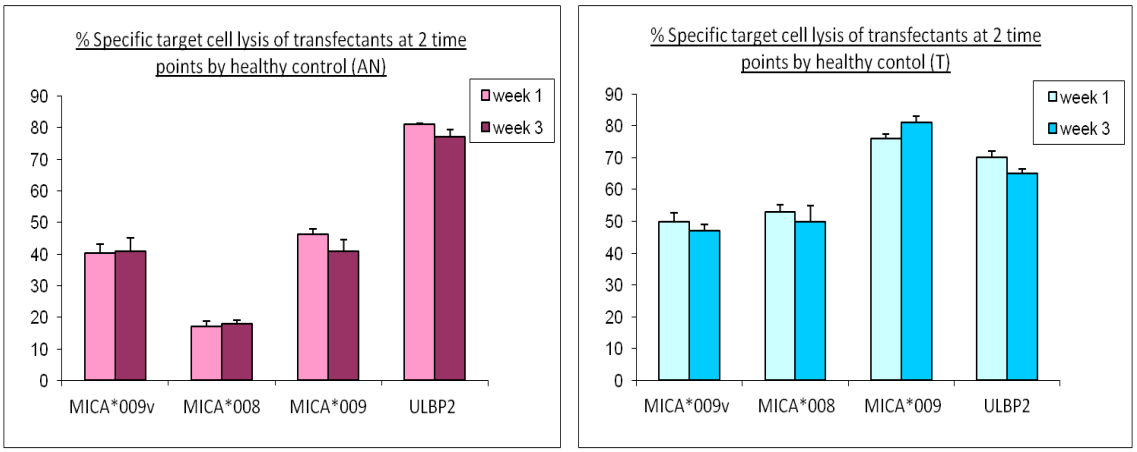


**Figure 3.1**: Killing assay data reveals a varied individual response to transfectants which is stable longitudinally (A) percentage specific lysis of MICA and ULBP2 transfectants by freshly isolated PBMC's from one healthy donor (n=2) (B) i) Killing of transfectants by 2 healthy controls at 3 different time points ii) Killing of transfectants by 2 healthy controls at 2 different time points. The assay was carried

out in triplicate, where a mean of the results was obtained (Data are means of triplicate wells +/- SD). Duration of the assays was 12 hours (n=2).

---

## 3.2 An analysis of the hierarchy of varied killing by healthy donors

PBMC's from 22 healthy donors were used in *in vitro* killing assays. An extreme variation in hierarchy was evident in this analysis. Approximately one third of donors specifically targeted MICA*008 cells more efficiently than MICA*009v cells, despite the low cell surface expression of MICA*008 compared to the highest cell surface expression of MICA*009v. (Fig 3.2) There was no correlation of MICA*009 and MICA*027 expression levels with their capacity to be targeted. Furthermore, certain individuals, example donors number 2, 8 and 15 targeted transfectants extremely well, whereas donor number 4, 5, 6 and 9 were less effective. This had no obvious relation to hierarchies. Approximately 8 donors targeted ULBP2 to about 80-90% effectiveness. In relation to MICA*008 transfectant killing, donor number 2 killed MICA*008 transfectants effectively (approximately 90%), whereas donor number 17 killed MICA*008 poorly (10%). An inter-individual variation in PBMC's targeting ULBP2 was also observed, where PBMC's from 3 healthy donors showed little or no capacity to target ULBP2 cells, despite their capacity to target the MICA transfectants.

In addition, all the donors were MICA typed, to analyse whether the MICA type of the individuals correlated to the killing of the different transfectants (Figure 3.8, see section 3.3) .The percentages of $NKG2D^+$ NK cells and γδ T cells and the mean fluorescence intensity (MFI) of the expression of NKG2D on NK cells from 8 donors used in the assay (Table 3.1) were analysed. On average the healthy donors have similar percentages of $NKG2D^+$ cells and similar surface expression of NKG2D on NK cells (see table 3.1), thus the variable killing of transfectants is surprising. For example donor 6 and 17 have similar percentages of NK cells and γδ T cells, yet $NKG2D^+$ cells from donor 6 targeted the transfectants very poorly compared to donor 17, who targeted the transfectants with a higher efficiency.The $NKG2D^+$ expression data confirmed that all NK cells are positive for the NKG2D receptor, while most γδ

T cells are NKG2D$^{+}$, with a small percentage being negative for the receptor. Another intriguing observation was that donor 14 has the highest percentage of NK cells (21.91%) and γδ T cells (11.28%), displayed variable killing efficiencies of the transfectants, compared to donor 15, who had much lower percentage of NK cells (10.75%) and γδ T cells (2.97%) yet killed all the transfectants with a much higher cytotoxic potential. This shows that the reduced killing of the transfectants is not attributable to lower percentages of circulating NKG2D$^{+}$ cells (Table 3.1). Correlation analysis showed no correlation between the killing of MICA and ULBP2 transfectants and the percentage of NKG2D$^{+}$ NK cells (figure 3.3) and the MFI (Mean fluorescence intensity) of NKG2D expressed on NK cells (figure 3.4) in all healthy controls.

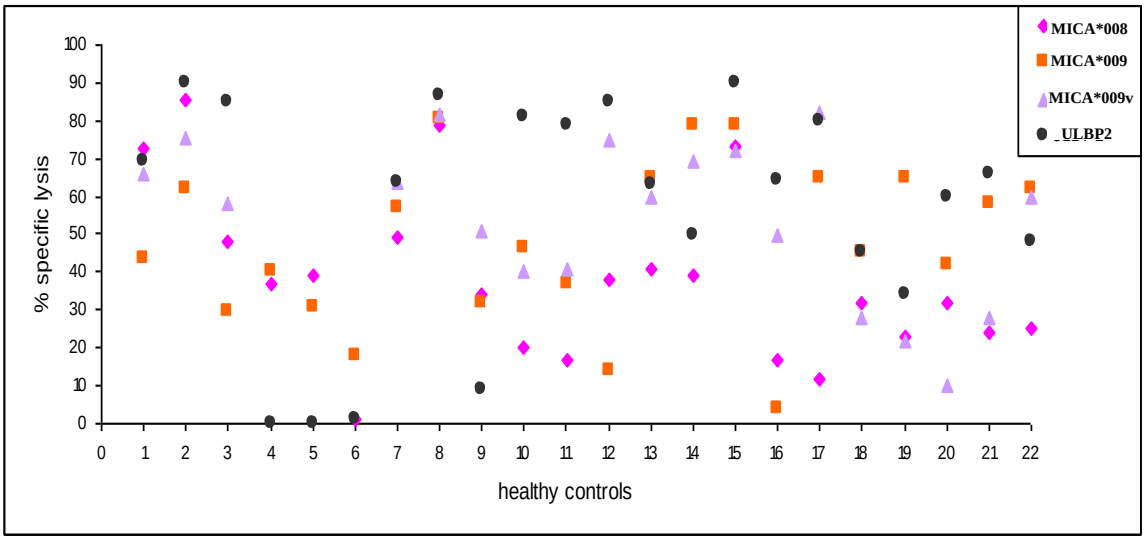


**Figure 3.2**: Variable killing of MICA and ULBP2 transfectants by PBMCs from 22 healthy donors (controls) (not all donors were tested against all targets). The target:effector ratio used was 1:20 for 12 hours, in triplicate. The assay was carried out in triplicate, where a mean of the results was obtained and percentage specific lysis of transfectants was calculated and compared. Standard deviation (SD) was consistently < 5%, but is not shown so as to preserve the clarity of the figure. Duration of the assays was 12 hours (n=1).

| CONTROL | MICA TYPE | % γδ (% NKG2D) | % NK (% NKG2D) | MFI OF NKG2D ON NK CELLS |
|---|---|---|---|---|
| HC(6) | 008*,009* | 1.07 (73.8) | 10.57 (100) | 449.92 |
| HC(13) | *002,008* | 5.03 (99.2) | 5.51 (100) | 504.86 |
| HC(14) | *008,*010 | 11.28 (95.2) | 21.91 (100) | 311.27 |
| HC(15) | *008,*009 | 2.97 (79.1) | 10.75 (100) | 379.1 |
| HC(16) | *002,*010 | 1.05 (79.5) | 8.92 (100) | 341.12 |
| HC(17) | *008,*010 | 1.72 (86.6) | 11.59 (100) | 426.32 |
| HC(18) | *008,*009 | 1.4 (87.9) | 9.28 (100) | 450.03 |
| HC(19) | *002,*008 | 3.46 (91.6) | 9.7 (100) | 356.46 |

**Table 3.1**. Percentages of γδ and NK cells in PBMC from 8 healthy donors (controls). MICA type, percentage of NKG2D$^{+}$ NK and γδT cells and the MFI (mean fluorescence intensity) of NKG2D expression on NK cells in peripheral blood from 8 controls in figure 3.2 (n=1).

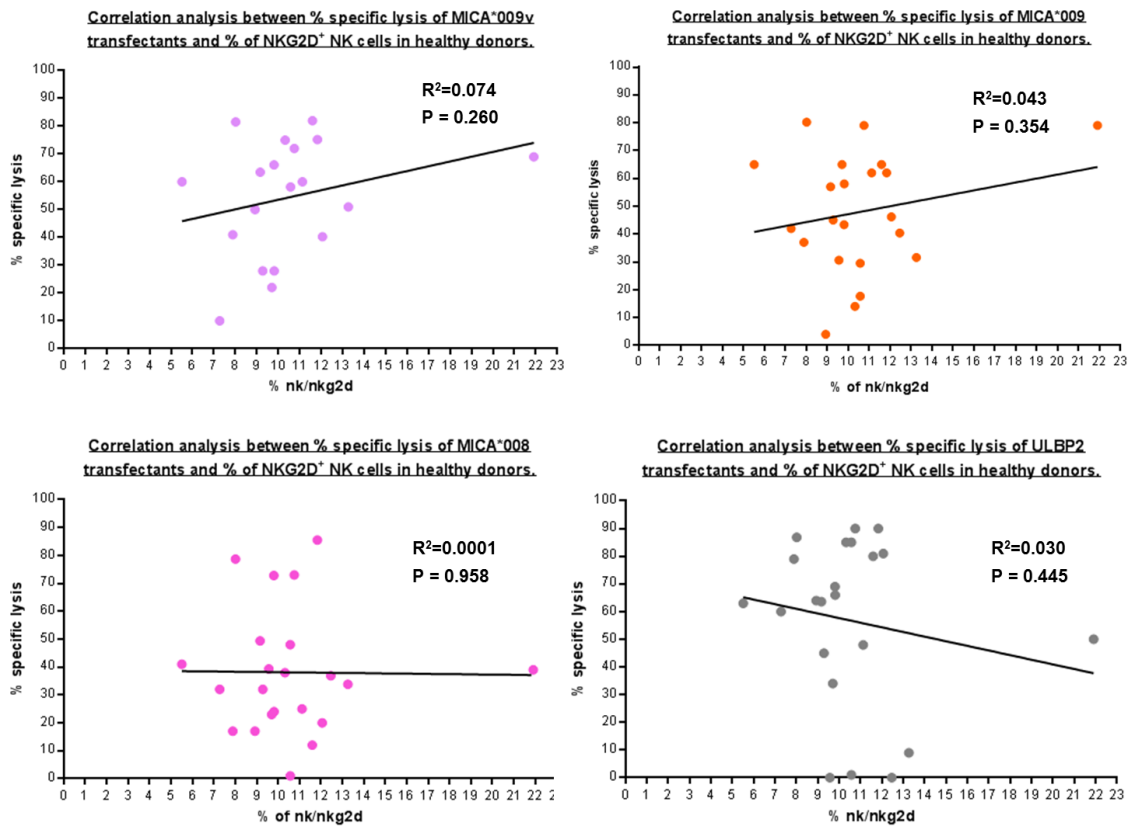


**Figure 3.3**: Graphical representation of the Correlation analysis between percentage of specific target lysis of MICA and ULBP2 transfectants and percentage of $NKG2D^+$ NK cells from 22 healthy donors (controls). The $R^2$ and P values are shown for each analysis graph, measured by linear regression analysis.

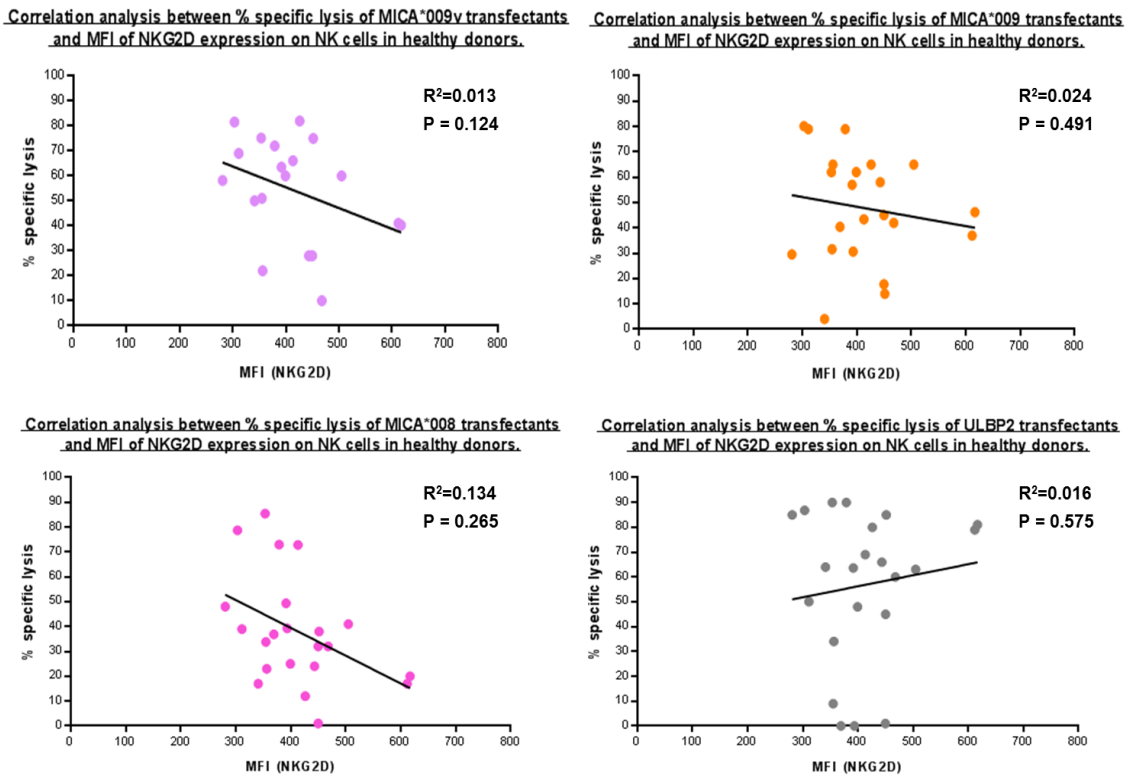


**Figure 3.4**: Graphical representation of the Correlation analysis between percentage of specific target lysis of MICA and ULBP2 transfectants and MFI (Mean fluorescence intensity) of expression of NKG2D on NK cells from 22 healthy donors (controls). The $R^2$ and P values are shown for each analysis graph, measured by linear regression analysis.

## 3.3 The hierarchy of varied killing by healthy donors is mirrored in BD patients

The variation in hierarchy of killing of transfectants using healthy donor PBMCs was mirrored when PBMC's from patients with BD were used in the killing assays against the transfectants (figure 3.5). In terms of the killing of MICA*009 transfectants, 2 cohorts of patients were highlighted, one cohort that killed the transfectants as their primary target (donor number: 1, 11, 14, 15, 17, 20 and 22) and the other cohort that killed the transfectants very poorly (donor number: 2, 4, 9, 13, 16 and 18). These data is intriguing, considering that MICA*009 is the BD associated isoform. Interestingly, the percentages of circulating NK and $\gamma\delta^+$ T cells in patient peripheral blood, were on average much lower than that seen in healthy controls (discussed in chapter four). This however, did not affect the capacity for these NKG2D$^+$ cells to target the MICA and ULBP2 transfectants as efficiently as the healthy control NKG2D$^+$ cells.

For example, patient 13 has an unusually low percentage of NK cells (1.77%) ,yet displayed a variable targeting of the transfectants (ULBP2>MICA*008>MICA*009v>MICA*009) compared to patient 20 who has the highest percentage of NK cells (18.11%) and also targeted the transfectants variably (MICA*009>ULBP2>MICA*008>MICA*009v). There were no differences in killing between male and female patients.

Furthermore, the hierarchies did not obviously correlate to the donor MICA haplotype (Fig 3.8). The MICA*008$^+$ and MICA*009$^+$ individuals displayed a wide range of targeting the MICA*008 and MICA*009 transfectants. Similar to healthy controls, correlation analysis showed no correlation between the killing of MICA and ULBP2 transfectants and the percentage of NKG2D$^+$ NK cells (figure 3.6) and the MFI (Mean fluorescence intensity) of NKG2D expressed on NK cells (figure 3.7) in all BD patients. Therefore these studies did not explain the reasons for the preferential responses of NKG2D lymphocytes from both healthy controls and patients.

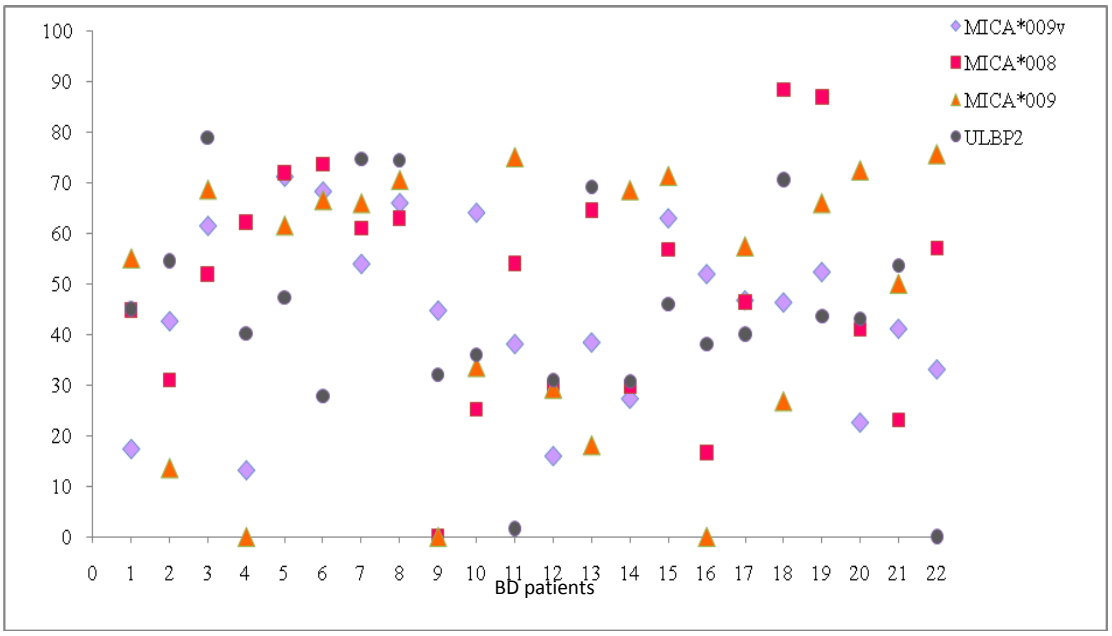


**Figure 3.5**: Variable killing of MICA and ULBP2 transfectants by PBMCs from 22 Behcet's patients. The target:effector ratio used was 1:20 for 12 hours. The assay was carried out in triplicate and the mean of the results and percentage specific lysis was calculated and compared. Standard deviation (SD) was consistently < 5%, but is not shown so as to preserve the clarity of the figure. Duration of the assays was 12 hours (n=1).

| BD patient | MICA type | % γδ (% NKG2D) | % NK (% NKG2D) | MFI of NKG2D onNK cells |
|---|---|---|---|---|
| BD(5) | *004,*009 | 2.51 (88) | 5.44 (100) | 350.55 |
| BD(6) | *004,*009 | 5.95 (79) | 13.06 (100) | 401.4 |
| BD(10) | *002,*009 | 3.65 (87) | 7.57 (100) | 454.4 |
| BD(11) | **009 | 1.07 (73.5) | 1.13 (100) | 542.23 |
| BD(12) | *044,*049 | 1.46 (89) | 19.04 (100) | 412.3 |
| BD(13) | *002,*043 | 1.78 (92) | 1.77 (100) | 398.23 |
| BD(14) | *008,*017 | 1.97 (83) | 10.32 (100) | 365.45 |
| BD(19) | *008,*009 | 2.92 (72) | 9.19 (100) | 504.34 |
| BD(20) | *008,*009 | 6.41 (91) | 18.11 (100) | 225.6 |

**Table 3.2**: Percentages of γδ and NK cells in PBMCs from 9 Behcet's disease patients. Table showing MICA type, percentage of NKG2D$^{+}$ NK and γδT cells in peripheral blood and MFI (mean fluorescence intensity) of NKG2D expression on NK cells from 9 BD patients used in used in figure 3.3 (n=1).

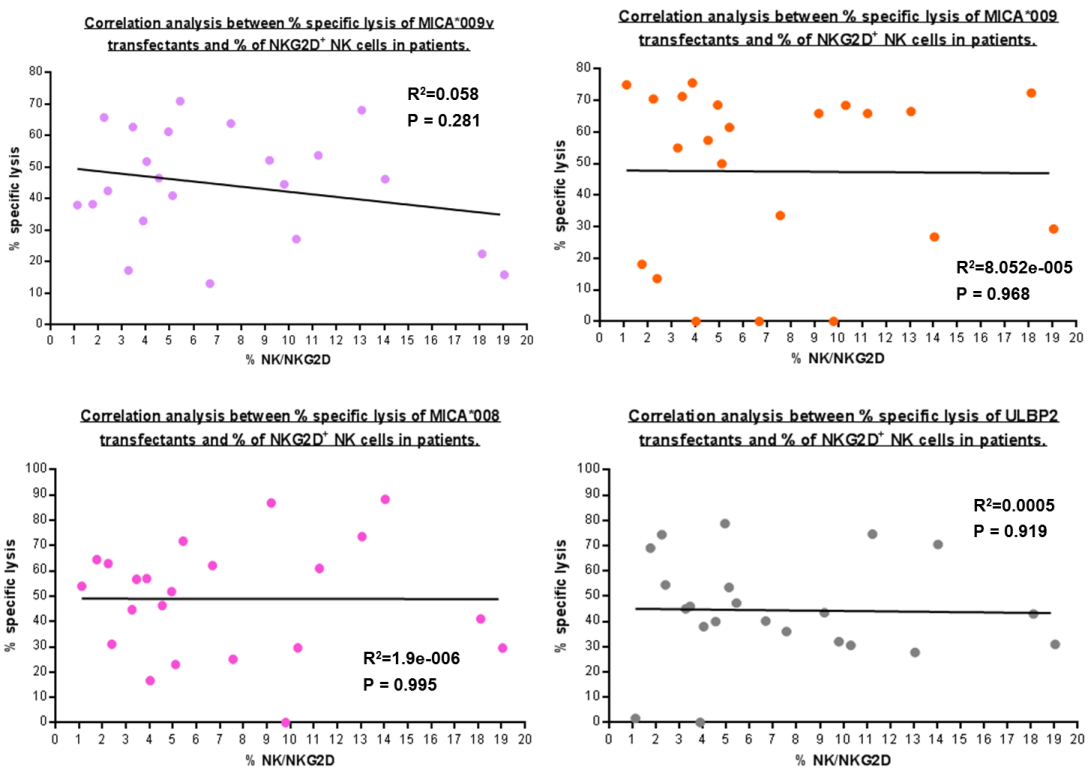


**Figure 3.6**: Graphical representation of the Correlation analysis between percentage of specific target lysis of MICA and ULBP2 transfectants and percentage of $NKG2D^+$ NK cells from 22 BD patients. The $R^2$ and P values are shown for each analysis graph, measured by linear regression analysis.

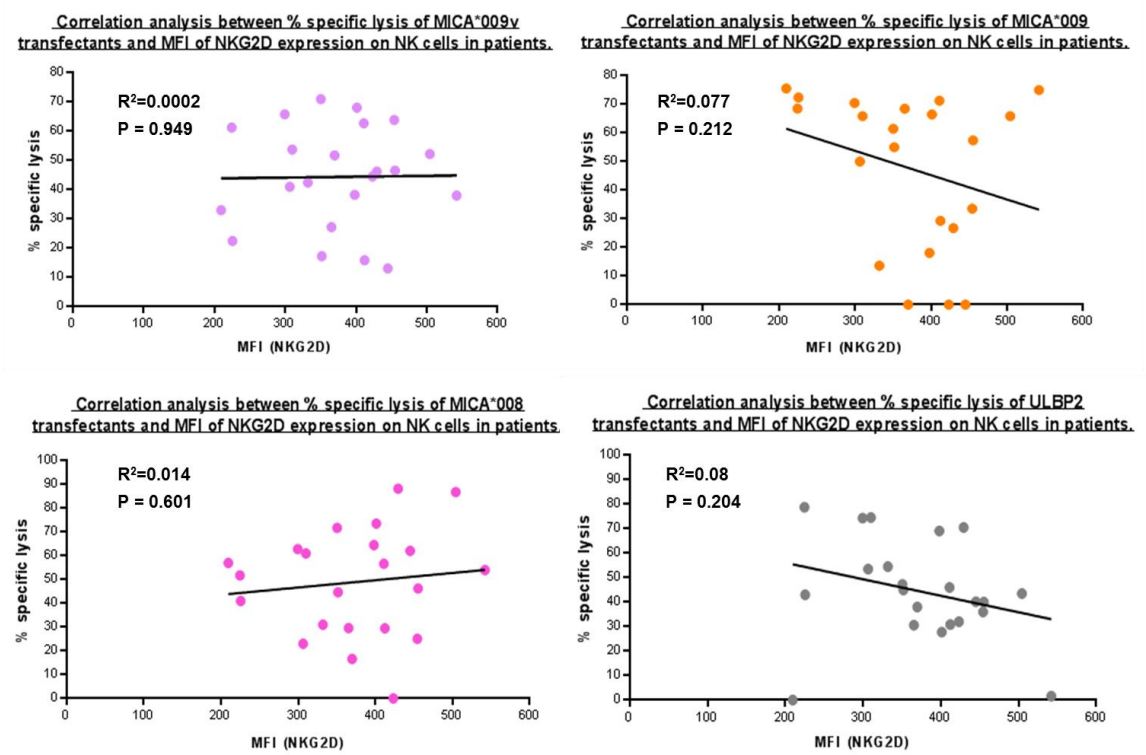


**Figure 3.7**: Graphical representation of the Correlation analysis between percentage of specific target lysis of MICA and ULBP2 transfectants and MFI (Mean fluorescence intensity) of expression of NKG2D on NK cells from 22 Behcet's disease patients. The $R^2$ and P values are shown for each analysis graph, measured by linear regression analysis.

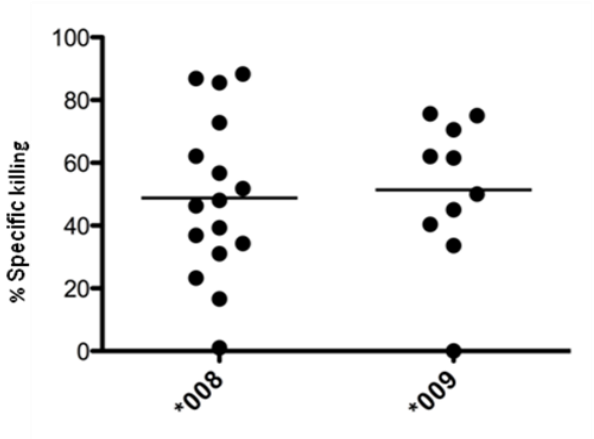


**Figure 3.8**: Percentage specific target lysis of matching target and donor isoforms. This graph shows the killing of MICA*008 targets by MICA*008 donors (healthy controls and patients) and killing of MICA*009 targets by MICA*009 donors to potentially explain the reason for the preferential responses.

## 3.4 Degranulation of NKG2D$^+$ cells using the CD107a assay

The CFSE assay determines the percentage specific lysis of the MICA and ULBP2 transfectants, however it does not take into account any non-specific lysis of the control CHO-FRT cells. Therefore, a complementary assay, the CD107a assay was employed. The CD107a assay measures the direct response of PBMCs to target cells via the cell surface expression of the degranulation marker, CD107a, released as a result of exocytosis of the cytolytic granules following activation of the immune cell. Degranulation is measured as the percentage of CD107a$^+$ cells, commonly from approximately 5 to 20% and the level, to which they degranulate, judged by their MFI (Mean fluorescence intensity). The CD107a$^+$ cells are phenotyped by staining for NK, γδ T and CD8$^+$ αβ T cells using specific antibodies. The CFSE assay was carried out on 3 healthy donors (Figure 3.9A) using only the MICA transfectants, which showed a high donor-donor variation, killing targets with different hierarchies. Similarly the NK cells from these donors degranulated in response to the MICA transfectants that reproducibly exceeded the degranulation response to CHO-FRT cells (Figure 3.9 C). Every donor showed a degranulation response by their NK cells to the MICA targets and a γδ T cell response to at least one MICA target. Although the MFI (Mean fluorescence intensity) of the NK cells and γδ T cells was comparable, the percentage of NK cell degranulation was much higher. Surprisingly, there was no CD8$^+$ NKG2D$^+$ αβ T cell granulation whatsoever to any of the MICA targets in any of the donors in spite of the down regulation of NKG2D on the surface of CD8$^+$ T cells, thus suggesting that there was engagement of NKG2D and MICA. The results from the CD107a assay validated the results from the CFSE assay, as they showed the same hierarchies of responses as observed in the killing assay: donor E lysed all the MICA targets effectively which was validated by comparable degranulation and donor A lysed MICA*027 and MICA*008 transfectants poorly and the NK and γδ T cells expressed very little CD107a.

(A)

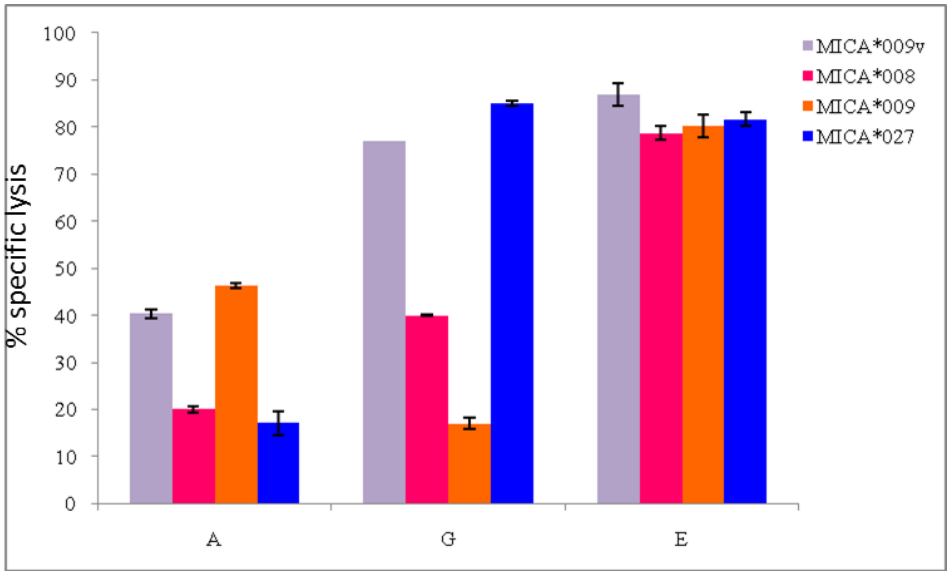
% specific lysis
100
90
80
70
60
50
40
30
20
10
0
A
G
E
MICA*009v
MICA*008
MICA*009
MICA*027

(B)

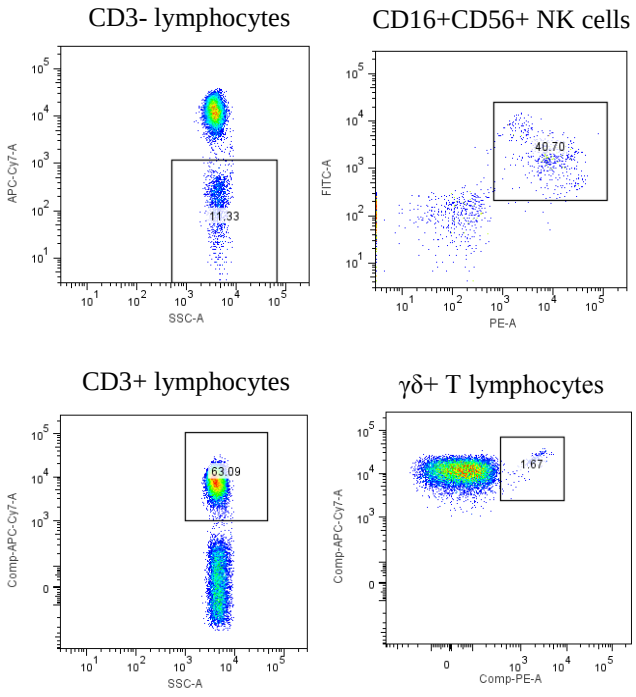
CD3- lymphocytes
CD16+CD56+ NK cells
CD3+ lymphocytes
γδ+ T lymphocytes
APC-Cy7-A
SSC-A
11.33
FITC-A
PE-A
40.70
Comp-APC-Cy7-A
63.09
1.67
Comp-PE-A

(C)

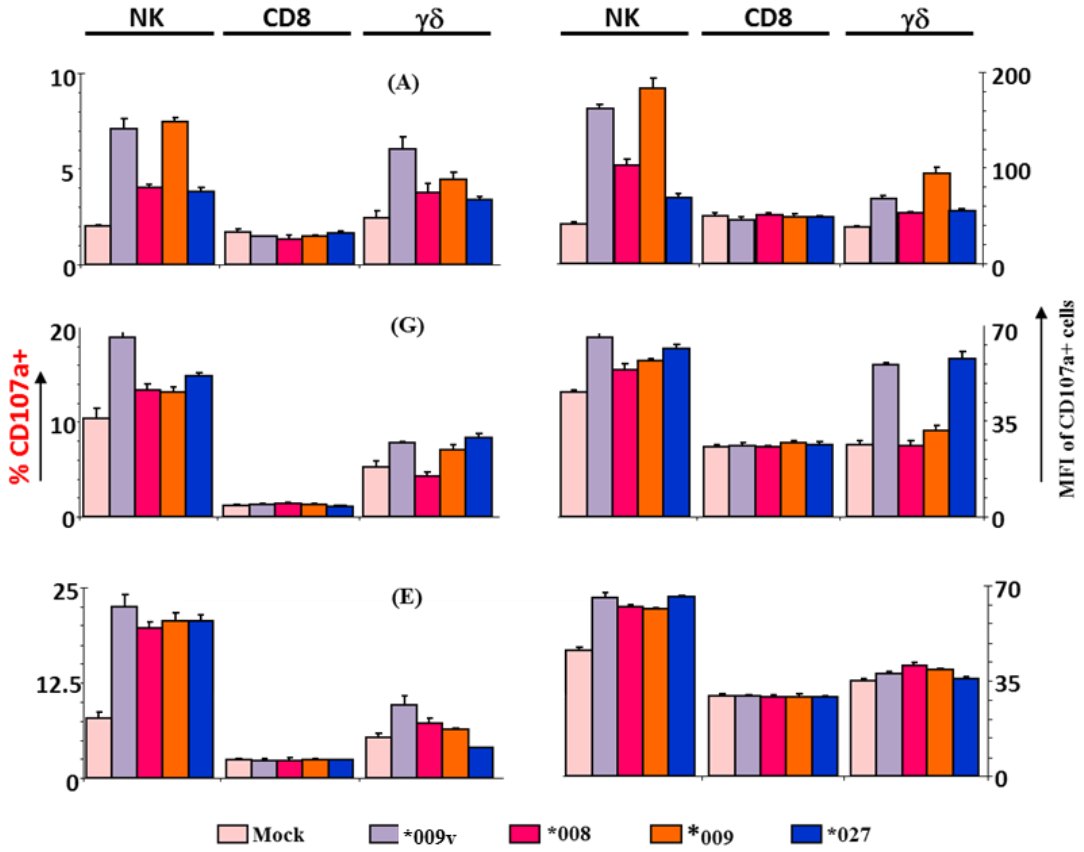


**Figure 3.9**: Percentage specific lysis of transfectants and CD107a degranulation of NKG2D positive cells. (A) Graph showing killing of transfectants (MICA*009v,*008,*009 and MICA*027) by 3 healthy controls (A, G and E). The assay was carried out in triplicate and the mean of the results were obtained (Data are means of triplicate wells +/- SD). Duration of the assay was 12 hours (n=2). (B) The CD107a degranulation assay: Representative data analysis: following 4 hours in culture with target CHO cell lines, PBMC were stained with fluorescently conjugated antibodies to delineate NK cells ($CD3^{-}CD16^{+}CD56^{+}$), $CD8^{+}$ T cells ($CD3^{+}CD8^{+}$) and γδ T cells ($CD3^{+}TCR\gamma\delta^{+}$) (n=2). The assay was carried out in triplicate and the mean of the results were obtained. (C) Graphical data demonstrated the percentage CD107a expression of NK, CD8 T and γδ cells from three healthy controls compared to the mock (CHO-FRT cells) as seen by flow cytometry using CD107a, NK, γδ and CD8 specific antibodies with the matching isotype controls. The MFI (mean fluorescence intensity) of the $CD107a^{+}$ cells was also calculated (shown above) (Data are means of

triplicate wells +/- SD). The data from the CD107a data compliments the killing assay data whereby showing a consistency of NKG2D positive effector cell activation and killing of targets from donor to donor. (This figure was performed in collaboration with Dr Pierre Vantourout, Kings College London).

---

## 3.5 ULBP2 as a target of cytolysis by healthy and patient donors.

Data from the killing assays using more than 40 donors revealed that specific cytolysis of ULBP2 was very varied between different individuals (Figure 3.2 and 3.3). This finding is most unpredictable and interesting, as ULBP2 is a non polymorphic NKG2D ligand. The fact that this gene is targeted with different efficiencies by different donors is shown by 3 donors that target ULBP2 effectively, and 3 donors that target it poorly (Figure 3.10A). This raises the question of whether the cell surface protein expression of ULBP2 may possibly affect the capacity for it to be targeted by $NKG2D^+$ cells. Different doses of ULBP2 (doses of cell surface protein expression) may give 2 different cytolytic responses (Figure 3.10 B): either the capacity to kill ULBP2 increases with increasing doses of ULBP2, or as the doses of ULBP2 begin to increase, there is an initial increase in the capacity to kill ULBP2, however, a further increase in expression causes a saturation effect, and the capacity to kill ULBP2 declines. Therefore a dose response study using 2 healthy donors (one which targets ULBP2 with high efficiency and the other that targets ULBP2 poorly) targeting ULBP2 transfectants with low, medium and high expression of the protein at the cell surface, would give an indication to whether the density of ULBP2 on the surface of cells can affect it's ability to be targeted more or less by the 2 donors.

(A)

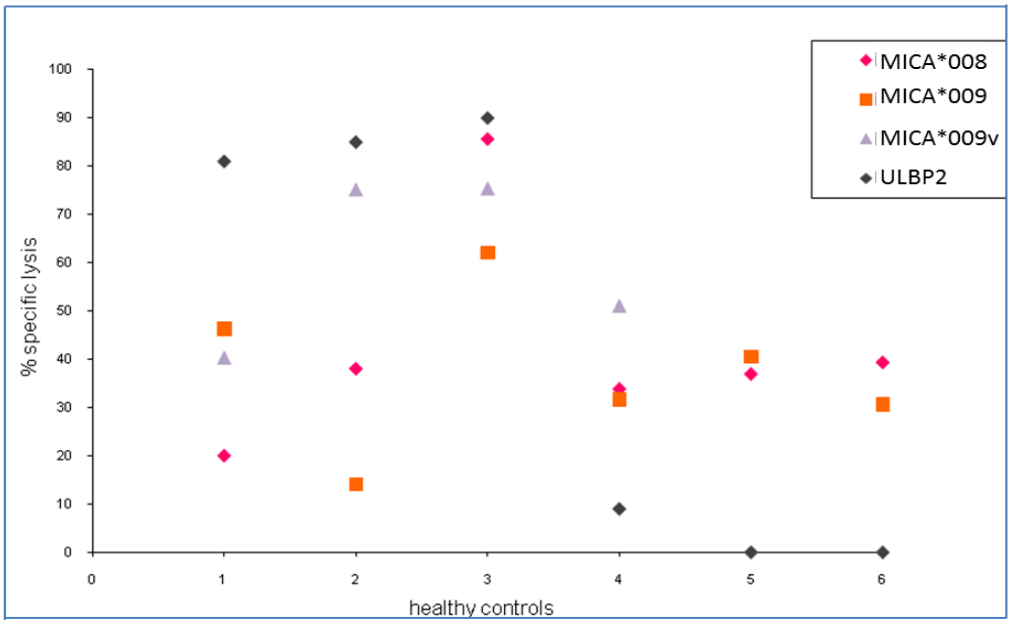


(B)

i)

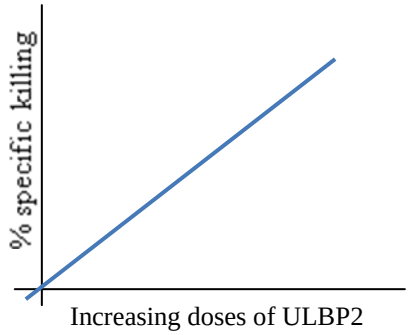


ii)

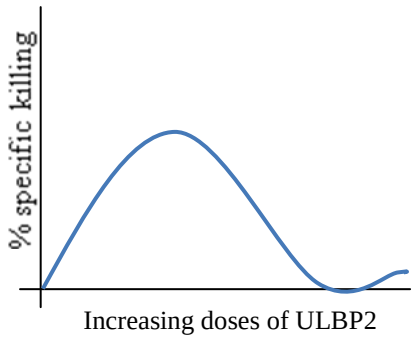


**Figure 3.10**: Variable ULBP2 killing. (A) The graph above is a representation of poor and high ULBP2 killing by 6 healthy donors (3 of each) (B) A depiction of the two proposed types of killing by healthy controls with increasing doses of ULBP2. i) a linear curve of killing as the doses of ULBP2 increase ii) a bell shaped curve with an initial exponential rise in killing as the doses of ULBP2 increase, however with a further increase, there is saturation and therefore a decrease in the percentage killing of ULBP2.

## 3.6 DISCUSSION

The use of a sizable cohort of 22 healthy controls has allowed us to identify the differences in the killing potential of $NKG2D^+$ cells from each individual and has shown that the hierarchy of inter-individual variation of targeting the MICA and ULBP2 transfectants, has indeed remained a consistent finding. Furthermore, longitudinal assays showed that over different time points killing of transfectants by cells from the same individual was fairly consistent, which further reinforces the hierarchy of inter-individual variation concept.

Furthermore, there is no correlation in the variation of killing of transfectants to the percentage of circulating $NKG2D^+$ NK cells and the MFI of expression of NKG2D on the surface of the NK cells in peripheral blood of the donors. This was evident in healthy controls, as they all have similar percentages of circulating $NKG2D^+$ cells and MFIs of NKG2D on NK cells, yet displayed varied cytolytic responses to the MICA and ULBP2 transfectants (Fig 3.2). Likewise, this phenomenon was true for BD patients, which all have on average lower percentages of $NKG2D^+$ circulating lymphocytes in their peripheral blood, yet display similar cytotoxic potential in targeting the MICA isoforms and ULBP2 protein as the healthy control counterparts (Fig 3.3).

. This decrease in percentages of $NKG2D^+$ circulating lymphocytes in the peripheral blood of BD patients may possibly be due to disease, steroid treatment, or their transition to sites of inflammation in tissues. This will be discussed further in chapter four. Interestingly, this hierarchy of varied responses to targeting the transfectants is not correlated to the MICA type of the individual (Fig 3.8), the percentage of circulating $NKG2D^+$ NK cells and the MFI (Mean fluorescence intensity) of NKG2D expressed on NK cells in all BD patients.

When analysing the targeting of MICA*009 transfectants, 2 cohorts of patients were highlighted, one cohort that killed the cells with a higher capacity than the other. This raises certain questions as to why one patient would efficiently kill the MICA*009 transfectants whereas others do not. In an attempt to confirm the supposition of high inter-individual variation in cytolysis of the transfectants, and also to validate the

observations from the in vitro CFSE killing assays in absolute terms, an assay for the expression of CD107a/LAMP-1 as a marker of cellular degranulation. For every individual, the MICA transfectants we directly recognised and targeted by NK cells and γδ T cells, without prior activation of any other receptors. The activation of NK cells and γδ T cells in the CD107a assay compliments the inter-individual variation in killing of the MICA transfectants observed in the CFSE killing assays.

In conclusion the data so far provides an insight into MICA polymorphism, in terms of surface expression, shedding of surface MICA (soluble MICA), and their potentials as targets for NKG2D positive cells in BD patients, disease and healthy controls. However, the influence of the other disease susceptibility gene, HLA-B*51, needed to be investigated in the context of inhibition in the cellular model of Behcet's disease (discussed in chapter four).

# CHAPTER FOUR- DECREASED NUMBERS OF CIRCULATING NKG2D POSITIVE LYMPHOCYTES IN PATIENTS AND THE ROLE OF HLA-B*51 IN BEHCET'S DISEASE

Behcet's disease is a multi-organ inflammatory disease, in which the status of peripheral blood lymphoid populations has been investigated for abnormalities. Increased numbers of $CD8^+$ T cells and γδ T cells (Freysdottir et al., 1999), $CD56^+$ NK cells and $CD8^{bright}CD56^+$ T cells (Ahn et al., 2005) in the peripheral blood of patients compared to controls have been reported. $CD4^+CD16^+$ and $CD4^+CD56^+$ T cell populations have been also shown to be increased in peripheral blood from patients (Eksioglu-Demiralp et al., 1999), as has a decrease in numbers of total $CD4^+$ cells (Freysdottir et al., 1999).

Genes associated with BD include HLA-B*51 and MICA*009. The receptors for these molecules are KIR3DL1 and NKG2D respectively. KIR3DL1 expression on NK and T cells in peripheral blood from patients has been reported to be the same as in control subjects (Saruhan-Direskeneli et al., 2004), however it has also been reported that KIR3DL1 expression varies in patients and is most abnormal in patients with severe eye disease (Takeno et al., 2004). This may be due to different ethnic groups being tested in these two studies from Turkey and Japan respectively.

It is not clear whether expression of NKG2D and on NK and T cells may alter with disease and therefore to address this and to confirm HLA ligand expression, $NKG2D^+$ and $KIR3DL1^+$ levels were assessed by flow cytometry on NK and T cells populations in the peripheral blood of BD patients and healthy controls.

The aim of this study was to determine differences, if any, in the percentage of circulating $NKG2D^+$ cells and $KIR3DL1^+$ NK, γδ T and $CD8^+$ T cells in the peripheral blood of BD patients, compared to disease controls (idiopathic uveitis patients on similar steroid treatment as BD patients) and healthy controls. All donors used in this study were aged between 25-65 years. All patients fulfilled the International Study Group criteria (ISG criteria). 69 Patients were on steroid treatment, 13 of whom had active disease, 8 were off treatment and 69 were classified as quiet patients with little or no disease activity. Clinical activity was assessed at the time of venipuncture from active signs and symptoms (oral ulcers, genital ulcers, ocular lesions, skin lesions, articular symptoms).

## 4.1 Patients have decreased percentages of NK cells in peripheral blood compared to healthy controls.

The percentages of $CD16^+/CD56^+$ NK cells from patients in all groups and disease controls are significantly lower when compared to healthy controls. This difference may be related to the treatment and not to the disease process, as there are no differences between patients with BD and uveitis disease controls. All $CD16^+/CD56^+$ NK cells in all cohorts are $NKG2D^+$ (Fig 4.2 A). Active patients seem to have significantly lower percentages of circulating $CD16^+/CD56^+$ NK cells on average compared to healthy controls. However a similar decrease was seen in disease controls suggesting that this was due to the presence of inflammation rather than specific to BD.

There are some patients with quiet disease who have no $NKG2D^+CD16^+$ and $NKG2D^+/CD56^+$ cells, thus suggesting flare ups in active disease. Most active patients have lower than 5% of circulating $CD16^+/NKG2D^+$ cells. Two groups of quiet patients, off treatment were analysed: one group that essentially have no $CD16^+/NKG2D^+$ cells, and the second group that have more than 10% of circulating $CD16^+/NKG2D^+$ cells (Fig 4.2 B). This segregation may be due to the length of time the patients have been off treatment.

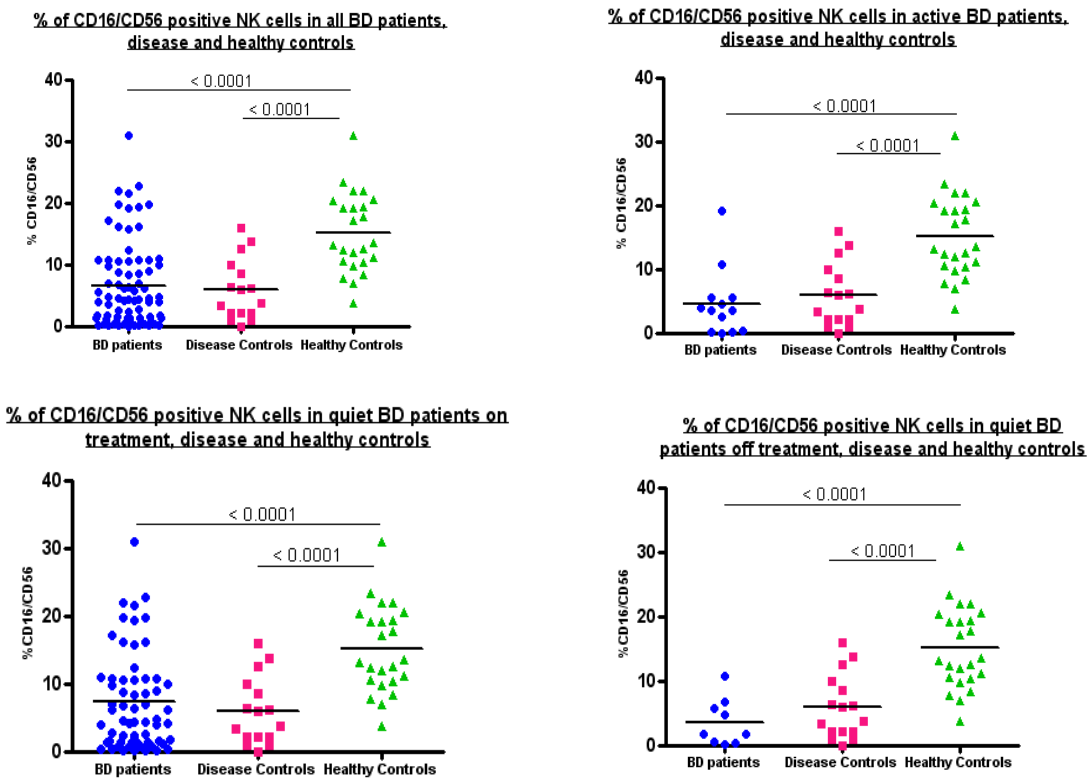


**Figure 4.1**: Comparative flow cytometry and graphical analysis of CD16/CD56 positive NK cells from patients, disease and healthy controls. The graphs outline the differences in percentages of CD16/CD56 positive NK cells from all BD patients (n=90), active patients on treatment (n=13), quiet patients undergoing treatment (n=69) and quiet patients off treatment (n=8) when compared with disease (n=16) and healthy (n=23) controls. P values indicate statistically significant differences: $p < 0.05$, measured by ANOVA statistical analysis.

(A)

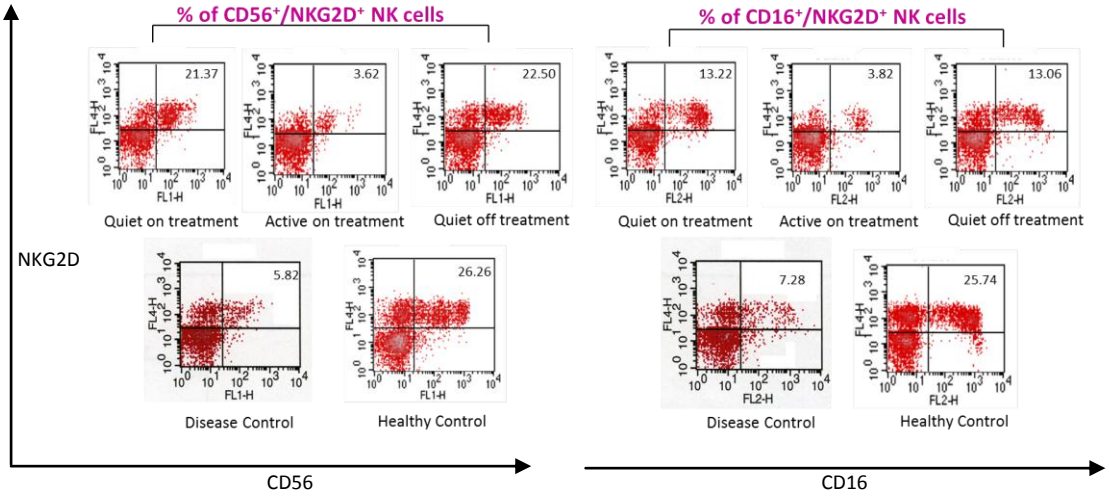
% of CD56+/NKG2D+ NK cells
% of CD16+/NKG2D+ NK cells
21.37
3.62
22.50
13.22
3.82
13.06
Quiet on treatment
Active on treatment
Quiet off treatment
Quiet on treatment
Active on treatment
Quiet off treatment
NKG2D
5.82
26.26
7.28
25.74
Disease Control
Healthy Control
Disease Control
Healthy Control
CD56
CD16

(B)

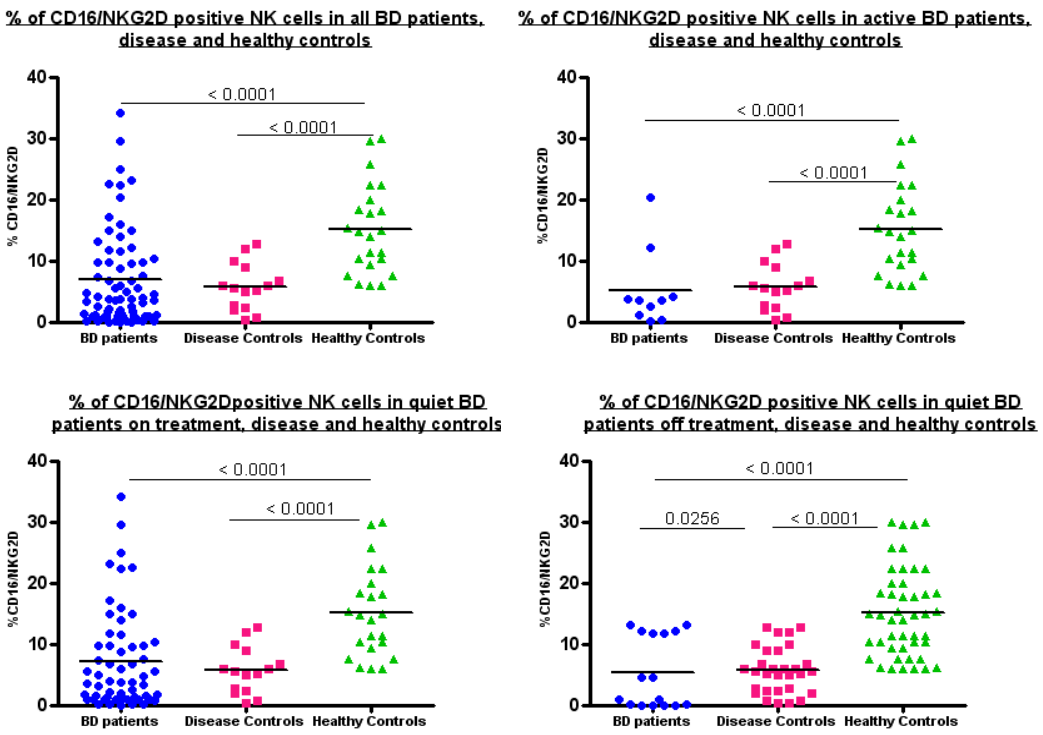
% of CD16/NKG2D positive NK cells in all BD patients, disease and healthy controls
% of CD16/NKG2D positive NK cells in active BD patients, disease and healthy controls
% of CD16/NKG2Dpositive NK cells in quiet BD patients on treatment, disease and healthy controls
% of CD16/NKG2D positive NK cells in quiet BD patients off treatment, disease and healthy controls
% CD16/NKG2D
%CD16/NKG2D
< 0.0001
0.0256
BD patients
Disease Controls
Healthy Controls

(C)

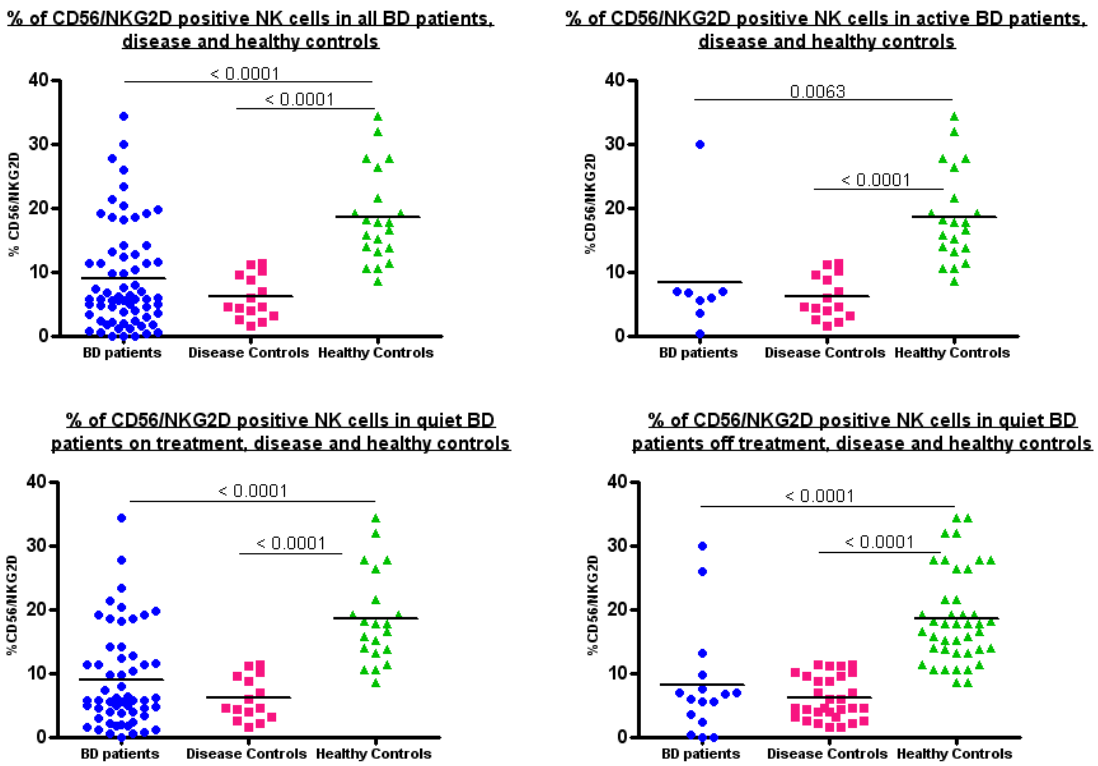


**Figure 4.2**: Comparative flow cytometry and graphical analysis of NKG2D positive NK cells from patients, disease and healthy controls. (A) FACS analysis: Example of the percentage of NK and T cells expressing CD16/CD56/NKG2D from active patients on treatment, quiet patients on treatment and quiet patients off treatment when compared with disease and healthy controls. The graphs outline the differences in percentages of (B) CD16/NKG2D and (C) CD56/NKG2D positive NK cells from all BD patients, active patients on treatment (n=13), quiet patients undergoing treatment (n=69) and quiet patients off treatment (n=8) when compared with disease (n=16) and healthy (n=23) controls. P values indicate statistically significant differences: $P < 0.05$, measured by ANOVA statistical analysis.

## 4.2 Patients on average have decreased percentages of NKG2D$^+$ γδT cells in peripheral blood.

The percentages of NKG2D$^+$ γδ T cells were significantly reduced in BD patients with active disease, but levels were restored in patients on treatment, and patients with quiescent disease showed no difference from controls. Most γδ T cells from each cohort are NKG2D$^+$ (Figure 4.3 A). CD8$^+$/NKG2D$^+$ cells were consistently reduced in patients with active BD and in disease controls. Normal levels were not restored by treatment. There is a spread of quiet patients on treatment with some that have high, moderate and low percentages of CD8+/NKG2D+ cells, whereas quiet patients off treatment all have percentages lower than 10%. (Figure 4.4)

(A)

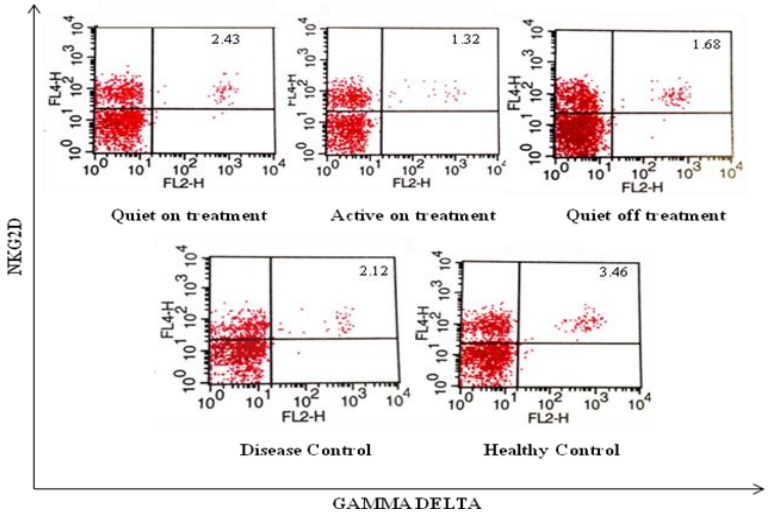


(B)

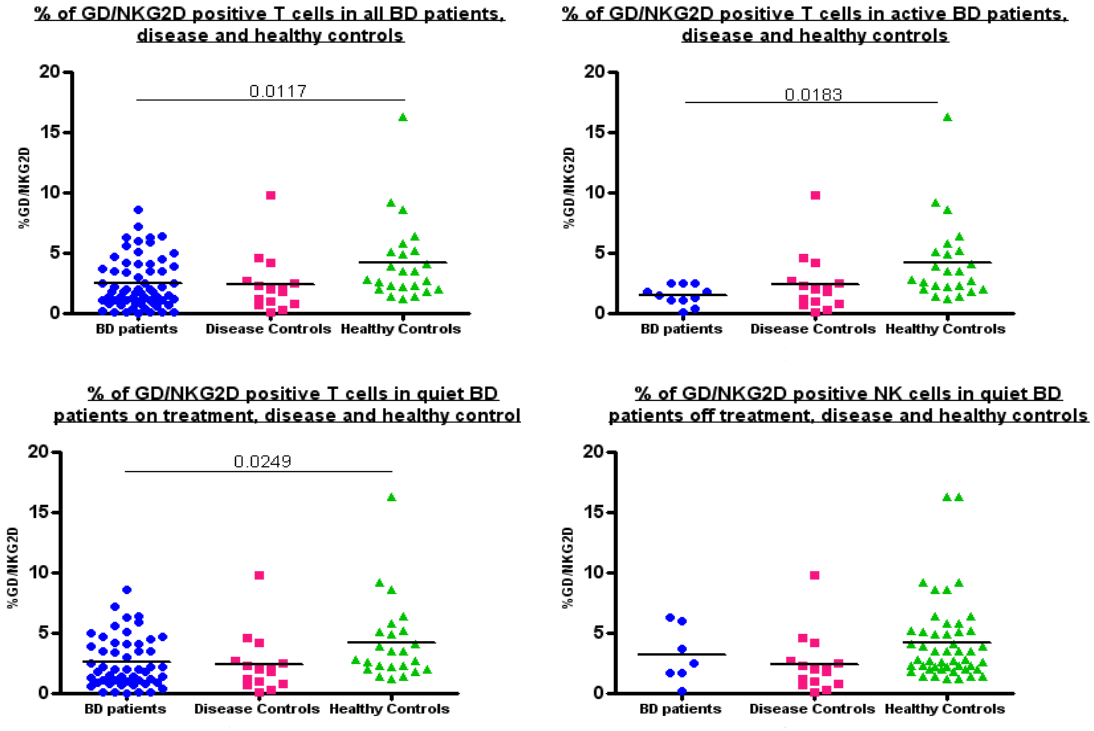


**Figure 4.3**: Comparative flow cytometry of NKG2D positive $\gamma\delta^+$ T cells from patients, disease and healthy controls. (A) FACS analysis: Example of the percentage of $\gamma\delta^+$ T cells expressing NKG2D from active patients on treatment, quiet patients on treatment and quiet patients off treatment when compared with disease and healthy controls. (B) Percentages of GD/NKG2D positive T cells from all BD patients, active

patients on treatment (n=13), quiet patients undergoing treatment (n=69) and quiet patients off treatment (n=8) when compared with disease (n=16) and healthy (n=23) controls. P values indicate statistically significant differences: $P < 0.05$, measured by ANOVA statistical analysis.

(A)

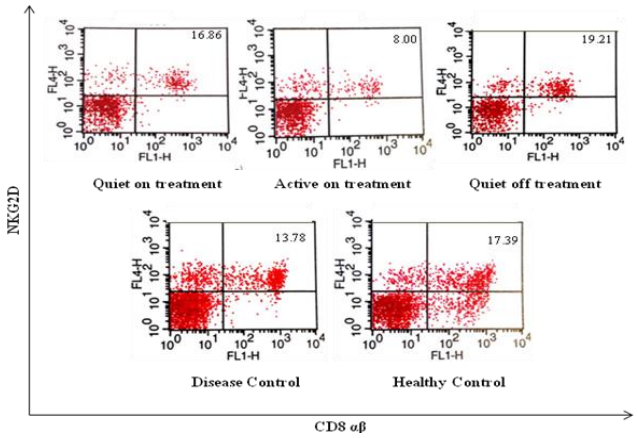


(B)

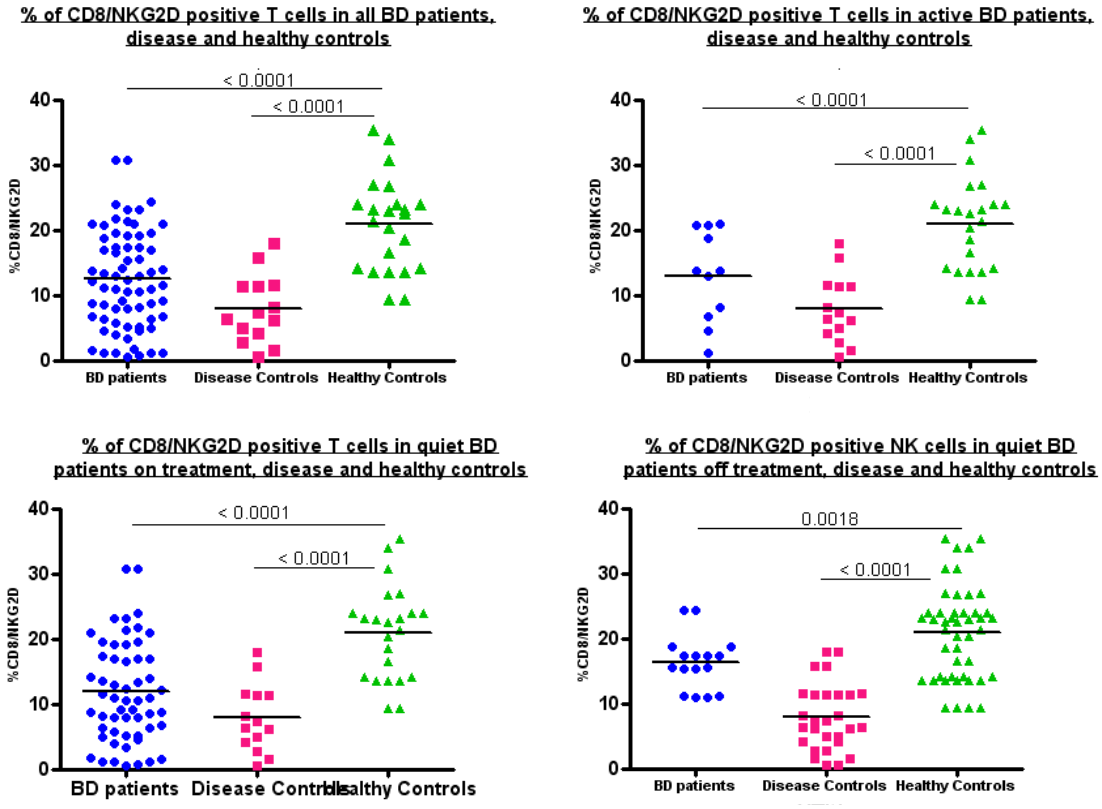


**Figure 4.4**: Comparative flow cytometry and graphical analysis of NKG2D positive $CD8^+$ T cells from patients, disease and healthy controls. (A) FACS analysis: Example of the percentage of $CD8^+$ T cells expressing NKG2D from active patients on treatment quiet patients on treatment and quiet patients off treatment when compared with disease and healthy controls. (B) The graphs below outline the

differences in percentages of CD8/NKG2D positive T cells from all BD patients (n=90), active patients on treatment (n=13), quiet patients undergoing treatment (n=69) and quiet patients off treatment (n=8) when compared with disease (n=16) and healthy (n=23) controls. P values indicate statistically significant differences: $P < 0.05$, measured by ANOVA statistical analysis.

---

## 4.3 Patients have decreased percentages of KIR3DL1$^+$ NK and T cells in peripheral blood.

The percentages of CD56$^+$/KIR3DL1$^+$ NK and T cells from patients and disease controls are significantly lower in peripheral blood when compared to healthy controls. These differences in patients may be accounted for by the change in disease activity and whether they are on treatment or not (Figure 4.5).

(A)

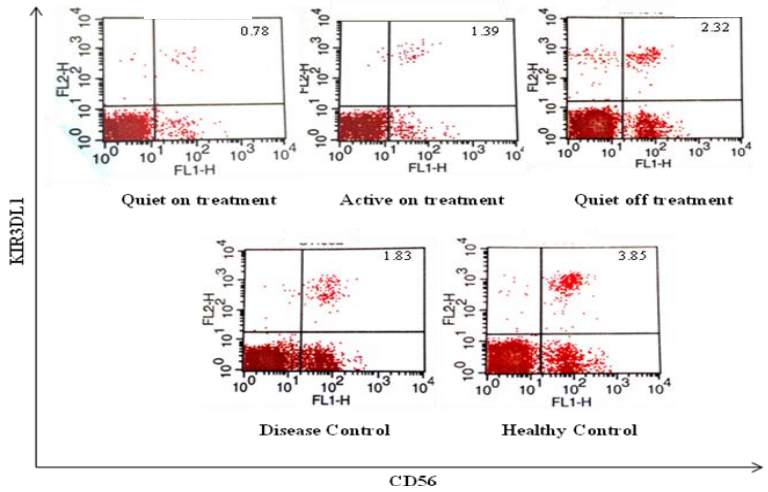


(B)

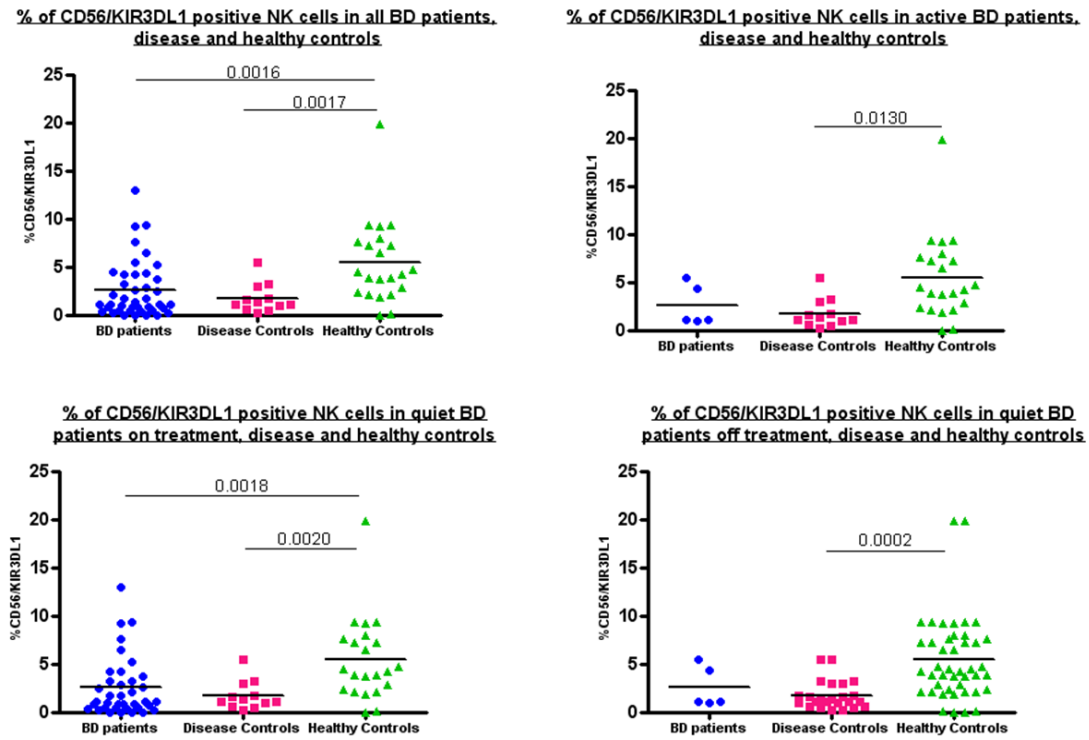


**Figure 4.5**: Comparative flow cytometry and graphical analysis of $CD56^+$ NK cells expressing KIR3DL1 from patients, disease and healthy controls. (A) FACS analysis: Example of the percentage of $CD56^+$ NK cells expressing KIR3DL1 from active patients on treatment, quiet patients on treatment and quiet patients off

treatment when compared with disease and healthy (n=23) controls. (B) The graphs below outline the differences in percentages of CD56/KIR3DL1 positive NK cells from all BD patients (n=90), active patients on treatment (n=13), quiet patients undergoing treatment (n=69) and quiet patients off treatment (n=8) when compared with disease (n=16) and healthy (n=23) controls. P values indicate statistically significant differences: $P < 0.05$, measured by ANOVA statistical analysis.

---

## 4.4 Percentages of $CD3^+/CD16^+$ T and $CD3^+/CD56^+$ T cells are significantly lower in patients with active disease

The percentages of $CD3^+/CD56^+$ T cells in all patient groups are similar and show no significant difference when compared to disease and healthy controls. (Figure 4.6) These data compared to Figure 4.2 suggest that NK cells and not $CD56^+$ T cells are most susceptible to dyregulation, seemingly by treatment. The percentages of $CD3^+/CD16^+$ T cells in active patients are significantly lower when compared to both disease and healthy controls. (Figure 4.7) This suggests that this difference may be attributable to an effect of the disease. $CD3^+/CD56^+/CD16^+$ T cells are probably NKT cells (Khvedelidze et al., 2008).

(A)

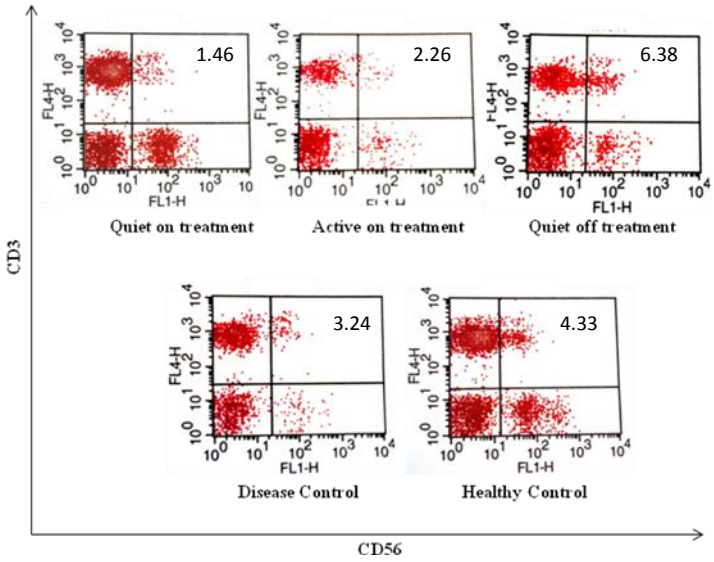


(B)

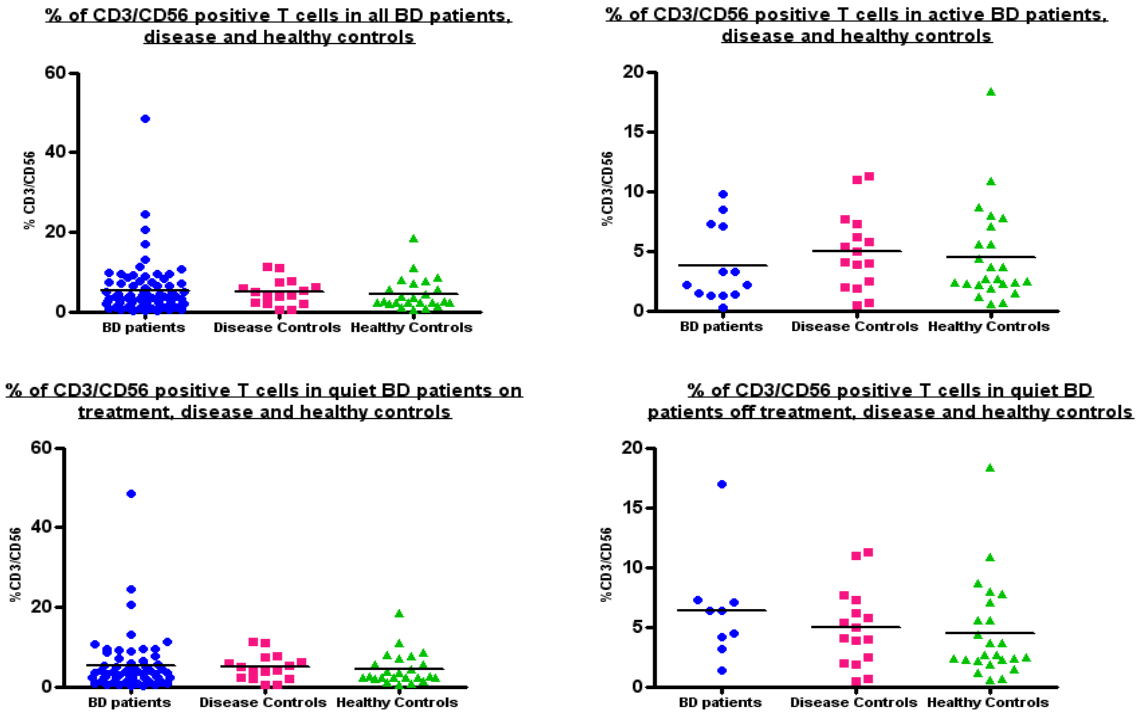


**Figure 4.6**: Comparative flow cytometry and graphical analysis of $CD3^+$ T cells expressing CD56 from patients, disease and healthy controls. (A) FACS analysis: Example of the percentage of $CD3^+$ T cells expressing CD56 from active patients on treatment, quiet patients on treatment and quiet patients off treatment when

compared with disease and healthy controls. (B) The graphs outline the differences in percentages of CD3/CD56 positive T cells from all BD patients (n=90), active patients on treatment (n=13), quiet patients undergoing treatment (n=69) and quiet patients off treatment (n=8) when compared with disease (n=16) and healthy (n=23) controls. P values indicate statistically significant differences: $P < 0.05$, measured by ANOVA statistical analysis.

(A)

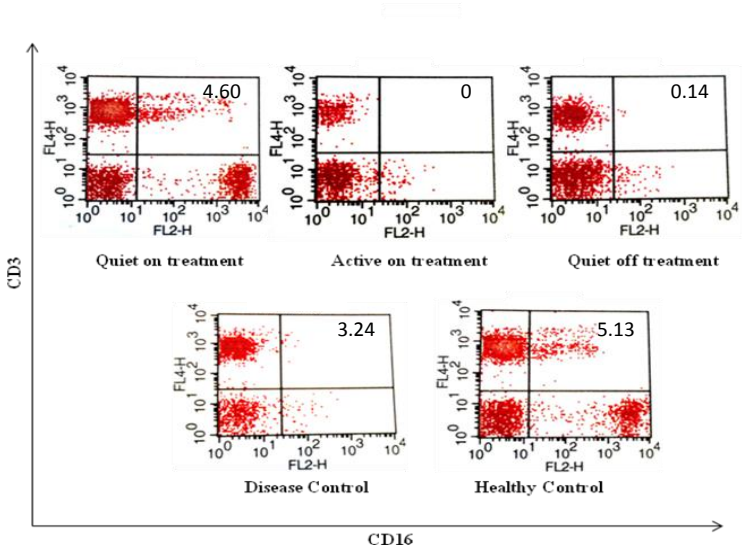


(B)

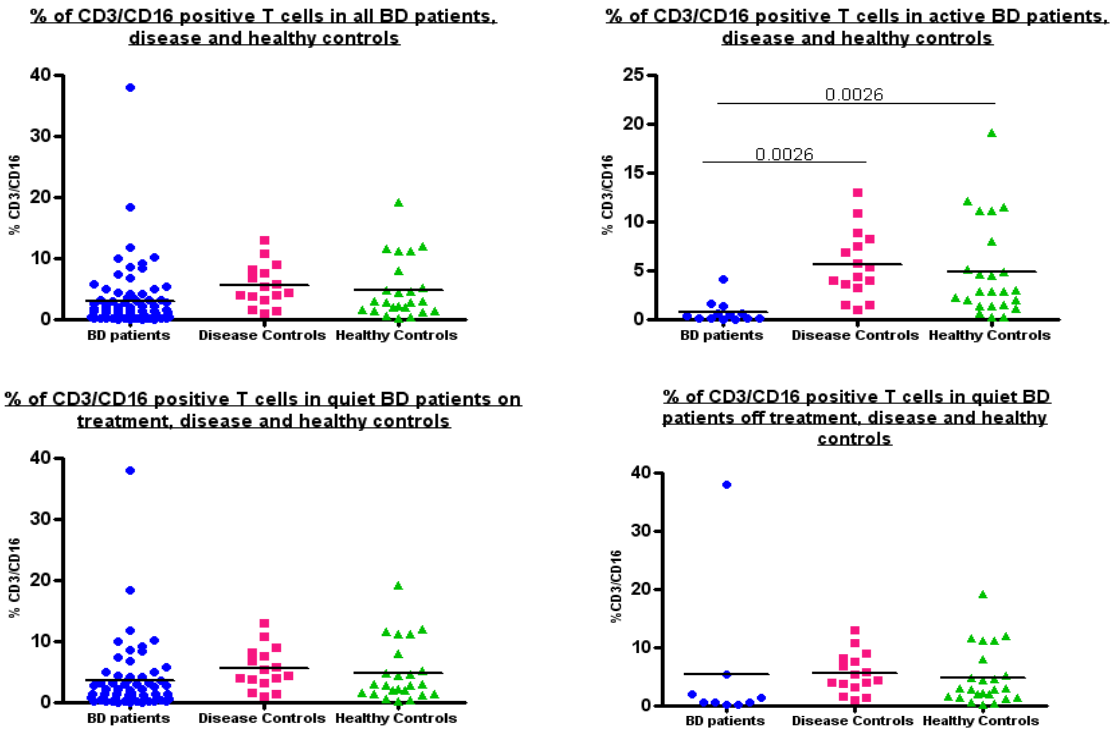


**Figure 4.7**: Comparative flow cytometry and graphical analysis of $CD3^+$ T cells expressing CD16 from patients, disease and healthy controls. (A) FACS analysis: Example of the percentage of $CD3^+$ T cells expressing CD16 from active patients on treatment, quiet patients on treatment and quiet patients off treatment when

compared with disease and healthy controls. (B) The graphs below outline the differences in percentages of CD3/CD16 positive T cells from all BD patients (n=90), active patients on treatment (n=13), quiet patients undergoing treatment (n=69) and quiet patients off treatment (n=8) when compared with disease (n=16) and healthy (n=23) controls. P values indicate statistically significant differences: $P < 0.05$, measured by ANOVA statistical analysis.

---

## 4.5 Percentages of $CD14^+/CD56^+$ monocytes are significantly higher in patients

The percentages of $CD14^+/CD56^+$ monocytes in active patients on treatment and quiet patients off treatment are significantly higher when compared to healthy controls. There are approximately 2 fold higher percentages of these cells in these patients versus healthy controls, however this has not been compared to disease controls, and thus the effects of steroid treatment cannot be accounted for (Figure 4.8). This data is very surprising, as CD56 is expressed on a minor percentage of monocytes (as can be seen in healthy controls). However, in patients, there is an increased percentage of $CD14^+/CD56^+$ monocytes circulating in peripheral blood. It is not known whether these cells express KIR3DL1 or NKG2D, and therefore it has not been investigated whether these cells have any cytolytic potential. Furthermore, the function of these $CD56^+$ monocytes in patients has not been explored and thus their role in disease not determined.

(A)

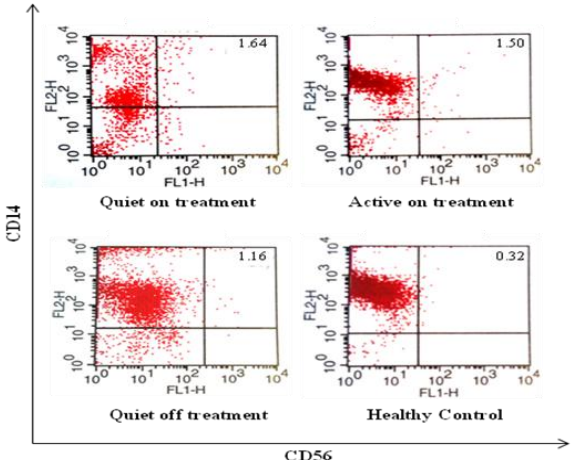


(B)

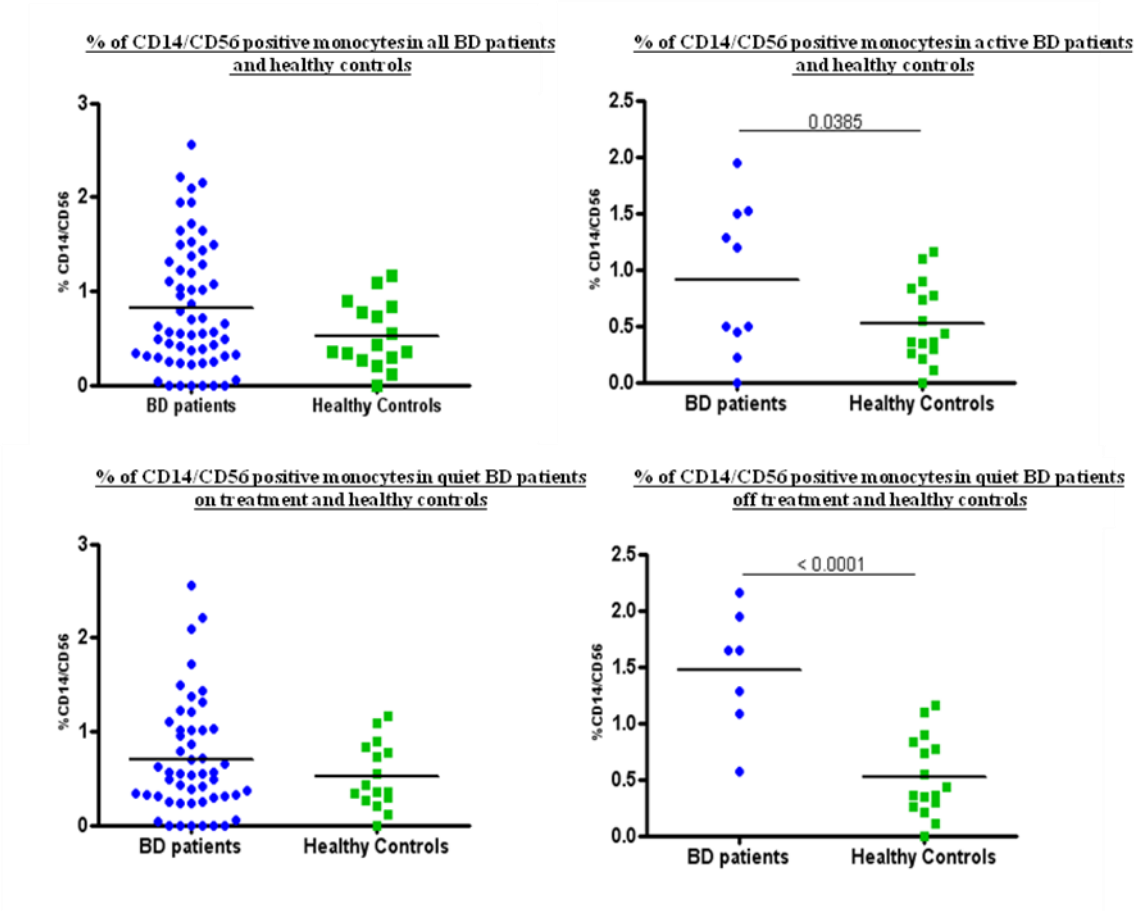


**Figure 4.8**: Comparative flow cytometry and graphical analysis of $CD14^+$ monocytes from patients and healthy controls. (A) FACS analysis: Example of the percentage of $CD14^+$ monocytes expressing CD56 from active patients on treatment, quiet patients on treatment and quiet patients off treatment when compared with disease and

healthy controls. The quadrant lines for each dot plot are different, as each patient was compared to their own isotype controls (data are not shown) (B) The graphs below outline the differences in percentages of CD14/CD56 positive monocytes from all BD patients (n=90), active patients on treatment (n=13), quiet patients undergoing treatment and quiet patients off treatment (n=8) when compared with disease (n=16) and healthy (n=23) controls. P values indicate statistically significant differences: $P<0.05$, measured by ANOVA statistical analysis.

---

## 4.6 The role of HLA-B*51 and B*52 in the proposed cellular model of Behcet's disease.

It has long been established that HLA-B*51 is the most important genetic factor that plays that an integral role in BD, in determining the pathogenesis with respect to disease susceptibility and expression. However, the mechanism underlying this is poorly understood. Until recently, it was difficult to venture into the functional importance of HLA-B*51 (disease associated isoform) in BD. However, integrating HLA-B*51 and HLA-B*52 (control isoform) into the developed CHO-FRT-MICA model to complete the cellular model of BD, made it possible to test the effects of HLA-B*51 and HLA-B*52 on the killing potential by $NKG2D^+$ NK and T cells from healthy controls and patients with BD. The data from these experiments would provide an insight into the pathogenesis of BD.

In this section I will describe the completion of the design of the cellular model of BD via the introduction of HLA-B*51 and HLA-B*52 into the CHO-MICA*009 cells to generate double transfectants which will be used in in vitro killing assays (described in chapter 2 and 3). This aim was to unravel the inhibitory potential of HLA-B subtypes on killing of MICA*009 cells and to determining if there are any differences between the inhibition seen in healthy controls and in patients.

## 4.7 Cloning and transfection of HLA-B*51 and HLA-B*52 genes

HLA-B*51 and HLA-B*52 genes were PCR amplified from the cell lines: AKIBA and JHAF respectively, using HLA-B specific primers and using a proof reading DNA polymerase enzyme. The PCR products were run on a 1% agarose gel. The bands corresponding to HLAB*51/*52 (1089bp) were cut out of the gel and purified, then cloned into a TOPO cloning vector. The chemically competent bacteria (*Escherichia coli* (E.coli), TOP10) were transformed with the recombinant plasmids and plated onto ampicillin after 24 hour's growth (Figure 4.9). Positive colonies were screened for the correct integration of the cDNA using restriction enzyme digestion and subsequently sequenced to confirm the successful inheritance of the correct ORF. The genes were then sub-cloned in to a pcDNA3.1-Neo vector that contains a neomycin resistance gene. The pcDNA3.1-Neo vector containing the GOI's (HLA-B*51 and HLA-B*52) were then transformed by chemically competent TOP10 bacteria. The colonies of bacteria were analysed for orientation of the GOI by restriction enzyme digestion (Figure 4.10). The vectors were then transfected into the CHO-FRT cells by electroporation. This results in GOI integrating randomly into the CHO genome. Positive cells expressing the GOI are then selected for neomycin resistance.

As a negative control, CHO-FRT cells were transfected with the parental pcDNA3.1-Neo vector for the generation of CHO-FRT neomycin resistant cells. After growth of the positive cells in neomycin resistant medium, the cells were then stained with an anti-HLA-B antibody and analysed for surface expression of the appropriate genes.

The full strategy is shown in Figure 4.11

(A)

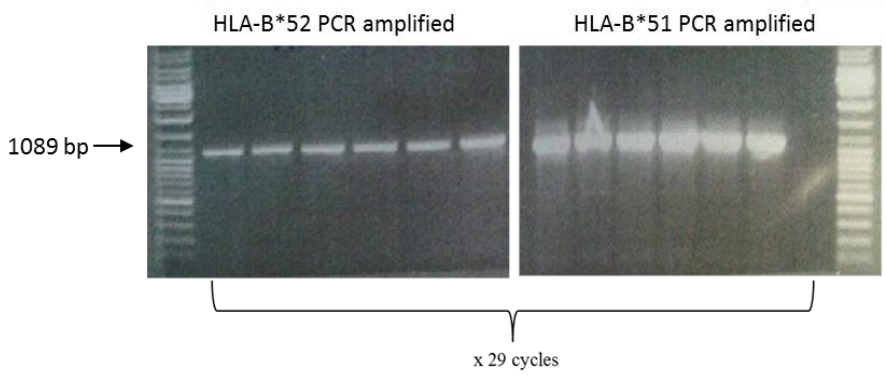


(B)

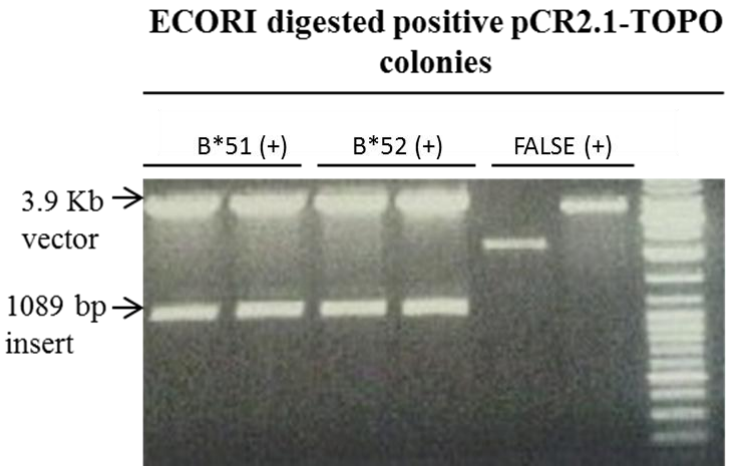


**Figure 4.9**: PCR amplification and cloning of HLA-B*51 and HLA-B*52 alleles. (A) PCR amplification of HLA-B alleles from the various cell lines: AKIBA (HLA-B*51) and JHAF (HLA-B*52). The PCR products were cloned into the pcr2.1 TOPO vector and (B) the positive colonies were digested with the ECORI restriction enzyme to determine which colonies incorporated the inserts (HLA-B*51 and *52). The positive colonies were then sequenced to obtain the colonies with perfect sequence data.

(A)

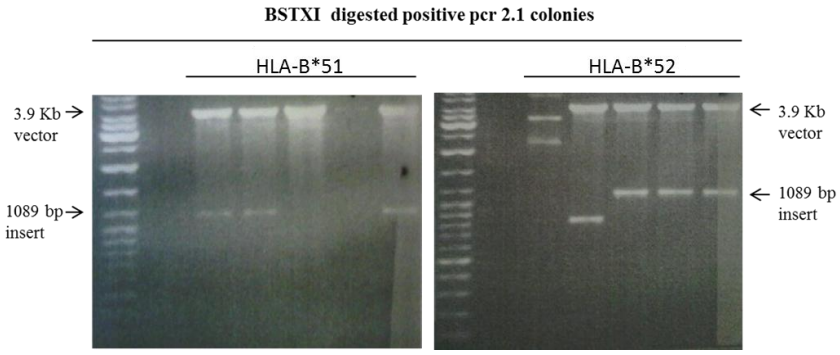


(B)

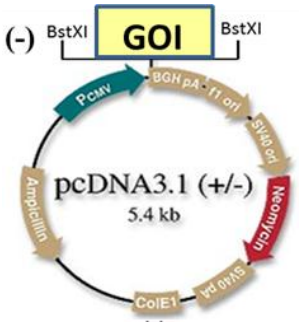


(C)

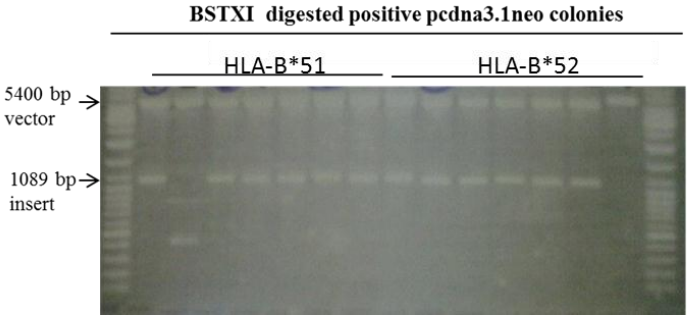


**Figure 4.10**: Subcloning of HLA-B*51 and HLA-B*52 alleles into the pcdna3.1 neo vector. HLA-B*51 and HLA-B*52 alleles were subcloned into the pcdna3.1 neo vector (expression vector) in the multiple cloning site (MCS), between the 2 BSTXI sites: (A) HLA-B*51 and HLA-B*52 alleles were cut out of the pcr2.1 TOPO vector, run on an agarose gel, gel purified and subcloned into the pcDNA3.1 neo vector. (B) Map of the pcdna3.1 neo vector with the multiple cloning site, showing where HLA -

B*51 and HLA-B*52 was inserted during cloning. (C) The positive colonies were digested with the BSTXI restriction enzyme to determine if any of the inserts had incorporated into the vector.

---

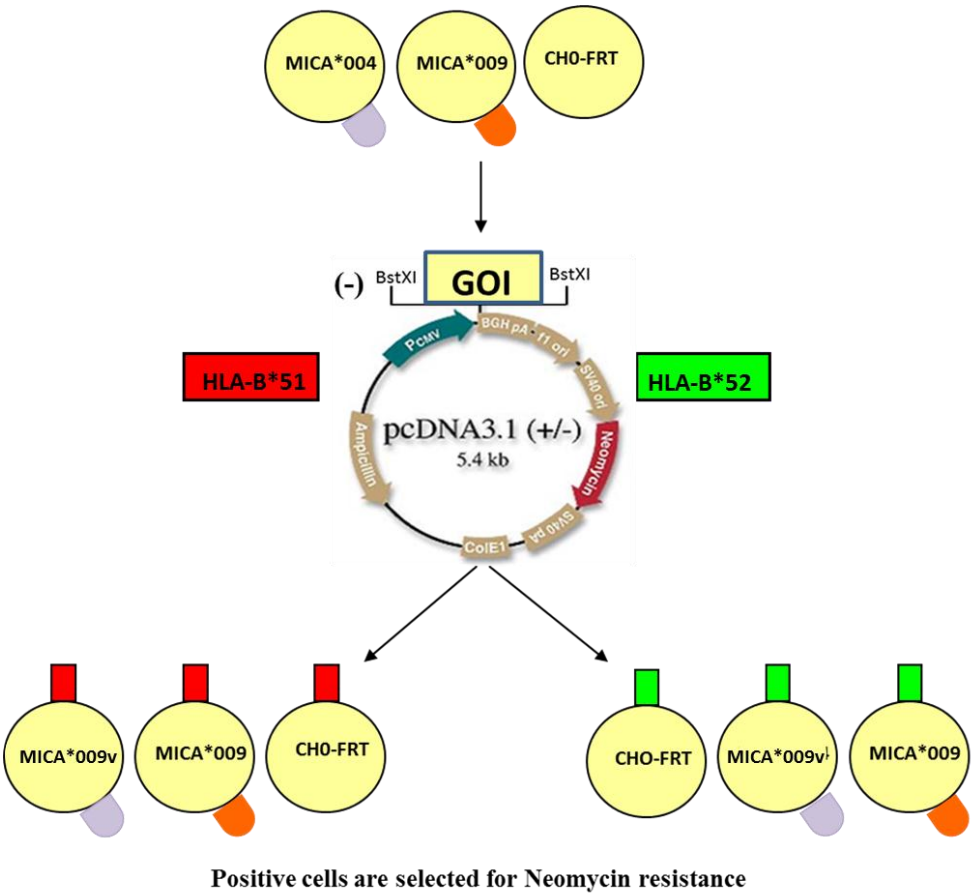


**Figure 4.11**: Diagram illustrating the cloning and transfection strategy of HLA-B*51 and HLA-B*52. Cloning of HLA-B*51 and HLA-B*52 into the pCDNA3.1-neo vector between the 2 BSTXI sites. Following transfection of the CHO-FRT, MICA*009v and MICA*009 cells with the HLA-B*51 and HLA-B*52-pCDNA3.1-neo vector, positive cells were maintained in 600ug/ml neomycin.

## 4.8 Lack of cell surface expression of HLA-B*51 and HLA-B*52

HLA-B*51 and HLA-B*52 surface protein expression was examined by staining using Flow cytometry analysis. The analysis showed a lack of surface protein expression by both HLA-B*51 and HLA-B*52 on both double-transfectants (MICA*009/ HLA-B*51 and MICA*009/ HLA-B*52) and the single transfectant (CHO-FRT-B*51). However, the PBMC's from one healthy donor (positive control) stained positive for HLA-B, illustrating that the anti-HLA antibody used for staining was indeed positively staining the HLA-B surface protein (Figure 4.12). Therefore, the double transfectants were tested for HLA-B*51 and B*52 RNA expression via PCR using HLA-B*5 specific primers, which showed a clear band of 1089bp corresponding to HLA-B*51 and B*52 RNA (Figure 4.13 A). Furthermore, the double transfectants were stained intracellularly with the anti-HLA-B antibody and compared to the negative control (CHO-FRT untransfected). The data produced from these staining confirmed the presence of intracellular pools of HLA-B*51 and HLA-B*52 protein (Figure 4.13 B). Thus it was intriguing to identify why the intracellular pools of protein were not translocating to the cell surface. For MHC class I molecules to be stably presented on the cell surface, they require association with beta-2-microglobulin ($\beta_2$M), however the CHO cells synthesise their own B2M. This however may not be sufficient in associating with human HLA genes and thus the observed absence of HLA-B*51 and *52 protein from the surface of the transfectants (Figure 4.12). Therefore human $\beta_2$M was PCR amplified using human $\beta_2$M specific primers and using a proof reading DNA polymerase enzyme. The PCR products were run on a 1% agarose gel. The bands corresponding to $\beta_2$M (1800bp) were cut out of the gel and purified, then cloned into a TOPO cloning vector. The chemically competent bacteria (TOP10) were transformed with the recombinant plasmids and plated onto ampicillin after 24 hour's. Positive colonies were screened for the correct integration of the cDNA using restriction enzyme digestion and subsequently sequenced to confirm the successful inheritance of the correct ORF. The genes were then sub-cloned in to a pCDNA3.1-Neo vector and transfected into the MICA*009/HLA-B*51 and MICA*009/HLA-B*52 and CHO-FRT-B*51 and B*52 cells. Positive cells were grown in neomycin resistant medium.

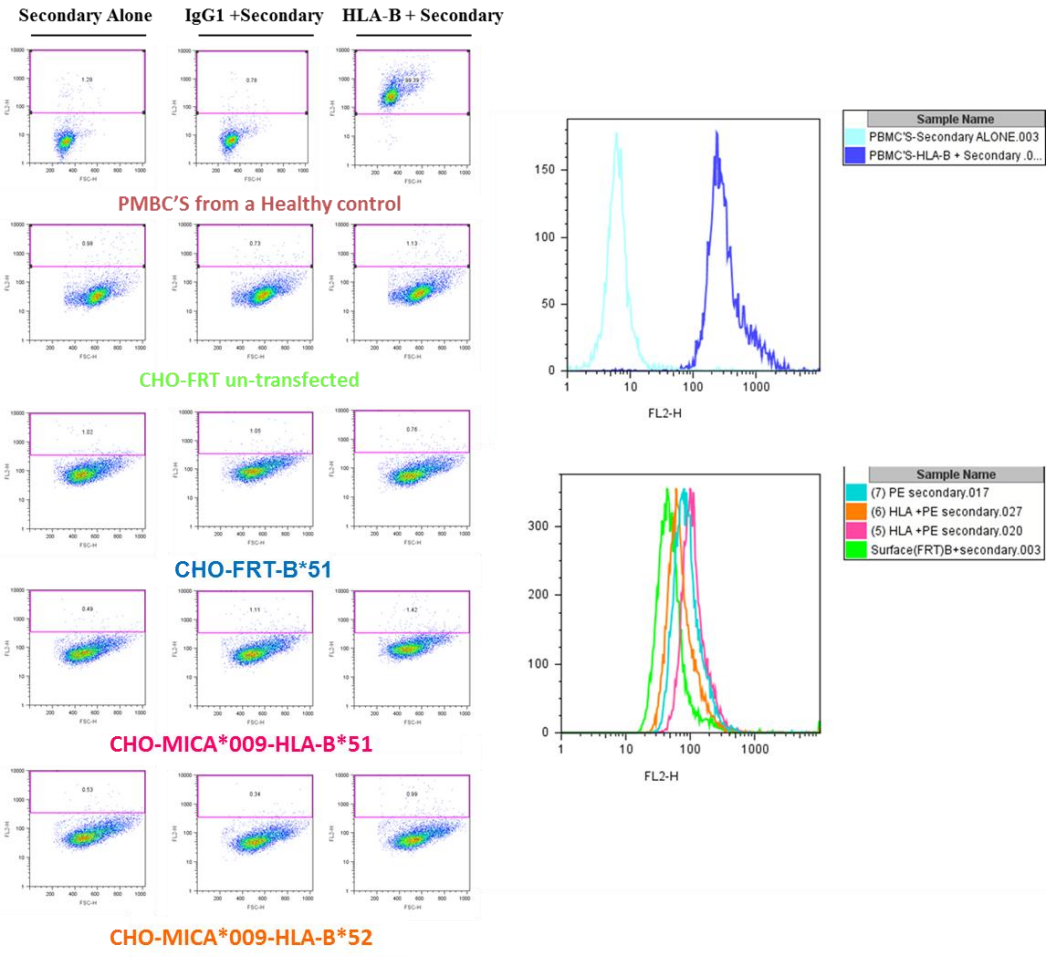


**Figure 4.12**: Surface expression profiles of MICA*009/HLA-B*51 and MICA*009/HLA-B*52 cells post transfection. Expression of HLA-B*51 and B*52 on the surface of the double transfectants (MICA*009/ HLA-B*51 and MICA*009/ HLA-B*52 cells) compared to the positive control; PBMC's (from one healthy individual) and the negative control; CHO-FRT-untransfected cells, analysed by flow cytometry. Data shown are representative dot plots, a comparative histogram of multiple stainings; with isotype control (mouse IgG1), mouse anti-human HLA-B and secondary antibody (goat anti-mouse IgG-PE). (representative of n>3)

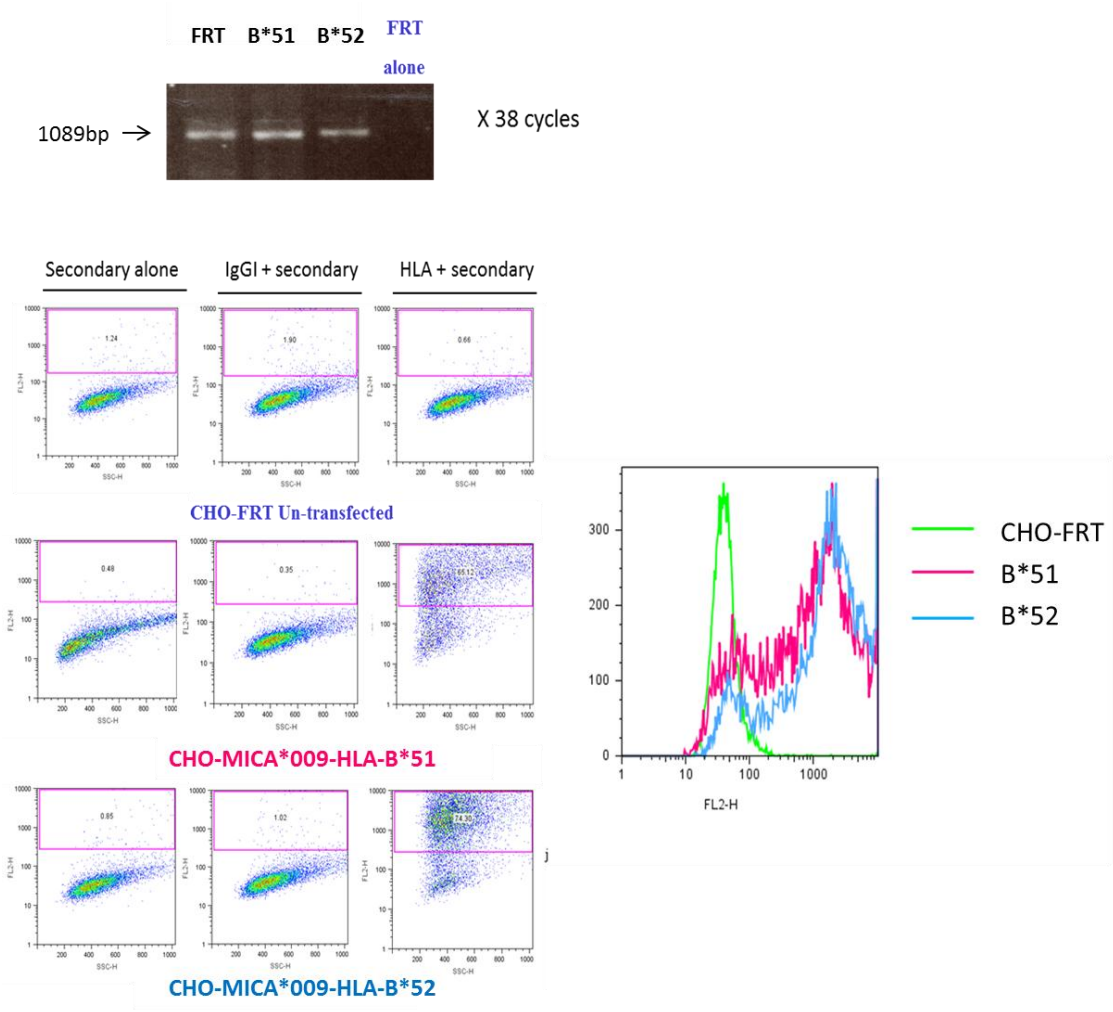


**Figure 4.13**: Intracellular expression profiles of HLA-B*51 and HLA-B*52. (A) RNA expression using HLA-B* specific primers showing the presence of HLA-B*51 and HLA-B*52 RNA in the CHO- MICA*009/ HLA-B*51 and MICA*009/ HLA-B*52 cells and CHO-FRT-B*51 cells compared to the negative control; CHO-FRT-untransfected cells, analysed by flow cytometry. Data shown are representative dot plots, a comparative histogram of multiple stainings; with isotype control (mouse IgG1), mouse anti-human HLA-B and secondary antibody (goat anti-mouse IgG-PE). (representative of n>3)

## 4.9 Detectable cell surface expression of HLA-B*51 and B*52 following transfection with human beta-2-microglobulin

Following transfection of β2M into the double transfectants (MICA*009/ HLA-B*51/ $\beta_2$M and MICA*009/ HLA-B*52/ $\beta_2$M cells) and single transfectants (CHO-FRT-B*51/ $\beta_2$M, CHO-FRT-B*52/ $\beta_2$M and CHO-MICA*009/ $\beta_2$M), the cells were stained with mouse anti-human HLA-B-PE and secondary antibody (goat anti-mouse IgG-PE) to detect any cell surface expression of protein. The data showed expression of both HLA-B*51 and B*52 at the surface of the cells. The data is representative of a number of stainings at different time points, which shows that at any given time point approximately 35% and 30% of cells express HLA-B*51 and HLA-B*52 respectively at the surface. (Figure 4.14) Thus this data confirms that human $\beta_2$M is a definite requirement for association with and HLA-B*51 and B*52 and their expression on the cell surface. Nevertheless, since the expression is not seen on most of the cells, in order to use these cells in subsequent assays, they had to be sorted using mouse anti-human HLA-B and secondary antibody (goat anti-mouse IgG-PE), such that most of the cells expressed the protein at the cell surface (Figure 4.15). These sorted cells were then used in cytotoxic *in vitro* killing assays using CFSE (as before) as target cells for PBMC's isolated from healthy donors and patients.

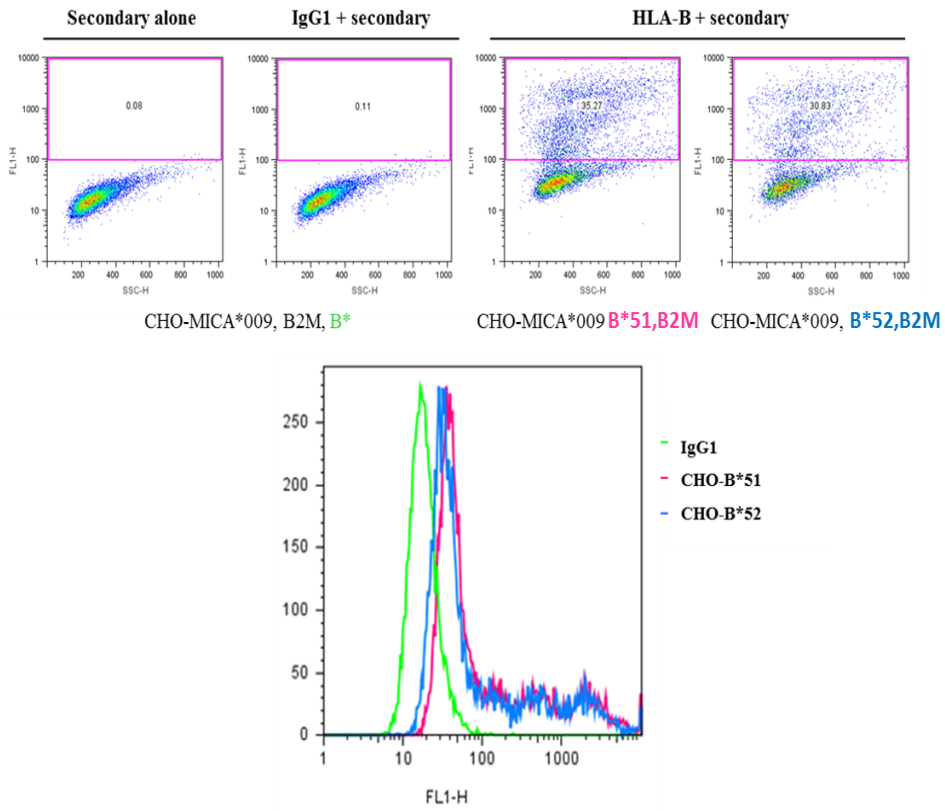


**Figure 4.14**: Cell surface protein expression of HLA-B*51 and HLA-B*52 proteins after transfection with human beta-2-microglobulin. MICA*009/ HLA-B*51/ $\beta_2$M and MICA*009/ HLA-B*52/ $\beta_2$M cells were stained for HLAB*51 and HLA-B*52 protein expression and compared to the negative control CHO-MICA*009/ $\beta_2$M transfectants. The cells were analysed by flow cytometry. Data shown are representative dot plots, a comparative histogram of multiple stainings; with isotype control (mouse IgG1), mouse anti-human HLA-B and secondary antibody (goat anti-mouse IgG-PE) (representative of n>3).

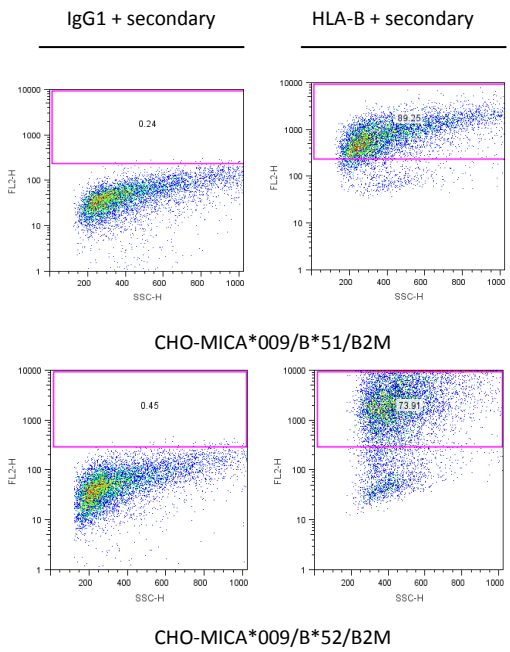


**Figure 4.15**: Cell surface protein expression of HLA-B*51 and HLA-B*52 after flow cytometry sorting of positive cells. MICA*009/HLA-B*51/$\beta_2$M and MICA*009/HLA-B*52/$\beta_2$M cells were stained for HLAB*51 and HLA-B*52 protein expression and the positive cells were sorted using the Flow cytometer. Approximately 24 hours later, 100,000 cells from each cell line (including CHO-FRT-HLA-B*51 and CHO-FRT-HLA-B*52, data not shown) were stained for HLA-B*51 and HLA-B*52 cell surface protein expression. Data shown are representative dot plots of multiple stainings; with isotype control (mouse IgG1), mouse anti-human HLA-B and secondary antibody (goat anti-mouse IgG-PE). (representative of n>3)

## 4.10 Selective inhibition of killing by HLA-B*51 in patients

The results determined by the analysis of the inhibitory potential of HLA-B*51 and HLA-B*52 in killing of the double transfectants was clearly observed in the killing assays (Figure 4.16 and 4.17). PBMC's from 13 healthy controls and 20 BD patients were used in killing assays as effector cells targeting the MICA*009 single transfectants and MICA*009/HLA-B*51 and MICA*009/HLA-B*52 double transfectants, the negative controls; CHO-FRT-B*51 and CHO-FRT-B*52. The data from the killing assays using the healthy controls (Figure 4.16) revealed that on average both B*51 and B*52 inhibited killing of the double transfectants compared to the killing of the single CHO-MICA*009 transfectants to the same extent by approximately 10% inhibition ($p=0.7495$) (Figure 4.18 (ii)). This indicates that there were no differences observed in the inhibitory potential of B*51 and B*52 in killing of the double transfectants by healthy controls. Data from KIR3DL1 typing showed that all healthy donors were KIR3DL1$^{+}$. (Table 4.1) The difference in percentages of KIR3DL1$^{+}$ NK cells revealed that this had no effect on the inhibitory potential of HLA-B*51 and B*52 (example healthy control 11 and 13) and correlation analysis showed no correlation between the inhibition of killing by HLA-B*51 and the the MFI (Mean fluorescence intensity) of KIR3DL1 expressed on NK cells (figure 4.19 (i)) and the percentage of KIR3DL1$^{+}$ NK cells (figure 4.19 (ii)) in all healthy controls.

The data from the killing assays using PBMC's from BD patients (Figure 4.17) was very intriguing. Similar to healthy controls, the KIR3DL1 typing showed that all patients were KIR3DL1$^{+}$ and the difference in percentages of KIR3DL1$^{+}$ NK cells shown, had no effect on the inhibitory potential of HLA-B*51 and HLA-B*52. (Table 4.2) However, most surprisingly, killing by the patient PBMC's was varied: B*51 inhibited killing of the double transfectants by approximately 45% of the patients compared to the killing of the single CHO-MICA*009 transfectants. In some cases B*51 inhibited killing by 35 and 50% ($p<0.052$) (patient number 1 and 3 respectively) (Figure 4.18 (ii)). By comparison, HLA-B*52 had no such effect and inhibition was similar to that seen in healthy controls (Figure 4.18 (i)). Similar to healthy controls, correlation analysis showed no correlation between inhibition of

killing by HLA-B*51 and the MFI (Mean fluorescence intensity) of KIR3DL1 expression on NK cells (figure 4.19 (i)) and percentages of KIR3DL1$^{+}$ NK cells (figure 4.19 (ii)) from BD patients used in this study.

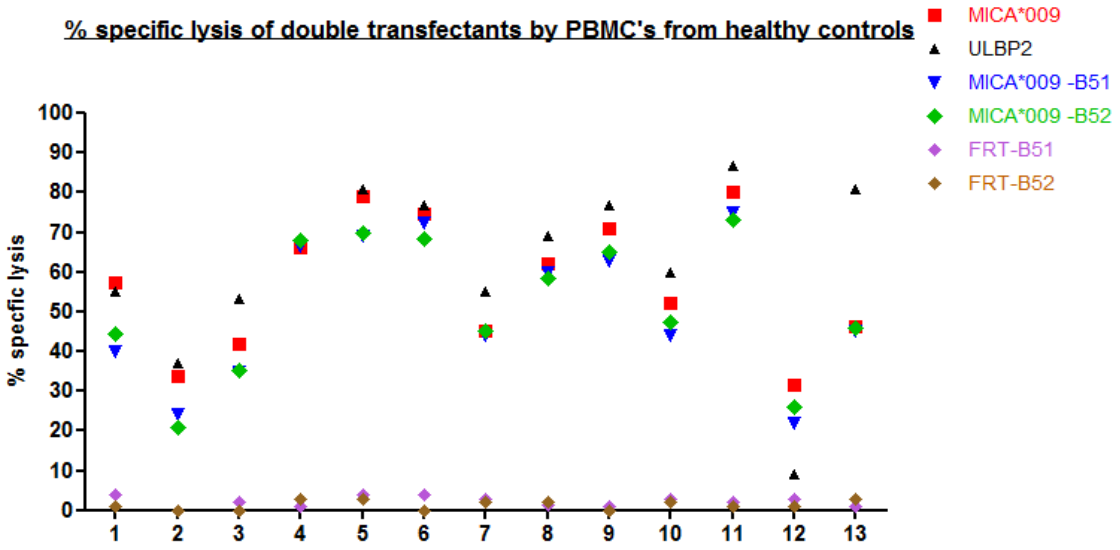


**Figure 4.16**: Killing of MICA*009/ HLA-B*51 and MICA*009/ HLA-B*52 cells by PBMCs from 13 healthy donors. Killing assay data from 13 healthy donors (controls) whereby the killing of MICA*009 single transfectants was compared to the double transfectants; MICA*009/HLA-B*51 and MICA*009/HLA-B*52 cells. The duration of the assay was 12 hours, and the target:effector ratio used was 1:20. The assay was carried out in triplicate, where a mean of the results was obtained, and percentage specific lysis of the transfectants was calculated and compared to the negative controls (CHO-FRT-B*51 and CHO-FRT-B*52) (n=1). Standard deviation (SD) was consistently < 5%, but is not shown so as to preserve the clarity of the figure.

| Healthy Donor | KIR3DL1 (+/-) | % inhibition by B51 | % inhibition by B52 | % of NK/KIR3DL1 | MFI of KIR3DL1 |
|---|---|---|---|---|---|
| 1 | + | 17.2 | 13 | 1.65 | 379.29 |
| 2 | + | 9.8 | 12.9 | 3.42 | 251.02 |
| 3 | + | 7.2 | 6.5 | 3.77 | 420.66 |
| 4 | + | 0 | 0 | 2.9 | 55.95 |
| 5 | + | 10 | 9 | 2.13 | 76.89 |
| 6 | + | 2.2 | 6.2 | 1.02 | 43.5 |
| 7 | + | 1 | 0 | 4.22 | 414.29 |
| 8 | + | 2 | 3.5 | 3.54 | 182.83 |
| 9 | + | 8 | 6 | 2.97 | 444.64 |
| 10 | + | 8 | 4.5 | 2.06 | 71.36 |
| 11 | + | 5.2 | 6.2 | 3.89 | 98.11 |
| 12 | + | 10 | 5 | 2.91 | 163.17 |
| 13 | + | 0.2 | 0.3 | 1.34 | 627.26 |

**Table 4.1**: Table illustrating KIR3DL1 (+/-) type, calculated percentage inhibition by HLA-B*51 and HLA-B*52, percentage of KIR3DL1$^{+}$ NK cells and the MFI (Mean fluorescence intensity) of KIR3DL1 expression on NK cells from 13 healthy donors (controls) in figure 4.16 (n=1).

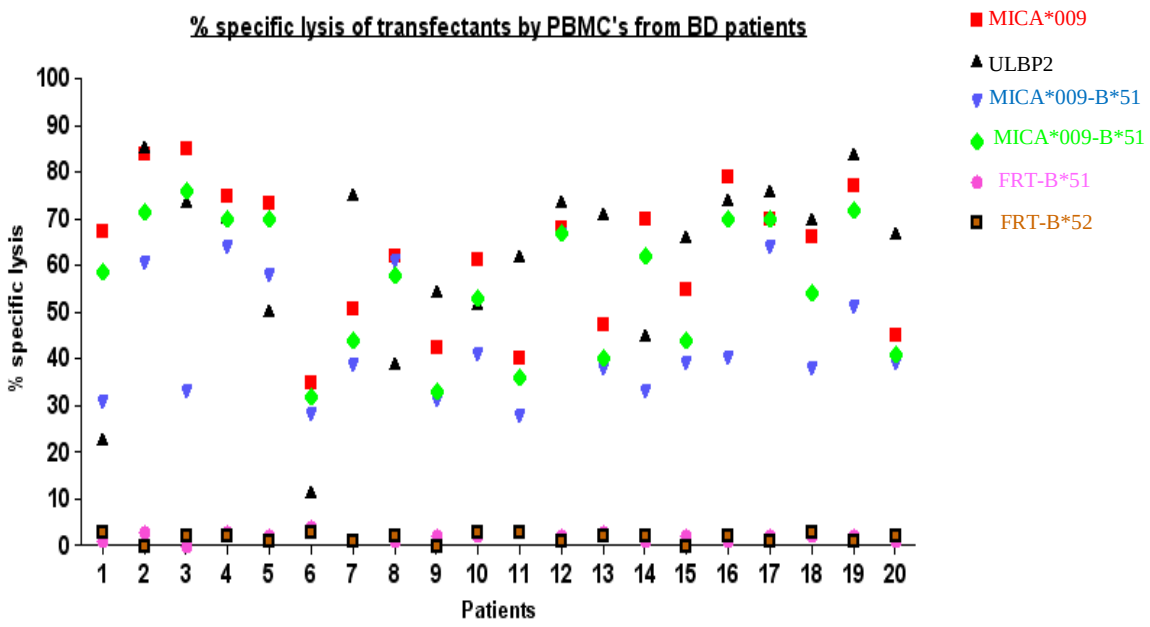


**Figure 4.17**: Killing of MICA*009/ HLA-B*51 and MICA*009/ HLA-B*52 cells by PBMCs from 20 Behcet's disease patients. Killing assay data from 20 BD patients, whereby the killing of MICA*009 single transfectants was compared to the double transfectants; MICA*009/ HLA-B*51 and MICA*009/ HLA-B*52 cells. The duration of the assay was 12 hours, and the target:effector ratio used was 1:20. The assay was carried out in triplicate, where a mean of the results was obtained, and percentage specific lysis of the transfectants was calculated and compared to the negative controls (CHO-FRT-B*51 and CHO-FRT-B*52) (n=1). Standard deviation (SD) was consistently < 5%, but is not shown so as to preserve the clarity of the figure.

| BD Patient | KIR3DL1 (+/-) | % inhibition by HLA- B*51 | % inhibition by HLA-B*52 | % of NK/KIR3DL1 | MFI of KIR3DL1 |
|---|---|---|---|---|---|
| 1 | + | 36.3 | 8.4 | 3.4 | 244.32 |
| 2 | + | 23.1 | 12.2 | 4.1 | 445.08 |
| 3 | + | 52.1 | 9.3 | 2.11 | 421.53 |
| 4 | + | 10.8 | 4.8 | 0.98 | 282.9 |
| 5 | + | 15.3 | 3.3 | 1.56 | 244.8 |
| 6 | + | 6.6 | 2.9 | 2.34 | 337.77 |
| 7 | + | 12.3 | 6.9 | 2.21 | 294.38 |
| 8 | + | 1 | 2 | 1.46 | 250.08 |
| 9 | + | 11.5 | 9.5 | 1.05 | 185.52 |
| 10 | + | 20.3 | 8.3 | 2.99 | 260.05 |
| 11 | + | 12.4 | 4.2 | 2.73 | 357.35 |
| 12 | + | 1.6 | 1.2 | 1.17 | 208.02 |
| 13 | + | 9.3 | 7.1 | 1.27 | 76.81 |
| 14 | + | 37 | 8 | 0.13 | 159.63 |
| 15 | + | 16 | 11 | 2.96 | 111.75 |
| 16 | + | 39 | 9 | 5.45 | 206.65 |
| 17 | + | 14 | 0 | 0.09 | 218.05 |
| 18 | + | 28 | 12 | 1.12 | 137.41 |
| 19 | + | 26 | 5 | 0.14 | 322.2 |
| 20 | + | 6 | 4 | 3.09 | 232.21 |

**Table 4.2**: Table illustrating KIR3DL1 (+/-) type, calculated percentage inhibition by HLA-B*51 and HLA-B*52, percentage of KIR3DL1$^{+}$ NK cells and the MFI (Mean fluorescence intensity) of KIR3DL1 expression on NK cells from 20 BD patients in figure 4.17 (n=1).

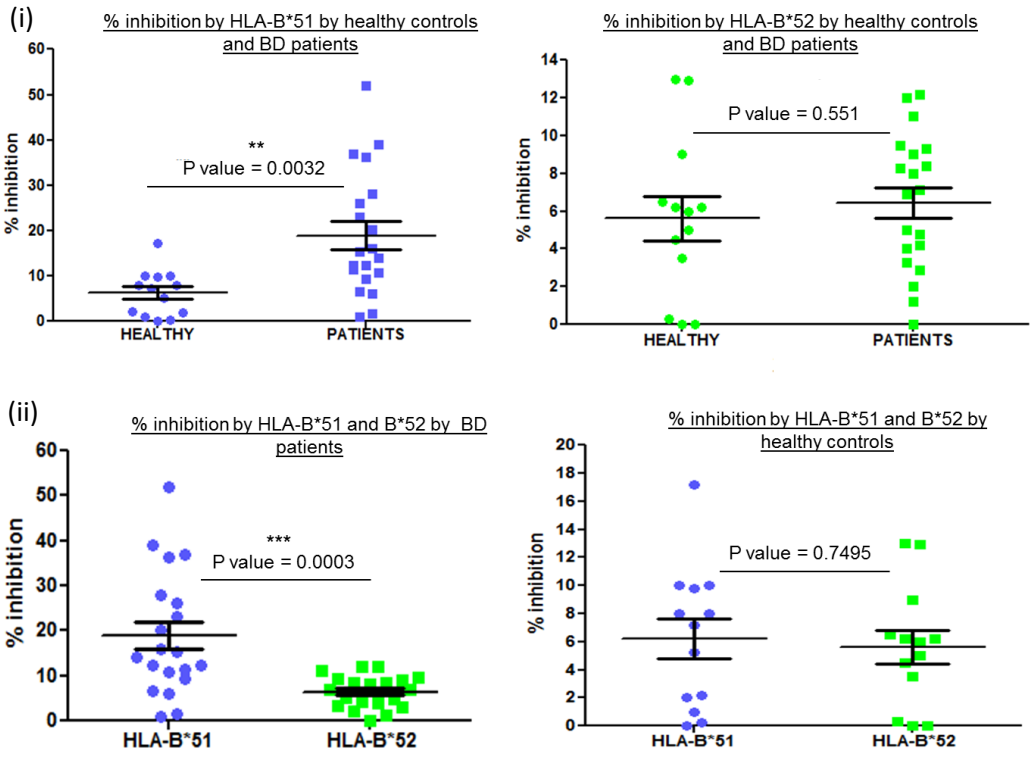


**Figure 4.18**: Graphical representation of the calculated percentage inhibition of killing of double transfectants by HLA-B*51 and HLA-B*52 by PBMCs from Behcet's disease patients and healthy donors (controls). (i) Percentage inhibition by HLA-B*51 and HLA-B*52 by healthy controls and BD patients (ii) Percentage inhibition by HLA-B*51 and HLA-B*52 by patients and healthy controls. P values indicate statistically significant differences: $P < 0.05$, measured by unpaired t-test statistical analysis.

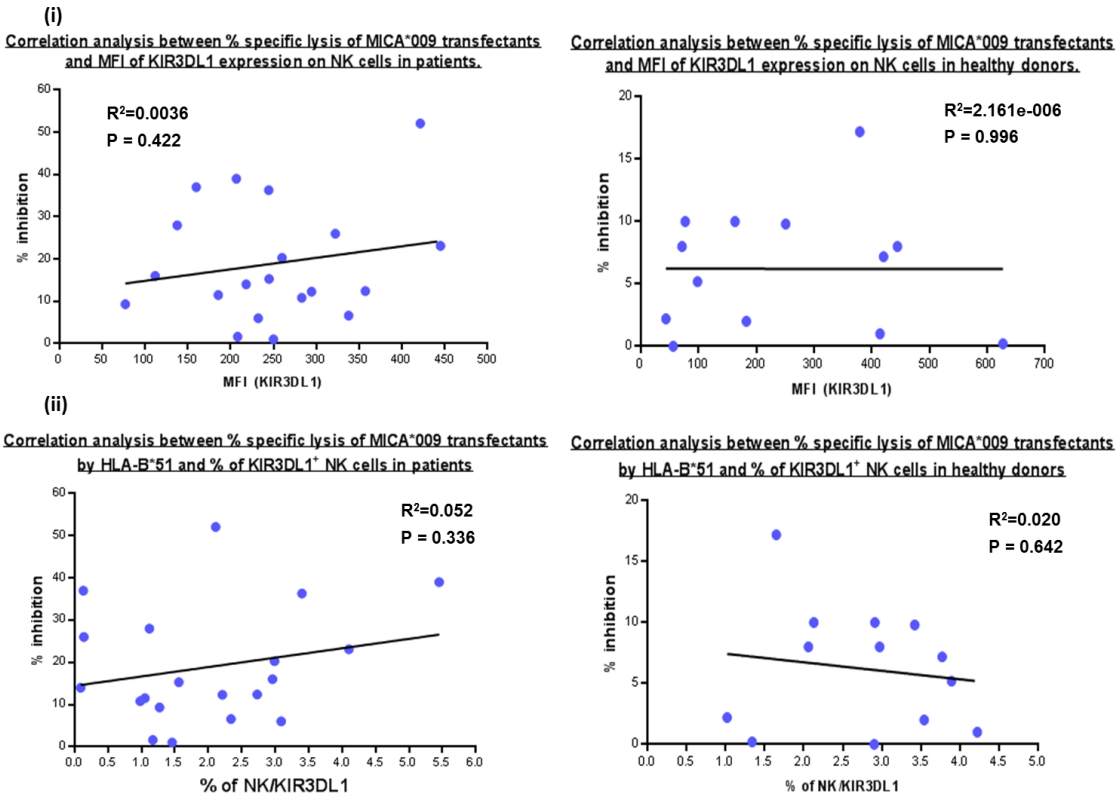


**Figure 4.19**: Graphical representation of the Correlation analysis between percentage inhibition of killing by HLA-B*51 and the percentage of KIR3DL1$^+$ NK cells and MFI of KIR3DL1 expression on NK cells from 22 Behcet's disease patients and 13 healthy donors (controls). (i) Correlation analysis between the percentage inhibition of killing of double transfectants by HLA-B*51 and the MFI (Mean fluorescence intensity) of expression of KIR3DL1 on NK cells from 22 BD patients and 13 healthy donors (controls) (ii) Correlation analysis between percentage inhibition by HLA-B*51 and percentage of KIR3DL1$^+$ NK cells from 22 BD patients and 13 healthy controls. The $R^2$ and P values are shown for each analysis graph, measured by linear regression analysis.

## 4.11 Discussion

Previous studies have reported an increase in NK cells, γδT cells, and memory $CD8^+$ T cells numbers in patients with active BD, and a decrease on treatment, including IFN2α. However, the data from the patients with BD, disease and healthy controls from this study showed $CD16^+CD56^+$ NK cells, γδT cells and $CD8^+$ T cells expressing NKG2D were all significantly decreased in active disease. On treatment numbers of γδ/NKG2D cells were restored to control levels, while the other populations remained low.

IL-15 has been shown to increase the expression of NKG2D on the surface on NK and T cells (Wu et al 2004). Previous studies by our group have shown that IL-15 is significantly raised in patients with BD, although there was no difference between active and quiescent patients or the level of treatment. (Curnow et al., 2008) Conversely, Hamzaoui reported an increase in serum IL-15 from patients with active BD compared to patients with quiet disease. The reason for the difference may be due to patients in this study having neuro-BD or because active disease developed when patients were off treatment (Hamzaoui et al., 2006). Further studies in other cohorts are required to determine the role of this cytokine in BD, particularly with regards to NKG2D expression.

As stated soluble MICA can down-regulate NKG2D expression. The levels of soluble MICA have not been investigated in this study therefore it is not possible to comment on any role in the significant decrease in the expression of NKG2D on NK and T cells when compared with healthy controls. Similarly, chronic expression of ligands can reduce NKG2D levels and this should be determined in tissue samples from patients with BD.

The data presented here shows a decrease in percentage of circulating $KIR3DL1^+$ NK cells, in patients which is different to that previously published (Saruhan-Direskeneli et al., 2004), where a similar percentage of positive cells was observed in patients and healthy controls. However, KIR3DL1 expression was found to be abnormal on $CD56^+$ cells in patients with severe eye disease (Takeno et al., 2004), and all of the patients used in our study had uveitis. Other reasons for these differences may be

ethnic, or due to other disease manifestations. Finally, as KIR3DL1 is polymorphic it would be of interest to type individuals to determine if specific isoforms are decreased more than others.

The effect of treatment of patients must also be taken into account. Treatments include cyclosporine and prednisone, which may have an adverse effect on the surrounding cytokine milieu and on chemokine and chemokine receptor expression which affects immune cell sequestration. This in turn may affect the expression of CD56, KIR3DL1 and NKG2D on the surface of $CD8^+$ T cells, γδ T cells (NKG2D expression significant only in patients on treatment) and NK cells, thus influencing the dynamics of the immune response. Finally, the decrease of $NKG2D^+$ cells in the peripheral blood of active BD patients may be due to these cells infiltrating the sites of inflammation in the tissues. Intraocular infiltration of TcRαβ $CD8^{bright}$ $CD56^+$ cells is a distinct feature of Behcet's disease, CD94 expression was increased and NKG2D expression down-regulated (Ahn et al., 2005).

The discovery of $CD14^+$ monocytes expressing CD56 is a novel finding. The function of these cells is not yet determined. Similarly, the $CD3^+CD56^+$ T cells and $CD3^+CD16^+$ T cells been described in one study, as being natural killer like T cells (Bojarska-Junak et al., 2010). The function of these cells needs to be investigated.

The concept of the inhibitory potential of HLA-B*51 in BD has not previously been studied. In this section, I sought to address the role of HLA-B*51 by the generation of the cellular model of BD. In this model HLA-B*51 and the control allele HLA-B*52 were introduced into CHO cells separately and used in two complementary *in vitro* assays of cytolysis. HLA-B*51 and B*52 were PCR amplified and subcloned into a pcdna3.1neo vector and transfected into the CHO-FRT-MICA*009 and CHO-FRT cells. Initial experiments determined that surface expression of HLA-B*51 and B*52 was null (Figure 4.4). However after intracellular staining of CHO-MICA*009/B*51 and CHO-MICA*009/B*52 cells, pools of intracellular B*51 and B*52 protein were observed, as was the presence of HLA-B*51 and B*52 RNA (Figure 4.5). The results of this instigated the cloning and transfection of human β2-microglobulin into the CHO-MICA*009/B*51, CHO-MICA*009/B*52 and CHO-FRT/B*51 and B*52 cells. Following this, cell surface expression of B*51 and B*52

was observed (Figure 4.6), but was not sufficient to be comparably used in killing assays with the CH0-MICA*009 high expresser cells (see chapter 2). This hurdle was overcome by specifically sorting the B*51 and B*52 single and double transfectants using specific antibodies (Figure 4.7) so that most cells expressed the protein on the surface.

The single MICA*009 transfectants and double transfectants were used as targets for freshly isolated PBMC from a sizeable cohort of both healthy controls and patients in killing assays to determine specific inhibition by B*51 on the killing of the CHO-MICA*009/B*51 transfectants compared to the CHO-MICA*009 cells. The results from the healthy controls showed a slight inhibitory potential equally by both B*51 and B*52 (approximately 10%) on the killing of the double transfectants compared to CHO-MICA*009 alone (Figure 4.8). However, the results from the killing assays using PBMC from patients were diverse and distinct. Approximately 45% of patients showed a clear and strong inhibition of killing of MICA*009 by B*51 compared to B*52. Correlation analysis showed no correlation between the inhibition of killing by HLA-B*51 and the percentage of circulating KIR3DL1+ NK cells or KIR3DL1 expression on NK cells in both the healthy control and BD patient cohorts. This specific inhibition of killing by B*51 in certain patients may suggest several potential theories such as the binding affinity of HLA-B*51 for KIR3DL1 in patients, for example: the different KIR3DL1 polymorphisms which may have an effect on the binding potential of these isoforms to HLA-B*51 and the increased expression of HLA-B*51 on patient cells which allows for the stronger binding of HLA-B*51 to KIR3DL1 in patients (discussed in chapter five).

In conclusion, there are many potential reasons for the selective inhibition of killing by B*51 seen only in patients, which remain unresolved. It would also be potentially important to carry out longitudinal studies on these patients to determine whether they show the same pattern of inhibition of killing over a set period of time, when the patients are in remission and when they are receiving treatment.

# CHAPTER FIVE - DISCUSSION

## 5.1 – Aim of the thesis

This thesis has investigated one component of Behcet's Disease, a significant unmet clinical need. That component is the genetic linkage to HLA-B*51 and to MICA*009. The genetic linkage to HLA-B*51 is widely accepted. However, the linkage to MICA*009 is more contentious, because it might simply reflect the linkage disequilibrium of MICA*009 with HLA-B*51. Nonetheless, the intriguing possibility exists that both genes are functionally linked to BD since they may both regulate the same target cells, NK cells or T cells, which have been implicated in disease by pathology and other related studies. In confronting this possibility, it is evident that there has been very little direct, head-to-head comparison of MICA isoforms for their capacity to evoke the functions of NK and/or T cells, and no comparison of the impact on this of polymorphic HLA-B isoforms. Therefore, this thesis undertook such investigations, examining how NK cells and T cells from different individuals respond to the products of different MICA isoforms, and how those responses are affected by HLA-B. It supported those studies by further phenotyping of NK cells and T cells in BD. In so doing, the goal was to provide information that would strengthen or weaken the hypothesis that NK and/or T cell dysregulation plays a fundamental role in the initiation or progression of BD.

More specifically, the thesis has focused on the comparative analysis of the products of Behcet's disease-associated isoform (MICA*009) and non-associated MICA isoforms (MICA*009v,*008,*027) for various properties including RNA stability, translational efficiency, protein stability, protein localisation and the ability of allelic forms to evoke responses from NKG2D-positive lymphocytes. NKG2D-mediated recognition of cell stress markers such as MICA and the ULBP family members is broadly implicated in infection, inflammatory disease and tumour surveillance. However, the functional significance of MICA polymorphisms is not yet fully understood. To evaluate this, this thesis together with ongoing studies employed PBMCs from a large number (44) of donors *in vitro* as effector cells targeting mammalian epithelial cells (CHO transfectants) that differ from control cells only by the expression of a single copy of a MICA isoform or ULBP2.

MICA*009 associates with and is in strong linkage disequilibrium with HLA-B*51 in Behcet's disease (BD). Therefore, the second aim of this study was to compare the inhibitory effects of HLA-B*51 with HLA-B*52 (control gene) on the killing potential of KIR3DL1-positive NK and γδ T cells from PBMCs from a large number of donors (33). This was approached by expressing different combinations of HLA-B*51 and HLA-B*52 and MICA in CHO cells, and examining the impact of these combinations on NK and γδ T cell stimulation. These studies provide a novel approach to investigating the mechanisms underpinning the disease-association of HLA-B*51 in BD: moreover, this approach may be useful in dissecting similar associations of linked genes with other diseases. Furthermore, the approach has provided new insights into the responses of T and NK cells to human stress-ligands in outwardly healthy individuals.

## 5.2 – MICA and ULBP2 provokes specific killing

The first finding of the thesis was that the allelic forms transcribed as single copy genes from identical transcriptional control elements were expressed at consistently different levels. It might have been anticipated that this would be the case for the protein products, particularly MICA*008, since amino acid differences and protein truncation can be expected to impact on protein stability. However, it was not anticipated that the differences in protein levels would be largely attributable to differences in RNA levels, implying that allelic sequence variation has a major impact on RNA stability. This is an issue that merits follow up. Clearly, stringent regulation of expression will be critical for a molecule to function as a stress-ligand. Furthermore, it is increasingly clear that this regulation is not simply manifest at the regulation of transcription initiation, but includes mRNA stability. Thus, there have been recent reports of MICA and MICB RNA regulation by micro RNAs (Stern-Ginossar et al., 2007, 2008; Nachmani et al., 2010; Yaday et al., 2009). However, to our knowledge there has not previously been an association of allelic variation with RNA levels.

A specific result of this regulation is that the protein encoded by MICA*008 is expressed at lower levels than that of other MICA isoforms. Moreover, it is expressed very poorly at the cell surface. However, this is evidently not because the truncated trans-membrane region reduces the ratio of membrane-associated protein to total protein as was implied by Spies and colleagues (Li et al., 2000). Indeed, most of the MICA*008 protein product appears on the cell surface, emphasising again that a primary level of regulation may be the stability and translation of RNA.

The differences in MICA protein expression begged the question as to whether cells expressing the different allelic forms could be equally well recognised by NK cells and/or T cells. This was assessed using an *in vitro* killing assay in which MICA or ULBP FRT-CHO transfectants were used as targets for effector PBMC from a large cohort of donors. The first and important observation was that every individual was able to specifically target these cells *via* their NK cells and γδ T cells without the obvious co-activation of other receptors: blocking NKG2D inhibited killing completely. These data are similar to those obtained by Spies and colleagues using MICA transfected C1R cells that also showed NKG2D-mediated killing (Bauer et al., 1999). The data are consistent with the Lymphoid Stress-Surveillance hypothesis that argues that molecular reflections of cellular stress are sufficient to activate an immune response (Hayday, 2009). Nonetheless, this issue is formally unresolved since some studies have argued that activation *via* the NKG2D receptor is insufficient to activate γδ T cells or NK cells, with the former requiring activation through the TCR (Favier et al., 2003) and the latter requiring activation through multiple receptors (Bryceson., et al 2005). Clearly the different results may reflect the use of different experimental systems, and following their original studies, Bryceson and colleagues modified their perspective by noting that NKG2D engagement by NK cells was sufficient to promote some level of activation (Bryceson., et al 2009). Additionally, Hermann and colleagues reported that human peripheral blood γδ cells could be activated solely *via* NKG2D (Rincon-Orozco et al., 2005). Our use of $MICA^{+}$ and $ULBP2^{+}$ CHO cells may have evoked responses from human cells because non-specific integrins and/or adhesins, despite their being heterologous, may have permitted cells sufficient "contact time" to be activated. We believe that this would be physiologically relevant in the context of human T and NK

cells confronting stressed target cells. It might be argued that the use of CHO cells was inappropriate because they lack human MHC molecules that would naturally inhibit activation of NK cells and possibly of γδ T cells. We would counter this argument in several ways. First, when we did provide ligands for inhibitory receptors (see below) they did not reduce activation to nothing. Second, NKG2D ligand upregulation is commonly commensurate with MHC Class I downregulation. Related to which, third, the experimental system provides an objective means to make multi-parameter biological comparisons of different MICA isoforms. In this regard, our studies revealed additional and sometimes unexpected findings.

First, there was an unexpected inter-individual variation that was stable longitudinally at least over several weeks in three individuals tested. Also unexpected was that most donors were able to respond to cells expressing MICA*008, despite its very low cell surface expression. Indeed, some individuals targeted MICA*008 transfectants better than cells expressing the other MICA isoforms. These data raise two important points. First, that human Lymphoid Stress-Surveillance can be extremely sensitive; second, that the cell surface density of a ligand may not necessarily indicate that the cell would have an increased chance of being recognised and targeted by effector cells bearing the receptor for the ligand, for example in the case of tumours which express very high levels MICA. Rather, the capacity of a cell to be targeted relies on other factors, at least some of which vary from person to person. This second point is not often considered; may even seem counter-intuitive; and has implications for immune-evasion. MICA can be shed from the surface of tumour cells by the action of metalloproteases as soluble MICA (sMICA) was understandably interpreted as a route to tumour immune evasion by reducing the quantity of MICA on cells, and by blocking the NKG2D receptor on responding cells. Provocatively, the data in this study suggest that both events might move a tumour cell into an optimal range for targeting by the immune system. Further experiments should be undertaken to test this concept because it may have implications for immunotherapy. That is, by understanding the optimal range of MICA to which an individual's cells respond, one might attempt to modulate the expression of MICA on tumour cells upwards or downwards from the existing levels revealed by tumour biopsies. Thus, counter-intuitively, treating some individuals

with a blocking anti-MICA antibody may enhance their responses to MICA, as the amount of ligand accessible on the surface of the cell would be reduced. While the data provided in this study point to the complexity of the Lymphoid Stress-Surveillance Response, they also demonstrate a practical and rapid way by which the "bandwidth" of a recipient's responses could be assessed. This may be particularly relevant in transplantation, where it could be useful to assess a recipient's responses in relation to the MICA haplotype of donors. The inter-individual variability in functional responses to allotypic MICA predicts diversity in the response to allografts expressing MICA as a result of severe stress. The increasing interest in MICA in transplantation (Flegel et al. 2007; Dragun et al 2012) should accommodate this perspective.

The finding of individual hierarchies of responsiveness begs the question of their underlying basis. The high inter-individual variation in healthy controls and in BD patients did not correlate with gender, disease activity, the percentage or cell surface expression of $NKG2D^{+}$ circulating NK cells in peripheral blood, or KIR3DL1 expression. Clearly, NKG2D ligands differ in their affinities for the receptor. However, with little known allelic variation in NKG2D itself, the affinity hierarchy should be largely the same from one person to another. Since the elucidation of the TCR synapse (Wulfing and Davis, 1998), it has been acknowledged that receptor-ligand interactions that promote lymphocye actvation can involve several heterologous molecules. In this regard, the protein products of different MICA isoforms may also differ in their association with other molecules such as ICAM-1, actin/talin and LFA-1 in the formation of intra-membrane protein clusters within or around the immune synapse between NK cells and T cells with their target cells. By this means, different MICA isoforms might render cells better or worse targets for immune surveillance. (Davis and Dustin, 2004; Vyas et al., 2002). As integrins and related molecules on PBMC's from different donors might vary, one could anticipate that individuals would vary in their capacity to make immunological synapses and that different hierarchies of targeting might thereby arise. Indeed, Bouma et al (2011) and Randall et al (2011) have attributed a series of human immunodeficiencies to variation in the capacity to make effective synapses between cytolytic T cells and their targets (Bouma et al., 2011; Randall et al., 2011).

There may be other unexplained ways in which NKG2D-ligands, including allelic forms of MICA differ. Thus, a recent study showed that not all ULBP proteins are equivalent in their targeting by human γδ T cells as part of a tumour surveillance response (Lanca et al., 2010). In particular, targeting of leukaemia cells by γδ T cells was facilitated uniquely by ULBP1 and not by MICA, ULBP3 of ULBP4, despite their all being ligands for NKG2D. The underlying basis for this was unexplained, but might conceivably differ from person to person. In this regard, a very unexpected and striking observation was the inter-individual variation in the capacity of NKG2D positive cells to respond to the non-polymorphic NKG2D ligand, ULBP2. Indeed, some individuals completely failed to target ULBP2, whilst targeting other cells expressing MICA isoforms. This intriguing observation led us to consider that different individual responses may be less reflective of MICA genetics than of individual bandwidths of responses to NKG2D-ligands. That is, individuals become tuned so as to respond in particular ways.

Tuning has previously been invoked to describe the experiential adjustment of T lymphocyte responsiveness to be most compatible with healthy immunoprotection (Grossman et al., 1992). The essence of the concept is that an individual's responses evolve over time. For NKG2D positive cells, we consider that there will be individual variation in NKG2D ligand expression levels in unstressed tissues, added to which there will be individual variation in the levels of stress-induced expression. The basis of such variation will be polymorphism in loci affecting gene expression (Li et al., 2008) Thus, it can be postulated that at early times in the developmental process, NKG2D-positive cells may become educated or "tuned" to the level of ligand expression in any one individual. One would want one's cells not to respond to basal levels of NKG2D expression, but to respond to levels typical of one's own stress-induced expression. If cells only responded to high levels, such as are phenocopied in this study by ULBP2 or MICA*009 expression, they may be inefficient at responding to lower levels more typical of those induced by stress in some individuals. Hence, one can readily consider the benefits of individual tuning (Gasser and Raulet, 2006; Yokoyama and Kim, 2006). How tuning might occur is currently unclear. One can consider at least two possibilities. First, at a population level, γδ T cells that recognise basal expression levels might be developmentally

deleted akin to negative selection in the αβ T cell compartment. Among surviving cells, those that respond to an individual's "typical" induced levels of NKG2D ligands clonally expand and come to dominate that person's peripheral population. Alternatively, tuning may be cell autonomous, whereby cells do not respond to basal levels of ligand expression, but respond and adapt to stress-induced levels of ligand most commonly encountered. Although a mechanism for this is not yet apparent, it is very clear that many cell types, from T cells through to neurons show altered levels of responsiveness, e.g. attenuation, to successive stimulation (Angelosanto et al., 2012; Wherry et al., 2011; Henderson, 2011). The hypothesis that individual responses might be tuned to different dose bandwidths in response to stress is illustrated in Fig 5.1 which was composed by my colleague, Dr Pierre Vantourout. Also shown in this Figure are some experiments undertaken by Dr Vantourout that were provoked by the findings of this thesis and that fulfil some predictions of the tuning hypothesis. In particular, the hypothesis predicts bell-shaped response curves for many donors that will "ignore" cells expressing MICA levels either above or below the bandwith. Consistent with this, treatment of MICA-transfectants with accutase that reduced MICA expression from the cell surface actually increased the targeting of transfectants by of cells from some donors (Fig 5.1B, C). Furthermore, by creating CH0-MICA*027 transfectants with different expression levels and using them in *in vitro* assays to determine the responsiveness of NK and γδ T cells compartments, it was possible to identify bell-shaped responses of two individuals tested (Fig 5.2). These experiments undertaken by Dr Vantourout have been published in our co-authored paper, Shafi et al 2011, and are reproduced here with permission of the author.

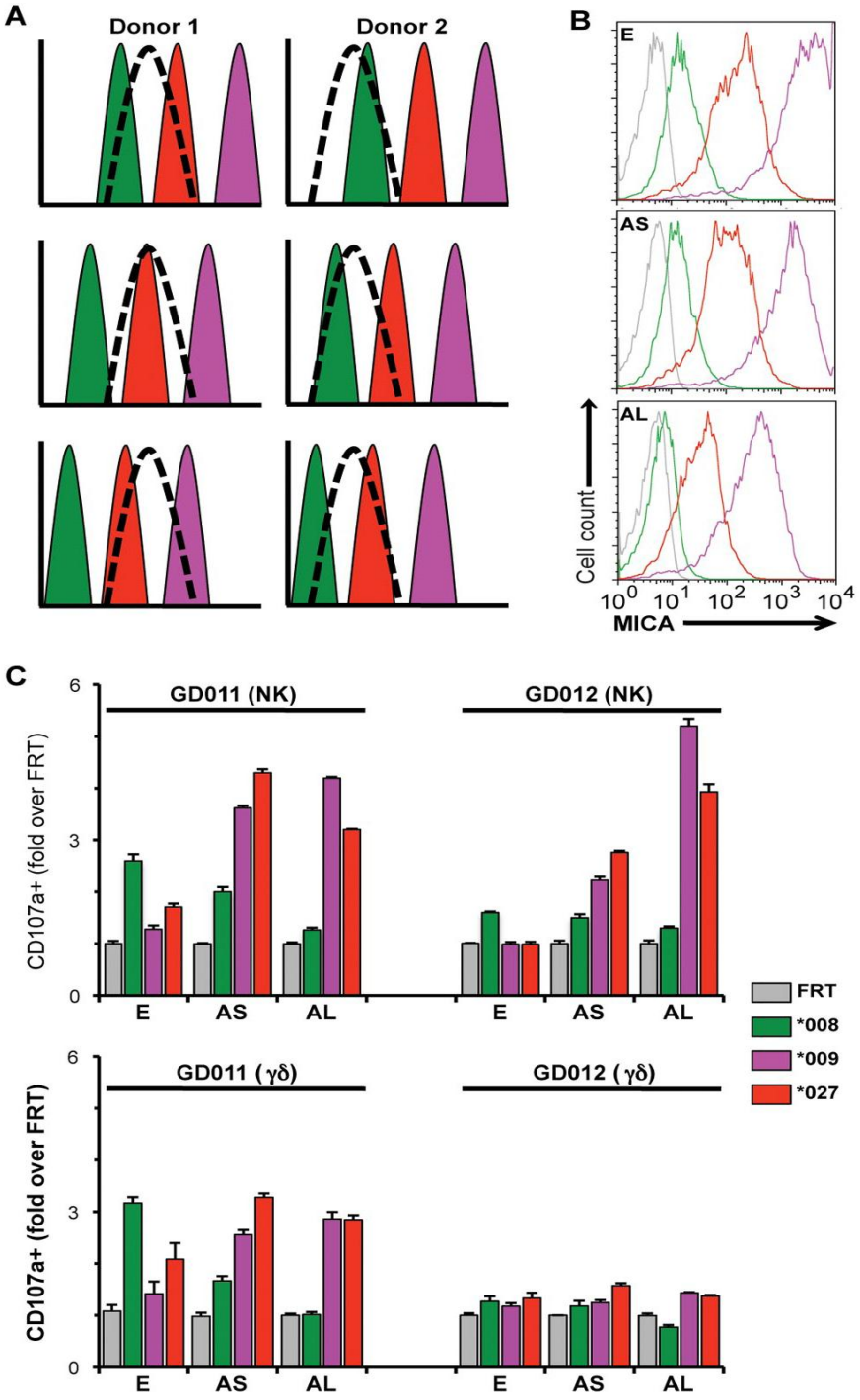


**Figure 5.1** Contribution of tuning to the preferential recognition of MICA isoforms. **(A)** Model for a bell-shaped response of effector cells from 2 donors tuned to different ranges (dashed curves) of MICA expression levels, set against the levels of MICA expressed by CHO-MICA*008 (green), CHO-MICA*027 (red), and CHO MICA*009 (purple) cells (top panels). As the expression of these allelic forms is gradually reduced (middle and bottom panels), the capacity to be targeted by donor 1

and donor 2 effector cells is increased for MICA*027 and MICA*009 cells whereas targeting of MICA*008 cells is decreased. **(B)** CHO cells were collected with PBS-10mM EDTA (E) or after a short (5min, AS) or long (20min, AL) treatment with Accutase and stained for cell surface MICA expression. Colors coded according to key box shown. **(C)** Target cells defined in panel B were used in a CD107a assay with NK (top panel) and γδ T cells (bottom panels) from two healthy donors (GD011 and GD012). Responses were normalized to the percentage of CD107a(+) cells in the presence of control vector-transfected FRT cells. Data are means of triplicate stimulations +/- SD. (Shafi et al 2011).

---

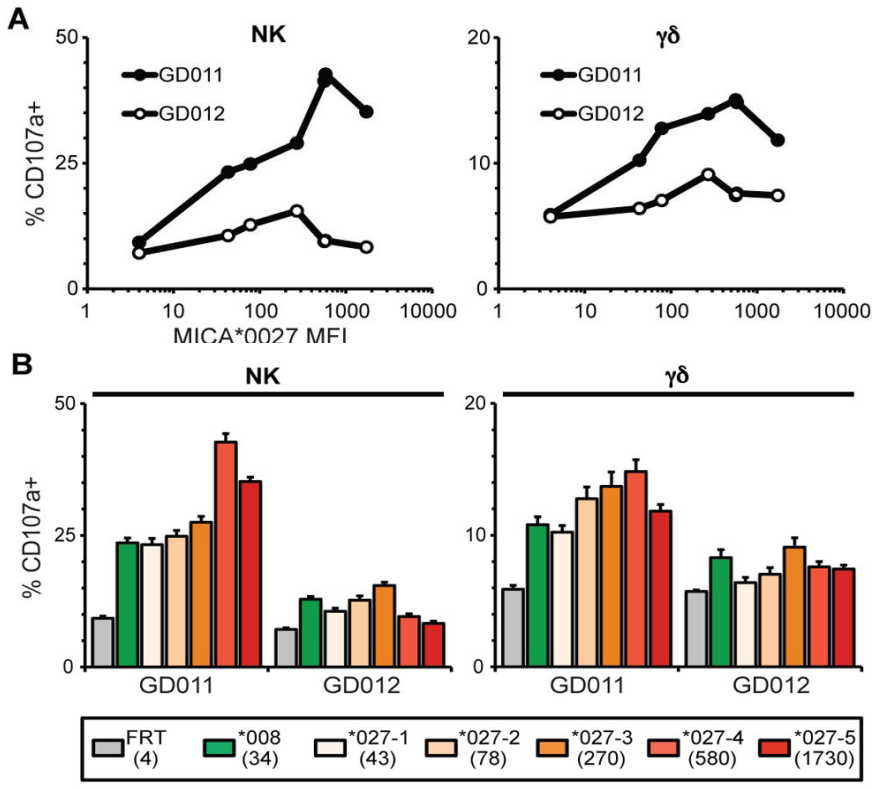


**Figure 5.2:** Quantitative and Qualitative aspects of the response to CHO-MICA cells**.** Clones expressing different MICA levels were generated and used in a CD107a assay to analyse the response of NK cells (left panel) and T cells (right panel) from the same donors as in Fig. 5.1. **(B)** Comparison of responses of NK cells (left panel) and γδT cells (right panel) to the different MICA*027 clones as well as to the MICA*008 FRT cell line. Numbers between brackets indicate the MICA MFI as

measured by flow cytometry. Data are means of triplicate wells +/- SD. (Shafi et al 2011).

---

Interestingly, the "typical" stress-induced level of NKG2D-ligands might change in inflammation and disease states, possibly dysregulating a tuned response. At the same time, it is also evident that there are distinct qualitative contributions to MICA recognition by different individuals in that there appear to be distinct responses to different isoforms when expressed at comparable levels (Fig 5.2B). This may reflect issues of affinity of inter-molecular protein aggregate formation considered above. Although much remains to be learned, it is evident from this thesis and from the collaborative studies of Dr Vantourout that the response of cells to stress-induced NKG2D ligands is highly complex even among outwardly healthy individuals. Given that stress-recognition is a form of autoimmunity, it is perhaps not surprising that its regulation will be complex and distinct to any one individual.

## 5.3 – Impaired expression of NKG2D on circulating leukocytes in patients with Behcet's Disease

Germane to the potential role of MICA-NKG2D signalling in BD, data from the current study illustrated a universally lower level of NKG2D positive cells circulating in peripheral blood of patients compared to healthy controls. However, this phenomenon was also observed in disease controls, who were receiving the same treatment as patients. Therefore, they may not represent the status of patients in the early stages of disease. Previous results from the phentoyping of NKG2D positive cells (NK cells, γδ T and $CD8^+$ T cells) from BD patients support the current findings. Thus, Ahn et al showed decreased NKG2D expression on both the $CD8^{bright}CD56^+$ T cells and $CD8^{bright}CD56^-$ T cells in BD compared with normal controls, both in PBMC and in cells infiltrating the eye. It was suggested that NKG2D engagement was involved in activation of these cells with NKG2D downregulation a result of chronic ligand exposure (Ahn et al., 2005). This would be

consistent with the MICA-NKG2D axis being an active component of disease. However, the contribution of treatment to these observations needs to be considered.

KIR3DL1 expression is also apparently decreased in on the surface of NK and T cells in patients compared to healthy controls. A lack of correlation between KIR3DL1 and BD has been reported in two studies (Saruhan-Direskeneli et al., 2004, Middleton et al., 2007). However recent analysis of polymorphic variants that regulate the frequency of subtype expression suggests that typing of donors would provide an insight into variable KIR3DL1 isoform expression (Li et al., 2008).

Taken together, the results suggest several possibilities. Firstly, the reduced percentages of NKG2D positive cells and KIR3DL1 positive cells may be due to the effect of treatment, which may affect the normal status of chemokine and chemokine receptor expression. This could affect cells directly; for example, NKG2D expression is known to be regulated by IL-15 (Jinushi et al., 2003). Ironically, however, raised levels of IL-15 expression have been reported in BD (Roberts et al., 2001; Hamzoaui et al., 2006; Curnow et al 2008). Alternatively, it may indirectly account for the observation, if altered; immune cell sequestration redistributes NKG2D-positive cells from the blood to sites in the tissues that are not easily sampled. Secondly, the reduced levels of circulating NKG2D-positive lymphocytes may suggest that these cells may have migrated to sites of inflammation in the tissues, irrespective of treatment. Thirdly, high levels of sMICA and/or chronic exposure to cell-expressed MICA (Oppenheim et al., 2005) in active patients may have decreased the surface expression of NKG2D on NK and T cells compared to healthy controls. The levels of sMICA in the serum of BD patients used in this study are currently being analysed. However a recent study showed no difference between BD patients and controls (Clemente et al., 2010).

In summary, the data from the patients with BD, disease and healthy controls, show a significant decrease of $CD16^{+}CD56^{+}$ NK cells, γδ T cells and $CD8^{+}$ T cells expressing NKG2D in patients with active disease. These data provide further evidence for the importance of understanding the NKG2D axis in BD, although the potential contribution of treatment has been noted. Following treatment, the

percentages of $\gamma\delta^+$/NKG2D$^+$ cells were restored to control levels, while the other populations remained low.

## 5.4- HLA-B*51 differentially inhibits killing in patients and controls.

The experimental system described in this thesis permitted the impact of MHC Class I engagement on NKG2D-mediated responses to be assessed. For cells from healthy controls, both HLA-B*51 and HLA-B*52 inhibited the killing of target cells by approximately 10%, compared to the killing of CHO-MICA*009 cells. However, the most striking results were obtained using PBMC from patients. Of note, killing of MICA*009-expressing cells by the PBMC of several patients showed a clear and strong inhibition by HLA-B*51, which is disease-associated, but not by HLA-B*52, which is not disease-associated. As with single transfectants, these effects did not correlate to the gender of the donors involved in the study, nor to the percentage and cell surface expression of KIR3DL1$^+$ circulating NK cells in peripheral blood. These unanticipated, discrete inhibitory effects of the two HLA isoforms on the cells of patients evoke several ideas. For example, the binding of KIR3DL1 to HLA-B*51 in a subset of patients may be stronger due to a higher affinity of their KIR3DL1 allotypes for HLA-B*51. This might be compounded by a higher level of expression of HLA-B*51, relative to HLA-B*52 since HLA-B*51 may bind more promiscuously to peptides of lower affinity than does HLA-B*52. In this regard, patients should be more thoroughly typed for the B*51 and KIR3DL1* subtypes as well as NKG2D polymorphisms, since it is highly possible that combinations of B*51 and KIR3DL1 subtypes may influence NKG2D-dependent killing responses. To address these outstanding issues, a larger cohort of donors needs to be used for longitudinal *in vitro* killing assays with the double transfectants, combined with typing of all four molecules HLA, NKG2D, KIR3DL1 and MICA. Nonetheless, it is striking that an allotype-specific effect of HLA-B has been observed with patients. Were HLA-B*51 to consistently exert profound inhibition on the NKG2D-dependent stress responses of some individuals, then one could hypothesise that those individuals would not clear infection/inflammation as well as would healthy individuals. This would lead to the prolonged mucosal inflammation seen in these

patients, increased levels of inflammatory cytokines and chemokines causing vasculitis and infiltration of neutrophils into immune-privileged sites such as the eye, the brain and joints. Such a state may be further compounded by dysregulation of genes such as IL-10 as considered in the Introduction. Additionally, one should consider that the patients might represent individuals in which profound effects of HLA-B*51 are exerted during licensing (Kim et al., 2005). Nonetheless, no evidence emerged in this thesis that NK or γδ T cells of patients have a fundamentally different spectrum of activities, as might be predicted would follow from alterations in licensing.

Finally, one inevitably considers what pressures may have led to the retention of genotypes that predispose to chronic inflammation. Possibly it is protective in responses to infectious agents. Similar consideration should be given to other data from our group. As discussed previously, single nucleotide polymorphisms in the TNF gene linked to its higher production have been associated with BD (Ahmad et al., 2003). A single nucleotide polymorphism PTPN22 was inversely correlated with disease in UK BD patients (Baranathan et al., 2007), while a SNP in TIRAP linked to its reduced function as well as low production of IL-10 both associates with disease (Durrani et al., 2011; Wallace et al., 2007). High levels of TNF are likely to be effective against infection, but too much may cause fatal symptoms, for example cerebral malaria or septic shock (Ahmad et al., 2003). Therefore matching high TNF with reduced killing via HLA-B*51 or TIRAP, which is also associated with protection against infection, might balance the response to control diseases that were prevalent threats in regions where the genotype flourished. The PTPN22 polymorphism might also limit the development of autoimmune T cells. However, reduced IL-10 would lead to less resolution from the reduced potent inflammatory response leading to a condition like BD. While many more genes are sure to be involved in a complex disease such as BD, this thesis provides an initial experimental approach to dissecting the role in disease of specific pathways, singly and in combination. Thus, more sophisticated systems might effectively begin to dissect the impact of multi-gene haplotypes. Moreover, as is often the case in clinically-motivated research, the results of this thesis have also provided new insight into the basic immunobiology of healthy individuals.

# CHAPTER SIX-MATERIALS AND METHODS

## 6.1 - Nucleic Acid Extraction & Analysis

### 6.1.1 RNA Isolation

Total RNA was isolated from cell lines using the Trizol method: approximately 5-10 million cells are lysed in 1ml of Trizol by repetitive pipetting and left at room temperature to incubate for 5 minutes. 0.2ml of chloroform was added to the lysed cells and the samples were vigorously shaken for about 15 seconds, and left to incubate for 2 to 3 minutes. The samples were the centrifuged at 13,000 rpm for 10 mins at 4 ˚C. After this point the sample separates into 3 phases: the lower red phenol:chloroform phase, and interphase (which contains DNA) and an upper aqueous phase (which contains RNA). The upper RNA phase was transferred to a fresh tube and 0.5ml isopropanol was added to precipitate the RNA and left to incubate for 10 minutes at room temperature before centrifuging at 13,000 rpm for 10 minutes at 4˚C. The RNA at this point formed a gel like pellet, which was washed with 1ml of 75% ethanol, after removal of the supernatant. The sample was mixed by vortexing, and then centrifuged for 5 minutes at 13,000 rpm and at 4 ˚C. The supernatant was removed again, and the RNA pellet was allowed to air dry for 5-10 minutes, before dissolving the pellet in 40µl RNAse free water. 5µl of DNAse buffer (10x) and 1µl of RQ DNAse (Promega) was added to the RNA and incubated at 37 ˚C for 20-30 minutes. Following this, 150µl of water was added to the sample followed by the addition of 200µl of phenol:chloroform:isoamylol (25:24:1 pH 5.6), mixed and spun at 13,000 rpm for 5 minutes at 4 ˚C. The upper aqueous phase is transferred again to a new tube, to which 20µl 3M sodium acetate (pH 5.2) and 500µl 100% ethanol was added and mixed thoroughly. The RNA was left to precipitate on ice for 15-20 minutes, and then centrifuged at 13,000 rpm for 20 minutes at 4 ˚C. The supernatant was discarded and the pellet left to air dry before resuspension in 12µl water.

### 6.1.2 cDNA Synthesis

Complementary DNA (cDNA) was synthesized via reverse transcription using SuperScript II Reverse Transcriptase (Invitrogen, cat. #18064-014) according to the supplied protocol. 12µl of total RNA was combined with 1µl of 500µg/ml oligo(dT)

and 1µl of 10mM dNTP mix, followed by a 5 minute incubation at 65˚C.The sample was then chilled on ice, prior to addition of 4µl of 5x First Strand buffer, 2µl of 0.1M dithiothreitol (DTT) and 1µl of RNase Out (40 units/µl ; Invitrogen, cat. #10777-019). Finally, the sample was incubated at 42˚ C for 2 minutes, followed by addition of 1µl of SuperScript II reverse transcriptase and incubation at 42˚ C for 50 minutes. The enzyme was inactivated by incubation of the sample at 70˚ C for 7 minutes, and then 50 µl of water was added to the newly synthesised cDNA sample.

### 6.1.3 Polymerase chain reaction (PCR)

Amplification of full length MICA*004,*008,*00901 and*027 cDNA sequences was performed using cDNA isolated from the Mou cells (B Lymphoblastoid Cell Line), Int407 cells (gut epithelial Cell Line) C1R cells (B Lymphoblastoid Cell Line) and SWEIG007 (B Lymphoblastoid Cell Line) respectively.

Sequence-specific forward and reverse primers used were:

MICA-Forward – 5’ CGGGGCCATGGGGCTGGGCCCGGT 3’

MICA-Reverse – 5’ AGCCGCCTGGCTGTAGAGTCTAGG 3’

Amplification of full length HLA-B*5101 and B*5201 cDNA sequences was performed using cDNA isolated from AKIBA cells (human B cell line) and JHAF cells (human B cell line).

Sequence-specific forward and reverse primers used were:

HLA-B*5-Forward – 5’ ATGCGGGTCACGGCGCCCCG 3’

HLA-B*5-Reverse – 5’ TCAAGCTGTGAGAGACACA 3’

Amplification of full length ULBP2 cDNA sequences was performed using cDNA isolated from Hacat cells UV(Ultra Violet light) treated for 24 hours (Human keratinocyte cell line).

Sequence-specific forward and reverse primers used were:

ULBP2-Forward – 5'GAGCTAGCTCCTTAATGGCAGCA 3'

ULBP2-Reverse – 5'TCAGATGCCAGGGAGGATGAA 3'

Amplification of full length human beta-2-microglobulin cDNA sequences was performed using cDNA isolated from human peripheral blood mono nuclear cells (PBMC's).

Sequence-specific forward and reverse primers used were:

Beta-2 microglubulin – forward - 5'ATGTCTCGCTCCGTGGCT 3'

Beta-2 microglubulin – reverse - 5' TTACATGTCTCGATCCCA 3'

All Sequence-specific primers pairs were used at a final concentration of 1µM and 300 µM of each dNTP. Finally, 10x proofstart buffer (contains 15 mM MgSO4) and distilled water were used to make up the volume, followed by addition of 1µl of proofstart enzyme per 50µl reaction. The samples were then placed in a thermal cycler, with a typical PCR reaction as outlined below:

Step1 : Initial activation step: 5 min at 95°

Step 2: Denaturation: 0.5–1 min at 94°C

Step 3: Annealing: 0.5–1 min at 65°C (for MICA and HLA-B*5 primers) and 60°C (for ULBP2 primers) (Approximately 5°C below *T*m of primers)

Step 4: Extension: 1 min/kb at 72°C

Repeat from step 2 for a total of 35–45 cycles

Step 5: 5 minutes at 72°c.

Step 6: End of PCR cycling: Indefinite 4°C

Annealing temperatures were optimized the primer pair using a temperature gradient (50˚ - 68˚C) prior to sample analysis.

### 6.1.4 Agarose Gel Electrophoresis

Visualisation of amplified DNA products from the PCR reactions was performed by agarose gel electrophoresis in the presence of ethidium bromide (EtBr). To make the gel, the appropriate amount of agarose was weighed and added into an appropriate volume of 1X TAE buffer to make a 1% TAE agarose gel and then microwaved for 2-3 minutes to fully dissolve the agarose in the 1X TAE buffer. This was followed by the addition of 10mg/ml EtBr (1µl per 100ml solution) before being poured in to a gel mould with a 17 well comb. The gel was then allowed to solidify before being placed in a gel tank containing sufficient TAE buffer to completely cover the gel. Samples were then combined with 6x Orange G loading buffer, loaded on to the gel and run through the gel at approximately 120V for 45-60 minutes, before visualization of DNA-EtBr bands under ultraviolet light.

TAE buffer (50x):

Tris base 242g

Glacial acetic acid 57.1ml

EDTA (0.5M; pH 8.0) 100ml

Distilled water to final volume of 1000ml.

TAE buffer (1x):

40 ml TAE buffer 50X

Distilled water to final volume of 2000ml

## 6.2 Molecular Cloning Techniques

### 6.2.1 Visualising the PCR product and Gel Extraction

Approximately one-fifth of the PCR reaction was visualized using a 1% EtBr-containing agarose gel electrophoresis, while the rest of the sample was run on a separate 1% EtBr-containing agarose gel. The appropriate band (MICA-1158bp, HLAB*5101 and B*5102- 1080bp and ULBP2-741bp) was then excised from the gel, and the DNA extracted and purified using the QIAquick Gel Extraction kit (QIAGEN, cat #28706) according to the manufacturer's protocol and eluted in 30µl elution buffer (from kit).

The purified PCR products were then sent for sequencing (Lark sequencing, UK) in order to obtain perfect sequences in order to use in cloning and sub cloning.

### 6.2.2 TOPO Cloning Reaction

As proofstart polymerase produces blunt-ended PCR products, after PCR purification and after sequencing, the correct DNA sequences were treated with Taq polymerase to sequentially add adenine overhangs to both ends of the purified PCR product to aid cloning into the pCR2.1-TOPO vector that has single 3'-thymidine overhangs (Invitrogen cat # K4500-40). The reaction with taq polymerase, buffer and dNTP's and incubated for 15 minutes at 72°C to add the 3' adenine residues at the ends.

The modified PCR product was then cloned into the TOPO vector in the following way: 4µl of fresh PCR product was combined with 1µl of salt solution (provided with kit) and 1µl of vector, and then incubated at room temperature for 5-30 minutes, before placing on ice and transforming chemically-competent TOP10 bacteria (with kit Invitrogen cat # K4500-40)

### 6.2.3 Bacterial Transformation and Growth

Chemically-competent *Escherichia coli* bacteria were transformed with plasmid vectors as follows: Approximately 2µl of either a TOPO cloning reaction or vector-insert ligation was added to a vial of One Shot Chemically Competent cells (with kit Invitrogen cat # K4500-40) were transformed with the ligate from the pcr2.1 TOPO vector and PCR product reaction by gentle pipetting, followed by incubation on ice for up to 30 minutes. Immediately afterwards, the cells were heat-shocked by incubation at 42°C for exactly 45 seconds, followed by immediate placing them on ice. 250µl of either SOC or Luria Bertani (LB) medium (without antibiotic) was then added to the vial. The bacteria were then incubated in a rotating shaking 37˚C incubator for an hour (set to 220rpm).

An hour later 50µl and 150 µl of each the transformation reactions was separately plated out on to pre-warmed LB-agar plates containing ampicillin (70µg/ml). The plates were then incubated overnight at 37˚C. Colonies that had grown were picked and placed in 5ml of LB broth containing ampicillin (70µg/ml) and incubated overnight at 37˚C in the shaking incubator. Extraction and purification of the plasmids was carried out using the QIAGEN Miniprep kit (for 3-5ml cultures; QIAGEN cat. #27106) and were screened for incorporation of the insert (see below), and positive plasmids were grown in larger volumes of bacteria by diluting 0.5ml of the 5ml culture in 500ml of LB broth containing ampicillin (70µg/ml) and leaving this overnight to shake in the 37˚C incubator.

### 6.2.4 Plasmid Preparation

Extraction and purification of plasmid DNA from the 500ml cultures was performed using QIAGEN Maxiprep (for 250-500ml cultures; QIAGEN, cat. #12163) according to the protocol:

<u>For the 5ml bacterial cultures:</u>

The bacterial cultures were centrifuged and the pelleted cells were resuspended in 250µl buffer P1 (containing RNase A) followed by the addition of an equal volume of buffer P2 (to lyse the cells), and this is thoroughly mixed. 350µl of buffer N3 is added

to the lysate, and again thoroughly mixed before centrifugation for 10 mins at 13,000rpm. The supernatant collected after the centrifugation was applied to the QIAprep spin column, so that the plasmid DNA could bind to the column and this was further centrifuged for 1 minute, and the flow through was discarded. The column was then washed by addition of 750µl buffer PE (contains ethanol) spun down for 1 minute, and then the purified plasmid DNA was eluted in 30µl elution buffer.

For the 500ml bacterial cultures:

The cells were pelleted at 6000g for 15 minutes and then resuspended in 10ml buffer P1. An equal volume of buffer P2 was then added to this. The sample was mixed thoroughly by inverting the sample a few times and left to incubate at room temperature for 5 minutes to allow the cells to lyse efficiently. 10mls of buffer P3 is then added to the lysed cells, and once again the sample is mixed thoroughly before incubation on ice for 20 minutes. The sample was then centrifuged at 20 000g for 30 minutes at 4˚C. At the same time the Qiagen columns were equilibrated with 10ml QBT buffer and allowed to empty by gravity flow. The centrifuged sample was then applied to the equilibrated column and passed through by gravity flow. The column was then washed twice with 30ml QC buffer and the DNA was eluted with 15ml buffer QF. To precipitate the DNA, 0.7 volumes (10.5ml) of room temperature isopropanol was added to the eluted DNA, mixed and centrifuged at 15,000g for 30 minutes at 4 ˚C. The supernatant is removed without disturbing the pellet, and then the pellet is washed in 5ml 70% ethanol and centrifuged at 15,000g for 10 minutes. The supernatant is carefully removed and the pellet is air dried for 5 to 10 minutes after being dissolved in 200µl water.

### 6.2.5 Screening for positive clones, cloning and sub-cloning: Using Restriction endonuclease enzymes.

Restriction enzymes (from New England Biolab) are used to screen vectors for incorporation and orientation of inserts, for cloning of inserts into vectors and for cloning from one vector of into another (sub-cloning). A variety of enzymes were used during this project: EcoRI was used to identify positive inserts cloned into the TOPO

vector. These positive with the inserts were sub-cloned (from the TOPO vectors) into different expression vectors by the use the BsTXI enzyme. Multiple enzymes were used to identify positive inserts in the correct orientation in the expression vectors. Restriction enzyme digestion reactions used either 1µg (from the minipreps) and 10µg (maxipreps) of DNA with an appropriate volume of restriction enzyme (final concentration is 1X), of 10X buffer (final concentration 1X), 10X bovine serum albumin (final concentration 1X) and water to a final volume of either 20µl (1µg DNA) or 50µl (10µg DNA). The restriction enzyme reactions were incubated at their optimal temperatures for 1 hour (1µg DNA) or 2.5 hours (10µg DNA) and then run on 1% agarose gel to be analysed. The appropriate bands (DNA, insert and vector) were cut out of the gel and purified using the Qiagen gel extraction protocol (see below).

### 6.2.6 Gel extraction and purification (Qiagen)

The appropriate gel pieces were weighed, and 3X the volume (100mg=100ul) of buffer QG is added, and left to incubate at 55°C until the gel had completely melted and dissolved. A 1X volume of 100% isopropanol was added to the sample, and the sample was mixed thoroughly by inversion. The sample was then added to the Qiagen columns and spun at 13,000rpm for 1 minute. The flow through was discarded and the column was washed with PE buffer (containing ethanol) and again spun at 13,000rpm for 1 minute. The flow through was discarded and the column was spun again for another minute, before adding 30µl elution buffer to the column resin, incubated for 1 minute at room temperature, and eluted by spinning for 1 minute at 13,000rpm.

### 6.2.7 Phosphatase Treatment of vectors

Treating of linearised vectors with antartic phosphatase ((New England Biolabs, cat. #M0289) to remove 5’ phosphate groups, and thus prevent self-ligation optimising the chances of an insert ligating into the vector. The linearised vector (after restriction enzyme digestion) is mixed with 1µl Antartic phosphatase, 10X Antartic phosphatase buffer (final concentration 1X) and water and incubated for 45 minutes at 37˚C, before inactivion of the enzyme by incubation at 65˚C for 5 minutes.

### 6.2.8 Ligation reactions

These reactions were performed between an insert and a vector with the help of a ligase enzyme and optimal reaction conditions such as: the insert and vector were combined at a 5:1 ratio (ratio can be tweaked based on sequence length) plus 10 X ligase buffer (final concentration 1X), 1µl T4 DNA ligase enzyme, and the volume was made up to 10µl with water. The reaction was left to incubate at 16˚C overnight. Most of the ligate was used to transform chemically competent bacteria, and 2µl of the ligate is run on a 1% agarose gel to confirm insert ligation into the vector based on size of the bands.

## 6.3 Transfection of cells and generation of isogenic and stable cell lines.

### 6.3.1 Flp-In method generation of isogenic stable cell lines

Chinese hamster ovary (CHO) cells were stably transfected using a sophisticated unique system: the Flp-In system (Invitrogen, cat. # K6010-02 (vectors) and R75807 (CHO-FRT cells), following the supplier's protocol. This process is described in greater detail in Chapter 4, whereby MICA*004,*008,*009,*027 and ULBP2 were transfected into CHO-FRT cells (CHO-Flp-In modified cells, purchased from Invitrogen cat # R758-07) containing a Flp-recombinase target site in the exact same location in every cell. Full length MICA*004,*008,*009,*027 and ULBP2 were subcloned from the TOPO vectors into the pCDNA5FRT (using the BsTXI restriction enzyme) expression vector which contains a hygromycin resistance gene and a flp-recombinase site. The pCDNA5FRT vector cloned with the genes of interest are co-transfected into the CHO-FRT cells with the pOG44 vector, (which contains the flp recombinase enzyme) at a 1:9 ratio of pCDNA5FRT:pOG44. Approximately 2 million cells were transfected by electroporation in 6 well plates, in complete medium (RPMI 10%FCS, PSG). The medium was replaced with fresh medium 24 hours post-transfection and 48 hours post-transfection medium with 450µg/ml hygromycin B (Invitrogen, cat. # 10687-010) was added to the cells. The resistant cells were then transferred into a 96 well plates and grew them in T25 flasks (Sigma Aldrich cat #

Z707813). A couple of weeks later, the confluent flasks of resistant cells were then processed to obtain single clones by the serial dilution method in the following way: approximately 100 resistant cells from each transfectant were resuspended in 5mls media with 450µg/ml hygromycin B and cells were added to a 96 well plate by serial dilution, wherby some wells had only 1 cell/well in 50µl media (these wells were circled with a pen). These plates were left in the 37˚C incubator for approximately 3.5 weeks, with regular checks under the microscope. After this time period the marked wells had cells growing (detected under the microscope and media colour change) and were further expanded into flasks. Different clones of cells from the same transfectant were then checked for surface protein expression and frozen down, leaving one clone of each transfectant in the incubator to continue growing.

### 6.3.2 Generation of double transfectants with HLA-B*51 and HLA-B*52.

The open reading frames (ORF) of HLA-B*5101, HLA-B*5102 and beta-2-microglobulin (ß2m) were separately subcloned from the TOPO vectors into the pCDNA3.1 (-) using the BsTXI restriction enzyme) expression vector which contains a neomycin resistance gene. The CHO-FRT cells, MICA*009 and MICA*004 cells were transfectanted separately with HLA-B*5101 and ß2m, and with HLA-B*5201 and ß2m. The resistant cells were grown and expanded in complete medium with 650µg/ml G418 (Sigma-Aldrich, cat. #G8168) in the same way described for the single transfectants.

### 6.3.3 Transfection of Chinese Hamster Ovary cells by electroporation

Electroporation was the technique used to transfect CHO cells in the following way: 2 million CHO cells were centrifuged at 1200rpm for 5 minutes at room temperature. The pelleted cells were then resuspended in 250µl of serum-free RPMI. Approximately 10µg of plasmid DNA was added to a 4mm gap electroporatiom cuvette (Molecular BioProducts, cat. #5540) to which the cells were added and electroporated using a Bio-Rad Gene Pulser II with the following settings:

- Set to high capacity (raised to 950)
- 250 V
- Set to high range

Under these settings a pulse length of 55-60ms was usually observed. Electroporated cells were then diluted using 1ml of complete medium, and then resuspended in a well (6-well plate) with pre-warmed medium complete medium.

## 6.4 Northern blot technique

### 6.4.1 RNA isolation

RNA from CHO-FRT (untransfected cells), CHO-MICA*004,*009,*008 and *027 was isolated using the method illustrated in section 6.1.1. The concentration of the RNA was quantified, and to check the quality of RNA, 1µg of each RNA was run on a 1% agarose 1 X TAE gel (containing ethidium bromide).

### 6.4.2 Electrophoresis of RNA through gel containing formaldehyde

This protocol was adapted from the Manniatis protocol.

10X MOPS

0.2M MOPS

0.05M Sodium acetate

0.01M EDTA

pH adjusted to 7.0 with sodium hydroxide (buffer is stored in the dark at 4 ˚C.

Formaldehyde gel

2.89 Agarose

155ml water

50ml 5X MOPS (diluted from 10X MOPS)

The agarose was allowed to cool for a short while before the addition of 45ml formaldehyde (in the fume hood). The gel was then poured into a gel tray and allowed to set (in the fume hood).

In the mean while 15.5µl of sample buffer (see below) was added to 4.5µl of each RNA (10µg), the samples were then heated at 65˚C for 15 minutes and then left to cool on ice for a few minutes, before the addition of 2µl of RNA loading dye (95% formamide, 0.025% SDS, 0.025% bromophenol blue, 0.025% xylene cyanol FF, 0.025% ethidium bromide and 0.5mM EDTA). To each of the samples 1µl of 1mg/ml of ethidium bromide was added and the samples were loaded into the gel and the gel was run in 1X MOPS (diluted with water from 10X MOPS) for 3-4 hours at 100V (in the fume hood).

Sample buffer

125ul deionized formamide

43.75µl formaldehyde

25ul 5X MOPS

After 4 hours, a picture of the RNA run on the gel was taken under the UV lamp (visualising the large ribosomal subunit is 28S (approximately 5kb) and the small ribosomal subunit is 18S (approximately 2kb) bands) using a ruler as a reference. The gel was then placed in a large plastic tank and left to shake in deionized water twice for 10 minutes to remove the formaldehyde, and the soaked in 10X SSC for 15 minutes prior to the transfer.

10X SSC

88.23g Tris-sodium citrate

175.32g sodium chloride

added to 2l of water (pH 7-8)

### 6.4.3 Transfer of RNA from gel to nylon membrane

- A large tray was filled with 10 X SSC
- A smaller tray (slightly bigger than the size of the gel) was turned upside down in the larger tray
- A glass weight (slightly bigger than the size of the gel) was placed on top of the inverted smaller tray.
- A long piece of 3mm whatmann paper (the wick) was placed on the inverted tray from one side of the tray to the other (as shown below) to soak up the 20 X SSC.
- 2 sheets of pre-wet (in 20 X SSC) 3mm whatmann sheets (size of the gel) were placed on top of the wick.
- The gel was placed on top of the whatmann sheets, with the RNA facing upwards, and the H-bond nylon membrane (same size as the gel) was placed on top of the gel. All bubbles were removed and approximately 5 dry 3mm whatmann sheets were placed above the membrane.
- Strips of parafilm were placed between the whatmann sheets under and above the gel to avoid short circuit.
- A stack of paper towels approximately 4-5 inches high were placed on top of the whatmann sheets, and a large weight was placed on top of the paper towels.
- The edges of the large plastic tray were covered with saran wrap cling film to avoid evaporation of the 20 X SSC.
- The transfer is run overnight at room temperature.

After the transfer of the RNA from the gel to the membrane, a picture of the gel was taken to check that all the RNA had successfully transferred. The membrane (blot) was then air-dried for 30 minutes, before baking at 80˚C for 2 hours (membrane was sandwiched lightly between 2 whatmann filter papers) to allow the RNA to be cross linked to the membrane. The membrane (sandwiched lightly between 2 whatmann filter papers) was then wrapped in foil and left at room temperature till further use.

### 6.4.4 Preparation of the Northern probe

The probes for MICA and beta actin were prepared as follows: full length MICA was restriction enzyme digested (BSTXI) for 2.5 hours at 55˚C and then run on a 1% agarose gel (with ethidium bromide) and the 1.2kb MICA fragment was cut out and purified. The beta actin probe (full length) was a gift from Dr Els Henckaerts, department of Infectious diseases, Kings College London. Both probes (MICA and Beta actin) were separately radioactively labelled in the following way:

Probe cDNA (30-50ng) - 1µl

Primers (Amersham kit) - 5µl

Autoclaved water - 44µl

The DNA was denatured for 5 minutes at 95˚C and then spun down briefly. At room temperature the following was added to the probe using the (Amersham kit):

Labelling buffer - 5µl

dNTP mix (4µl each, except dCTP) - 12µl

Hot α- dCTP ($P^{32}$ 18.5MBq) - 5µl

Klenow L enzyme - 2µl

The 2 reactions were mixed by pipetting and the contents were briefly spun down before incubation at 37˚C for 10 minutes. This reaction was then stopped with 5µl 0.2M EDTA. The probe was then purified in the following way:

- 2 Qiagen columns were equilibrated by spinning them for 1 minute at 3000rpm and discarding the flow through.
- The probes were then applied to the columns and spun for 2 minutes at 3000rpm and the purified probes were collected in a new epindorphs. The probes were then left at room temperature until ready to use.

### 6.4.5 Pre-hybridization of the membrane (blot) – using Sigma's perfect-hyb hybridization.

The membrane was rolled up into a perpex cyclindrical tube with the RNA facing upwards. 120µl of salmon sperm DNA (10mg/ml) was boiled at 95˚C for 10 minutes, quickly chilled on ice and then added to 12 mls of pre-warmed (68˚C) perfecthyb (Sigma Aldrich, cat. # H7033) and this was added to the membrane and left to prehybridize at 68˚C rotating for 15 minutes.

At the same time the purified probes were boiled and denatured for 5-10 minutes at 95˚C, quickly chilled on ice and then spun down briefly. The probes were then both added to the membrane and the perfecthyb (12mls) and then left to hybridize overnight rotating at 68˚C.

### 6.4.6 Washing of the membrane and exposure to photometer film

The next day membrane was removed from the perfecthyb and washed once for 5 mins at room temperature (on a shaker) in low stringency buffer. The wash buffer was discarded and the membrane was then washed twice in high stringency buffer for 20 mins at 68˚ C.

Low stringency buffer

100ml 20 X SSC

5ml 10% SDS

895ml water

High stringency buffer

25ml 20 X SSC

10ml 10% SDS

965ml water

The Geiger readings were then taken to check that the radioactivity levels on the membrane were not too high, and then the membrane was wrapped in saran wrap cling

film and put in a cassette with a photometer film, and left to incubate overnight at room temperature.

## 6.5 Southern Blot technique

### 6.5.1 DNA extraction from CHO cells

Lysis buffer

10mM Tris-HCL pH7.5

10mM EDTA

10Mm Sodium chloride

0.5% Sarkosyl

1mg/ml proteinase k (added fresh each time)

Approximately 4 million CHO-FRT (untransfected) cells and CHO MICA transfectants (*004, 8, 9 and 27) were pelleted by spinning down at 1200rpm for 5 minutes and the supernatant was discarded. The pelleted cells were resuspended in 250µl lysis buffer and incubated at 60˚ C for 3 hours. Following this, an equal volume (250µl) of phenol:chloroform (phenol:chloroform:isoamylalcohol, 25:42:1) pH 7.8 was added to the samples, and they were immediately shaken gently by hand until an emulsion had formed. The samples were then centrifuged for 5-10 minutes at 13,000rpm at room temperature. At this point, the phases were separated, and the DNA (in the aqueous phase) was transferred into a new tube. These spinning steps were repeated until no protein was visible at the interphase of the aqueous and organic phases, after which 250µl of chloroform was added to the samples, and the spinning steps were repeated again, to extract the DNA. Once extracted, 250µl of chloroform and 10µl of 5M NaCl was added to the samples, followed by the addition of exactly 2 volumes of ice cold ethanol. The samples were mixed and the DNA left to precipitate on ice for 30 minutes before centrifuging at 16,000g at 4˚C for 10 minutes. The supernatant was decanted, and the DNA pellets were washed with 500µl of 70% ethanol, and re-spun for 5

minutes 4˚C. The supernatant was sucked off and the DNA pellet was air dried for 5 minutes until the ethanol was evaporated and then the pellets were dissolved in 30µl of 10mM Tris pH 8.5. The concentration of the DNA from each sample was quantified using the nanodrop machine and then 1µg of DNA from each sample was run on a 1% agarose gel (containing ethidium bromide) to check the quality of the DNA.

The DNA from each cell line was then digested with BlpI enzyme in the following way:

24µl of DNA (20µg)

3µl of NEB buffer 4

3µl of BlpI enzyme

These reactions were left to digest overnight at 37˚C.

### 6.5.2 Electrophoresis of DNA through a gel containing formaldehyde

A 0.7% agarose gel (Seakem LE agarose) was prepared in 500mls of 1X TAE buffer, and the gel was allowed to set with a 17 well comb. To the digested DNA samples and the 1Kb DNA ladder (New England Biolabs, cat # N3232L), 4ul of green loading buffer (buffer turns blue when mixed with samples and colour changes to green/yellow during depurination) was added and the samples and the DNA ladder were added to the wells of the gel. The gel was run at 40-60 V for 4-6 hours till the DNA had run 10cm down the gel. A photograph was taken of the gel under the UV lamp against a ruler for reference. The gel was then placed in a large plastic tank and shaken in depurination solution (see below) for 15 minutes and the colour of the DNA changed from blue to green to yellow. The depurination solution was then discarded and the gel was left to shake for 30 minutes in denaturation solution (see below), where the colour of the DNA changes from yellow to blue.

Depurination solution (0.25M HCL)

50ml of 10M HCL

1950ml water

Denaturation solution

88g of Sodium chloride

20g of Sodium hydroxide

2000ml water

The transfer of DNA from gel to nylon membrane technique was the same as the Transfer of RNA from gel to nylon membrane technique (Northern blot technique) with only one difference: the buffer used for transfer was 20 X SSC (not 10 X SSC). Preparation of the Southern probe was the same as in the northern (section 6.4.4) but only the full length MICA probes were used, and not beta actin. The Pre-hybridization of the membrane (blot) using Sigma's perfect-hyb (Sigma Aldrich, cat. # H7033), the hybridization steps and the washing steps were the same as for the northern blot.

### 6.5.3 Exposure of the membrane to a Kodak film

The membrane was wrapped in saran wrap cling film and put in a cassette (in the dark) with a kodak film (Sigma Aldrich, Kodak Biomax MS film, MS-1 size 35cm x 43cm) , and left to expose overnight at -80˚ C. The next day the film was exposed and developed.

## 6.6 Western blot technique

### 6.6.1 Preparation of cell lysates and supernatants

CHO-FRT (untransfected) and CHO-MICA transfectants were added to a 6 well plate with 4 mls of complete medium (CHO-FRT) with hygromycin B (CHO-MICA transfectants) and left in the 37 ˚C incubator for 24 hours. After this time point, the medium was taken off, the cells were washed twice with RPMI (serum-free) and 4mls of RPMI (serum-free) were added to the cells and left in the incubator for 6 hours. Following this, the supernatant was taken off gently and centrifuged at maximum speed for 30 minutes to pellet and debris of dead cells. The actual supernatants were then gently taken off, filtered by a 0.2µm Millex filter units, 33mm (Miillipore, UK, cat # SLGN033NS) and spun down in Amicon Ultra-4' 10,000 MWCO (Millipore cat # UFC801024) tubes at 4000 rpm for 20 minutes to concentrate them to 300µl.

Preparation of the lysates involved washing the cells in ice cold 1X PBS (all steps were carried out on ice) before addition of 500µl of freshly prepared cold lysis buffer (containing protease inhibitors) to each well. This was left to incubate on ice for 30 mins before scraping off the cells from the wells, adding them to individual epindorphs and snap freezing them in liquid nitrogen for 30 seconds. The lysates were then allowed to thaw on ice for up to 1 hour. Following this, the lysates were then centrifuged at 13,000rpm for 30 minutes at 4 ˚C to pellet the cells, and the actual lysates were taken off and added to new epindorphs.

Lysis buffer

580 µL Nonidet P40

0.58 g CHAPS

0.150 g HEPES

0.508 g NaCl

9.93 g Saccharose

0.022 g $Na_2EDTA$

### 6.6.2 Determining the concentration of protein in the lysates and supernatants

This technique was carried out using the micro BCA protein assay kit (Thermoscientific cat # 23235). The samples (lysates and supernatants) and standards (BSA 10mg/ml, New England Biolabs, UK cat # B9001S) were prepared in the following way:

Standards: dilutions of BSA 10mg/ml in 1X PBS:

- 10mg/ml stock BSA
- 5mg/ml
- 2.5mg/ml
- 1.25mg/ml
- 0.625mg/ml
- 0.313mg/ml

A blank sample was also prepared which consisted of 150µl of lysis buffer (only).

Approximately 150µl of standards, blank, lysates and supernatants were added to a 96 well plate and the detection mixture was made up in the following way:

Detection mixture

1000µl MA reagent

960µl MB reagent

40µl MC reagent

These were mixed together and 150µl was added to each of the blank, samples and standards and mixed thoroughly by pipetting up and down. The 96 well plate was then incubated at 37 ˚C for 1-2 hours. Following the incubation, all the samples in the 96 well plate were read at 562nm wavelength. A standard curve was produced, and the protein concentration of each sample was calculated.

### 6.6.3 Preparation of a 12% gel using and Gel electrophoresis

Two 12% gels were prepared using ProtoGel (Fisher, Uk, cat # EC-890) in the following way:

12%Resolving gel

20mls ProtoGel

12.5mls Resolving buffer (Fisher, Uk, cat # EC-892)

20.3mls deionized water

500µl 10% ammonium persulphate

50µl TEMED

The contents of the gel were then mixed by swirling and poured into the gel casting cassettes. The top layers of the gels were covered with water, to eliminate bubbles and to provide a sharp interface.

4% Stacking gel

650µl ProtoGel EC-890

1.250ml ProtoGel Stacking buffer (Fisher, Uk, cat # EC-893)

3.050ml deionized water

25µl 10% ammonium persulphate

10µl TEMED

For each 12percentage gel, 10µg of protein from each lysate and supernatant was then added to new epindorphs, to which lysis buffer was added to a total volume of 15µl. 5µl of loading buffer and 2µl of dithiothreitol (DTT) reducing agent were added to the samples. The molecular weight (MW) marker was also prepared: 10µl marker was added to 3.3µl loading buffer and 2 µl of DTT. The samples and the MW marker were

boiled at 70 ˚C for 10 minutes, quickly centrifuged and then loaded into the wells. Both gels were run at 200V for 1 hour in 1X running buffer.

1X Running buffer

3.03 g Trizma base (= 0.25 M)

14.4 g Glycine (= 1.92 M)

1 g SDS (= 1%)

### 6.6.4 Transfer of protein from gel to the nitrocellulose membrane

The transfer from gel to the membrane was set up as follows: The black side of the transfer cassette was emerged in transfer buffer with a sponge layered on top of it, two 3mm whatmann filter papers were placed on top of the sponge, followed by the gel, the nitrocellulose membrane, two more whatmann papers and finally a sponge. The transfer cassette was then closed in and tightly shut, before inserting into the tank filled with transfer buffer. An ice block was added to the tank to ensure that the buffer does not over heat during the transfer process. Transfer occurs at 100V for 1 hour in 1X transfer buffer. After the transfer, the membrane is blocked with 10% BSA in PBS 0.05% Tween for 30 minutes to 2 hours.

10X transfer buffer stock - stored at 4° C

144.1 g Tris base

144.1 g glycine

water to 1 liter

1X transfer buffer - stored at 4° C

- 100 ml 10X stock
- 500 ml $H_2O$

- 200 ml methanol

- water to 1 L

- chill to 4° C

### 6.6.5 Probing for MICA and Beta actin, washing and exposing of membrane to Kodak film.

The mouse anti-human MICA monoclonal antibody (R&D systems, UK, cat # MAB1300) and goat polyclonal beta-actin antibody (Abcam, UK cat # ab8229) were diluted to 1µg/ml in 10% BSA in 1X PBS 0.05% Tween and left to incubate overnight at 4 ˚C. The following day, the membranes were washed four times with 1XPBS 0.05% Tween for 15 minutes on the shaker at room temperature. The secondary antibodies: horseradish peroxidase (HRP)-conjugated goat anti-mouse IgG (R&D systems, UK, cat # HAF007) and HRP-conjugated rabbit anti goat IgG (R&D systems, UK, cat # HAF017) were prepared. Both antibodies were diluted 1/5000 in 10% BSA in 1X PBS 0.05% Tween and left to incubate for 30 minutes at room temperature. The membranes were then washed and antibody binding to membranes was visualized using the ECL chemiluminescence system (Amersham, UK, cat # RPN2108) using the Image Quant machine.

## 6.7 Staining of PBMCs from Behcet's patients, disease and healthy controls and analysis by Flow cytometry

Blood from 90 patients (37 males and 53 females), 16 Disease (11 male and 5 female diopathic uveitis patients on similar steroid treatment as BD patients) and 23 healthy Controls (18 males and 5 females) was collected. All donors were aged 25-65.All patients fulfilled the International Study Group criteria (ISG criteria). 69 Patients were on steroid treatment, 13 of whom had active disease, 8 were off treatment (present this as a table of patient criteria) and 69 were classified as quiet patients with little or no disease activity. Clinical activity was assessed at the time of venipuncture from active signs and symptoms (oral ulcers, genital ulcers, ocular lesions, skin lesions, articular symptoms).

Peripheral blood lymphocytes were isolated from heparinized samples by conventional Ficoll-Hypaque centrifugation and washed twice with RPMI (No-serum) and once with PBS 1% FCS (FACS Buffer). For 2 and 3 Colour-cytofluorimetric analysis, 200,000 cells were stained for each patient and control sample.

Phenotype of lymphocyte sub-populations was determined by immunofluorescence with monoclonal antibodies Cells were stained with the appropriate fluorescently labelled antibodies against specific surface markers: CD3, CD16, CD56, NKT, CD8, KIR3DL1, NKG2D, and γδ. For each sample, cells were also stained using the matched labelled isotype control. Cells were washed once using FACS Buffer and then re-suspended in 300µl buffer to be analysed.

## 6.8 In vitro Cytotoxicity Assay

A cytotoxic assay using the CFSE fluorescent dye was employed as the techniques to investigate the % specific killing of CHO-transfected cells by PBMCs isolated from healthy controls and BD patients. To achieve this, the control (CHO-FRT) and target cell lines (CHO-MICA and ULBP2) were stained with carboxyfluorescein succinimidylester (CFSE; Invitrogen, cat. #C34554) and then incubated with effector cells (PBMC's) overnight (protocol outlined below).

### 6.8.1 CFSE staining of control and target cells

CHO-FRT (untransfected) and CHO-MICA and ULBP2 transfectants are stained with a final concentration of 0.5µM CFSE and 5µM CFSE separately. Cells were first pelleted by centrifugation at 1200rpm for 5 minutes, the supernatant was aspirated off. The control cells were resuspended in 0.5ml of 1x PBS 0.5µM CFSE and the CHO-transfectants in 0.5ml of 1x PBS 5µM CFSE drop wise and mixed by gentle vortexing. The cells were then left to incubate for 10 minutes at room temperature. The cells were then washed twice in 10mls RPMI 1640 15% FCS and then resuspended in 1ml of complete medium (RPMI 1640 10%FCS).

### 6.8.2 Staining of effector cells with DDAO-SE

PBMC's (effector cells) freshly isolated from the blood of healthy controls and patients were stained with 2µM dodecyldimethylamine oxide succinimidyl ester (DDAO-SE; Invitrogen, cat. #C34553) in the following way: the effector cells were pelleted by centrifuging at 1200rpm for 5 minutes and resuspended in 500µlserum-free medium (RPMI 1640) 2µM DDAO-SE and then incubated on ice for 10 minutes in the dark. The cells were then washed twice with complete medium and placed on ice.

### 6.8.3 Cytotoxicity assay protocol

After staining the control and target CHO cells with CFSE, the cells were counted and diluted to a cell density of 2 x $10^5$ cells/ml each and then control and target samples combined at a 1:1 ratio. Therefore 100µl of control (CHO-FRT) and target (CHO-MICA and ULBP2) was plated in to each well of a 96-well plate resulting in 1 x $10^4$ control control and 1 x $10^4$ target cells per well. Effector cells were then counted, such that 6, 2 and 0.6 x $10^5$ were added to each well and spun down on to the target cells, resulting in effector:target (E:T) ratios of 20:1, 10:1 and 3:1. The assay was carried out in triplicate (3 wells of control: targets/effector). The plate was then incubated for 12 hours at 37˚C/5% CO2. After 12 hours, cells were detached from the plate using accutase (Sigma Aldrich, UK, cat # A6964) and resuspended in 330µl FACS buffer (1XPBS 2%FCS) to be analysed immediately by flow cytometry.

### 6.8.4 Analysis

Specific lysis of target cells was generated by analysis of the samples on the BD FACSCalibur. Live CHO cells were gated on by side scatter (CHO cells larger in size than PBMC's) and distinguished from any infiltrating effector cells (into the CHO cell gate) by CFSE fluorescence and a lack of DDAO-SE staining. The ratio of CFSEHigh (target cells) to CFSELow (control cells) was analysed from all samples. If no specific lysis of target CHO cells has occurred then the ratio should of control: targets should be 1:1, whereas if specific lysis of target cells *has* occurred, then there will be fewer

CFSEHigh cells, and the ratio of CFSELow: CFSEHigh will be greater than 1:1. To calculate the percentage specific lysis, the following equation was used:

% specific lysis = 100(1-((control ratio)/ (experimental ratio) whereby the control ratio refers to the CFSELow: CFSEHigh value in the absence of effector cells, and the experimental ratio refers to the CFSELow: CFSEHigh value in the presence of effector cells. The values for specific lysis against all CHO cell targets and at all E: T ratios were calculated in this way (mean of triplicate wells +/- SD) and then compiled and analysed statistically using Prism software.

## 6.9 CD107a Degranulation Assay

### 6.9.1 In vitro Cytotoxicity assay (CD107a)

For the analysis of cytotoxic cell activation, 2 x $10^5$ effector cells (PBMC's) were mixed with target cells at a 1:1 ratio in round bottom 96 wells plates in the presence of the anti-CD107a-PE antibody (BD Pharmingen, UK, cat # 555801) at a 1/30 final dilution. The cells were then pelleted by brief centrifugation at 400g and incubated for 5h at 37˚C 5% $CO_2$. Cells were then washed once, stained for the indicated cell surface markers for 30min at 4˚C in PBS 2% FCS (FACS buffer), washed and resuspended in 100µL FACS buffer. Staining with a combination of cell-type specific surface antigens (e.g. anti-human CD3 for T cells, CD3-CD16+CD56+ for NK cells and gamma delta TCR antibody for gamma delta cells), was then performed in the well in a 100µl final volume with FACS buffer for 30 minutes on ice. Following washing, the cells were then immediately analysed by flow cytometry to detect expression of CD107a on each cell type. Data were acquired on a FACScalibur flow cytometer and analysed with the FlowJo software (mean of triplicate wells +/- SD).

## 6.10 Surface and Intracellular staining of MICA transfectants

MICA transfectants were stained for cell surface expression of MICA with three different anti-MICA antibodies: mouse anti-human MICA-PE antibody (R&D systems, UK, cat # FAB13001P, clone 159207) antibody and mouse $IgG_{2a}$-PE isotype control

(R&D systems, UK, cat # IC003P, clone 20102), mouse anti-human MICA-PE antibody (R&D systems, UK, cat # FAB1300P, clone 159227) and mouse IgG2b-PE isotype control (R&D systems, UK, cat # IC0041P, clone 133303) and purified anti-human MICA/B antibody (BD Pharmingen, UK, cat # 558032, clone 6D4) and purified $IgG2a,_k$ isotype control (BD Pharmingen, UK, cat # 555571, clone G155-178) with secondary Goat Anti-Mouse IgM Phycoerythrin, Goat IgG (R&D systems F0116). For intracellular staining, cells were collected with accutase, washed in complete medium and seeded in 96 wells plates ($2 \times 10^5$ cells per well). Cells were then fixed for 10 minutes at room temperature and then incubated with the mouse anti MICA/B-PE (R&D systems, UK, cat # FAB13001P) antibody and mouse $IgG_{2a}$-PE (R&D systems, UK, cat # IC003P) antibody diluted in BD Cytofix/Cytoperm™ Fixation and Permeabilization Solution (BD, Pharmingen, UK, cat # 554722) at a 1/50 final dilution for 30min at 4° C in the dark. Cells were then washed once in permeabilization buffer, once in FACS buffer, and resuspended in 200µL FACS buffer. Data were acquired on a FACScalibur flow cytometer and analysed with the FlowJo software.

## 6.11 Immunoflourescence microscopy to determine intensity of surface and intracellular protein.

200,000 CHO-FRT and MICA transfectants were added separately to wells with coverslips, coated with poly-L-lysine (10mg/ml), and left overnight in the incubator. The next day medium was taken off and cells were washed once with 1X PBS. For extracellular staining, cells were blocked with 2% BSA in PBS at R.T for 1 hour, after which mouse anti-human MICA antibody (10µg/ml) and the relevant isotype control antibody (10µg/ml) were added for 1 hour at R.T.) The cells were stained with purified anti-human MICA/B antibody (BD Pharmingen, UK, cat # 558032, clone 6D4) and purified $IgG2a,_k$ isotype control (BD Pharmingen, UK, cat # 555571, clone G155-178) with secondary FITC Rat Anti-Mouse IgG1 (BD Pharmingen, UK, cat # 553443, clone A85-1). Cells were then washed 3x in 1XPBS, and then fixed with 3% paraformaldehyde for 10 mins, washed with 1XPBS, and mounted the coverslips onto the slides. For the intracellular staining, cells were first fixed with 3% paraformaldehyde for 10 mins, permeabilised with 0.2% Triton for 5 mins, and then stained and mounted in the same way as the extracellular staining protocol.

## 6.12 Soluble MICA ELISA (sMICA)

This experiment was carried out to determine if the MICA transfectants shed MICA from the surface of the cells into the surrounding media. The sMICA ELISA measures the shedding of MICA in actual concentration of the soluble protein (pg/ml) which allows for comparison of shedding between the MICA alleles.

### 6.12.1 Reagents required

- Capture antibody (360µg/ml)-mouse anti-human MICA (reconstituted with 1ml PBS (phosphate buffered saline)). A working concentration of 2.0 µg/ml in PBS was used.
- Detection antibody (72 µg/ml) biotynalated goat anti-human MICA reconstituted with reagent diluent*. A working concentration of 400ng/ml in PBS was used.
- Standards: 220ng/ml of recombinant human MICA reconstituted with 0.5ml reagent diluent*. Standard curve using 2-fold serial dilutions in reagent diluent*.
- Streptavidin-HRP (1ml).
- Phosphate buffered saline (PBS)
- W\ash buffer (0.05% Tween20 in PBS)
- Reagent diluent (1% BSA in PBS, 0.2µm filtered)
- Substrate solution (1:1 mixture of colour reagent A, hydrogen peroxide and colour reagent B.
- Stop solution-2M sulphuric acid.

  *Reagent diluent- 2% normal goat serum (heat inactivated) in PBS

### 6.12.2 Protocol for the sMICA ELISA

- A 96-flat bottomed ELISA plate was coated with 100µl of capture antibody (diluted to the working concentration of 2.0 µg/ml) and kept at room temperature overnight.

- After two successive washes (with wash buffer), 300µl of reagent diluent was added to the wells for one hour at room temperature.
- The plate was once again washed twice and the 100µl of standards and samples were added in the following way:

The standards for the ELISA used was serial dilutions of recombinant MICA:

(A) 4000 pg/ml
(B) 2000 pg/ml
(C) 1000 pg/ml
(D) 800 pg/ml
(E) 400 pg/ml
(F) 100 pg/ml
(G) 40 pg/ml

Samples

Approximately 200,000 MICA*008,*004 and MICA*009 CHO transfectants were separately plated into a 6-well plate with 1ml of media (RPMI 10% FCS with 600µg/ml) for 24 hours, after which the media was aspirated off the cells, the cells were then washed with 1X PBS to remove any traces of FCS. 1 ml of serum free RPMI was added to the cells for 6 hours. Following this, the supernatant was gently taken off the cells, and spun down for 30 mins at 13,000rpm: the final supernatant was then carefully removed from the pelleted dead cells. Approximately 100µl of the supernatant from each transfectant was added to the 96 well sMICA ELISA plate.

Both the standards and the samples were added to the wells in duplicates and allowed to incubate in the plate for 2 hours at room temperature.

- After 2 hours, the plates were washed twice, and 100µl of detection antibody (diluted in reagent diluent to a working concentration of 400µg/ml) was added to the wells to incubate for 2 hours at room temperature.
- The wells were then washed again twice, and 100ul of substrate solution was added to the wells and incubated at room temperature for 20 minutes.

- Following this, 50µl of stop solution is added to each well.
- The plate is then read in the plate reader at 540nm and 450nm wavelength.
- A standard curve was then obtained and the sMICA concentration from each sample was then calculated.

# REFERENCES


1. Adrain C, Murphy BM, Martin SJ. 2005. Molecular ordering of the caspase activation cascade initiated by the cytotoxic T lymphocyte/natural killer (CTL/NK) protease granzyme B. J Biol Chem 280(6):4663-73.

2. Ahmad T, Wallace GR, James T, Neville M, Bunce M, Mulcahy-Hawes K, Armuzzi A, Crawshaw J, Fortune F, Walton R, Stanford MR, Welsh KI, Marshall SE, Jewell DP. 2003. Mapping the HLA association in Behçet's disease: a role for tumor necrosis factor polymorphisms? Arthritis Rheum 48(3):807-13.

3. Ahn JK, Seo JM, Yu J, Oh FS, Chung H, Yu HG. 2005. Down-regulation of IFN-gamma-producing CD56+ T cells after combined low-dose cyclosporine/prednisone treatment in patients with Behçet's uveitis. Invest Ophthalmol Vis Sci 46(7):2458-64.

4. Akdeniz, N., Esrefoglu, M., Keles, M.S., Karakuzu, A., Atasoy, M., 2004. Serum interleukin-2, interleukin-6, tumour necrosis factor-alpha and nitric oxide levels in patients with Behcet's disease. Ann Acad Med Singapore 33(5): 596–599.

5. Aki, A T., Karincaoglu, Y., Seyhan, M., Batcioglu, K., 2006. Serum substance P and calcitonin gene-related peptide levels in Behcet's disease and their association with disease activity. Clin Exp Dermatol 31(4): 583–587.

6. Anderson P, Caligiuri M, Ritz J, SchlossmanSF. 1989. CD3-negative natural killer cells express ζ TCR as part of a novel molecular complex. Nature 341(6238):159–62.

7. Angelosanto JM, Blackburn SD, Crawford A, Wherry EJ. 2012. Progressive loss of memory T cell potential and commitment to exhaustion during chronic viral infection. J Virol 86(15):8161-70.

8. Altenburg, A., Papoustis, N., Orawa, H., Martus, P., Krause, L., Zouboulis, C.C., 2006. Epidemiology and clinical manifestations of Adamantiades-Behcet

disease in Germany-current pathogenetic concepts and therapeutic possibilities. J Dtsch Dermatol Ges 4(1): 49–65.

9. Alter G, Martin MP, Teigen N, Carr WH, Suscovich TJ, Schneidewind A, Streeck H, Waring M, Meier A, Brander C, Lifson JD, Allen TM, Carrington M, Altfeld M. 2007. Differential natural killer cell-mediated inhibition of HIV-1 replication based on distinct KIR/HLA subtypes. J Exp Med 204(12):3027-36.

10. Ambros V. 2004. The functions of animal microRNAs. Nature 431(7006):350-5.

11. Ando, K., Fujino, Y., Hijikata, K., Izawa, Y., Masuda, K., 1999. Epidemiological features and visual prognosis of Behcet's Disease. Jpn J Ophthalmol 43(4): 312–317.

12. Arase, N., H. Arase, S. Y. Park, H. Ohno, C. Ra, and T. Saito. 1997. Association with FcRgamma is essential for activation signal through NKR-P1 (CD161) in natural killer (NK) cells and NK1.1$^{+}$ T cells. J Exp Med 186(12): 1957–1963.

13. Arida A, Fragiadaki K, Giavri E, Sfikakis PP. 2011. Anti-TNF agents for Behçet's disease: analysis of published data on 369 patients. Semin Arthritis Rheum 41(1):61-70.

14. Arnheim L, Dillner J, Sanjeevi CB. 2005. A population-based cohort study of KIR genes and genotypes in relation to cervical intraepithelial neoplasia. Tissue Antigens 65(3):252-9.

15. Arnon TI, Lev M, Katz G, Chernobrov Y, Porgador A, Mandelboim O. 2001. Recognition of viral hemagglutinins by NKp44 but not by NKp30. Eur J Immunol 31(9):2680-9.

16. Arreygue-Garcia NA, Daneri-Navarro A, del Toro-Arreola A, Cid-Arregui A, Gonzalez-Ramella O, Jave-Suarez LF, Aguilar-Lemarroy A, Troyo-Sanroman

R, Bravo-Cuellar A, Delgado-Rizo V, Garcia-Iglesias T, Hernandez-Flores G, Del Toro-Arreola S. 2008. Augmented serum level of major histocompatibility complex class I-related chain A (MICA) protein and reduced NKG2D expression on NK and T cells in patients with cervical cancer and precursor lesions. BMC Cancer 8:16.

17. Aust JG, Gays F, Mickiewicz KM, Buchanan E, Brooks CG. 2009. The expression and function of the NKRP1 receptor family in C57BL/6 mice. J Immunol 183(1):106-16.

18. Bahram S, Bresnahan M, Geraghty DE, Spies T, 1994. A second lineage of mammalian major histocompatibility complex class I genes. Proc Natl Acad Sci USA 91(14):6259–62.

19. Bahram S. MIC genes: from genetics to biology. 2000. Adv Immunol 76:1-60.
20. Barber, L.D, P. Parham. 1993. Peptide binding to major histocompatibility complex molecules. Annu. Rev. Cell Biol 9:163-206.
21. Baranathan V, Stanford MR, Vaughan RW, Kondeatis E, Graham E, Fortune F, Madanat W, Kanawati C, Ghabra M, Murray PI, Wallace GR. 2007 .The association of the PTPN22 620W polymorphism with Behcet's disease. Ann Rheum Dis 66(11):1531-3.
22. Bauer S, Groh V, Wu J, Steinle A, Phillips JH, Lanier LL, Spies T. 1999. Activation of NK cells and T cells by NKG2D, a receptor for stress-inducible MICA. Science 285(5428):727-9

23. Ben Ahmed, M., Houman, H., Miled, M., Dellagi, K., Louzir, H., 2004. Involvement of chemokines and Th1 cytokines in the pathogenesis of mucocutaneous lesions of Behcet’s disease. Arthritis Rheum 50(7): 2291–2295.

24. Biassoni R, Cantoni C, Pende D, Sivori S, Parolini S, Vitale M, Bottino C, Moretta A. 2001. Human natural killer cell receptors and co-receptors. Immunol Rev 181:203-14.

25. Biassoni R, Bottino C, Cantoni C, Moretta A. 2002. Human natural killer receptors and their ligands. Curr Prot Immunol chapter 14 :Unit 14.10.

26. Binstadt BA, Brumbaugh KM, Dick CJ, Scharenberg AM, Williams BL, Colonna M, Lanier LL, Kinet JP, Abraham RT, Leibson PJ. 1996. Sequential involvement of Lck and SHP-1 with MHC-recognizing receptors on NK cells inhibits FcR-initiated tyrosine kinase activation. Immunity 5(6):629–38.

27. Binstadt BA, Billadeau DD, Jevremović D, Williams BL, Fang N, Yi T, Koretzky GA, Abraham RT, Leibson PJ. 1998. SLP-76 is a direct substrate of SHP-1 recruited to killer cell inhibitory receptors. J Bio Chem 273(42):27518–23.

28. Bloushtain N, Qimron U, Bar-Ilan A, Hershkovitz O, Gazit R, Fima E, Korc M, Vlodavsky I, Bovin NV, Porgador A. 2004. Membrane associated heparan sulfate proteoglycans are involved in the recognition of cellular targets by NKp30 and NKp46. J Immunol 173(4): 2392–2401.

29. Bojarska-Junak A, Hus I, Sieklucka M, Wasik-Szczepanek E, Mazurkiewicz T, Polak P, Dmoszynska A, Rolinski J. 2010. Natural killer-like T CD3+/CD16+CD56+ cells in chronic lymphocytic leukemia: intracellular cytokine expression and relationship with clinical outcome. Oncol Rep 24(3):803-10.

30. Bouma G, Mendoza-Naranjo A, Blundell MP, de Falco E, Parsley KL, Burns SO, Thrasher AJ. 2011. Cytoskeletal remodeling mediated by WASp in dendritic cells is necessary for normal immune synapse formation and T-cell priming. Blood 118(9):2492-501.

31. Brandt CS, Baratin M, Yi EC, Kennedy J, Gao Z, Fox B, Haldeman B, Ostrander CD, Kaifu T, Chabannon C, Moretta A, West R, Xu W, Vivier E, Levin SD. 2009. The B7 family member B7-H6 is a tumor cell ligand for the activating natural killer cell receptor NKp30 in humans. J Exp Med 206(7): 1495–1503.

32. Braud VM, Allan DS, O'Callaghan CA, Söderström K, D'Andrea A, Ogg GS, Lazetic S, Young NT, Bell JI, Phillips JH, Lanier LL, McMichael AJ. 1998. HLA-E binds to natural killer cell receptors CD94/NKG2A, B and C. Nature 391(6669):795–799.

33. Brodin P., Karre K., Hoglund P. 2009. NK cell education: not an on-off switch but a tunable rheostat. Trends Immunol 30(4):143–149.
34. Brown MH, Boles K, van der Merwe PA, Kumar V, Mathew PA, Barclay AN. 1998. 2B4, the natural killer and T cell immunoglobulin superfamily surface protein, is a ligand for CD48. J Exp Med 188(11): 2083–2090.
35. Bryceson YT, March ME, Barber DF, Ljunggren HG, Long EO. 2005. Cytolytic granule polarization and degranulation controlled by different receptors in resting NK cells. J Exp Med 202(7):1001-12.
36. Bryceson YT, Ljunggren HG, Long EO. 2009. Minimal requirement for induction of natural cytotoxicity and intersection of activation signals by inhibitory receptors. Blood 114(13):2657-66.
37. Campbell JA, Trossman DS, Yokoyama WM, Carayannopoulos LN.2007. Zoonotic orthopoxviruses encode a high-affinity antagonist of NKG2D. J Exp Med 204(6):1311-7.
38. Cantoni, C., S. Verdiani, M. Falco, A. Pessino, R. Cilli, R. Conte, D. Pende, M. Ponte, M. S. Mikaelsson, L. Moretta, and R. Biassoni. 1998. p49, a putative HLA class I-specific inhibitory NK receptor belonging to the immunoglobulin superfamily. Eur J Immunol. 28(6):1980-90.
39. Cantoni C, Bottino C, Vitale M, Pessino A, Augugliaro R, Malaspina A, Parolini S, Moretta L, Moretta A, Biassoni R. 1999. "NKp44, a triggering receptor involved in tumor cell lysis by activated human natural killer cells, is a novelmember of the immunoglobulin superfamily," J Exp Med 189(5):787–795.
40. Carletto A, Pacor ML, Biasi D, Caramaschi P, Zeminian S, Bellavite P, Bambara LM. 1997. Changes of neutrophil migration without modification of in vitro metabolism and adhesion in Behçet's disease. J Rheumatol 24(7): 1332-36.
41. Carlyle, J. R., A. Martin, A. Mehra, L. Attisano, F. W. Tsui, and J. C. Zuniga-Pflucker. 1999. Mouse NKR-P1B, a novel NK1.1 antigen with inhibitory function. J Immunol 162(10): 5917–5923.

42. Carr, W. H., M. J. Pando, and P. Parham. 2005. KIR3DL1 polymorphisms that affect NK cell inhibition by HLA-Bw4 ligand. J. Immunol 175(8): 5222–5229.

43. Carretero, M., G. Palmieri, M. Llano, V. Tullio, A. Santoni, D.E. Geraghty, and M. Lopez-Botet. 1998. Specific engagement of the CD94/NKG2-A killer inhibitory receptor by the HLA-E class Ib molecule induces SHP-1 phosphatase recruitment to tyrosine-phosphorylated NKG2-A: evidence for receptor function in heterologous transfectants. Eur J Immunol 28(4):1280–1291.

44. Carrington, M., and M. Cullen. 2004. Justified chauvinism: advances in defining meiotic recombination through sperm typing. Trends Genet 20(4):196–205.

45. Cella, M., A. Longo, G. B. Ferrara, J. L. Strominger, and M. Colonna. 1994. NK3-specific natural killer cells are selectively inhibited by Bw4-positive HLA alleles with isoleucine 80. J Exp Med 180(4): 1235–1242.

46. Chan HW, Kurago ZB, Stewart CA, Wilson MJ, Martin MP, Mace BE, Carrington M, Trowsdale J, Lutz CT. 2003. DNA methylation maintains allele-specific KIR gene expression in human natural killer cells. J Exp Med 197(2): 245–255.

47. Chan A, Hong DL, Atzberger A, Kollnberger S, Filer AD, Buckley CD, McMichael A, Enver T, Bowness P. 2007. CD56 bright human NK cells differentiate into CD56dim cells: role of contact with peripheral fibroblasts. J Immunol 179(1):89-94.

48. Chalupny NJ, Rein-Weston A, Dosch S, Cosman D. 2006. Down-regulation of the NKG2D ligand MICA by the human cytomegalovirus glycoprotein UL142. Biochem Biophys Res Commun 346(1):175-81.

49. Choy,MK., Phipps,ME. 2003. Possible polyphyletic origin of major histocompatibility complex class i chain-related gene A (MICA) alleles. J Mol Evol 57(1):38–43

50. Chenna, R., H. Sugawara, T. Koike, R. Lopez, T. J. Gibson, D. G. Higgins, and J. D. Thompson. 2003. Multiple sequence alignment with the Clustal series of programs. Nucleic Acids Res 31(13):3497-3500.

51. Clayberger, C., M. Rosen, P. Parham, and A.M. Krensky. 1990. Recognition of an HLA public determinant (Bw4) by human allogeneic cytotoxic T lymphocytes. J Immunol 144(11):4172-4176.

52. Clemente A, Cambra A, Munoz-Saá I, Crespí C, Pallarés L, Juan A, Matamoros N, Julià MR. 2010. Phenotype markers and cytokine intracellular production by CD8+ gammadelta T lymphocytes do not support a regulatory T profile in Behçet's disease patients and healthy controls. Immunol Lett 129(2):57-63.

53. Cooper MA, Fehniger TA, Turner SC, Chen KS, Ghaheri BA, Ghayur T, Carson WE, Caligiuri MA. 2001. Human natural killer cells: a unique innate immunoregulatory role for the CD56 (bright) subset. Blood 97(10):3146-51.

54. Correa I, Raulet DH. 1995. Binding of diverse peptides to MHC class I molecules inhibits target cell lysis by activated natural killer cells. Immunity 2(1): 61–71.

55. Correia DV, Fogli M, Hudspeth K, da Silva MG, Mavilio D, Silva-Santos B. 2011. Differentiation of human peripheral blood Vδ1+ T cells expressing the natural cytotoxicity receptor NKp30 for recognition of lymphoid leukemia cells. Blood 118(4):992-1001.

56. Cosman D, Müllberg J, Sutherland CL, Chin W, Armitage R, Fanslow W, Kubin M, Chalupny NJ. 2001. ULBPs, novel MHC class I-related molecules, bind to CMV glycoprotein UL16, and stimulate NK cytotoxicity through the NKG2D receptor. Immunity 14(2):123–133.

57. Coudert JD, Zimmer J, Tomasello E, Cebecauer M, Colonna M, Vivier E, Held W. 2005. Altered NKG2D function in NK cells induced by chronic exposure to NKG2D ligand-expressing tumor cells. Blood 106(5):1711-7.

58. Coudert JD, Scarpellino L, Gros F, Vivier E, Held W. 2008. Sustained NKG2D engagement induces cross-tolerance of multiple distinct NK cell activation pathways. Blood 111(7):3571-8.

59. Cullen SP, Adrain C, Luthi AU, Duriez PJ, Martin SJ. 2007. Human and murine granzyme B exhibit divergent substrate preferences. J Cell Biol 176(4):435–444.

60. Curnow SJ, Pryce K, Modi N, Knight B, Graham EM, Stewart JE, Fortune F, Stanford MR, Murray PI, Wallace GR. 2008. Serum cytokine profiles in Behçet's disease: is there a role for IL-15 in pathogenesis? Immunol Lett 121(1):7-12.

61. Dam J, Guan R, Natarajan K, Dimasi N, Chlewicki LK, Kranz DM, Schuck P, Margulies DH, Mariuzza RA. 2003. Variable MHC class I engagement by Ly49 natural killer cell receptors demonstrated by the crystal structure of Ly49C bound to H-2K(b). Nat Immunol 4(12): 1213–1222.

62. Davatchi F, Baygan F, Chams H, Chams C, Contractor M. 1984. Levamisole in Behcet’s disease. Rev Int Rhumatol 14:109–13.

63. Davatchi F, Shahram F, Chams H, Jamshidi AR, Nadji A, Chams C, Akbarian M, Gharibdoost F. 2003. High dose methotrexate for ocular lesions of Behcet’s disease.Preliminary short-term results. Adv Exp Med Biol 528:579–84.

64. Davatchi F, Shahram F, Chams H, Akbarian M. 2004. Pulse cyclophosphamide in ocular manifestations of Behcet’s Disease. A double blind crossover study. Arch Iran Med 7:201–5.

65. Davatchi F, Sadeghi Abdollahi B, Tehrani Banihashemi A, Shahram F, Nadji A, Shams H, Chams-Davatchi C. 2009. Colchicine versus placebo in Behcet’s Disease; randomized double blind controlled crossover trial. Mod Rheumatol 19(5):542-9.

66. Davies, G. E., S. M. Locke, P. W. Wright, H. Li, R. J. Hanson, J. S. Miller, and S. K. Anderson. 2007. Identification of bidirectional promoters in the human KIR genes. Genes Immun 8(3):245-53.

67. Davis DM, Dustin ML.2004. What is the importance of the immunological synapse? Trends Immunol 25(6):323-7.

68. de Menthon M, Lavalley MP, Maldini C, Guillevin L, Mahr A. 2009. HLA-B51/B5 and the risk of Behçet's disease: a systematic review and meta-analysis of case-control genetic association studies. Arthritis Rheum 61(10):1287-96.

69. Denman AM, PJ Fialkow PJ, P Elton BK, Salo AC, Appleford DJ. 1979. Attempts to establish a viral aetiology for Behcets syndrome. In: Lehner T and Barnes CG (eds). Behcets syndrome, London, Academic Press 91-105.

70. Deuter CM, Kötter I, Wallace GR, Murray PI, Stübiger N, Zierhut M. 2008.Behçet's disease: ocular effects and treatment. Prog Retin Eye Res 27(1):111-36.

71. Dilsen, N., Konice, M., Aral, O., 1986. Our diagnostic criteria of Behcet's Disease-an overview, recent advances in Behcet's Disease. London Royal Society of Medicine Services. Int Congr Sympos Series 103:177–180.

72. Direskeneli H, Keser G, D'Cruz D, Khamashta MA, Akoğlu T, Yazici H, Yurdakul S, Hamuryudan V, Ozgün S, Goral AJ, et al. 1995. Anti-endothelial cell antibodies, endothelial proliferation and von Willebrand factor antigen in Behcet's disease. Clin Rheumatology 14(1):55–61.

73. Direskeneli H, Ekşioglu-Demiralp E, Yavuz S, Ergun T, Shinnick T, Lehner T, Akoglu T. 2000. T cell responses to 60/65 kDa heat shock protein derived peptides in Turkish patients with Behçet's disease. J Rheumatol 27(3):708-13.

74. Direskeneli H, Saruhan-Direskeneli G.2003. The role of heat shock proteins in Behçet's disease. Clin Exp Rheumatol 21(4 Suppl 30):S44-8.

75. Direskeneli H. 2006. Autoimmunity vs autoinflammation in Behcet's disease: do we oversimplify a complex disorder? Rheumatology (Oxford) 45(12):1461-5.

76. Doğan P, Tanrikulu G, Soyuer U, Köse K. 1994. Oxidative enzymes of polymorphonuclear leucocytes and plasma fibringen, ceruloplasmin, and copper levels in Behçet's disease. Clin Biochem 27(5):413-18.

77. Doubrovina ES, Doubrovin MM, Vider E, Sisson RB, O'Reilly RJ, Dupont B, Vyas YM. 2003. Evasion from NK cell immunity by MHC class I chain-related molecules expressing colon adenocarcinoma. J Immunol 171(12):6891-9.

78. Dragun D, Philippe A, Catar R. 2012. Role of non-HLA antibodies in organ transplantation. Curr Opin Organ Transplant 17(4):440-5.

79. Duan X, Deng L, Chen X, Lu Y, Zhang Q, Zhang K, Hu Y, Zeng J, Sun W. 2011. Clinical significance of the immunostimulatory MHC class I chain-related molecule A and NKG2D receptor on NK cells in pancreatic cancer. Med Oncol 28(2):466-74.

80. Dummer R, Potoczna N, Häffner AC, Zimmermann DR, Gilardi S, Burg G. 1996. A primary cutaneous non-T, non-B CD4+, CD56+ lymphoma. Arch Dermatol 132(5):550-3.

81. Durrani O, Banahan K, Sheedy FJ, McBride L, Ben-Chetrit E, Greiner K, Vaughan RW, Kondeatis E, Hamburger J, Fortune F, Stanford MR, Murray PI, O'Neill LA, Wallace GR. 2011. TIRAP Ser180Leu polymorphism is associated with Behcet's disease. Rheumatology 50(10):1760-5

82. Eagle RA, Traherne JA, Ashiru O, Wills MR, Trowsdale J. 2006. Regulation of NKG2D ligand gene expression. Hum Immunol 67(3):159-69.

83. Efthimiou J, Addison IE, Johnson BV.1989: In vivo leucocyte migration in Behçet's syndrome. Ann Rheum Dis 48(3):206-10.

84. Eksioglu-Demiralp E, Direskeneli H, Ergun T, Fresko I, Akoglu T. 1999; Increased CD4+CD16+ and CD4+CD56+ T cell subsets in Behcet's disease. Rheumatol Int 19(1-2):23-6.

85. Ekşioglu-Demiralp E, Kibaroglu A, Direskeneli H, Yavuz S, Karsli F, Yurdakul S, Yazici H, Akoglu T. 1999. Phenotypic characteristics of B cells in

Behcet’s Disease: increased activity in B cell subsets. J Rheumatol 26(4):526–32.

86. Eleme K, Taner SB, Onfelt B, Collinson LM, McCann FE, Chalupny NJ, Cosman D, Hopkins C, Magee AI, Davis DM. 2004. Cell surface organization of stress-inducible proteins ULBP and MICA that stimulate human NK cells and T cells via NKG2D. J Exp Med 199(7):1005-10

87. Falk, K., Rotzschke, O., Takiguchi, M., Gnau, V., Stevanovic, S., Jung,G., Rammensee, H.G. 1995. Peptide motifs of HLA-B51, -B52 and-B78 molecules, and implications for Behcet’s disease. Int Immunol 7(2):223–228.

88. Favier B, Espinosa E, Tabiasco J, Dos Santos C, Bonneville M, Valitutti S, Fournié JJ. 2003. Uncoupling between immunological synapse formation and functional outcome in human gamma delta T lymphocytes. J Immunol 171(10):5027-33.

89. Feng XG, Ye S, Lu Y, Xu XJ, Gu YY, Shen N, Ye P, Cheng FP, Wang AM, Chen SL. 2007. Antikinectin autoantibody in Behçet's disease and several other autoimmune connective tissue diseases. Clin Exp Rheumatol 25(4 Suppl 45):S80-5.

90. Fischer G, Argüello JR, Pérez-Rodríguez M, McWhinnie A, Marsh SG, Travers PJ, Madrigal JA. 2000. Sequence-specific oligonucleotide probing for MICB alleles reveals associations with MICA and HLA-B. Immunogenetics 51(7):591-9

91. Flegel WA. 2007. Will MICA glitter for recipients of kidney transplants? N Engl J Med 357(13):1337-9.

92. Fodil N, Pellet P, Laloux L, Hauptmann G, Theodorou I, Bahram S. 1999. MICA haplotypic diversity. Immunogenetics 49(6):557-60.

93. Fortune F, Walker J, Lehner T. 1990. The expression of gd T cell receptor and the prevalence of primed, activated and IgA-bound T cells in Behcet's syndrome. Clin Exp Immunol 82(2):326-32.

94. Frassanito MA, Dammacco R, Cafforio P, Dammacco F. 1999. Th1 polarization of the immune response in Behçet's disease: a putative pathogenetic role of interleukin-12. Arthritis Rheum 42(9):1967-74.

95. Freud AG, Becknell B, Roychowdhury S, Mao HC, Ferketich AK, Nuovo GJ, Hughes TL, Marburger TB, Sung J, Baiocchi RA, Guimond M, Caligiuri MA.. 2005. A human CD34 (+) subset resides in lymph nodes and differentiates into CD56bright natural killer cells. Immunity 22(3): 295–304.

96. Freysdottir J, Lau S, Fortune F. 1999. Gammadelta T cells in Behcet's disease (BD) and recurrent aphthous stomatitis (RAS). Clin Exp Immunol 118(3):451-7.

97. Gardiner, C. M., L. A. Guethlein, H. G. Shilling, M. Pando, W. H. Carr, R. Rajalingam, C. Vilches, and P. Parham. 2001. Different NK cell surface phenotypes defined by the DX9 antibody are due to KIR3DL1 gene polymorphism. J Immunol 166(5): 2992–3001.

98. Gardiner CM. 2008. Killer cell immunoglobulin-like receptors on NK cells: the how, where and why. Int J Immunogenet 35(1): 1–8.

99. Garni-Wagner BA, Purohit A, Mathew PA, Bennett M, Kumar V. 1993. A novel function associated molecule related to non-MHC-restricted cytotoxicity mediated by activated natural killer cells and T cells. J Immunol 151(1): 60–70.

100. Garrity D, Call ME, Feng J, Wucherpfennig KW. 2005. The activating NKG2D receptor assembles in the membrane with two signaling dimers into a hexameric structure. Proc Natl Acad Sci USA 102(21):7641-6.

101. Gascoigne NR, Palmer E. 2011. Signaling in thymic selection. Curr Opin Immunol 23(2):207-12.

102. Gasser S, Raulet DH. 2006. Activation and self-tolerance of natural killer cells. Immunol Rev 214:130-42.

103. Gebreselassie, D., Spiegel, H., Vukmanovic, S. 2006. Sampling of major histocompatibility complex class I-associated peptidome suggests relatively

looser global association of HLA-B*5101 with peptides. Hum Immunol 67(11):894–906.

104. Geri G, Terrier B, Rosenzwajg M, Wechsler B, Touzot M, Seilhean D, Tran TA, Bodaghi B, Musset L, Soumelis V, Klatzmann D, Cacoub P, Saadoun D. 2011 .Critical role of IL-21 in modulating TH17 and regulatory T cells in Behçet disease. J Allergy Clin Immunol 128(3):655-64.

105. Gilfillan S, Ho EL, Cella M, Yokoyama WM, Colonna M. 2002. NKG2D recruits two distinct adapters to trigger NK cell activation and costimulation.Nat Immunol 3(12):1150-5.

106. Groh V, Bahram S, Bauer S, Herman A, Beauchamp M, Spies T. 1996. Cell stress-regulated human major histocompatibility complex class I gene expressed in gastrointestinal epithelium. Proc Natl Acad Sci USA 93(22):12445–12450

107. Groh V, Steinle A, Bauer S, Spies T. 1998. Recognition of stress-induced MHC molecules by intestinal epithelial gammadelta T cells. Science 279(5357):1737-1740.

108. Groh V, Rhinehart R, Secrist H, Bauer S, Grabstein KH, Spies T. 1999. Broad tumor associated expression and recognition by tumor-derived gd T cells of MICA and MICB. Proc Natl Acad Sci USA 96(12):6879–6884.

109. Groh V, Rhinehart R, Randolph-Habecker J, Topp MS, Riddell SR, Spies T. 2001. Costimulation of CD8alphabeta T cells by NKG2D via engagement by MIC induced on virus-infected cells. Nat Immunol 2(3):255–260.

110. Groh V, Wu J, Yee C, Spies T. 2002. Tumor-derived soluble MIC ligands impair expression of NKG2D and T-cell activation. Nature 419(6908):734–8.

111. Groh V, Smythe K, Dai Z, Spies T. 2006. Fas-ligand-mediated paracrine Tcell regulation by the receptor NKG2D in tumor immunity. Nat Immunol 7(7):755–762

112. Grossberger, D., and P. Parham. 1992. Reptillian class I major histocompatibility complex genes reveal conserved elements in class I structure. Immunogenetics 36(3):166-174.

113. Grossman, Z., and W. E. Paul. 1992. Adaptive cellular interactions in the immune system: the tunable activation threshold and the significance of subthreshold responses. Proc Natl Acad Sci USA 89(21):10365-10369.

114. Guerra N, Tan YX, Joncker NT, Choy A, Gallardo F, Xiong N, Knoblaugh S, Cado D, Greenberg NM, Raulet DH. 2008. NKG2D-deficient mice are defective in tumor surveillance in models of spontaneous malignancy. Immunity 28(4):571-80.

115. Gul, A., Inanc, M., Ocal, L., Aral, O., Konice, M., 2000. Familial aggregation of Behcet's disease in Turkey. Ann Rheum Dis 59(8):622–625.

116. Gul A .2001. Behcet's disease: an update on the pathogenesis. Clin Exp Rheumatol 19(5 Suppl.24): S6–12.

117. Gul A. 2005. Behcet's disease as an autoinflammatory disorder. Curr Drug Targets Inflamm Allergy 4(1):81–3.

118. Gur-Toy, G., Lenk, N., Yalcin, B., Aksaray, S., Alli, N., 2005. Serum interleukin-8 as a serologic marker of activity in Behcet's disease. Int J Dermatol 44(8):657–660.

119. Hamuryudan V, Mat C, Saip S, Ozyazgan Y, Siva A, Yurdakul S, Zwingenberger K, Yazici H. 1998 Thalidomide in the treatment of the Mucocutaneous lesions of Behcet's syndrome. A randomized double-blind, placebo controlled trial. Ann Intern Med 128(6):443-50.

120. Hamza M. 1986. Treatment of Behcet's disease with thalidomide. Clin Rheumatol 5(3):365–71.

121. Hamza M, Hamzaoui K, Ayed K. 1989. Treatment of Behcet's disease with dapsone. Clin Rheumatol 8(1):113–4.

122. Hamzaoui K, Hamzaoui A, Hentati F, Kahan A, Ayed K, Chabbou A, Ben Hamida M, Hamza M. 1994 .Phenotype and functional profile of T cells expressing gamma delta receptor from patients with active Behçet's disease. J Rheumatol 21(12):2301-6.

123. Hamzaoui K, Gorgi Y, Kahan A, Hamza M, Ayed K. 1998.Functional and phenotypic analysis of T cells cloned from the skin of patients with Behcet's disease. Tunis Med 76(6-7):184-9.

124. Hamzaoui K, Hamzaoui A, Houman H. 2006. CD4+CD25+ regulatory T cells in patients with Behçet's disease. Clin Exp Rheumatol 24(5 Suppl 42):S71-8.

125. Hanke T, Takizawa H, McMahon CW, Busch DH, Pamer EG, Miller JD, Altman JD, Liu Y, Cado D, Lemonnier FA, Bjorkman PJ, Raulet DH. 1999. Direct assessment of MHC class I binding by seven Ly49 inhibitory NK cell receptors. Immunity 11(1): 67–77.

126. Hasan A, Fortune F, Wilson A et al. 1996. Role of γδ T cells in pathogenesis and diagnosis of Behcet's disease. Lancet 347(9004):789–94.

127. Hayday A, Theodoridis E, Ramsburg E, Shires J. 2001. Intraepithelial lymphocytes: exploring the Third Way in immunology. Nat Immunol 2(11):997-1003.

128. Hayday AC. 2009. Gammadelta T cells and the lymphoid stress-surveillance response. Immunity 31(2):184-96.

129. Henderson AP, Altmann DR, Trip SA, Miszkiel KA, Schlottmann PG, Jones SJ, Garway-Heath DF, Plant GT, Miller DH. 2011. Early factors associated with axonal loss after optic neuritis. Ann Neurol 70(6):955-63. .

130. Hirohata S, Kikuchi H.2003. Behçet's disease. Arthritis Res Ther 5(3):139-46.

131. Hirohata S. 2008. Histopathology of central nervous system lesions in Behçet's disease. J Neurol Sci 267(1-2):41-7.

132. Iizuka, K., O. V. Naidenko, B. F. Plougastel, D. H. Fremont, and W. M. Yokoyama. 2003. Genetically linked C-type lectin-related ligands for the NKRP1 family of natural killer cell receptors. Nat Immunol 4(8): 801–807.

133. Inngjerdingen M, Kveberg L, Naper C, Vaage JT. 2011. Natural killer cell subsets in man and rodents. Tissue Antigens 78(2):81-8.

134. Jinushi M, Takehara T, Tatsumi T, Kanto T, Groh V, Spies T, Suzuki T, Miyagi T, Hayashi N. 2003. Autocrine/paracrine IL-15 that is required for type I IFN-mediated dendritic cell expression of MHC class I-related chain A and B is impaired in hepatitis C virus infection. J Immunol 171(10):5423-9.

135. Kahan A, Kahan A, Picard F, Menkès CJ, Amor B. 1991. Abnormalities of T lymphocyte subsets in systemic sclerosis demonstrated with anti-CD45RA and anti-CD29 monoclonal antibodies. Ann Rheum Dis 50(6):354-8.

136. Kaiser BK, Yim D, Chow IT, Gonzalez S, Dai Z, Mann HH, Strong RK, Groh V, Spies T. 2007. Disulphide-isomerase-enabled shedding of tumour-associated NKG2D ligands. Nature 447(7143):482-6.

137. Kaneko F, Takahashi Y, Muramatsu R, Adachi K, Miura Y, Nakane A, Minagawa T. 1985. Natural killer cell numbers and function in peripheral lymphoid cells in Behcet's disease. Br J Dermatol 113(3):313-8.

138. Kaneko F, Oyama N, Nishibu A. 1997. Streptococcal infection in the pathogenesis of Behçet's disease and clinical effects of minocycline on the disease symptoms. Yonsei Med J 38(6):444–454.

139. Karlhofer, F. M., and W. M. Yokoyama. 1991. Stimulation of murine naturalkiller (NK) cells by a monoclonal antibody specific for the NK1.1 antigen. IL-2-activated NK cells possess additional specific stimulation pathways. J Immunol 146(10): 3662–3673.

140. Kärre K. 2008. Natural killer cell recognition of missing self. Nat Immunol 9(5):477-80

141. Kato N, Tanaka J, Sugita J, Toubai T, Miura Y, Ibata M, Syono Y, Ota S, Kondo T, Asaka M, Imamura M. 2007 . Regulation of the expression of MHC class I-related chain A, B (MICA, MICB) via chromatin remodeling and its impact on the susceptibility of leukemic cells to the cytotoxicity of NKG2D-expressing cells. Leukemia 21(10):2103-8.

142. Khakoo SI, Thio CL, Martin MP, Brooks CR, Gao X, Astemborski J, Cheng J, Goedert JJ, Vlahov D, Hilgartner M, Cox S, Little AM, Alexander GJ, Cramp

ME, O'Brien SJ, Rosenberg WM, Thomas DL, Carrington M. 2004. HLA and NK cell inhibitory receptor genes in resolving hepatitis C virus infection. Science 305(5685):872-4.

143. Khvedelidze M, Chkhartishvili N, Abashidze L, Dzigua L, Tsertsvadze T. 2008. Expansion of CD3/CD16/CD56 positive NKT cells in HIV/AIDS: the pilot study. Georgian Med News 165:78-83.

144. Kim S, Poursine-Laurent J, Truscott SM, Lybarger L, Song YJ, Yang L, French AR, Sunwoo JB, Lemieux S, Hansen TH, Yokoyama WM. 2005. Licensing of natural killer cells by host major histocompatibility complex class I molecules. Nature 436(7051):709-1.

145. Kim S, Sunwoo JB, Yang L, Choi T, Song YJ, French AR, Vlahiotis A, Piccirillo JF, Cella M, Colonna M, Mohanakumar T, Hsu KC, Dupont B, Yokoyama WM. 2008. HLA alleles determine differences in human natural killer cell responsiveness and potency. Proc Natl Acad Sci USA 105(8):3053-8.

146. Kone-Paut I, Yurdakul S, Bahabri SA et al. 1998. Clinical features of Behcet's disease in children: an international collaborative study of 86 cases. J Pediatr 132(4):721–725.

147. Kotter, I., Stu¨ biger, N., Zierhut, M., 2003a. Use of interferon-a in Behcet's disease. In: Zierhut, M., Ohno, S. (Eds.), Immunology of Behcet's Disease. Swets & Zeitlinger Publishers, Lisse, Netherlands, pp. 155–159.

148. Kotter, I., Zierhut, M., Eckstein, A.K., Vonthein, R., Ness, T., Guenaydin, I., Grimbacher, B., Blaschke, S., Meyer-Riemann, W., Peter, H.H., Stubiger, N., 2003b. Human recombinant interferon alfa-2a for the treatment of Behcet's disease with sight threatening posterior or panuveitis. Br J Ophthalmol 87(4):423–431.

149. Kotter, I., Gunaydin, I., Zierhut, M., Stubiger, N., 2004. The use of interferon alpha in Behcet disease: review of the literature. Semin Arthritis Rheum 33(5):320–335.

150. Kotter, I., Koch, S., Vonthein, R., Ruckwaldt, U., Amberger, M., Gunaydin, I., Zierhut, M., Stubiger, N., 2005. Cytokines, cytokine antagonists and soluble adhesion molecules in patients with ocular Behcet's disease treated with human recombinant interferon-alpha 2a. Results of an open study and review of the literature. Clin Exp Rheumatol 23 (suppl. 38): S20–S26.

151. Krause, L., Turnbull, J.R., Torun, N., Pleyer, U., Zouboulis, C.C., Forster, M.H., 2003. Interferon alfa-2a in the treatment of ocular Adamantiades-Behcet's disease. Adv Exp Med Biol 528:511–519.

152. Kubin, M. Cassiano L., Chalupny J, Chin W., Cosman D., Fanslow W., Mullberg J., Rousseau A.M., Ulrich D., Armitage R. 2001. ULBP1, 2, 3: novel MHC class I-related molecules that bind to human cytomegalovirus glycoprotein UL16, activate NK cells. Eur J Immunol 31(5):1428–1437.

153. Kullberg MC, Jankovic D, Feng CG, Hue S, Gorelick PL, McKenzie BS, Cua DJ, Powrie F, Cheever AW, Maloy KJ, Sher A. 2006. IL-23 plays a key role in Helicobacter hepaticus-induced T cell-dependent colitis. J Exp Med 203(11):2485-94.

154. Kung, S. K., R. C. Su, J. Shannon, and R. G. Miller. 1999. The NKR-P1B gene product is an inhibitory receptor on SJL/J NK cells. J Immunol 162(10): 5876–5887.

155. Kurhan-Yavuz S, Direskeneli H, Bozkurt N, Ozyazgan Y, Bavbek T, Kazokoglu H, Eksioglu-Demiralp E, Wildner G, Diedrichs-Möhring M, Akoglu T. 2000. Anti-MHC autoimmunity in Behcet's disease: T cell response to an HLA-B derived peptide cross-reactive with retinal-S Ag in patients with uveitis. Clin Exp Immunol 120(1):162–6.

156. Lanca, T., D. V. Correia, C. F. Moita, H. Raquel, A. Neves-Costa, C. Ferreira, J. S. Ramalho, J. T. Barata, L. F. Moita, A. Q. Gomes, and B. Silva-Santos. 2010. The MHC class Ib protein ULBP1 is a nonredundant determinant of leukemia/lymphoma susceptibility to gammadelta T-cell cytotoxicity. Blood 115(12):2407-2411.

157. Lanier LL, Phillips JH, Hackett J Jr, Tutt M, Kumar V. 1986. Natural killer cells: definition of a cell type rather than a function. J Immunol 137(9):2735-9.

158. Lanier LL. 1998. NK cell receptors. Annu Rev Immunol 16:359-93.

159. Lanier LL, Corliss BC, Wu J, Leong C, Phillips JH. 1998. Immunoreceptor DAP12 bearing a tyrosine-based activation motif is involved in activating NK cells. Nature 391(6668):703–7

160. Lanier LL. 2005. NK cell recognition. Annu Rev Immunol 23:225-74.

161. Latchman Y, McKay PF, Reiser H. 1998. Identification of the 2B4 molecule as a counter receptor for CD48. J Immunol 161(11): 5809–5812.

162. Le Thi Huong D, Du LT, Wechsler B, et al.1991. Pulse cyclophosphamide in Behcet's Disease. In: O'Duffy JD, Kokmen E (eds) Behcet's Disease, Basic and Clinical Aspects, pp. 569–73. Marcel Decker Inc., New York.

163. Lee N, Llano M, Carretero M, Ishitani A, Navarro F, López-Botet M, Geraghty DE. 1998. HLA-E is a major ligand for the natural killer inhibitory receptor CD94/NKG2A. Proc Natl Acad Sci USA 95(9):5199-204.

164. Lee KH, Chung HS, Kim HS, Oh SH, Ha MK, Baik JH, Lee S, Bang D. 2003. Human alpha-enolase from endothelial cells as a target antigen of anti-endothelial cell antibody in Behcet's disease. Arthritis Rheum 48(7):2025–35.

165. Lee KM, McNerney ME, Stepp SE, Mathew PA, Schatzle JD, Bennett M, Kumar V. 2004. 2B4 acts as a non-major histocompatibility complex binding inhibitory receptor on mouse natural killer cells. J Exp Med 199(9): 1245–1254.

166. Lefrançois L, Fuller B, Huleatt JW, Olson S, Puddington L. 1997. On the front lines: intraepithelial lymphocytes as primary effectors of intestinal immunity. Springer Semin Immunopathol 18(4):463-75.

167. Lehner T. 1997.The role of heat shock protein, microbial and autoimmune agents in the aetiology of Behçet's disease. Int Rev Immunol 14(1):21–32

168. Levitz SM, Mathews HL, Murphy JW. 1995. Direct antimicrobial activity of T cells. Immunol Today 16(8):387-91.

169. Li H, Pascal V, Martin MP, Carrington M, et al. 2008. Genetic Control of Variegated KIR Gene Expression: Polymorphisms of the Bi-Directional KIR3DL1 Promoter Are Associated with Distinct Frequencies of Gene Expression. PLoS Genet 4(11): e1000254.

170. Li P, Willie ST, Bauer S, Morris DL, Spies T, Strong RK. 1999. Crystal structure of the MHC class I homolog MIC-A, a gammadelta T cell ligand. Immunity 10(5):577–584.

171. Li P, Morris DL, BE, Steinle A, Spies T, Strong RK. 2001. Complex structure of the activating immunoreceptor NKG2D and its MHC class I-like ligand MICA. Nat Immunol 2(5):443–451

172. Li JJ, Pan K, Gu MF, Chen MS, Zhao JJ, Wang H, Liang XT, Sun JC, Xia JC. 2012. Prognostic value of soluble MICA levels in the serum of patients with advanced hepatocellular carcinoma. Chin J Cancer doi: 10.5732/cjc.012.10025.

173. Li Z, Groh V, Strong RK, Spies T. 2000. A single amino acid substitution causes loss of expression of a MICA allele. Immunogenetics 51(3):246-8

174. Livneh A, Aksentijevich I, Langevitz P, Torosyan Y, G-Shoham N, Shinar Y, Pras E, Zaks N, Padeh S, Kastner DL, Pras M. 2001. A single mutated MEFV allele in Israeli patients suffering from familial Mediterranean fever and Behçet's disease (FMF-BD). Eur J Hum Genet 9(3):191-6.

175. Long EO, Barber DF, Burshtyn DN, Faure M, Peterson M, Rajagopalan S, Renard V, Sandusky M, Stebbins CC, Wagtmann N, Watzl C. 2001. Inhibition of natural killer cell activation signals by killer cell immunoglobulin-like receptors (CD158). Immunol Rev 181:223-33.

176. López-Larrea C, Suárez-Alvarez B, López-Soto A, López-Vázquez A, Gonzalez S. 2008. The NKG2D receptor: sensing stressed cells. Trends Mol Med 14(4):179-89.

177. Lu Y, Ye P, Chen SL, Tan EM, Chan EK. 2005. Identification of kinectin as a novel Behcet's disease autoantigen. Arthritis Res Ther 7(5):R1133–9.

178. Mandelboim O, Lieberman N, Lev M, Paul L, Arnon TI, Bushkin Y, Davis DM, Strominger JL, Yewdell JW, Porgador A. 2001 .Recognition of haemagglutinins on virus-infected cells by NKp46 activates lysis by human NK cells. Nature 409(6823):1055-60.

179. Mantas C, Direskeneli H, Ekşioglu-Demiralp E, Akoglu T. 1999. Serum levels of Th2 cytokines IL-4 and IL-10 in Behçet's disease. J Rheumatol 26(2):510-2.

180. Mantas C, Direskeneli H, Oz D, Yavuz S, Akoglu T. 2000. IL-8 producing cells in patients with Beheçet's disease. Clin Exp Rheumatol 18(2): 249-51.

181. Martin MP, Gao X, Lee JH, Nelson GW, Detels R, Goedert JJ, Buchbinder S, Hoots K, Vlahov D, Trowsdale J, Wilson M, O'Brien SJ, Carrington M. 2002. Epistatic interaction between KIR3DS1 and HLA-B delays the progression to AIDS. Nat Genet 31(4):429–434

182. Martin SJ, Amarante-Mendes GP, Shi L, Chuang TH, Casiano CA, O'Brien GA, Fitzgerald P, Tan EM, Bokoch GM, Greenberg AH, Green DR. 1996. The cytotoxic cell protease granzyme B initiates apoptosis in a cell-free system by proteolytic processing and activation of the ICE/CED-3 family protease, CPP32, via a novel two-step mechanism. EMBO J 15(10): 2407–2416.

183. Mason LH, Willette-Brown J, Mason AT, McVicar D, Ortaldo JR. 2000. Interaction of Ly-49D+ NK cells with H-2Dd target cells leads to Dap-12 phosphorylation and IFN-gamma secretion. J Immunol 164(2): 603–611.

184. Mathew SO, Rao KK, Kim JR, Bambard ND, Mathew PA. 2009. Functional role of human NK cell receptor 2B4 (CD244) isoforms. Eur J Immunol 39(6):1632–1641.

185. McGonagle D, McDermott MF. 2006. A proposed classification of the immunological diseases. PLoS Med 3(8):e297.

186. McNerney ME, Lee KM, Kumar V.2005. 2B4 (CD244) is a non-MHC binding receptor with multiple functions on natural killer cells and CD8+ T cells. Mol Immunol 42(4):489–494.

187. McQueen KL, Parham P. 2002. Variable receptors controlling activation and inhibition of NK cells. Curr Opin Immunol 14(5): 615–621.

188. Mege JL, Dilsen N, Sanguedolce V, Gul A, Bongrand P, Roux H, Ocal L, Inanç M, Capo C. 1993. Overproduction of monocyte derived tumor necrosis factor alpha, interleukin (IL) 6, IL-8 and increased neutrophil superoxide generation in Behçet's disease. A comparative study with familial Mediterranean fever and healthy subjects. J Rheumatol 20(9):1544-9.

189. Mehta IK, Wang J, Roland J, Margulies DH, Yokoyama WM. 2001. Ly49A allelic variation and MHC class I specificity. Immunogenetics 53(7): 572–583.

190. Michaëlsson J, Achour A, Salcedo M, Kâse-Sjöström A, Sundbäck J, Harris RA, Kärre K. 2000. Visualization of inhibitory Ly49 receptor specificity with soluble major histocompatibility complex class I tetramers. Eur J Immunol 30(1): 300–307.

191. Middleton D, Gonzelez F. 2010. The extensive polymorphism of KIR genes. Immunology 129(1):8-19.

192. Mincheva-Nilsson L, Nagaeva O, Chen T, Stendahl U, Antsiferova J, Mogren I, Hernestål J, Baranov V. 2006. Placenta-derived soluble MHC class I chain-related molecules down-regulate NKG2D receptor on peripheral blood mononuclear cells during human pregnancy: a possible novel immune escape mechanism for fetal survival. J Immunol 176(6):3585-92.

193. Misumi, M., Hagiwara, E., Takeno, M., Takeda, Y., Inoue, Y., Tsuji, T., Ueda, A., Nakamura, S., Ohno, S., Ishigatsubo, Y. 2003. Cytokine production profile in patients with Behcet’s disease treated with infliximab. Cytokine 24(5):210–213.

194. Mizuki N, Inoko H, Ando H, Nakamura S, Kashiwase K, Akaza T, Fujino Y, Masuda K, Takiguchi M, Ohno S. 1993. Behcet's disease associated with one of the HLA-B51 subantigens, HLA-B* 5101. Am J Ophthalmol 116 (4): 406-409.

195. Mizuki N, Inoko H, Sugimura K, Nishimura K, Nakamura S, Tanaka H, Mizuki N, Mizuki H, Inaba G, Tsuji K and Ohno S. 1992. RFLP analysis in the TNF β gene and susceptability to alloreactive NK cells in Behçet's disease. Inv Ophthalmol Vis Sci 33(11):3084–90.

196. Mizuki, N., Inoko, H., Ohno, S. 1997. Molecular genetics (HLA) of Behcet's disease. Yonsei Med J 38(6):333–349.

197. Mizuki N, Meguro A, Ota M, Ohno S, Shiota T, Kawagoe T, Ito N, Kera J, Okada E, Yatsu K, Song YW, Lee EB, Kitaichi N, Namba K, Horie Y, Takeno M, Sugita S, Mochizuki M, Bahram S, Ishigatsubo Y, Inoko H. 2010 .Genome-wide association studies identify IL23R-IL12RB2 and IL10 as Behçet's disease susceptibility loci. Nat Genet 42(8):703-6.

198. Mizushima Y, Matsumura N, Mori M, Shimizu T, Fukushima B, Mimura Y, Saito K, Sugiura S. 1977. Colchicine in Behcet's Disease. Lancet 2(8046):1037.

199. Molinero LL, Domaica CI, Fuertes MB, Girart MV, Rossi LE, Zwirner NW. 2006. Intracellular expression of MICA in activated CD4 T lymphocytes and protection from NK cell-mediated MICA-dependent cytotoxicity. Hum Immunol 67(3):170–82.

200. Mor P, Weinberger A, Cohen IR. 2002. Identification of alpha-tropomyosin as a target self antigen in Behcet's syndrome. Eur J Immunol 32(2):356–65.

201. Moretta A, Biassoni R, Bottino C, Mingari MC, Moretta L. 2000. Natural cytotoxicity receptors that trigger human NK-cell-mediated cytolysis. Immunol Today 21(5):228-34.

202. Moretta L, Ferlazzo G, Bottino C, Vitale M, Pende D, Mingari MC, Moretta A. 2006. Effector and regulatory events during natural killer-dendritic cell interactions. Immunol Rev 214:219-28.

203. Mostov KE, Verges M, Altschuler Y. 2000. Membrane traffic in polarized epithelial cells. Curr Opin Cell Biol 12(4):483-90.

204. Muftuoglu, A.U., Yazici, H., Yurdakul, S., Pazarli, H., Ozyazgan, Y., Tuzun, Y., Altac, M., Yalcin, B., 1981. Behcet's disease: lack of correlation of clinical manifestations with HLA antigens. Tissue Antigens 17(2):226–230.

205. Nachmani D, Lankry D, Wolf DG, Mandelboim O. 2010. The human cytomegalovirus microRNA miR-UL112 acts synergistically with a cellular microRNA to escape immune elimination. Nat Immunol 11(9):806-13.

206. Nagafuchi H, Takeno M, Yoshikawa H, Kurokawa MS, Nara K, Takada E, Masuda C, Mizoguchi M, Suzuki N. 2005. Excessive expression of Txk, a member of the Tec family of tyrosine kinases, contributes to excessive Th1 cytokine production by T lymphocytes in patients with Behcet's disease. Clin Exp Immunol 139(2):363–70.

207. Nedellec, S., C. Sabourin, M. Bonneville, and E. Scotet. 2010. NKG2D costimulates human V gamma 9V delta 2 T cell antitumor cytotoxicity through protein kinase C theta-dependent modulation of early TCR-induced calcium and transduction signals. J Immunol 185(1):55-63.

208. Niwa, Y., Mizushima, Y. 1990. Neutrophil-potentiating factors released from stimulated lymphocytes; special reference to the increase in neutrophil-potentiating factors from streptococcus-stimulated lymphocytes of patients with Behcet's disease. Clin Exp Immunol 79(3):353–360.

209. O'Duffy, J.D. 1974. Suggested criteria for diagnosis of Behcet's Disease. J Rheumatol 1:18.

210. Oppenheim DE, Roberts SJ, Clarke SL, Filler R, Lewis JM, Tigelaar RE, Girardi M, Hayday AC. 2005. Sustained localized expression of ligand for the activating NKG2D receptor impairs natural cytotoxicity in vivo and reduces tumor immunosurveillance. Nat Immunol 6(9):928-37.

211. Orihuela M, Margulies DH, Yokoyama WM. 1996. The natural killer cell receptor Ly-49A recognizes a peptide-induced conformational determinant on

its major histocompatibility complex class I ligand. Proc Natl Acad Sci USA 93(21): 11792–11797.

212. Ortaldo JR, Bere EW, Hodge D, Young HA. 2001. Activating Ly-49 NK receptors: central role in cytokine and chemokine production. J Immunol 166(8): 4994–4999.

213. Palmieri G, Tullio V, Zingoni A, Piccoli M, Frati L, Lopez-Botet M, Santoni A. 1999. CD94/NKG2-A inhibitory complex blocks CD16-triggered syk and extracellular regulated kinase activation, leading to cytotoxic function of human NK cells. J Immunol 162(12):7181–88.

214. Pando, M. J., C. M. Gardiner, M. Gleimer, K. L. McQueen, and P. Parham. 2003. The protein made from a common allele of KIR3DL1 (3DL1*004) is poorly expressed at cell surfaces due to substitution at positions 86 in Ig domain and 182 in Ig domain 1. J Immunol 171(12):6640–6649.

215. Paschen A, Sucker A, Hill B, Moll I, Zapatka M, Nguyen XD, Sim GC, Gutmann I, Hassel J, Becker JC, Steinle A, Schadendorf D, Ugurel S. 2009. Differential clinical significance of individual NKG2D ligands in melanoma: soluble ULBP2 as an indicator of poor prognosis superior to S100B. Clin Cancer Res 15(16):5208-15.

216. Pay, S., Erdem, H., Pekel, A., Simsek, I., Musabak, U., Sengul, A., Dinc, A. 2006. Synovial proinflammatory cytokines and their correlation with matrix metalloproteinase-3 expression in Behcet's disease. Does interleukin-1beta play a major role in Behcet's synovitis? Rheumatol Int 26(7):608–613.

217. Pende D, Parolini S, Pessino A, Sivori S, Augugliaro R, Morelli L, Marcenaro E, Accame L, Malaspina A, Biassoni R, Bottino C, Moretta L, Moretta A. 1999. Identification and molecular characterization of NKp30, a novel triggering receptor involved in natural cytotoxicity mediated by human natural killer cells. J Exp Med 190(10):1505-16.

218. Pekiner FN, Aytugar E, Demirel GY, Borahan MO. 2012. Interleukin-2, interleukin-6 and T regulatory cells in peripheral blood of patients with

Behçet's disease and recurrent aphthous ulcerations. J Oral Pathol Med 41(1):73-9.

219. Pelham HR. 1999. The Croonian Lecture 1999. Intracellular membrane traffic: getting proteins sorted. Philos Trans R Soc Lond B Biol Sci 354(1388):1471-8.

220. Pessino A, Sivori S, Bottino C, Malaspina A, Morelli L, Moretta L, Biassoni R, Moretta A. 1998. Molecular cloning of NKp46: A novel member of the immunoglobulin superfamily involved in triggering of natural cytotoxicity. Journal of Experimental Medicine 188(5): 953–960.

221. Petersdorf EW, Shuler KB, Longton GM, Spies T, Hansen JA. 1999. Population study of allelic diversity in the human MHC class I-related MIC-A gene. Immunogenetics 49(7-8):605-12.

222. Plougastel, B., C. Dubbelde, and W. M. Yokoyama. 2001. Cloning of Clr, a new family of lectin-like genes localized between mouse Nkrp1a and Cd69. Immunogenetics 53(3): 209–214.

223. Pogge von Strandmann E, Simhadri VR, von Tresckow B, Sasse S, Reiners KS, Hansen HP, Rothe A, Böll B, Simhadri VL, Borchmann P, McKinnon PJ, Hallek M, Engert A. 2007. Human leukocyte antigen-B-associated transcript 3 is released from tumor cells and engages the NKp30 receptor on natural killer cells. Immunity 27(6):965–974

224. Pronai L, Ichikawa Y, Nakazawa H, Arimori S. 1991.Enhanced superoxide generation and the decreased superoxide scavenging activity of peripheral blood leukocytes in Behçet's disease--effects of colchicine. Clin Exp Rheumatol 9(3):227-33.

225. Radaev S, Rostro B, Brooks AG, Colonna M, Sun PD. 2001. Conformational plasticity revealed by the cocrystal structure of NKG2D and its class I MHC-like ligand ULBP3. Immunity 15(6):1039-49.

226. Rajagopalan S, Fu J, Long EO. 2001. Cutting edge: induction of IFN-c production but not cytotoxicity by the killer cell Ig-like receptor KIR2DL4 (CD158d) in resting NK cells. J Immunol 167(4):1877–81.

227. Rajagopalan S, Long EO. 2012. KIR2DL4 (CD158d): An activation receptor for HLA-G. Front Immunol 3:258.

228. Rajasekaran K, Xiong V, Fong L, Gorski J, Malarkannan S. 2010 . Functional dichotomy between NKG2D and CD28-mediated co-stimulation in human CD8+ T cells. PLoS One 5(9): pii: e12635.

229. Randall KL, Chan SS, Ma CS, Fung I, Mei Y, Yabas M, Tan A, Arkwright PD, Al Suwairi W, Lugo Reyes SO, Yamazaki-Nakashimada MA, Garcia-Cruz Mde L, Smart JM, Picard C, Okada S, Jouanguy E, Casanova JL, Lambe T, Cornall RJ, Russell S, Oliaro J, Tangye SG, Bertram EM, Goodnow CC. 2011. DOCK8 deficiency impairs CD8 T cell survival and function in humans and mice. J Exp Med 208(11):2305-20.

230. Raulet DH, Held W, Correa I, Dorfman JR, Wu MF, Corral L. 1997. Specificity, tolerance and developmental regulation of natural killer cells defined by expression of class I-specific Ly49 receptors. Immunol Rev 155: 41–52.

231. Raulet DH, Vance RE. 2006. Self-tolerance of natural killer cells. Nat Rev Immunol 6(7):520-31.

232. Raziuddin S, al-Dalaan A, Bahabri S, Siraj AK, al-Sedairy S. 1998. Divergent cytokine production profile in Behçet's disease. Altered Th1/Th2 cell cytokine pattern. J Rheumatol 25(2):329-33.

233. Remmers EF, Cosan F, Kirino Y, Ombrello MJ, Abaci N, Satorius C, Le JM, Yang B, Korman BD, Cakiris A, Aglar O, Emrence Z, Azakli H, Ustek D, Tugal-Tutkun I, Akman-Demir G, Chen W, Amos CI, Dizon MB, Kose AA, Azizlerli G, Erer B, Brand OJ, Kaklamani VG, Kaklamanis P, Ben-Chetrit E, Stanford M, Fortune F, Ghabra M, Ollier WE, Cho YH, Bang D, O'Shea J, Wallace GR, Gadina M, Kastner DL, Gül A.2010. Genome-wide association study identifies variants in the MHC class I, IL10, and IL23R-IL12RB2 regions associated with Behçet's disease. Nat Genet 42(8):698-702.

234. Reth M. 1989. Antigen receptor tail clue. Nature 338(6214):383–84.

235. Rincon-Orozco B, Kunzmann V, Wrobel P, Kabelitz D, Steinle A, Herrmann T. 2005. Activation of V gamma 9V delta 2 T cells by NKG2D. J Immunol 175(4):2144-51.

236. Roberts AI, Lee L, Schwarz E, Groh V, Spies T, Ebert EC, Jabri B. 2001. NKG2D receptors induced by IL-15 costimulate CD28-negative effector CTL in the tissue microenvironment. J Immunol 167(10):5527-30.

237. Salih HR, Rammensee HG, Steinle A. 2002. Cutting edge: down-regulation of MICA on human tumors by proteolytic shedding. J Immunol 169(8):4098-102.

238. Salih HR, Antropius H, Gieseke F, Lutz SZ, Kanz L, Rammensee HG, Steinle A. 2003. Functional expression and release of ligands for the activating immunoreceptor NKG2D in leukemia. Blood 102(4):1389-96.

239. Sakaguchi T, Ibe M, Miwa K, et al. 1997. Binding of 8-mer to 11-mer peptides carrying the anchor residues to slow assembling HLA class I molecules (HLAB* 5101). Immunogenetics 45(4): 259-265.

240. Saruhan-Direskeneli G, Celet B, Eksioglu-Demiralp E, Direskeneli H. 2001. Human HSP 60 peptide responsive T cell lines are similarly present in both Behcet's disease patients and healthy controls. Immunology Letters 79(3):203–8.

241. Saruhan-Direskeneli G, Uyar FA, Cefle A, Onder SC, Eksioglu-Demiralp E, Kamali S, Inanc M, Ocal L, Gul A. 2004. Expression of KIR and C-type lectin receptors in Behcet's disease. Rheumatology (Oxford) 43(4):423-7.

242. Savage NW, Mahanonda R, Seymour GJ, Bryson GJ, Collins RJ. 1988. The proportion of suppressor-inducer T-lymphocytes is reduced in recurrent aphthous stomatitis. J Oral Pathol 17(6):293-7.

243. Schreiner B, Voss J, Wischhusen J, Dombrowski Y, Steinle A, Lochmüller H, Dalakas M, Melms A, Wiendl H. 2006. Expression of toll-like receptors by human muscle cells in vitro and in vivo: TLR3 is highly expressed in inflammatory and HIV myopathies, mediates IL-8 release and upregulation of NKG2D-ligands. Faseb J 20(1):118–120.

244. Shafi S, Vantourout P, Wallace G, Antoun A, Vaughan R, Stanford M, Hayday A. 2011. An NKG2D-mediated human lymphoid stress surveillance response with high interindividual variation. Sci Transl Med 3(113):113ra124.

245. Shao L, Serrano D, Mayer L. 2001 The role of epithelial cells in immune regulation in the gut. Semin Immunol 13(3):163-76.

246. Shiina T, Tamiya G, Oka A, Takishima N, Yamagata T, Kikkawa E, Iwata K, Tomizawa M, Okuaki N, Kuwano Y, Watanabe K, Fukuzumi Y, Itakura S, Sugawara C, Ono A, Yamazaki M, Tashiro H, Ando A, Ikemura T, Soeda E, Kimura M, Bahram S, Inoko H. 1999. Molecular dynamics of MHC genesis unraveled by sequence analysis of the 1,796,938-bp HLA class I region. Proc Natl Acad Sci USA 96(23):13282–13287.

247. Shimizu T, Ehrlich GE, Inaba G & Hayashi K. 1979. Behcet disease (Behcet syndrome). Semin Arthritis Rheum 8(4):223–260.

248. Shimizu J, Takai K, Fujiwara N, Arimitsu N, Ueda Y, Wakisaka S, Yoshikawa H, Kaneko F, Suzuki T, Suzuki N. 2012. Excessive CD4+ T cells co-expressing interleukin-17 and interferon-γ in patients with Behçet's disease. Clin Exp Immunol 168(1):68-74.

249. Silver ET, Gong DE, Chang CS, Amrani A, Santamaria P, Kane KP. 2000. Ly-49P activates NK-mediated lysis by recognizing H-2Dd. J Immunol 165(4): 1771–1781.

250. Silver ET, Gong D, Hazes B, Kane KP. 2001. Ly-49W, an activating receptor of nonobese diabetic mice with close homology to the inhibitory receptor Ly-49G, recognizes H-2D(k) and H-2D(d). J Immunol 166(4): 2333–2341.

251. Single, R. M., M. P. Martin, X. Gao, D. Meyer, M. Yeoger, J. R. Kidd, K. K. Kidd, and M. Carrington. 2007. Global diversity and evidence for coevolution of KIR and HLA. Nat Genet 39(9):1114–1119.

252. Sivori S, Vitale M, Morelli L, Sanseverino L, Augugliaro R, Bottino C, Moretta L, Moretta A. 1997. p46, a novel natural killer cell-specific surface molecule that mediates cell activation. J Exp Med 186 (7):1129–1136.

253. Smith KM, Wu J, Bakker AB, Phillips JH, Lanier LL. 1998. Ly-49D and Ly-49H associate with mouse DAP12 and form activating receptors. J Immunol 161(1): 7–10.

254. Soderquest K, Walzer T, Zafirova B, Klavinskis LS, Polić B, Vivier E, Lord GM, Martín-Fontecha A. 2011. Cutting edge: CD8+ T cell priming in the absence of NK cells leads to enhanced memory responses. J Immunol 186(6):3304-8.

255. Stebbins CC, Watzl C, Billadeau DD, Leibson PJ, Burshtyn DN, Long EO. 2003. Vav1 dephosphorylation by the tyrosine phosphatase SHP-1 as a mechanism for inhibition of cellular cytotoxicity. Mol Cell Biol 23(17):6291–99.

256. Steinle A, Li P, Morris DL, Groh V, Lanier LL, Strong RK, Spies T. 2001. Interactions of human NKG2D with its ligands MICA, MICB, and homologs of the mouse RAE-1 protein family. Immunogenetics 53(4):279-87.

257. Stern-Ginossar N, Elefant N, Zimmermann A, Wolf DG, Saleh N, Biton M, Horwitz E, Prokocimer Z, Prichard M, Hahn G, Goldman-Wohl D, Greenfield C, Yagel S, Hengel H, Altuvia Y, Margalit H, Mandelboim O. 2007. Host immune system gene targeting by a viral miRNA. Science 317(5836):376–381

258. Stern-Ginossar N, Gur C, Biton M, Horwitz E, Elboim M, Stanietsky N, Mandelboim M, Mandelboim O. 2008. Human microRNAs regulate stress induced immune responses mediated by the receptor NKG2D. Nat Immunol 9(9):1065–1073.

259. Stewart, C. A., J. Van Bergen, and J. Trowsdale. 2003. Different and divergent regulation of the KIR2DL4 and KIR3DL1 promoters. J Immunol 170(12):6073–6081.

260. Stojanov S, Kastner DL. 2005. Familial autoinflammatory diseases: genetics, pathogenesis and treatment. Curr Opin Rheumatol 17(5):586–99.

261. Strid J, Roberts SJ, Filler RB, Lewis JM, Kwong BY, Schpero W, Kaplan DH, Hayday AC, Girardi M. 2008. Acute upregulation of an NKG2D ligand

promotes rapid reorganization of a local immune compartment with pleiotropic effects on carcinogenesis. Nat Immunol 9(2):146-54.

262. Strid J, Sobolev O, Zafirova B, Polic B, Hayday A. 2011. The intraepithelial T cell response to NKG2D-ligands links lymphoid stress surveillance to atopy. Science 334(6060):1293-7

263. Strong, R.K. 2000. Class (I) will come to order – not. Nat Struct Biol 7(3):173–176.

264. Sutherland CL, Chalupny NJ, Cosman D. 2001. The UL16-binding proteins, a novel family of MHC class I-related ligands for NKG2D, activate natural killer cell functions. Immunol Rev 181:185-92.

265. Sutherland CL, Chalupny NJ, Schooley K, VandenBos T, Kubin M, Cosman D. 2002. UL16-binding proteins, novel MHC class I-related proteins, bind to NKG2D and activate multiple signalling pathways in primary NK cells. J Immunol 168(2):671–679.

266. Sutherland CL, Rabinovich B, Chalupny NJ, Brawand P, Miller R, Cosman D. 2006. ULBPs, human ligands of the NKG2D receptor, stimulate tumor immunity with enhancement by IL-15. Blood 108(4):1313-9.

267. Suemizu, H., M. Radosavljevic, M. Kimura, S. Sadahiro, S. Yoshimura, S. Bahram, and H. Inoko. 2002. A basolateral sorting motif in the MICA cytoplasmic tail. Proc Natl Acad Sci USA 99(5):2971-2976.

268. Suzuki, N., Nara, K., Suzuki, T. 2006. Skewed Th1 responses caused by excessive expression of Txk, a member of the Tec family of tyrosine kinases, in patients with Behcet's disease. Clin Med Res 4(2):147–151.

269. Takahashi E., Kuranaga N., Satoh K., Habu Y., Shinomiya N., Asano T., Seki S., Hayakawa M. 2007. Induction of $CD16^{+}$ CD56 bright NK cells with antitumour cytotoxicity not only from $CD16^{-}$ CD56bright NK Cells but also from $CD16^{-}$ CD56dim NK cells. Scand J Immunol 65(2):126–138.

270. Takeno M, Shimoyama Y, Kashiwakura J, Nagafuchi H, Sakane T, Suzuki N. 2004. Abnormal killer inhibitory receptor expression on natural killer cells in patients with Behçet's disease. Rheumatol Int 24(4):212-6.

271. Tang KF, Ren H, Cao J, Zeng GL, Xie J, Chen M, Wang L, He CX. 2008. Decreased Dicer expression elicits DNA damage and up-regulation of MICA and MICB. J Cell Biol 182(2):233-9.

272. Thananchai H, Gillespie G, Martin MP, Bashirova A, Yawata N, Yawata M, Easterbrook P, McVicar DW, Maenaka K, Parham P, Carrington M, Dong T, Rowland-Jones S. 2007. Cutting edge: Allele-specific and peptide-dependent interactions between KIR3DL1 and HLA-A and HLA-B. J Immunol 178(1):33–37.

273. The MHC sequencing consortium. 1999. Complete sequence and gene map of a human major histocompatibility complex. The MHC sequencing consortium. Nature 401(6756):921–923.

274. Thomas M, Wills M, Lehner PJ. 2008. Natural killer cell evasion by an E3 ubiquitin ligase from Kaposi's sarcoma-associated herpesvirus. Biochem Soc Trans 36(Pt 3):459–463.

275. Tormo J, Natarajan K, Margulies DH, Mariuzza RA. 1999. Crystal structure of a lectin-like natural killer cell receptor bound to its MHC class I ligand. Nature 402(6762):623–631.

276. Tosh K, Ravikumar M, Bell JT, Meisner S, Hill AV, Pitchappan R. 2006. Variation in MICA and MICB genes and enhanced susceptibility to paucibacillary leprosy in South India. Hum Mol Genet 15(19):2880-7.

277. Trowsdale J. 2001. Genetic and functional relationships between MHC and NK receptor genes. Immunity 15(3):363-74.

278. Trowsdale J, Moffett A. 2008. NK receptor interactions with MHC class I molecules in pregnancy. Semin Immunol 20(6):317-20.

279. Tugal-Tutkun, I., Guney-Tefekli, E., Urgancioglu, M., 2006a. Results of interferon-alfa therapy in patients with Behcet uveitis. Graefe's Arch Clin Exp Ophthalmol 244(12):1692–1695.

280. Turan B, Gallati H, Erdi H, Gurler A, Michel BA, Villiger PM. 1997. Systemic levels of the T cell regulatory cytokines IL-10 and IL-12 in Behcet's disease; soluble TNFR-75 as a biological marker of disease activity. J Rheumatol 24(1):128–32.

281. Türsen U. 2012. Pathophysiology of the Behçet's Disease. Patholog Res Int 2012:493015.

282. Ugolini, S., C. Arpin, N. Anfossi, T. Walzer, A. Cambiaggi, R. Forster, M. Lipp, R. E. Toes, C. J. Melief, J. Marvel, and E. Vivier. 2001. Involvement of inhibitory NKRs in the survival of a subset of memory-phenotype CD8+ T cells. Nat Immunol 2(5):430–435.

283. Uhrberg, M., N. M. Valiante, B. P. Shum, H. G. Shilling, K. Lienert-Weidenbach, B. Corliss, D. Tyan, L. L. Lanier, and P. Parham. 1997. Human diversity in killer cell inhibitory receptor genes. Immunity 7(6):753–763.

284. Unni AM, Bondar T, Medzhitov R. 2008. Intrinsic sensor of oncogenic transformation induces a signal for innate immunosurveillance. Proc Natl Acad Sci USA 105(5):1686-91.

285. Valiante NM, Trinchieri G. 1993. Identification of a novel signal transduction surface molecule on human cytotoxic lymphocytes. J Exp Med 178(4): 1397–1406.

286. Valiante NM, Phillips JH, Lanier LL, Parham P. 1996. Killer cell inhibitory receptor recognition of human leukocyte antigen (HLA) class I blocks formation of a pp36/PLC-γ signaling complex in human natural killer (NK) cells. J Exp Med 184(6):2243–50

287. Valiante NM, Uhrberg M, Shilling HG, Lienert-Weidenbach K, Arnett KL, D'Andrea A, Phillips JH, Lanier LL, Parham P. 1997. Functionally and

structurally distinct NK cell receptor repertoires in the peripheral blood of two human donors. Immunity 7(6):739-51.

288. Van Laar, J.A.M., Missotten, T., van Daele, P.L.A., Jamnitski, A.,Baarsma, G.S., van Hagen, P.M., 2007. Adalimumab: a new modality for Behçet's disease? Ann Rheum Dis 66(4):565–566.

289. Vance RE, Kraft JR, Altman JD, Jensen PE, Raulet DH. 1998. Mouse CD94/NKG2A is a natural killer cell receptor for the nonclassical major histocompatibility complex (MHC) class I molecule Qa-1(b). J Exp Med 188(10): 1841–1848.

290. Veillette A. 2006. NK cell regulation by SLAM family receptors and SAP-related adapters. Immunol Rev 214: 22–34.

291. Veinotte LL, Wilhelm BT, Mager DL, Takei F. 2003. Acquisition of MHC-specific receptors on murine natural killer cells. Crit Rev Immunol 23(4): 251–266.

292. Verity DH, Marr JE, Ohno S, Wallace GR, Stanford MR. 1999. 'Behcet's disease, The Silk Road and HLA-B51: historical and geographical perspectives. Tissue antigens 54(3):213-20.

293. Vilches, C., and P. Parham. 2002. KIR: diverse, rapidly evolving receptors of innate and adaptive immunity. Annu Rev Immunol 20:217–251.

294. Vitale M, Bottino C, Sivori S, Sanseverino L, Castriconi R, Marcenaro E, Augugliaro R, Moretta L, Moretta A. 1998. NKp44, a novel triggering surface molecule specifically expressed by activated natural killer cells, is involved in non-major histocompatibility complex-restricted tumor cell lysis. J Exp Med 187(12):2065–2072.

295. Vivier E, Nunès JA, Vély F. 2004. Natural killer cell signaling pathways. Science 306(5701):1517-9.

296. Vivier E, Tomasello E, Baratin M, Walzer T, Ugolini S. 2008 .Functions of natural killer cells. Nat Immunol 9(5):503-10

297. Vyas YM, Maniar H, Dupont B. 2002. Visualization of signalling pathways and cortical cytoskeleton in cytolytic and noncytolytic natural killer cell immune synapses. Immunol Rev 189:161-78.

298. Waggoner SN, Cornberg M, Selin LK, Welsh RM. 2011. Natural killer cells act as rheostats modulating antiviral T cells. Nature 481(7381):394-8.

299. Waldhauer I, Goehlsdorf D, Gieseke F, Weinschenk T, Wittenbrink M, Ludwig A, Stevanovic S, Rammensee HG, Steinle A. 2008. Tumor-associated MICA is shed by ADAM proteases. Cancer Res 68(15):6368–6376.

300. Wallace GR, Verity DH, Delamaine LJ, Ohno S, Inoko H, Ota M, Mizuki N, Yabuki K, Kondiatis E, Stephens HA, Madanat W, Kanawati CA, Stanford MR, Vaughan RW. 1999. MICA allele profiles and HLA class I associations with Behcet's disease. Immunogenetics 49(7-8):613–617.

301. Wallace GR, Kondeatis E, Vaughan RW, Verity DH, Chen Y, Fortune F, Madanat W, Kanawati CA, Graham EM, Stanford MR. 2007. IL-10 genotype analysis in patients with Behçet's disease. Hum Immunol 68(2):122-7.

302. Walzer T, Dalod M, Robbins SH, Zitvogel L, Vivier E. 2005. Natural-killer cells and dendritic cells: "l'union fait la force". Blood 106(7):2252-8.

303. Welte S, Kuttruff S, Waldhauer I, Steinle A. 2006. Mutual activation of natural killer cells and monocytes mediated by NKp80-AICL interaction. Nat Immunol 7(12): 1334–1342.

304. Wherry EJ. 2011. T cell exhaustion. Nat Immunol 12(6):492-9.

305. Wiemann K, Mittrücker HW, Feger U, Welte SA, Yokoyama WM, Spies T, Rammensee HG, Steinle A. 2005. Systemic NKG2D down-regulation impairs NK and CD8 T cell responses in vivo. J Immunol 175(2):720-9.

306. Wu J, Song Y, Bakker AB, Bauer S, Spies T, Lanier LL, Phillips JH. 1999. An activating immunoreceptor complex formed by NKG2D and DAP10. Science 285(5428):730-2.

307. Wu JD, Higgins LM, Steinle A, Cosman D, Haugk K, Plymate SR. 2004. Prevalent expression of the immunostimulatory MHC class I chain-related molecule is counteracted by shedding in prostate cancer. J Clin Invest 114(4):560-8.

308. Wülfing C, Davis MM. 1998. A receptor/cytoskeletal movement triggered by costimulation during T cell activation. Science 282(5397):2266-9.

309. Yadav D, Ngolab J, Lim RS, Krishnamurthy S, Bui JD. 2009. Cutting edge: down-regulation of MHC class I-related chain A on tumor cells by IFN-gamma-induced microRNA. J Immunol 182(1):39-43.

310. Yasici H, Pazarli H, Barnes CG. 1990. A controlled trial of azathioprine in Behcet's syndrome. N Engl J Med 322(5):281–5.

311. Yasuoka H, Okazaki Y, Kawakami Y, Hirakata M, Inoko H, Ikeda Y, Kuwana M. 2004. Autoreactive CD8þ cytotoxic T lymphocytes to major histocompatibility complex class I chain-related gene A in patients with Behcet's disease. Arthritis Rheum 50(11):3658–62.

312. Yawata, M., N. Yawata, M. Draghi, A. M. Little, F. Partheniou, and P. Parham. 2006. Roles for HLA and KIR polymorphisms in natural killer cell repertoire selection and modulation of effector function. J Exp Med 203(3):633–645.

313. Yazici, H., Tuzun, Y., Pazarli, H., Yurdakul, S., Ozyazgan, Y., Ozdogan, H., Serdaroglu, S., Ersanli, M., Ulku, B.Y., Muftuoglu, A.U. 1984b. Influence of age of onset and patient's sex on prevalence and severity of manifestations of Behcet's syndrome. Ann Rheum Dis 43(6):783–789.

314. Yazıcı H. 1997.The place of Behcet's Syndrome among the autoimmune diseases. Intern Rev Immunol 14(1):1–10.

315. Yokoyama WM, Kim S. 2006. How do natural killer cells find self to achieve tolerance? Immunity 24(3):249-57

316. Yu HG, Lee DS, Seo JM, Ahn JK, Yu YS, Lee WJ, Chung H. 2004. The number of CD8+ T cells and NKT cells increases in the aqueous humor of patients with Behçet's uveitis. Clin Exp Immunol 137(2):437-43.

317. Yurdakul S, Tüzüner N, Yurdakul I, Hamuryudan V, Yazici H. 1996. Gastrointestinal involvement in Behcet's syndrome: a controlled study. Ann Rheum Dis 55(3):208–210.

318. Zafirova B, Mandarić S, Antulov R, Krmpotić A, Jonsson H, Yokoyama WM, Jonjić S, Polić B. 2009. Altered NK cell development and enhanced NK cell-mediated resistance to mouse cytomegalovirus in NKG2D-deficient mice. Immunity 31(2):270-82.

319. Zhang Y, Lazaro AM, Zou Y, Lavingia B, Moraes EM, Moraes RJ, Stastny P. 2002. MICA polymorphism in South American Indians. Immunogenetics 53(10-11):900-6.

320. Zouboulis, C.C. 2003. Epidemiology of Adamantiades-Behcet's Disease. In: Zierhut, M., Ohno, S. (Eds.), Immunology of Behcet's Disease. Swets & Zeitlinger Publishers, Nisse, pp. 1–16.

321. Zwirner NW, Fernandez-Vina MA, Stastny P. 1998. MICA, a new polymorphic HLA related antigen, is expressed mainly by keratinocytes, endothelial cells, and monocytes. Immunogenetics 47(2):139–48.

# Presentations and Publications

- British Society of Immunology – 2008-2010
- 13th International Conference on Behçet's Disease, 2008 – Received Poster Award.
- 14th International Conference on Behçet's Disease, 2010
- Graduate Research Showcase event Kings College London, 2010 - Received Oral Presentation Award.

- Shafi S, Vantourout P, Wallace G, Antoun A, Vaughan R, Stanford M, Hayday A. 2011. **An NKG2D-mediated human lymphoid stress surveillance response with high interindividual variation.** Sci Transl Med. Dec 14;3(113):113ra124. Epub 2011 Nov 30.